ORNL-5259
(ENDF-258)

SB4. Measurements and Calculations of the ORNL CRBR Upper Axial Shield Experiment

R. E. Maerker
F. J. Muckenthaler
C. E. Clifford

OAK RIDGE NATIONAL LABORATORY
OPERATED BY UNION CARBIDE CORPORATION · FOR THE DEPARTMENT OF ENERGY

Printed in the United States of America. Available from
National Technical Information Service
U.S. Department of Commerce
5285 Port Royal Road, Springfield, Virginia 22161
Price: Printed Copy $7.25; Microfiche $3.00

OAK RIDGE NATIONAL LABORATORY
OPERATED BY
UNION CARBIDE CORPORATION
NUCLEAR DIVISION

POST OFFICE BOX X
OAK RIDGE, TENNESSEE 37831

January 12, 1978

To: ENDF Distribution

Subject: ORNL-5259 (ENDF-258), "Measurements and Calculations of the ORNL CRBR Upper Axial Shield Experiment"

The experiment described in the enclosed report is expected to become a CSEWG benchmark restricted to U.S. distribution. Your attention is called to the restrictions specified for the distribution of this document on its cover, and you are requested to handle the report and the information contained therein accordingly.

Ernest G. Silver, for
W. O. Harms, Director
Breeder Reactor Program

ORNL-5259
(ENDF-258)
Distribution Category UC-79d

Contract No. W-7405-eng-26

Neutron Physics Division

SB4. MEASUREMENTS AND CALCULATIONS OF THE ORNL CRBR UPPER AXIAL SHIELD EXPERIMENT

R. E. Maerker
F. J. Muckenthaler
C. E. Clifford

Date Published: June 1977

OAK RIDGE NATIONAL LABORATORY
Oak Ridge, Tennessee 37830
operated by
UNION CARBIDE CORPORATION
for the
ENERGY RESEARCH AND DEVELOPMENT ADMINISTRATION

Experiment Performed By:

F. J. Muckenthaler
R. M. Freestone
K. M. Henry
J. L. Hull
J. J. Manning
J. N. Money

Analysis Performed By:

R. E. Maerker

Report Written By:

R. E. Maerker

Work Directed By:

C. E. Clifford

Manuscript Typed By:

Susan L. Rider

TABLE OF CONTENTS

	Page
ABSTRACT	v
I. MEASUREMENTS	1
A. Introduction	1
B. Geometry	2
C. Materials	37
D. Source	37
E. Detectors	43
F. Measured Results	46
II. ANALYSIS	66
A. General	66
B. Method of Calculation	67
C. ANISN Scaling Calculations	71
D. Calculated Results and Comparisons with Experiment	79
E. Discussion of Comparisons	79
F. 171 Group ANISN Scaling Calculations	100
G. Conclusions	105
APPENDIX	107

ABSTRACT

The measurements and analysis of the upper axial shield experiment performed at the Tower Shielding Facility using the large beam collimator have been described in a format suitable for eventual adoption as a CSEWG shielding benchmark. Neutron transmissions through various combinations of stainless steel followed by sodium and carbon steel over a range of attenuations of the order of 10^{12} were measured in this experiment. Calculations using a standard design cross section set based on ENDF/IV with a standard transport code reveal disagreements with measurements behind the thickest shields by at most a factor of about three, but in most of the cases the agreement is within $\sim$ 30%. One-dimensional scaling of this experiment has also been verified, and fine-group calculations indicate that the basic ENDF/IV cross section data must be updated for sodium.

I. Measurements

A. INTRODUCTION

One of the controlling factors in the biological dose on the top deck of the proposed Clinch River Breeder Reactor is the neutron penetration through the upper axial shield. The neutron attenuation model of this shield consists of $\sim$ 30-45 cm. of SS-304 followed by $\sim$ 450-600 cm. of sodium followed by $\sim$ 60-125 cm. of carbon steel. In order to test the accuracy of design calculations based on a standard transport method and a standard set of group cross sections, and in addition to test the basic ENDF/IV cross section data, this integral experiment was devised and performed at the Tower Shielding Facility at Oak Ridge in the time interval March 1975 through April 1976.

Because the anticipated attenuation through the thickest shield mock-up was of the order of 10^{12}, the leakage from the TSR-II reactor was increased over that of earlier experiments by opening up the collimator to the diameter of the core ($\sim$ 86 cm.) and shortening the length of the collimator to $\sim$ 30 cm.. Maximum steady state power level operation capability was also increased from 100 kW to 1 MW over that of earlier experiments. The resulting maximum overall increase in the flux levels at the incident surface of a shield configuration was about three orders of magnitude over the earlier experiments. This increase in intensity comes at the expense of source definition, however, since the beam is no longer well-collimated.

Measurements were made only of neutrons. The shield was set up, one component at a time, and measurements made behind each portion of the configuration before additional components were added. This procedure allowed comparisons between calculation and measurement at intermediate thicknesses of the shield, so that trends and the appearance of local discrepancies could be better assessed.

Measurements of the 4-in. Bonner ball counting rates were made behind all configurations, and were supplemented by an NE-213 spectral measurement and a 12-in. Bonner ball counting rate behind $\sim$ 46 cm. of stainless steel and hydrogen counter spectral measurements behind both 46 cm. of stainless

steel and ∿ 150 cm. of sodium preceded by the stainless steel.

A sensitivity analysis of some of the thicker configurations in this experiment to the 4-in. Bonner ball counting rates (see Appendix) indicates that the important energy and material regions vary remarkably with the particular configuration. Generally speaking, the fluxes leaking the configurations with little or no carbon steel behind them are most sensitive to the sodium cross sections below 2 keV, but the fluxes leaking those configurations backed by considerable thicknesses of carbon steel are most sensitive to the 300 keV window in sodium, the 24 keV window and below in iron, and the cross sections above 2 MeV in both stainless steel and sodium.

B. GEOMETRY

A top view of the TSR-II and collimator geometry is shown in Fig. 1. The reactor geometry may be assumed to be spherical and the collimator geometry to have cylindrical symmetry about the horizontal centerline. The source can be represented as a disc source located on the inner surface of the collimator, as shown, and will be described in another section of this document. The beginning of the shielding configuration occurs at a centerline distance of 87.15 cm. from the core or 33.49 cm. from the source plane, as shown, when the thinner aluminum facing was used, and at a distance of 91.30 from the core (37.64 from the source plane) when the thicker aluminum facing was used.

The stainless steel-304, carbon steel, and lithium hydride slabs (the latter serving as a background reducing material) used in the shield configurations were approximately square, being 152.4 cm. on a side. The sodium filled aluminum-walled tanks were cylindrical, 335.3 cm. in diameter. The front and rear faces of the tanks had a thickness of 1.27 cm. of aluminum. Square concrete collars surrounded the sodium-filled tanks to produce an overall outside dimension of 426.7 cm. on a side. A photograph of the sodium tanks enclosed in their concrete collars is shown in Fig. 2.

The geometry of each of the configurations for which measurements were made is shown in Figs. 3-33. Although repeated in each figure for clarity, it should be pointed out that the geometry preceding the carbon steel slabs is the same for Figs. 5-9. Similarly, the geometry preceding the carbon

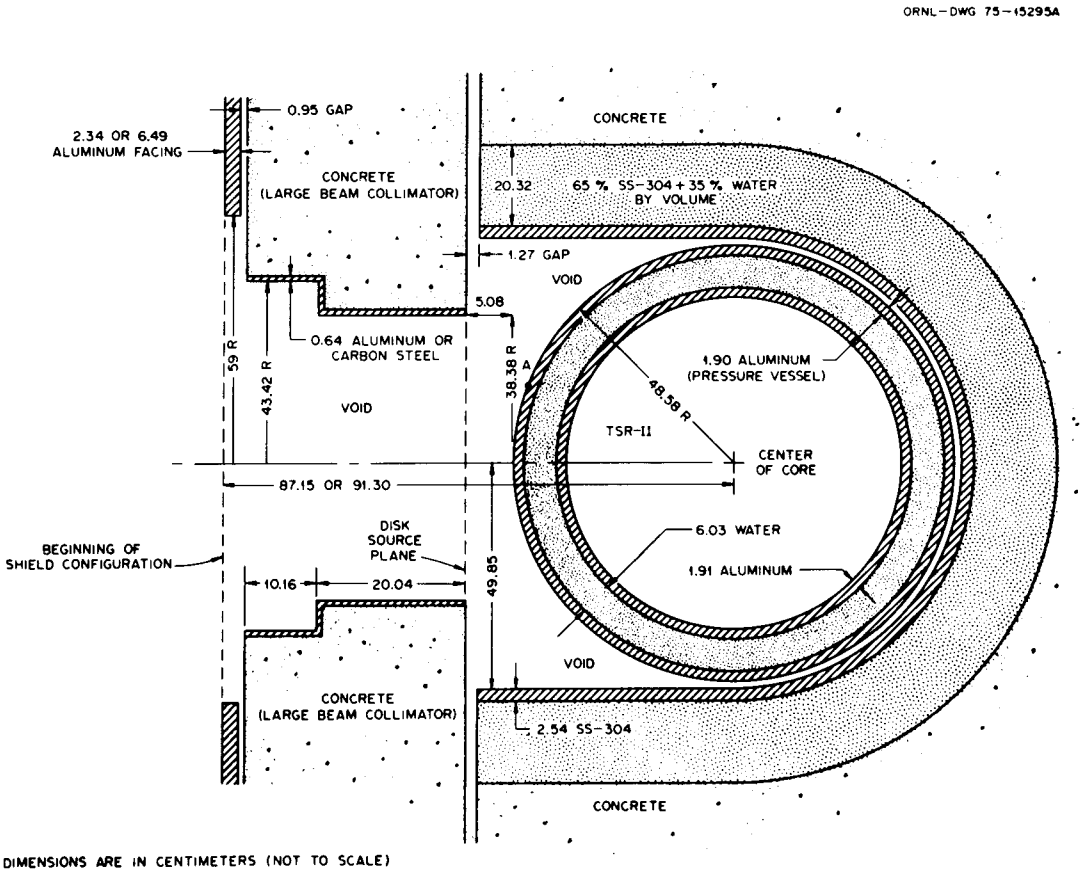

Fig. 1. Top view of reactor and large beam collimator geometry.

Fig. 2. Photograph of the sodium tanks. The concrete collar had not as yet been attached to the 5-ft. tank in the background.

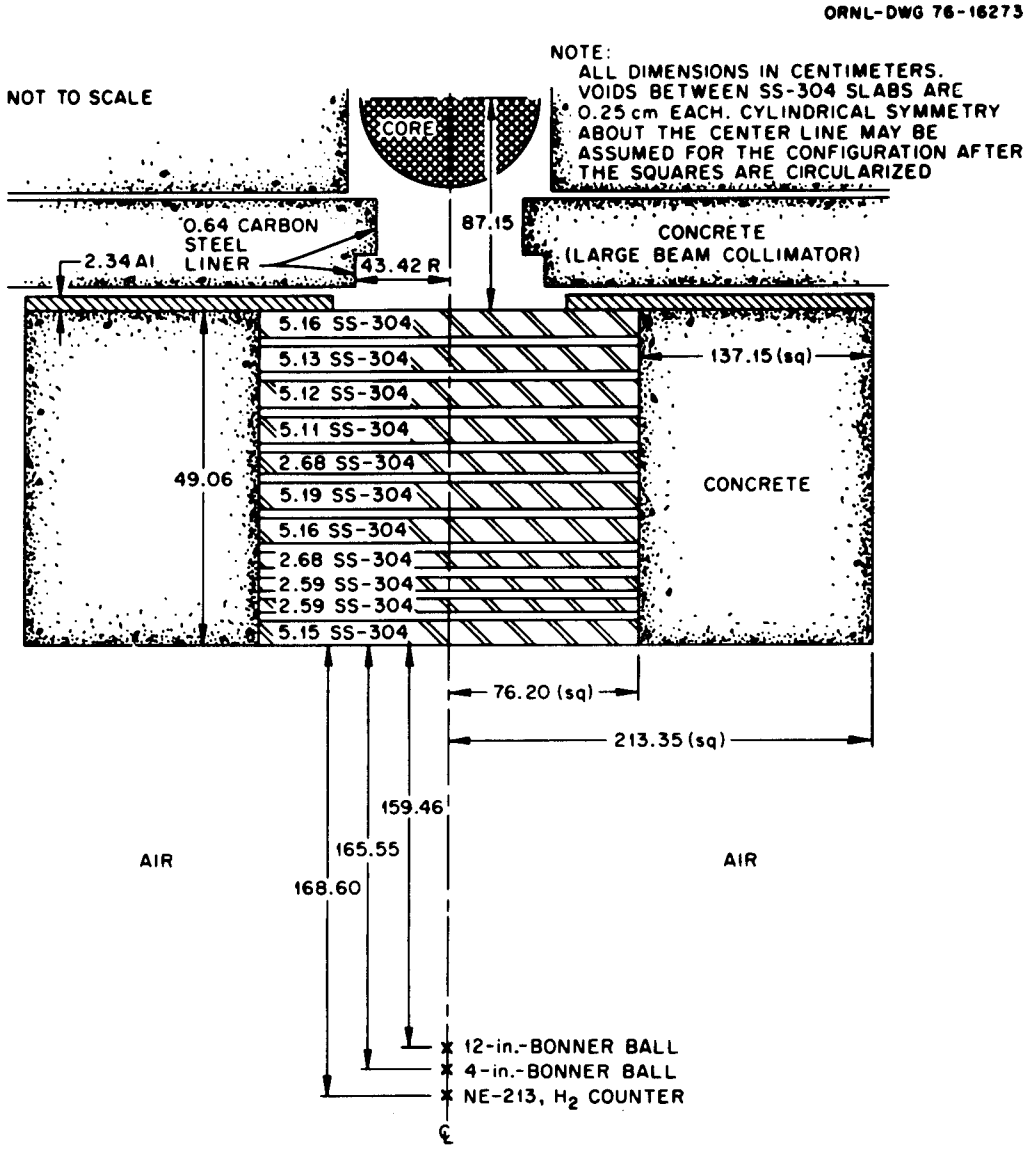

Fig. 3. Top view of the geometry of the measurements behind 46.56 cm. SS.

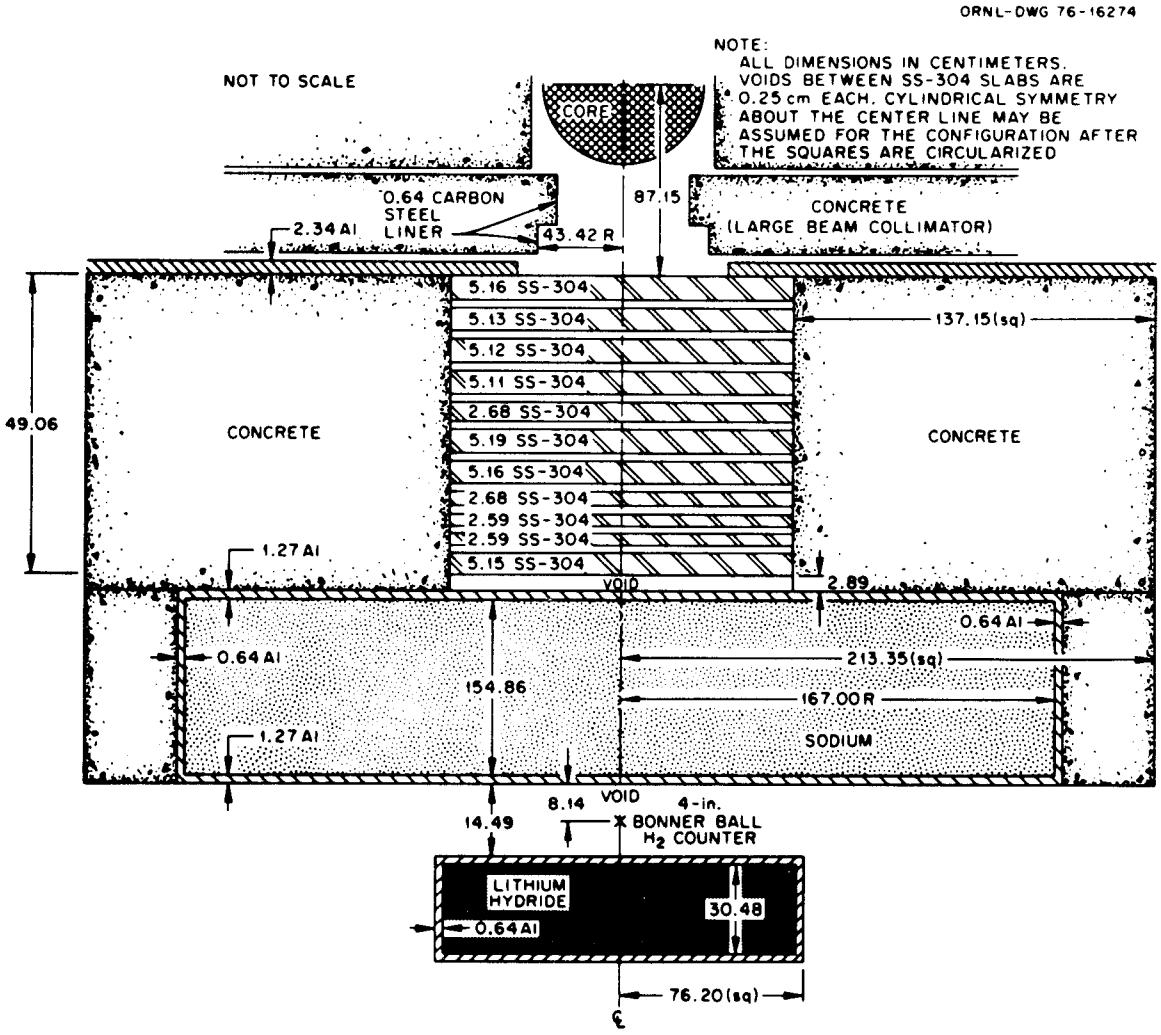

Fig. 4. Top view of the geometry of the measurements behind 46.56 cm. SS + 154.86 cm. Na.

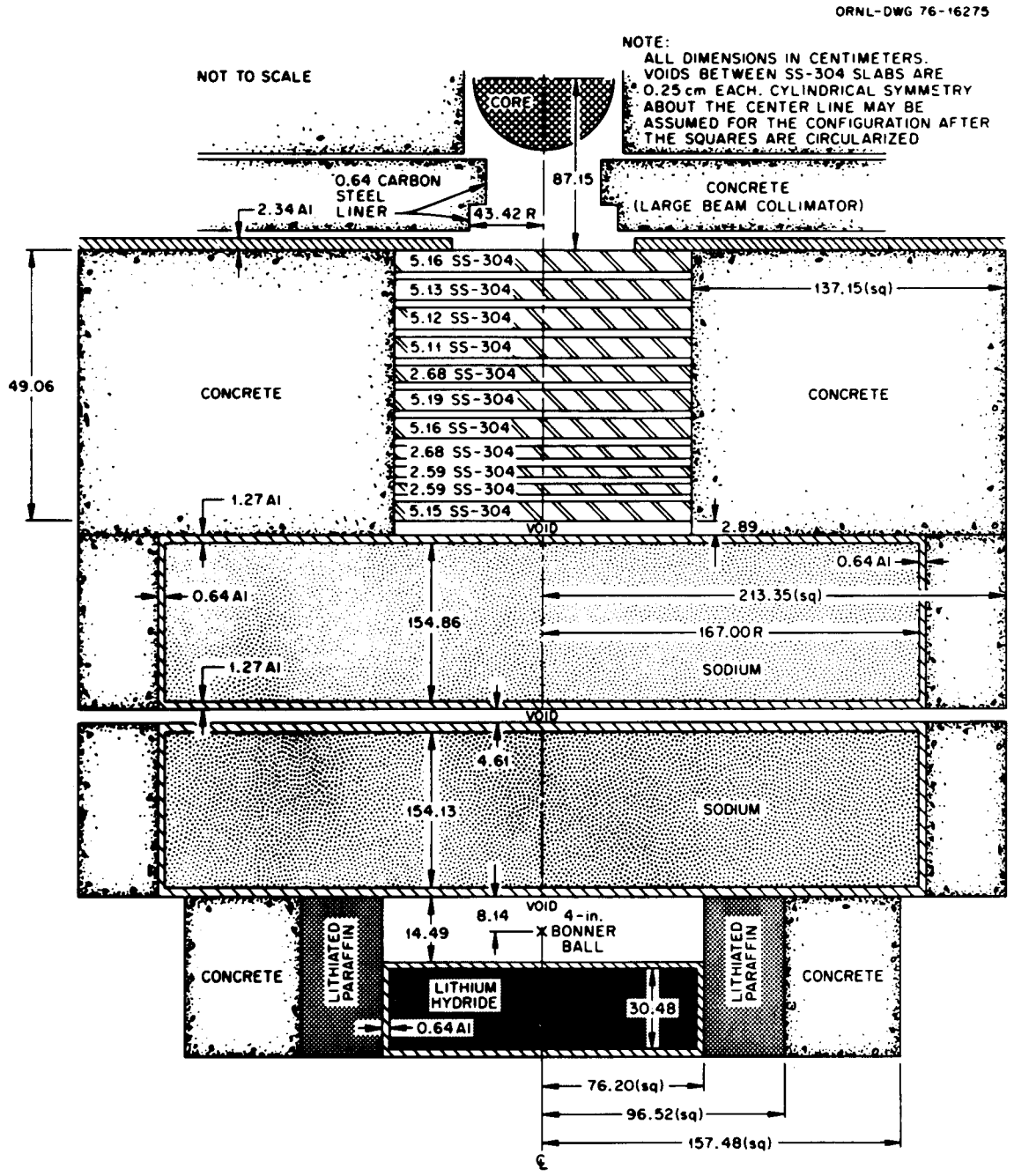

Fig. 5. Top view of the geometry of the measurements behind 46.56 cm. SS + 308.99 cm. Na.

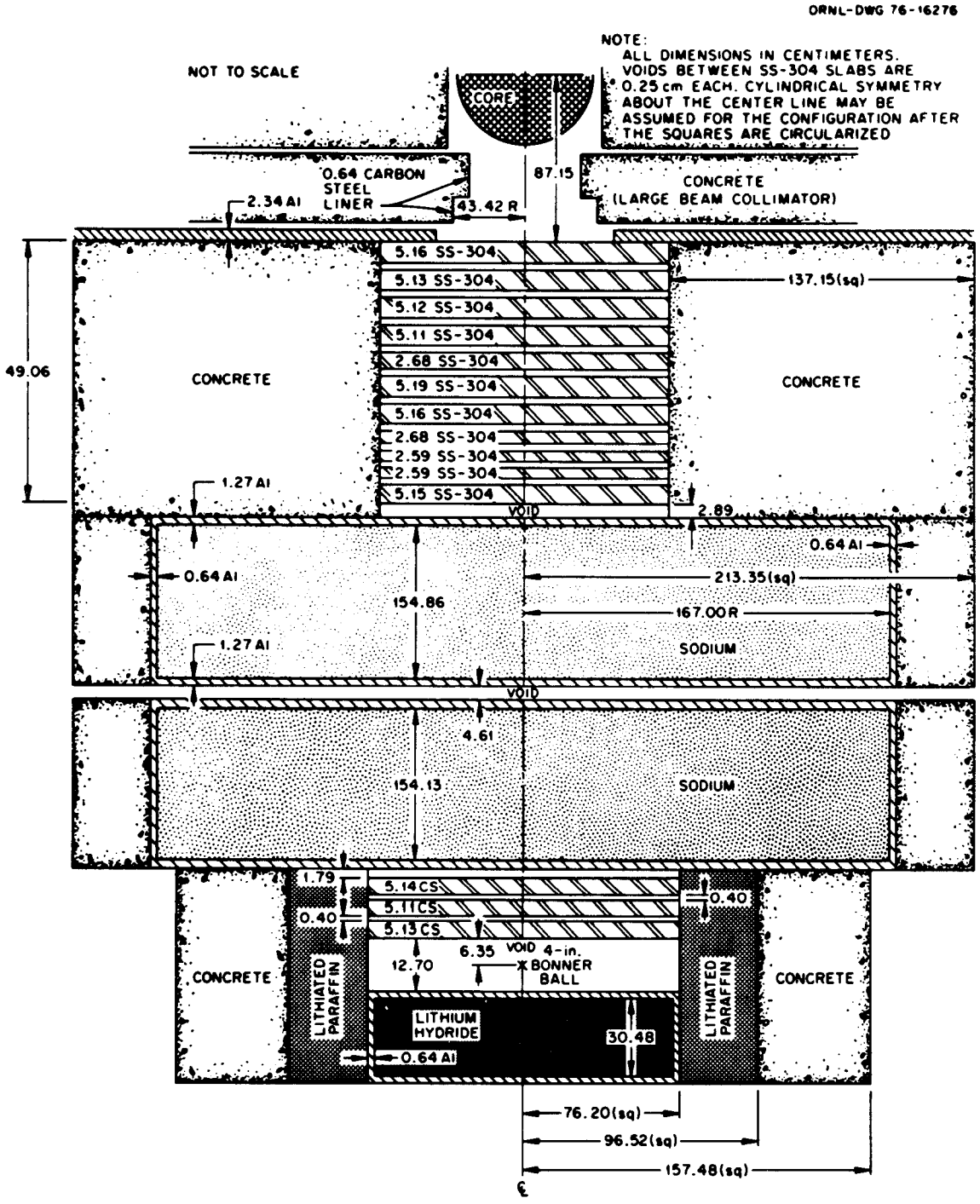

Fig. 6. Top view of the geometry of the measurements behind 46.56 cm. SS + 308.99 cm. Na + 15.38 cm. CS.

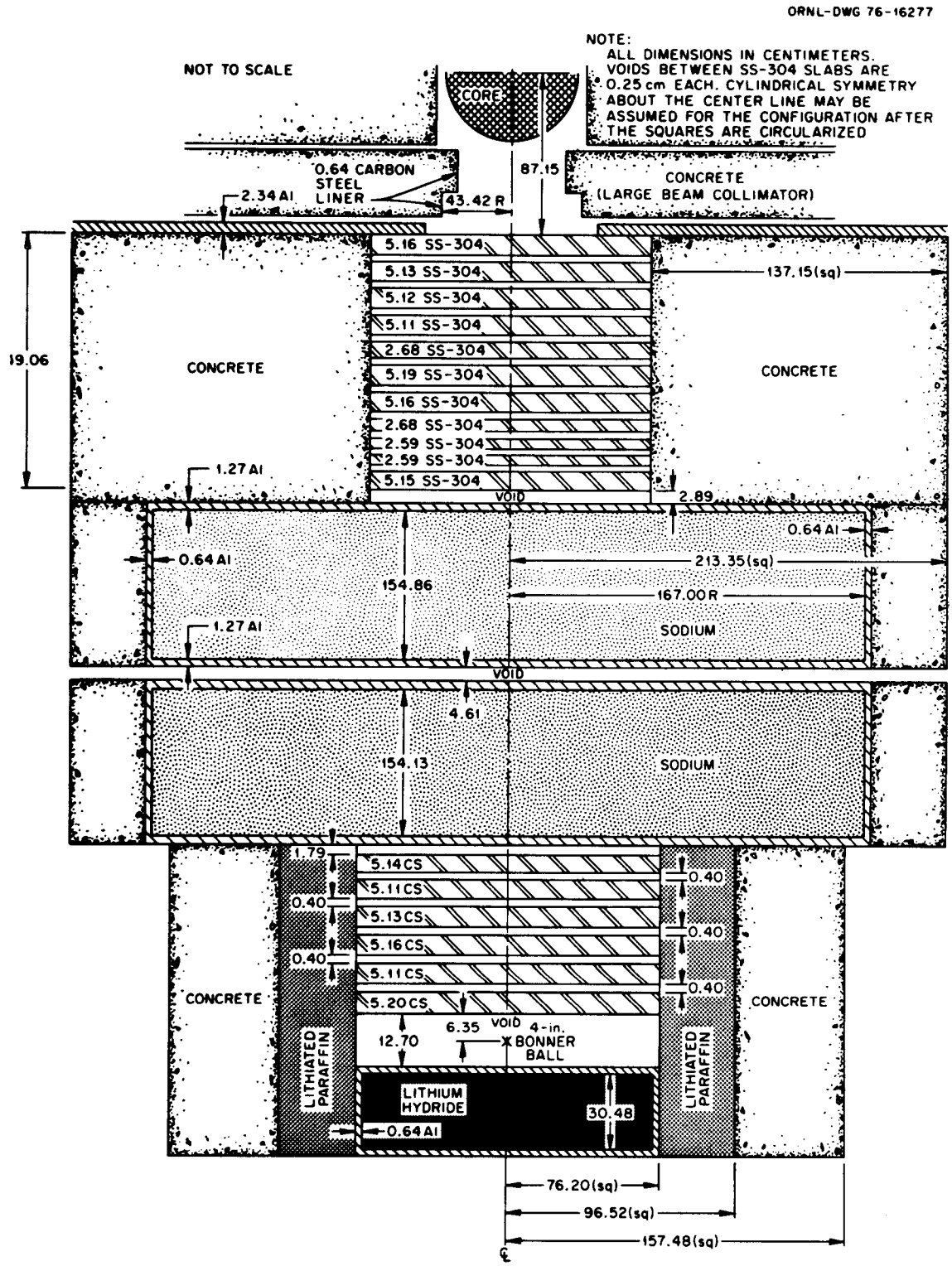

Fig. 7. Top view of the geometry of the measurements behind 46.56 cm. SS + 308.99 cm. Na + 30.85 cm. CS.

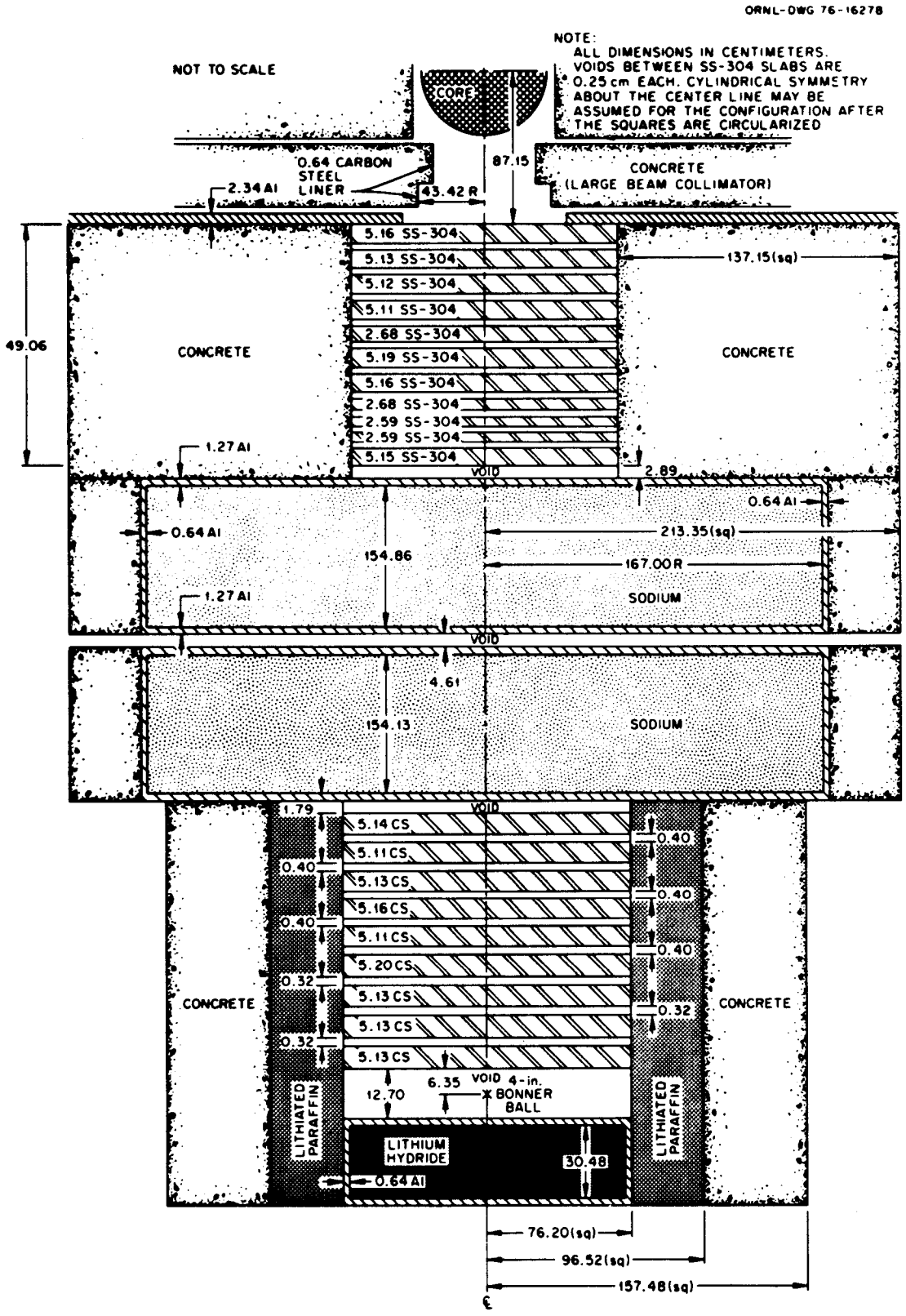

Fig. 8. Top view of the geometry of the measurements behind 46.56 cm. SS + 308.99 cm. Na + 46.24 cm. CS.

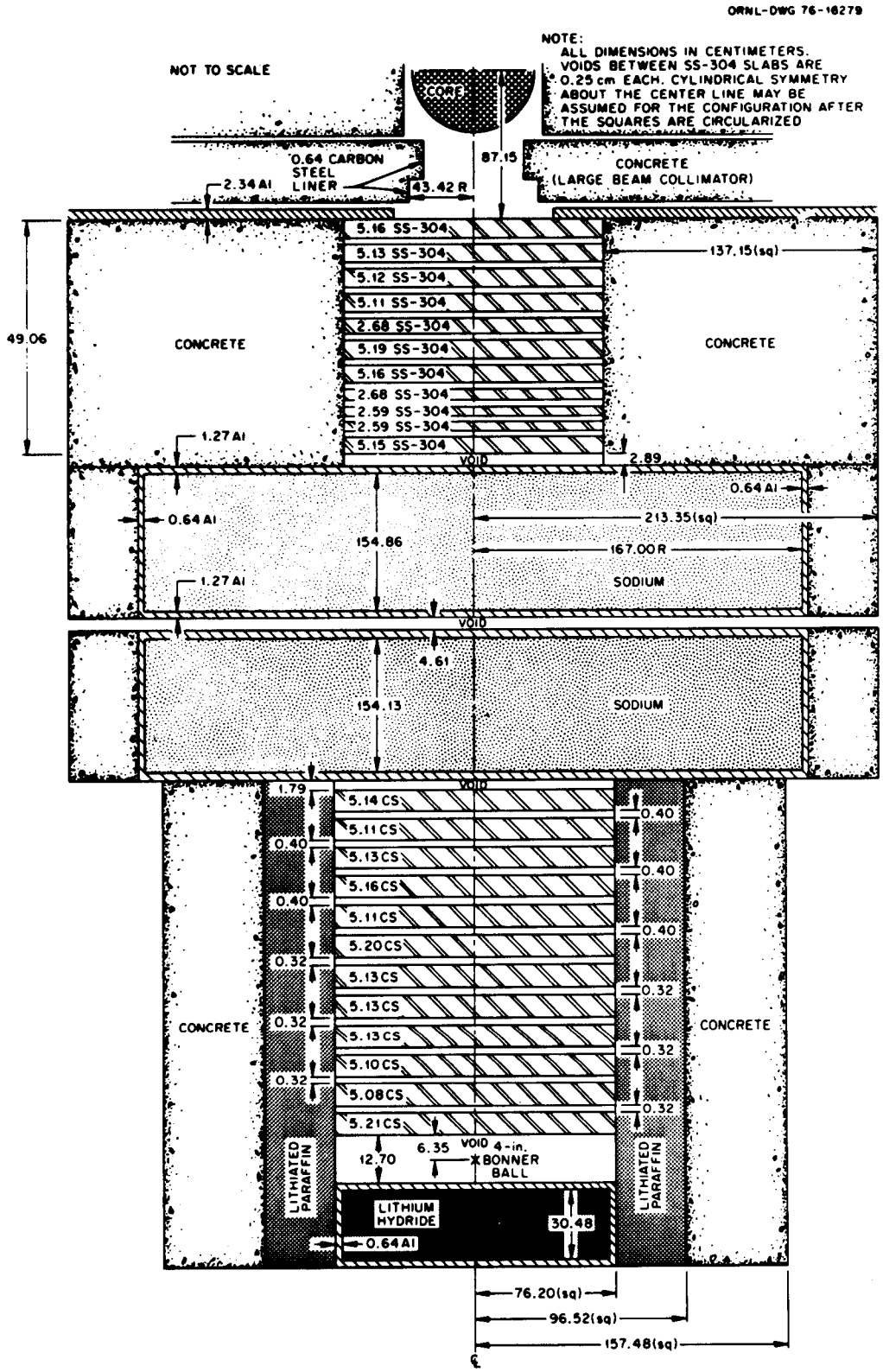

Fig. 9. Top view of the geometry of the measurements behind 46.56 cm. SS + 308.99 cm. Na + 61.63 cm. CS.

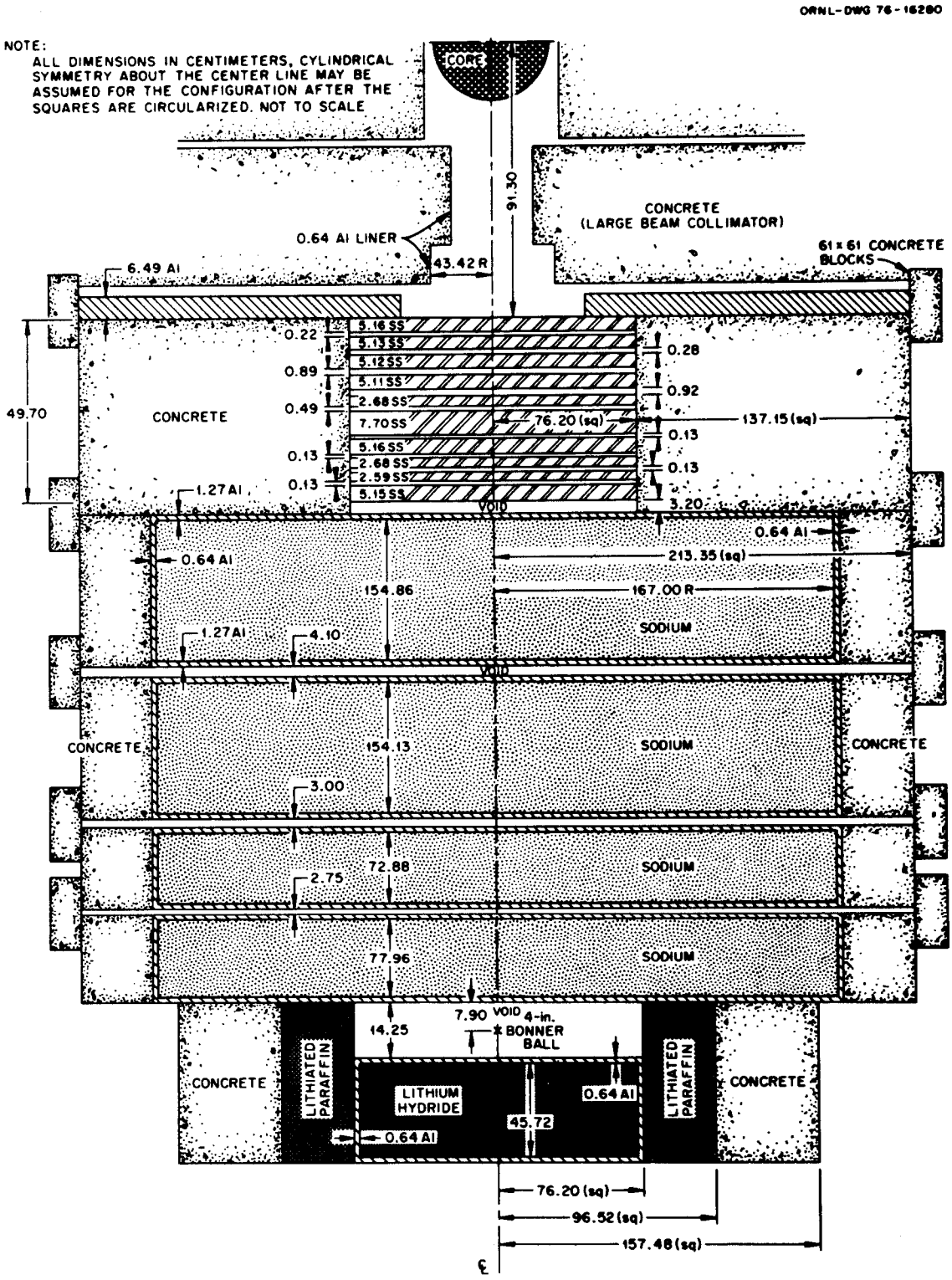

Fig. 10. Top view of the geometry of the measurements behind 46.56 cm. SS + 459.83 cm. Na.

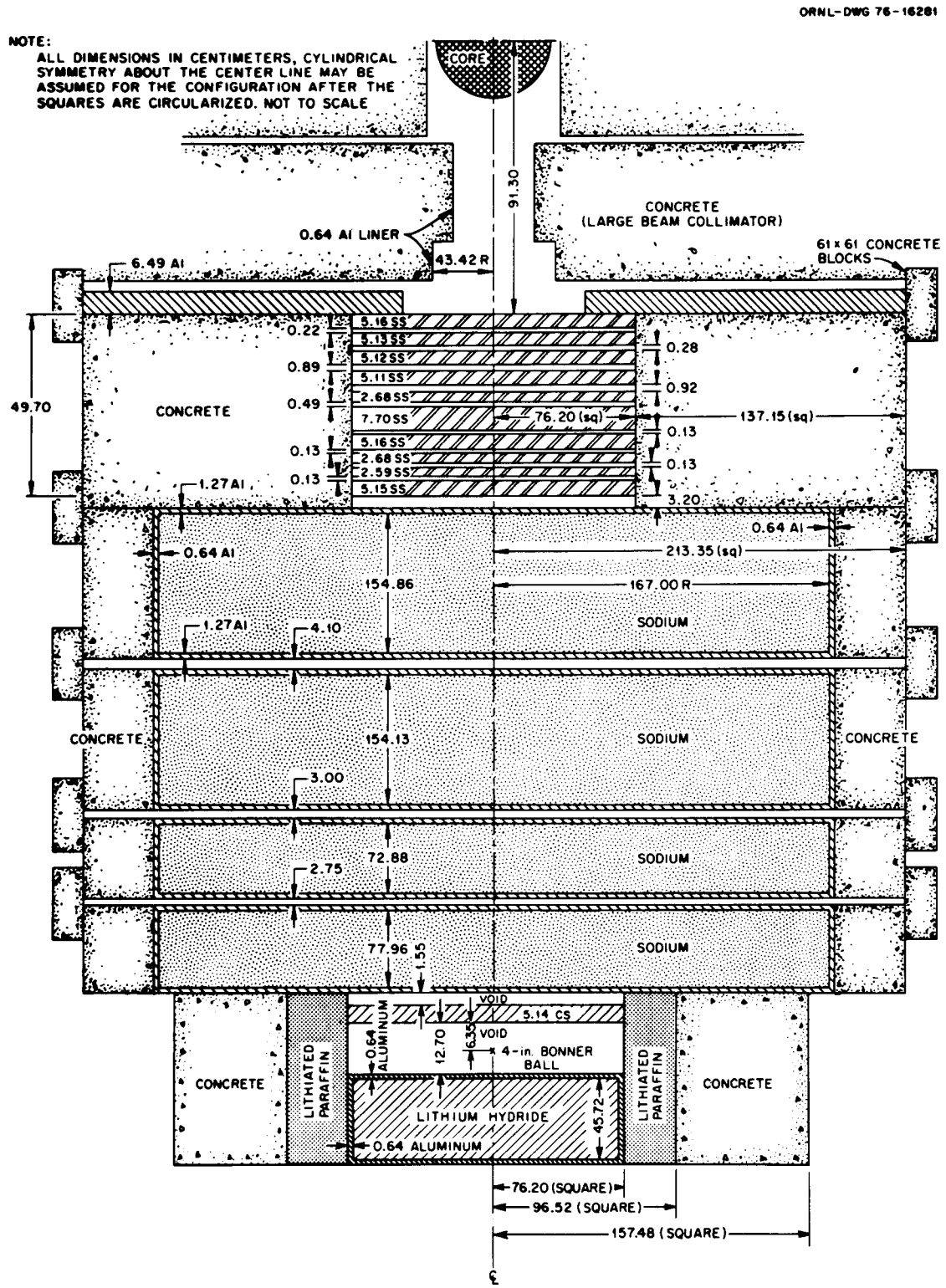

Fig. 11. Top view of the geometry of the measurements behind 46.56 cm. SS + 459.83 cm. Na + 5.14 cm. CS.

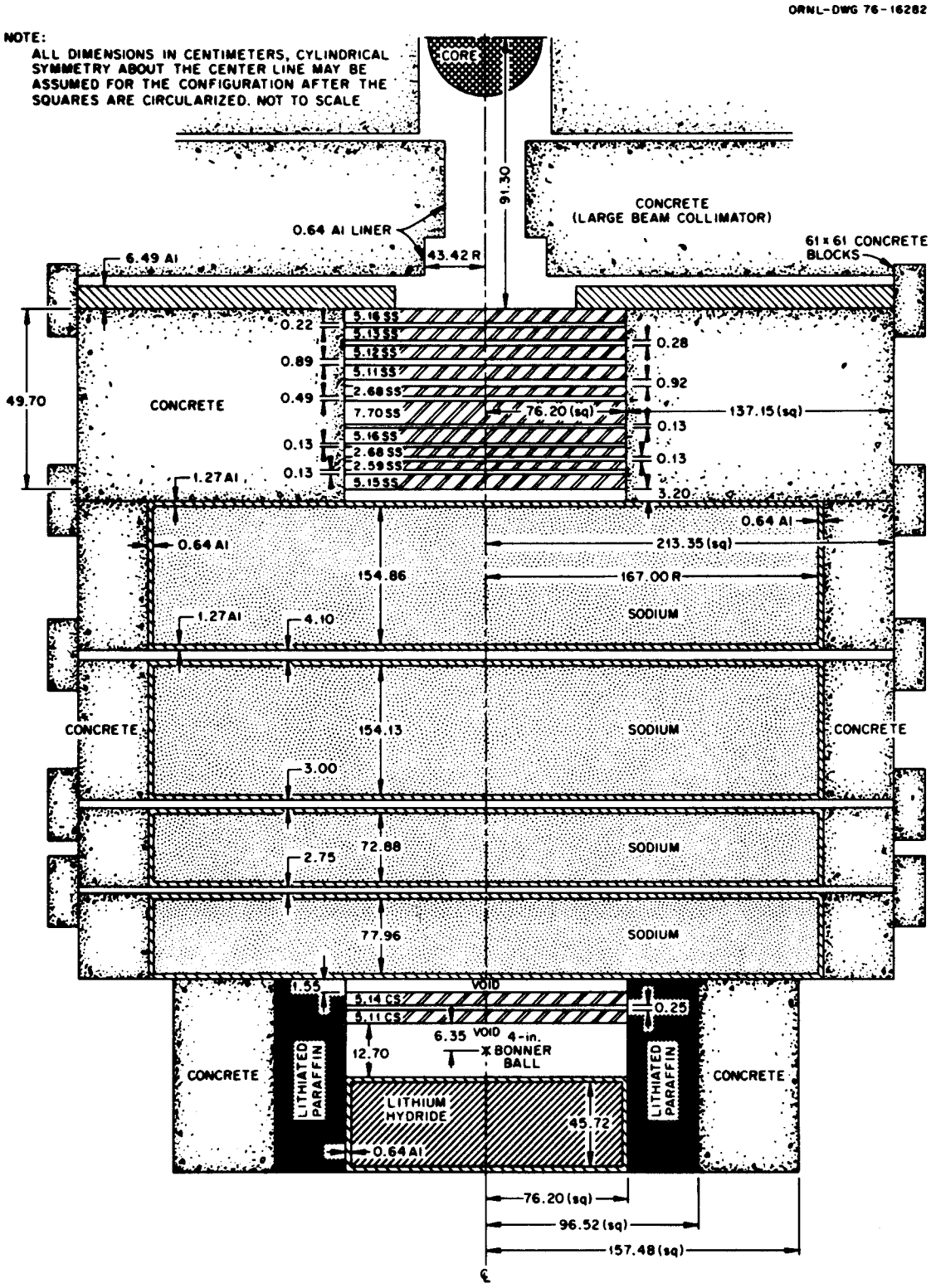

Fig. 12. Top view of the geometry of the measurements behind 46.56 cm. SS + 459.83 cm. Na + 10.25 cm. CS.

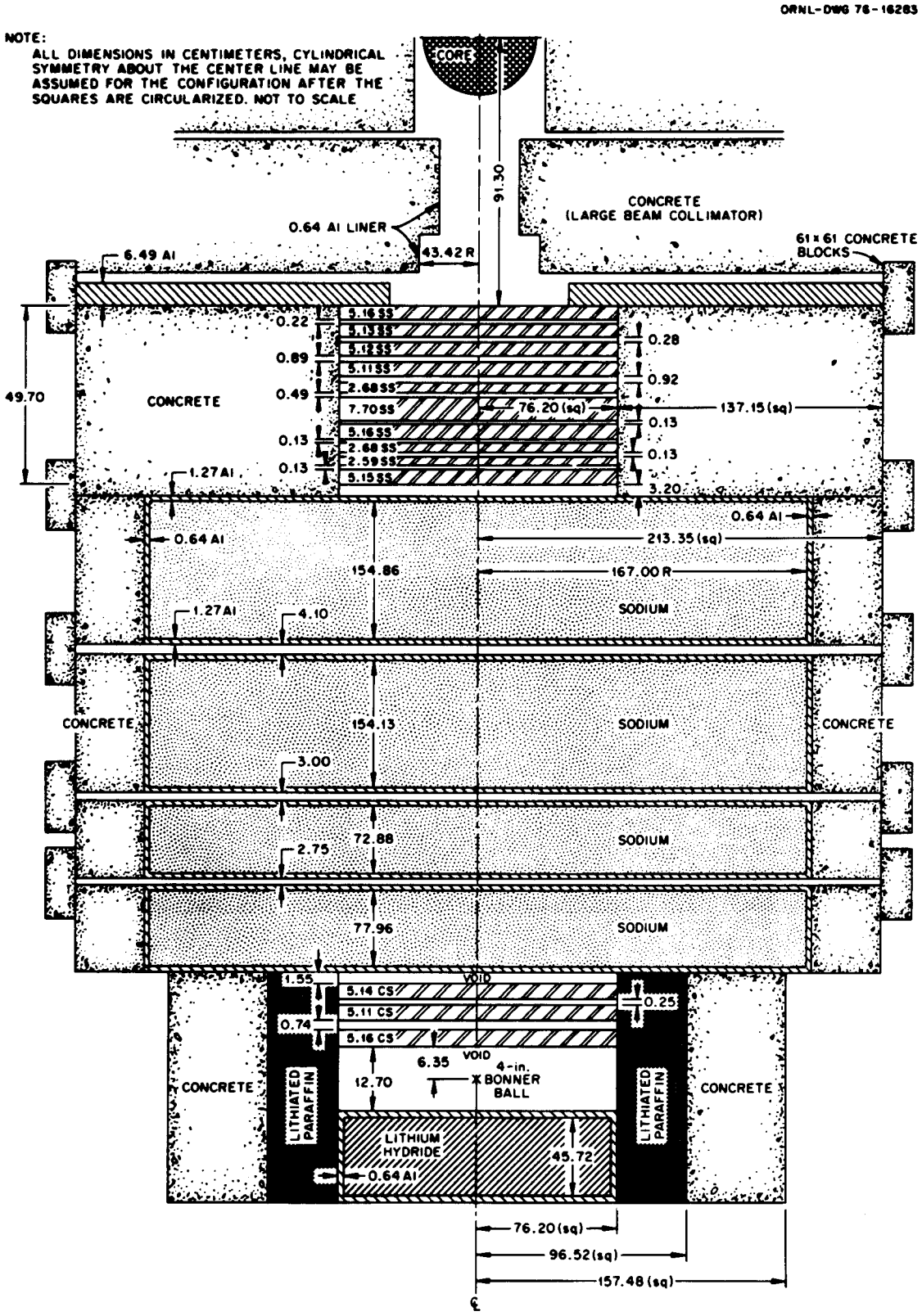

Fig. 13. Top view of the geometry of the measurements behind 46.56 cm. SS + 459.83 cm. Na + 15.41 cm. CS.

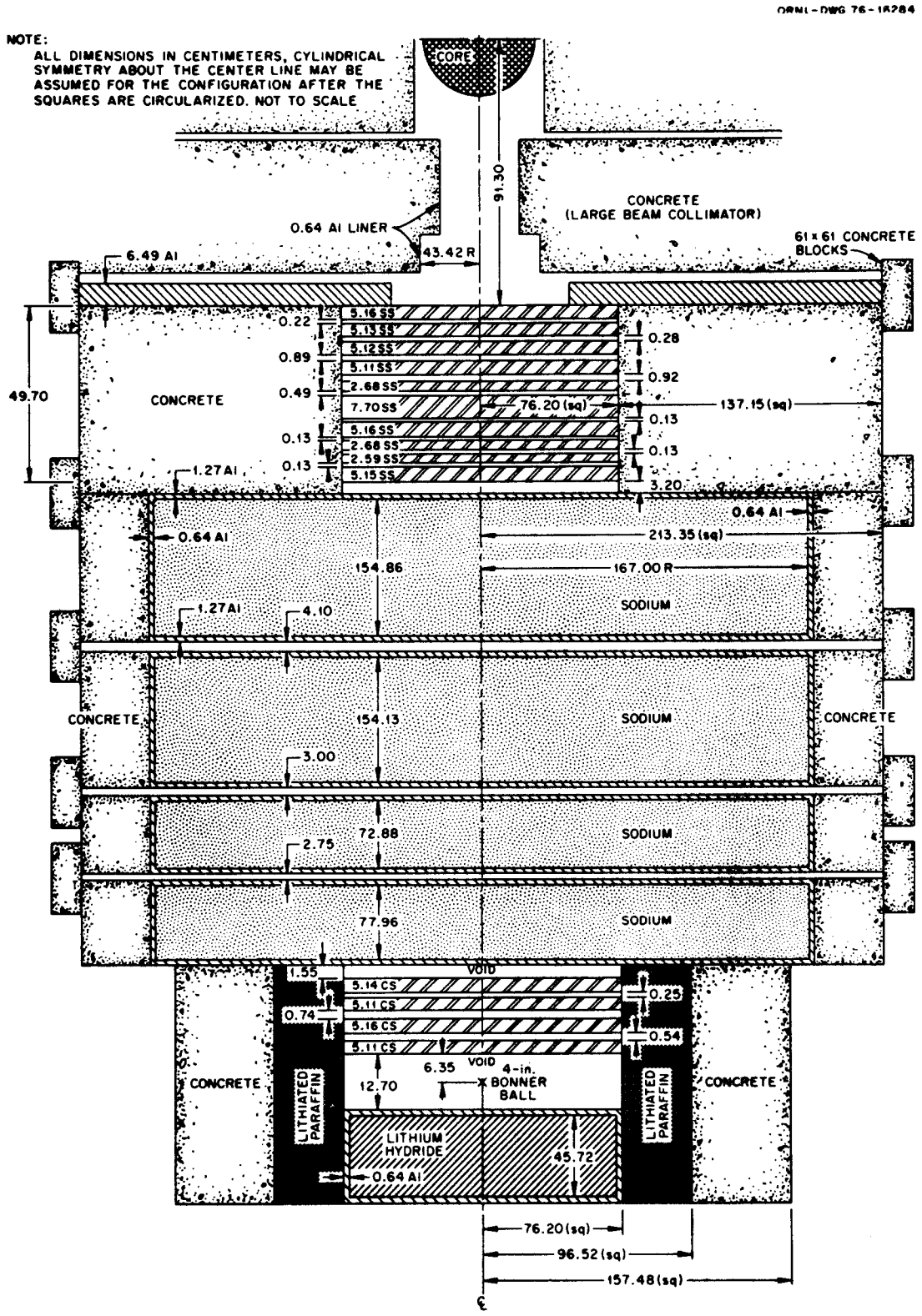

Fig. 14. Top view of the geometry of the measurements behind 46.56 cm. SS + 459.83 cm. Na + 20.52 cm. CS.

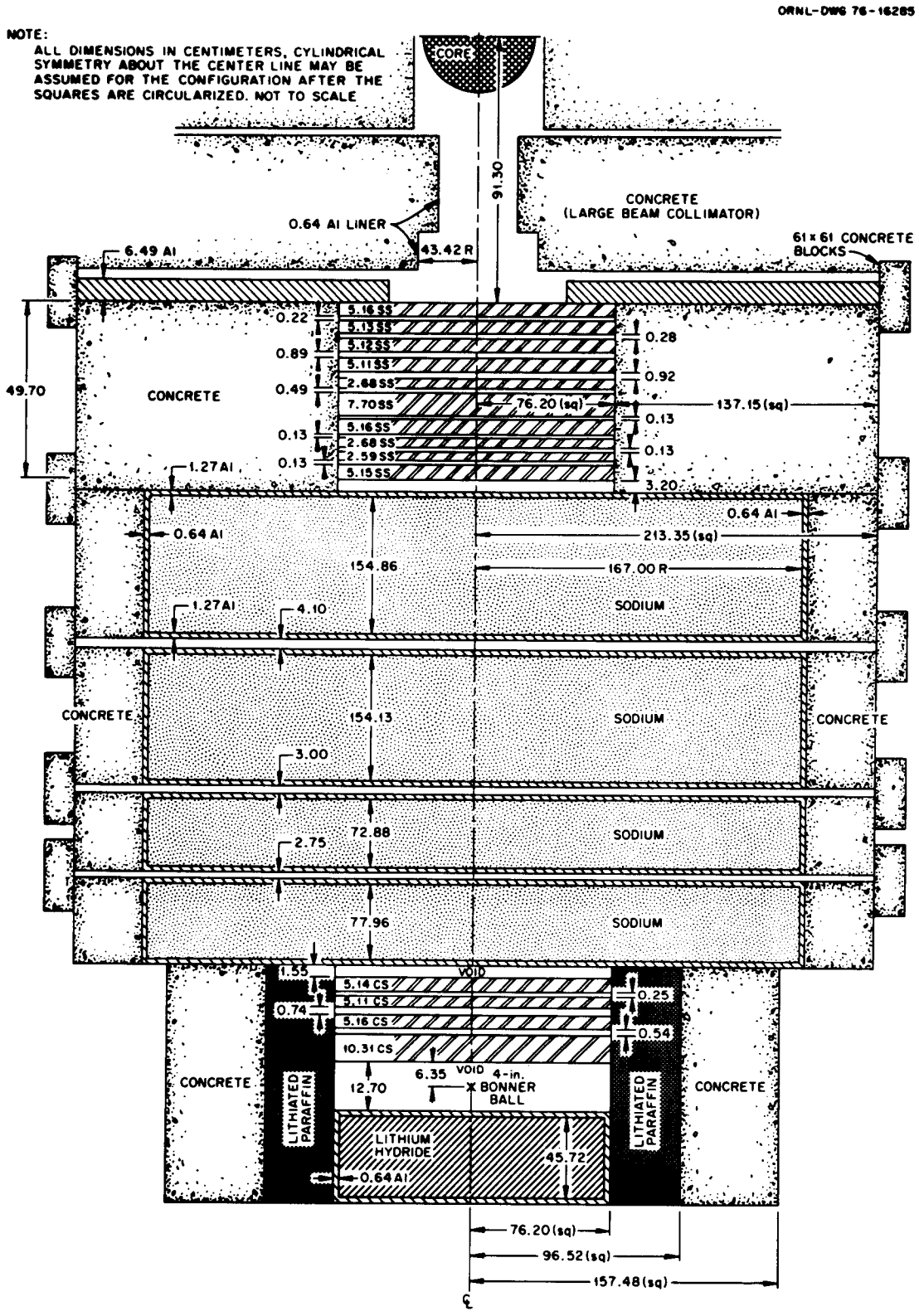

Fig. 15. Top view of the geometry of the measurements behind 46.56 cm. SS + 459.83 cm. Na + 25.72 cm. CS.

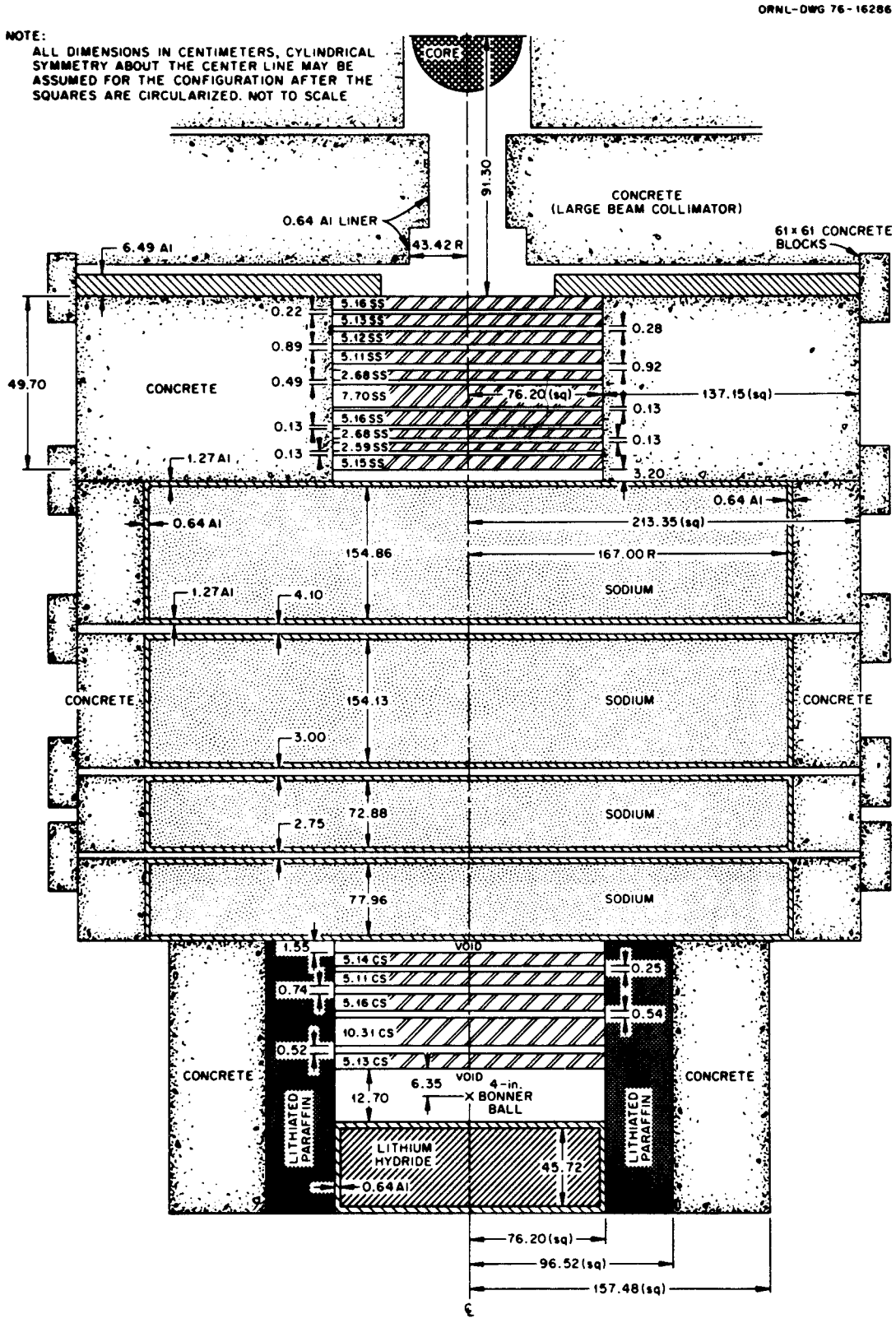

Fig. 16. Top view of the geometry of the measurements behind 46.56 cm. SS + 459.83 cm. Na + 30.85 cm. CS.

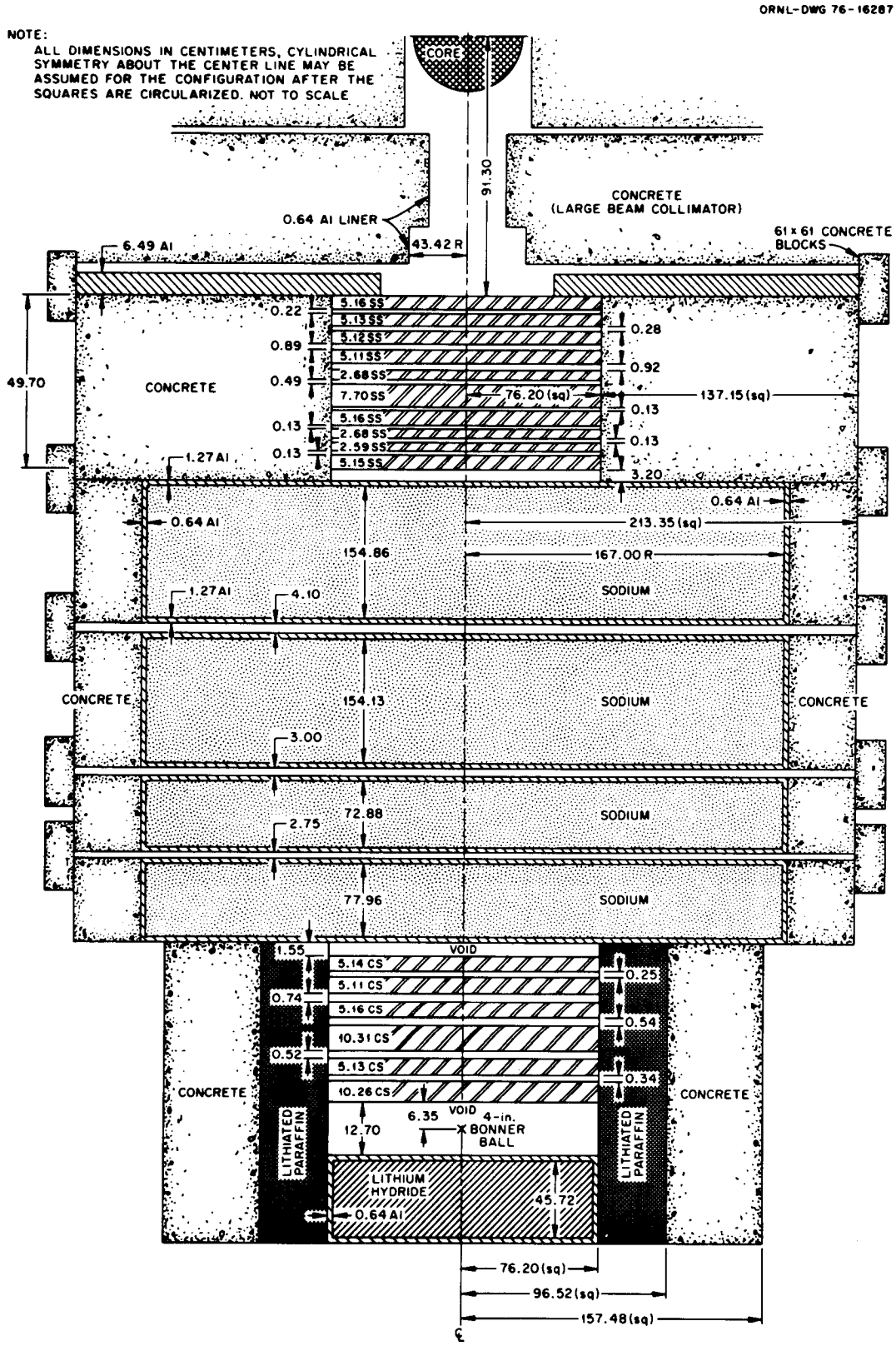

Fig. 17. Top view of the geometry of the measurements behind 46.56 cm. SS + 459.83 cm. Na + 41.11 cm. CS.

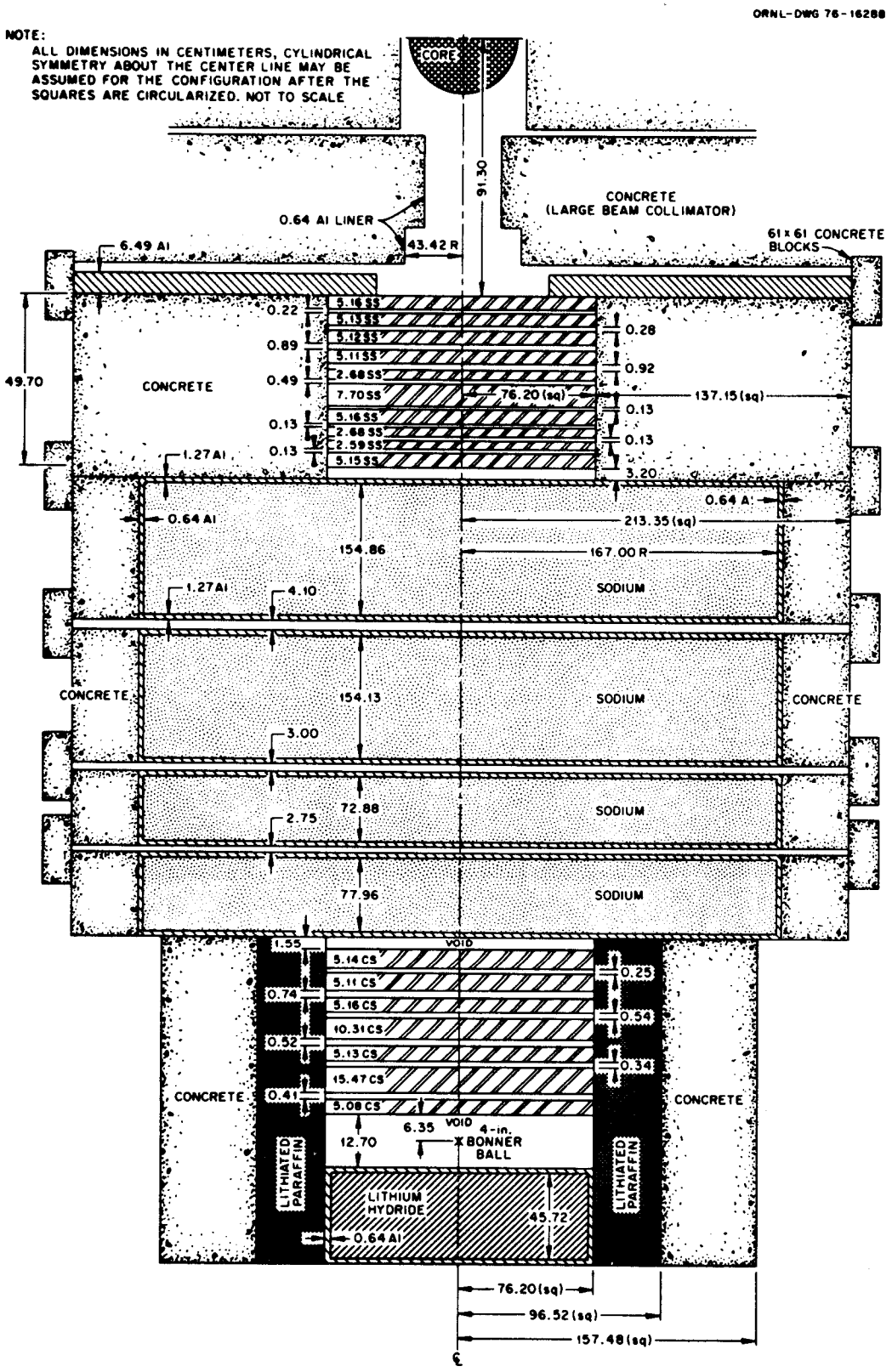

Fig. 18. Top view of the geometry of the measurements behind 46.56 cm. SS + 459.83 cm. Na + 51.40 cm. CS.

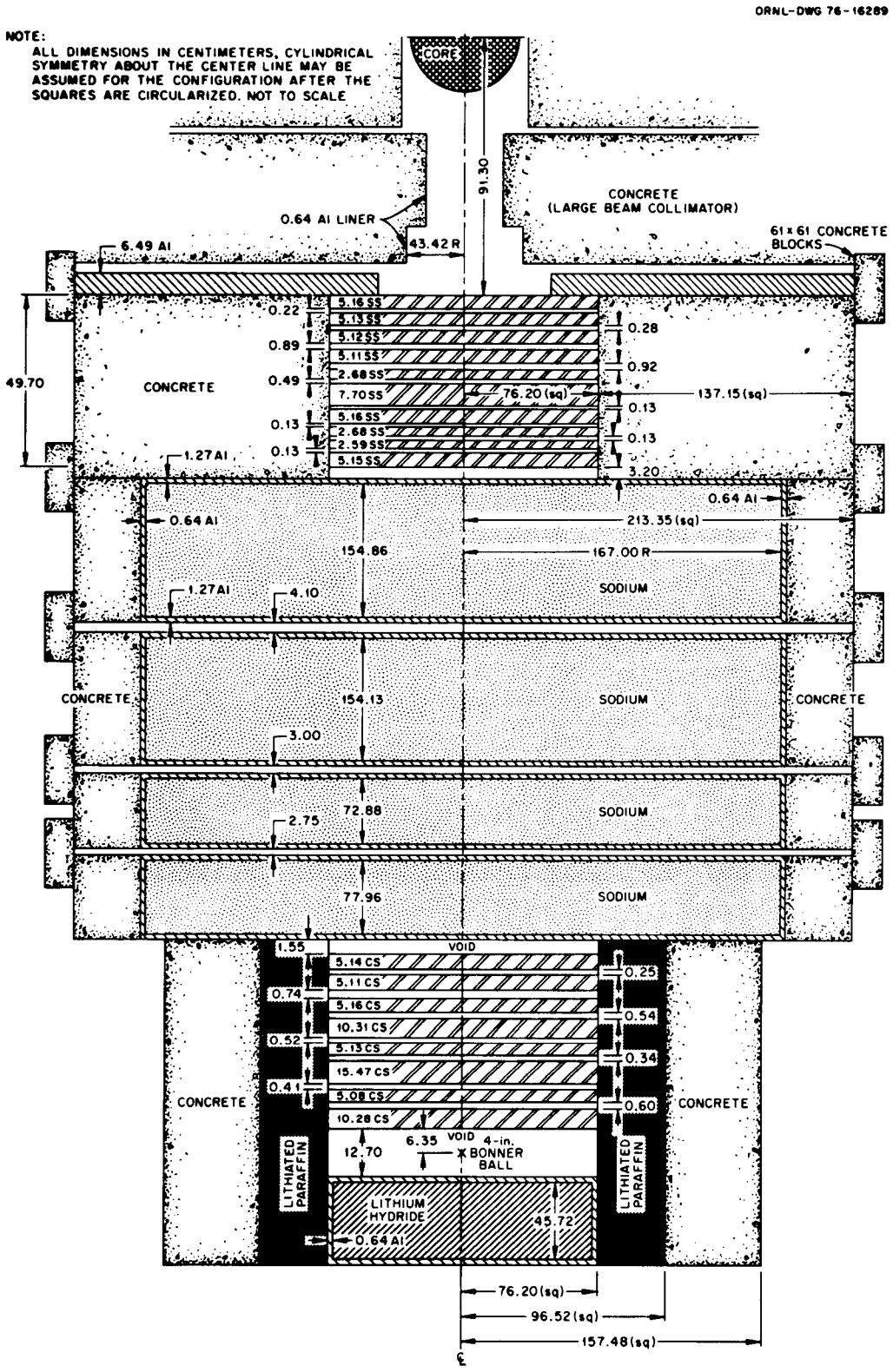

Fig. 19. Top view of the geometry of the measurements behind 46.56 cm. SS + 459.83 cm. Na + 61.68 cm. CS.

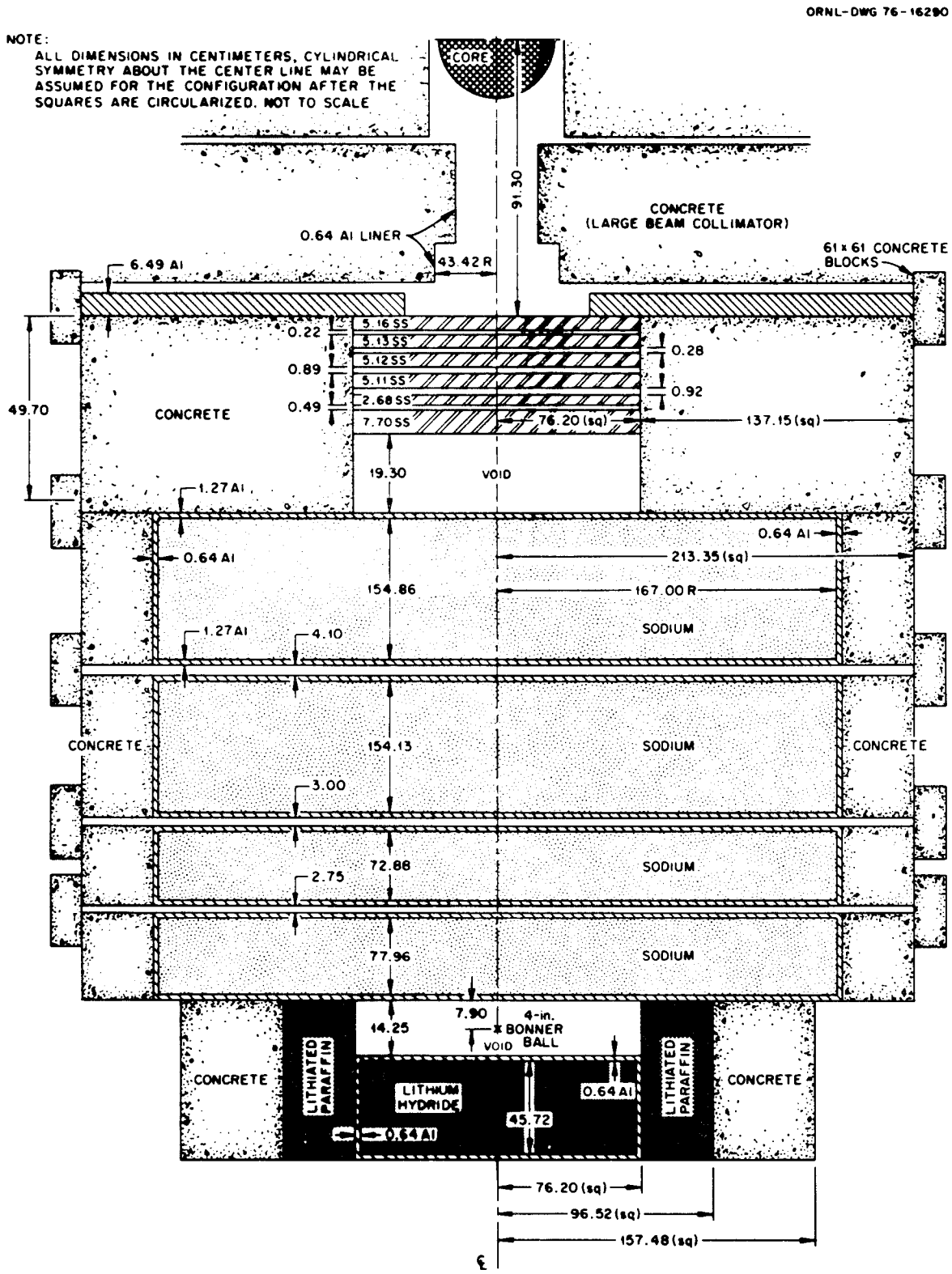

Fig. 20. Top view of the geometry of the measurements behind 30.90 cm. SS + 459.83 cm. Na.

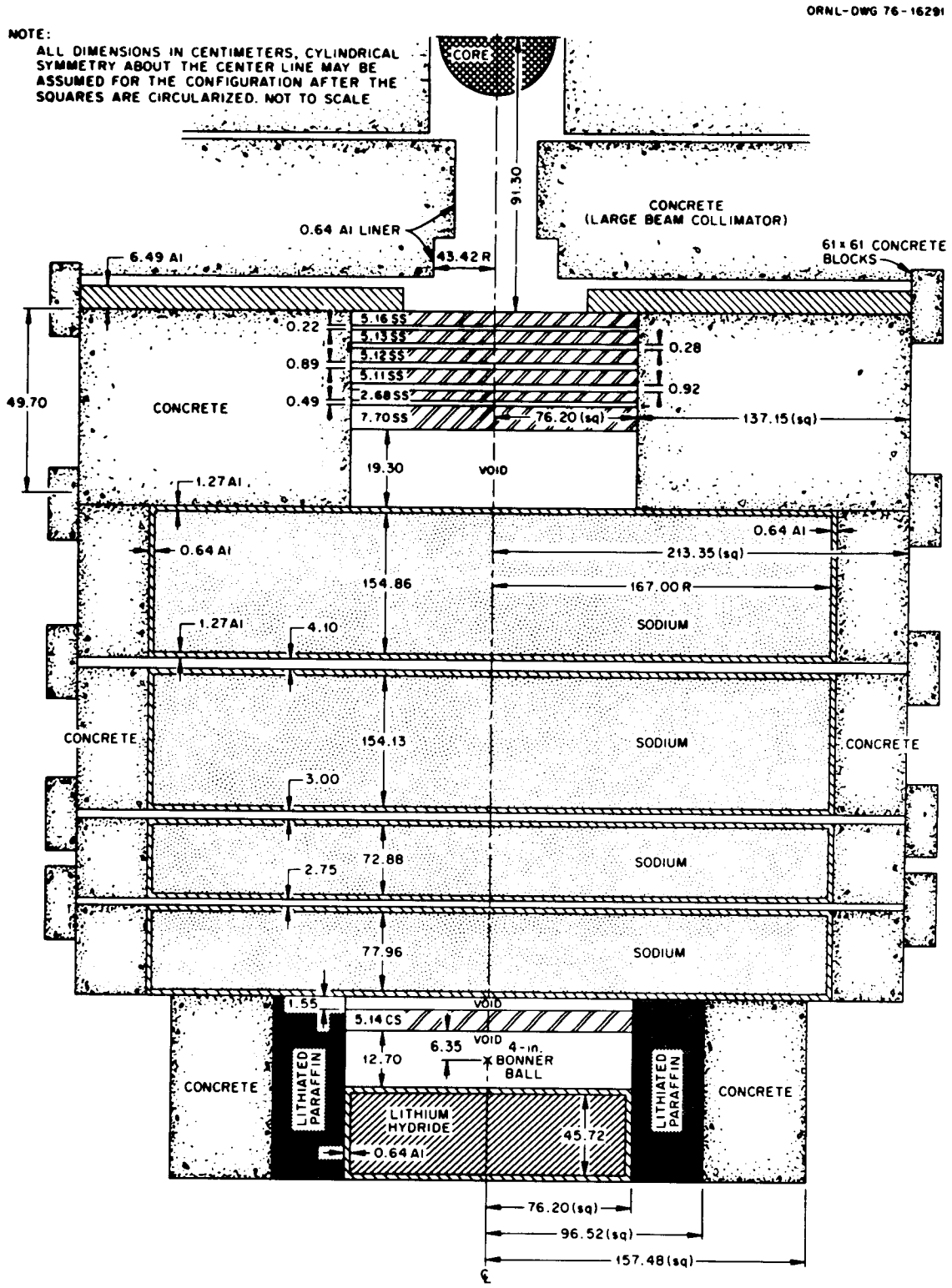

Fig. 21. Top view of the geometry of the measurements behind 30.90 cm. SS + 459.83 cm. Na + 5.14 cm. CS.

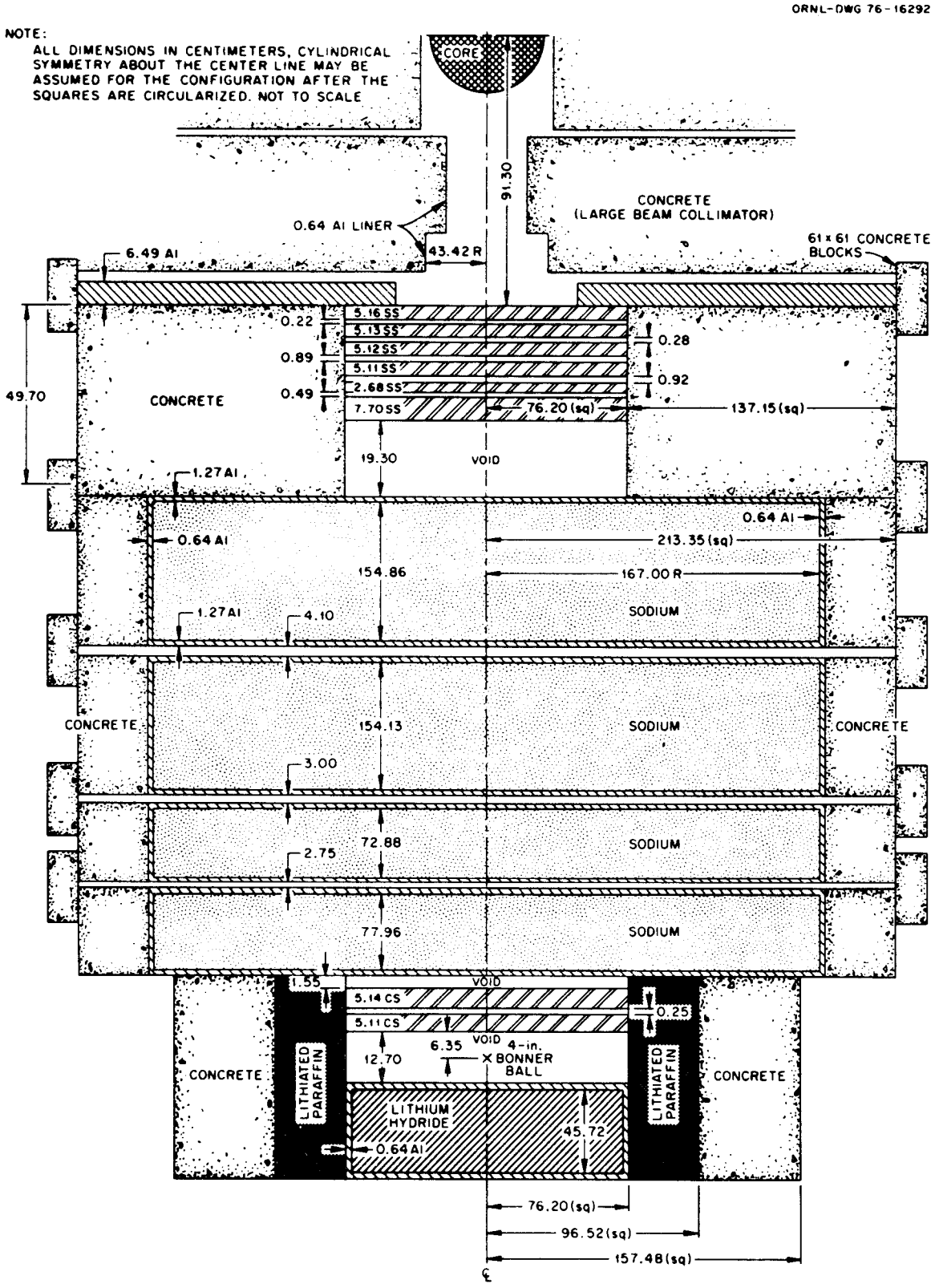

Fig. 22. Top view of the geometry of the measurements behind 30.90 cm. SS + 459.83 cm. Na + 10.25 cm. CS.

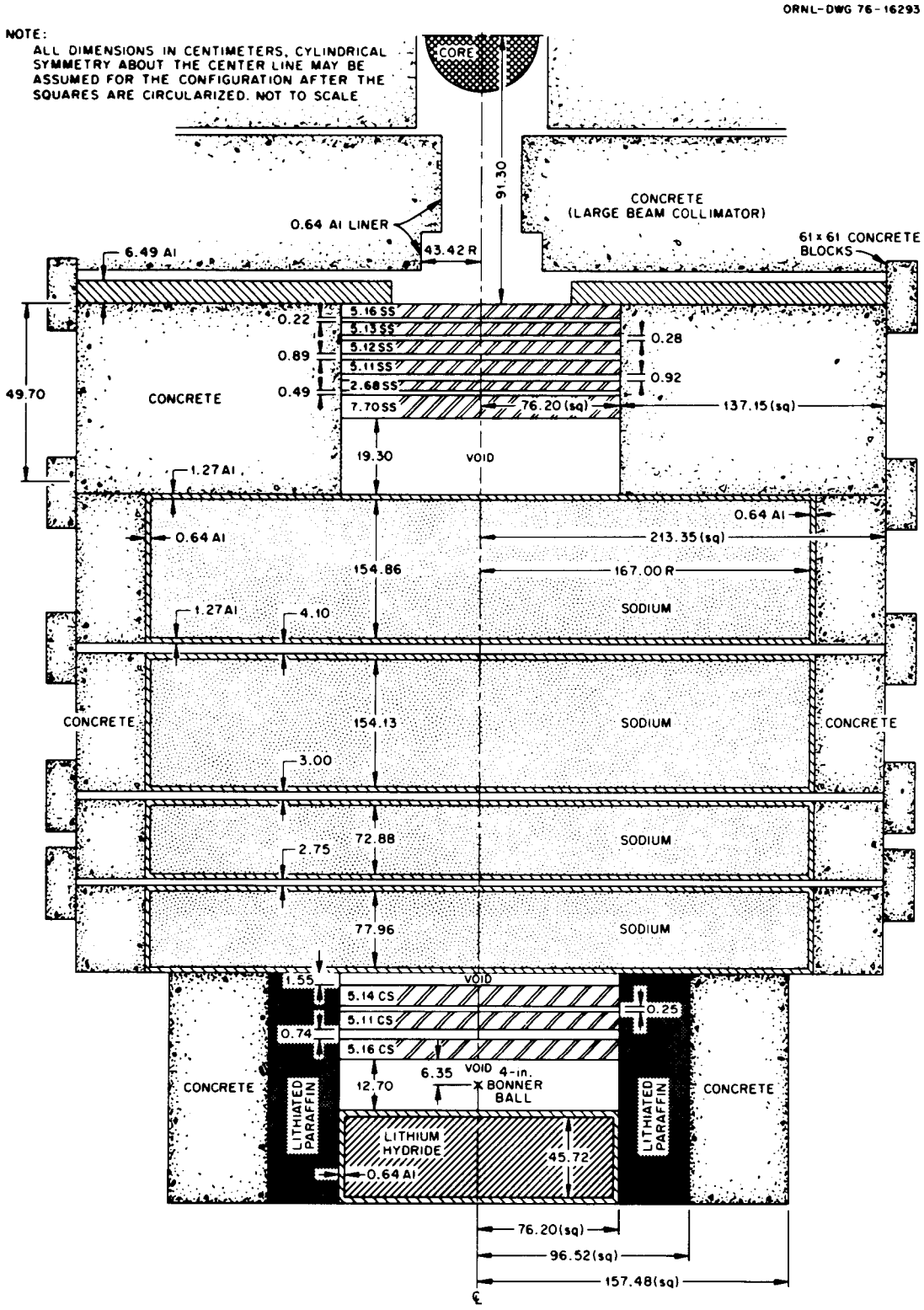

Fig. 23. Top view of the geometry of the measurements behind 30.90 cm. SS + 459.83 cm. Na + 15.41 cm. CS.

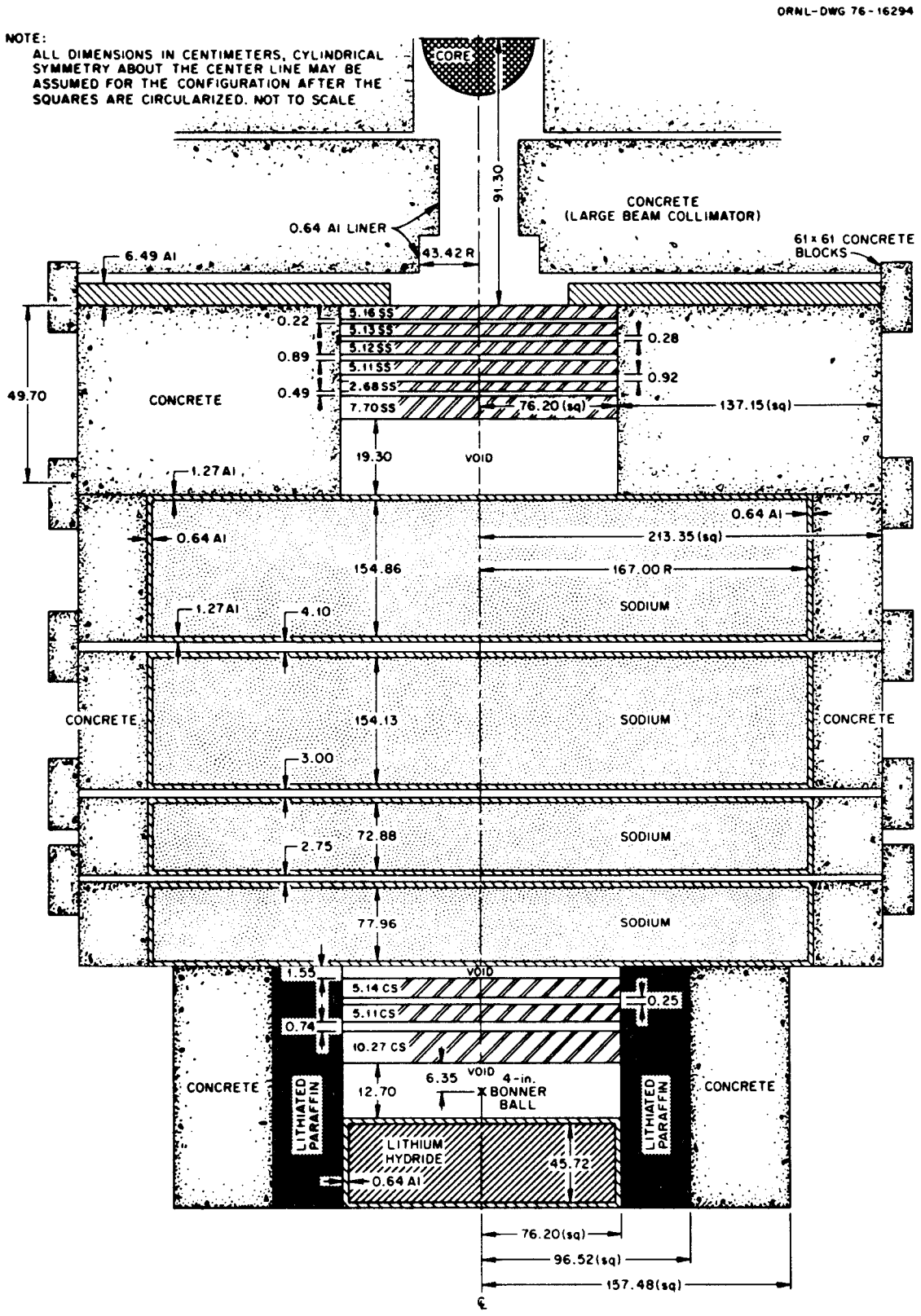

Fig. 24. Top view of the geometry of the measurements behind 30.90 cm. SS + 459.83 cm. Na + 20.52 cm. CS.

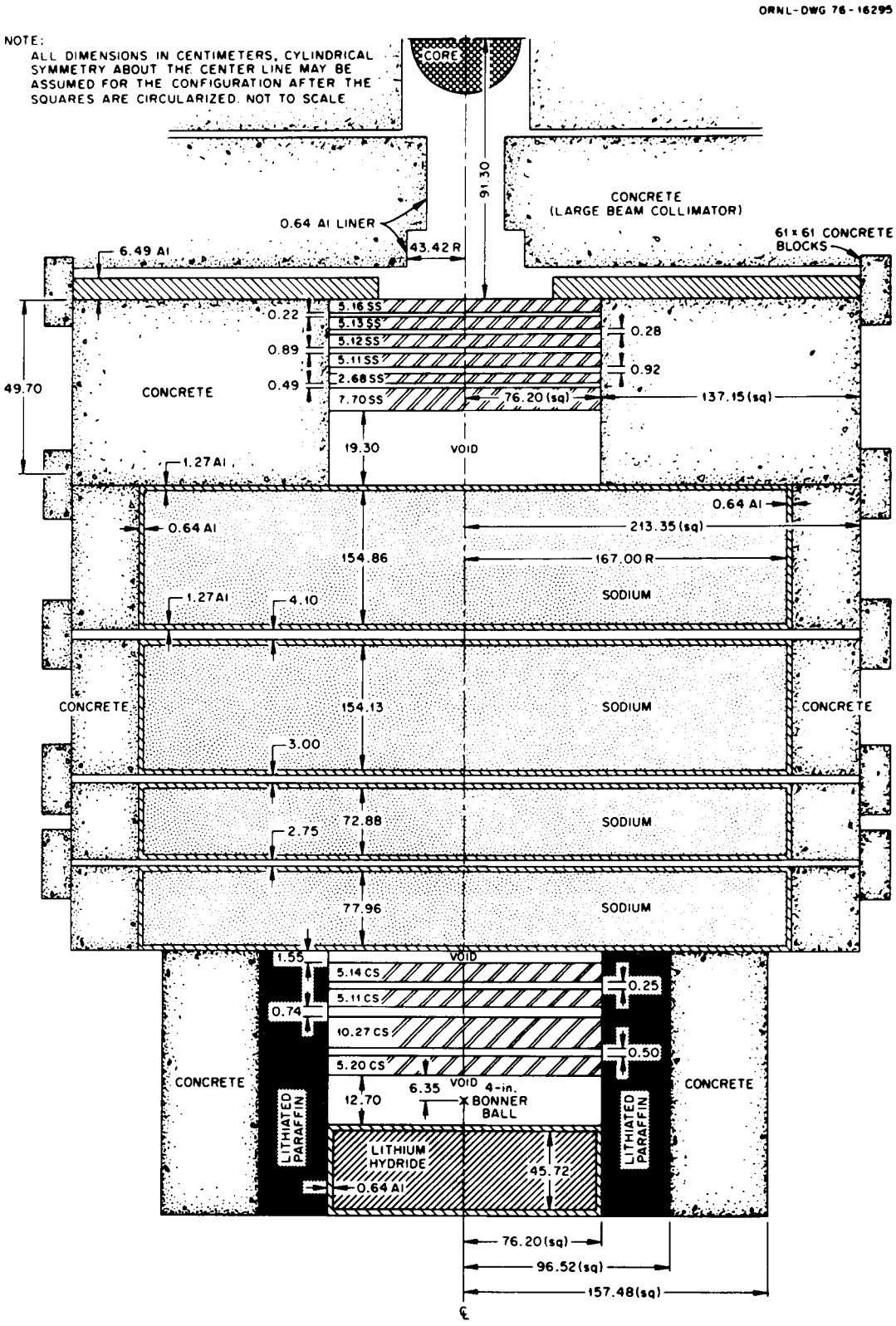

Fig. 25. Top view of the geometry of the measurements behind 30.90 cm. SS + 459.83 cm. Na + 25.72 cm. CS.

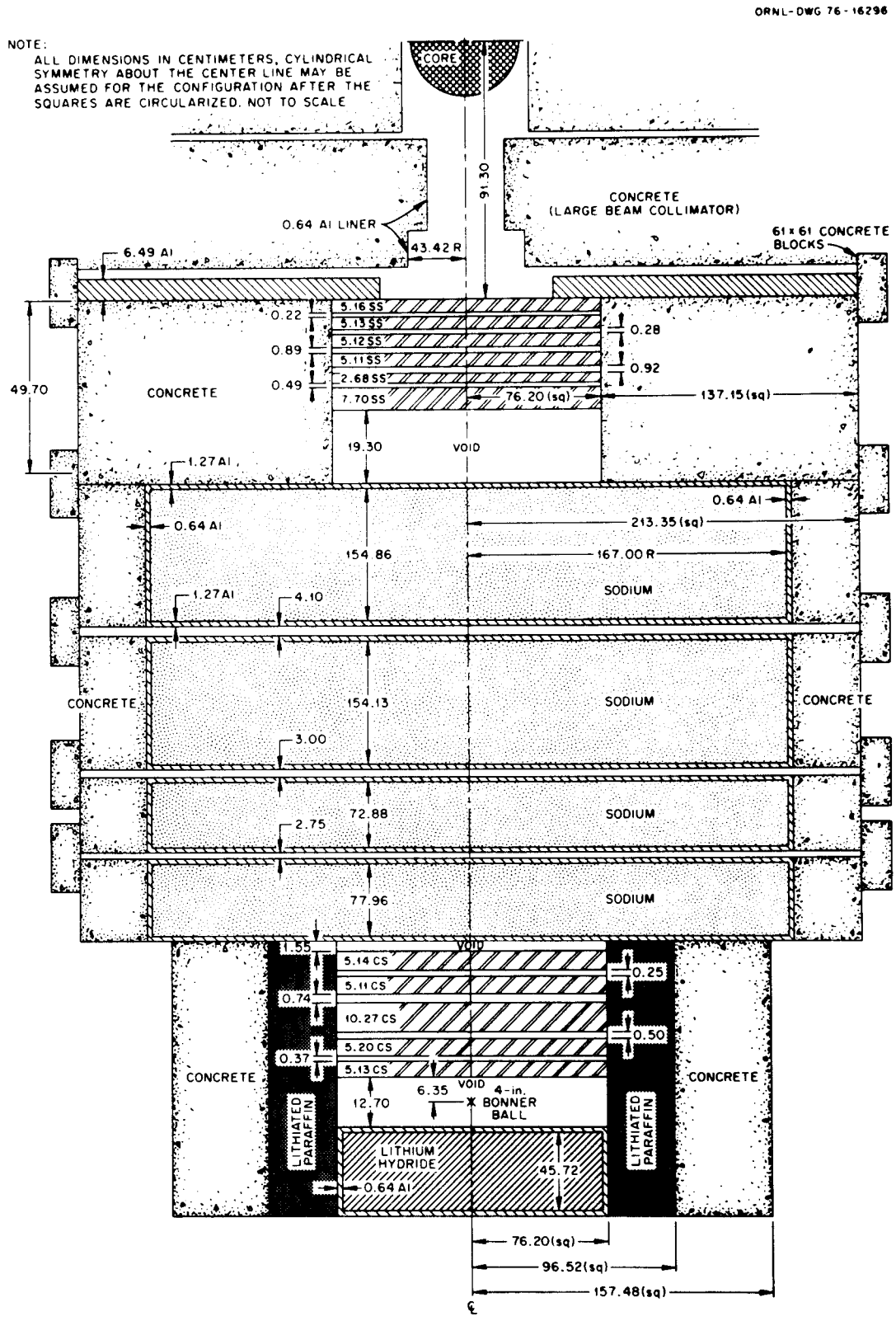

Fig. 26. Top view of the geometry of the measurements behind 30.90 cm. SS + 459.83 cm. Na + 30.85 cm. CS.

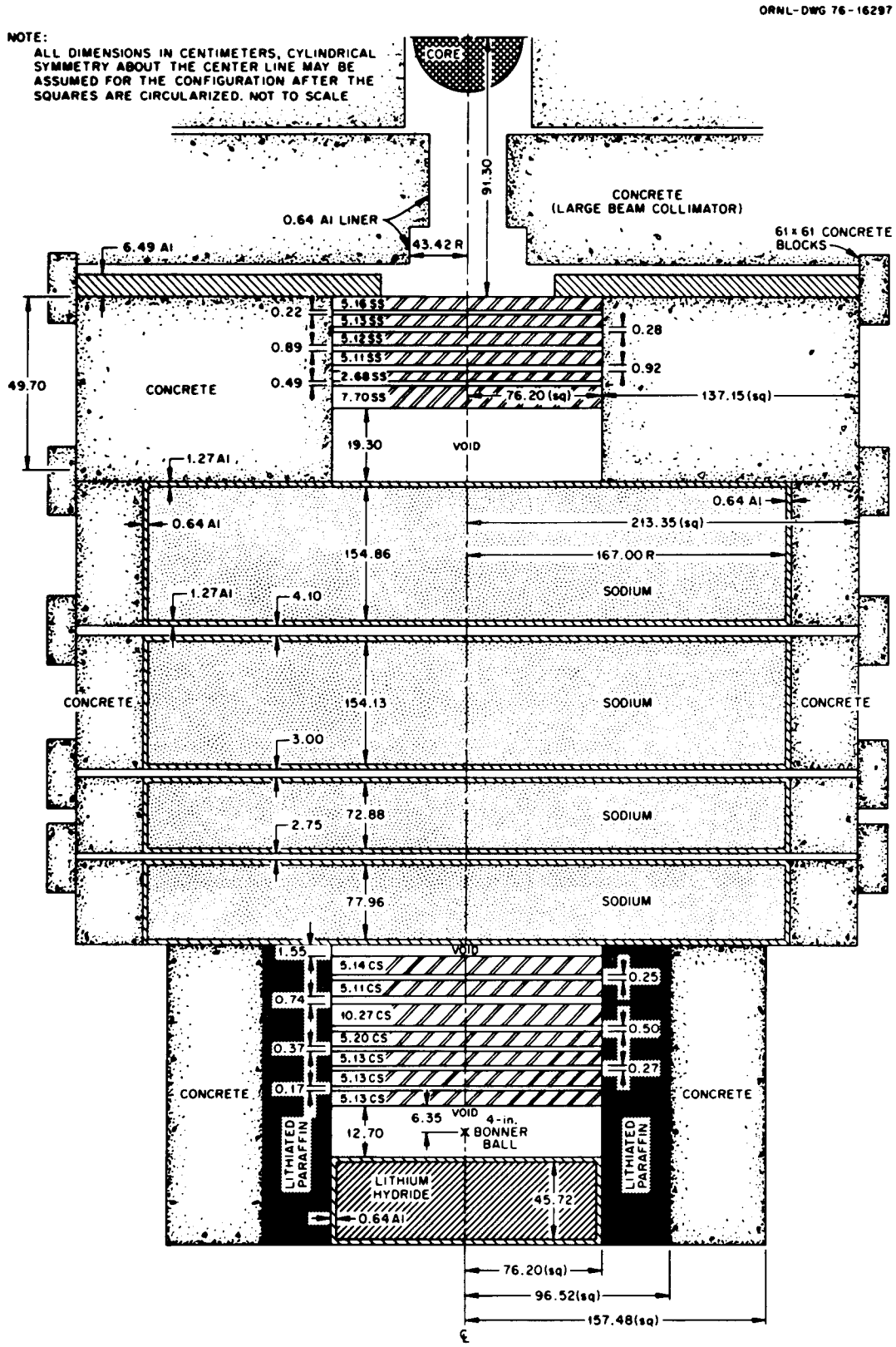

Fig. 27. Top view of the geometry of the measurements behind 30.90 cm. SS + 459.83 cm. Na + 41.11 cm. CS.

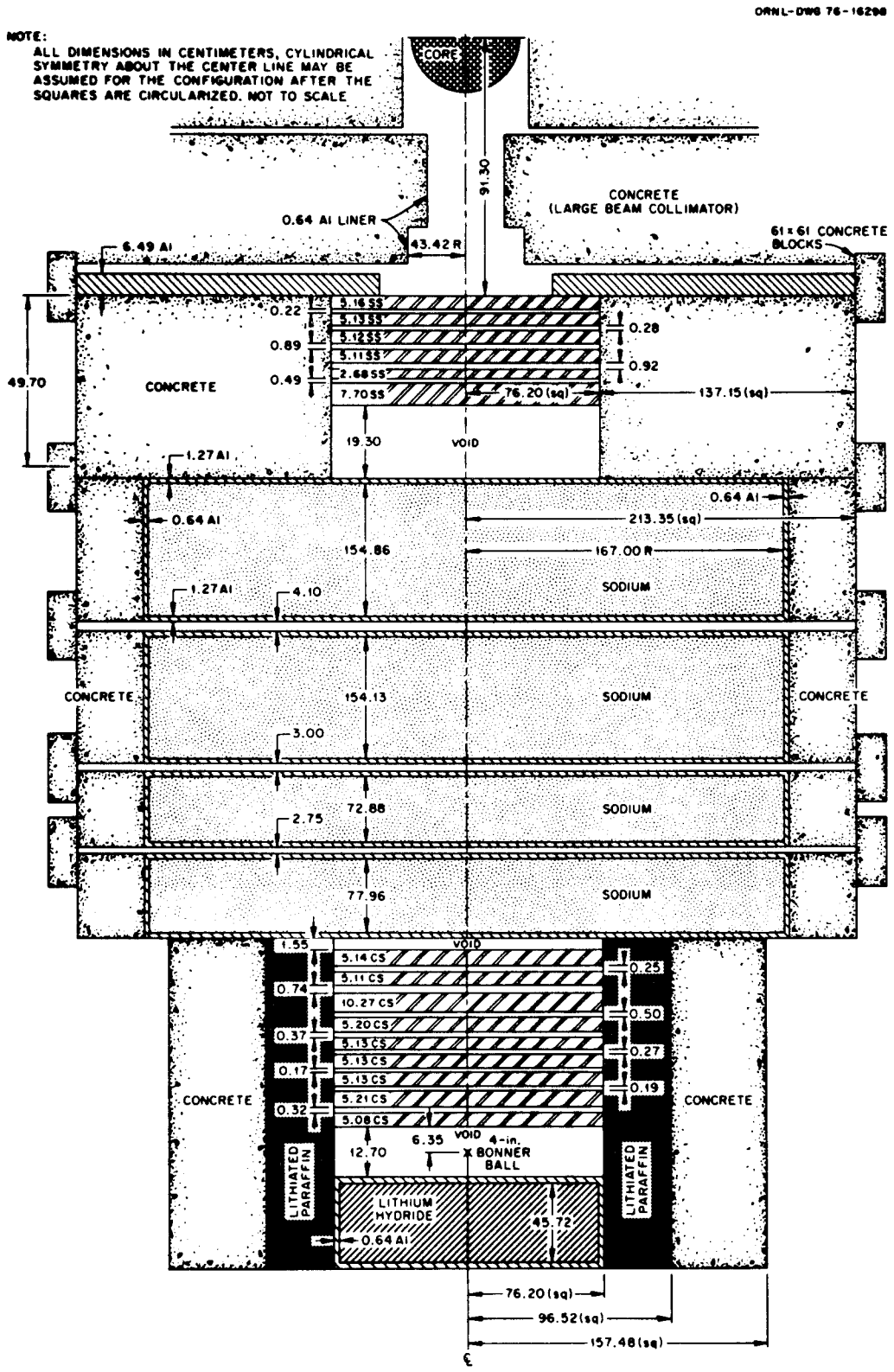

Fig. 28. Top view of the geometry of the measurements behind 30.90 cm. SS + 459.83 cm. Na + 51.40 cm. CS.

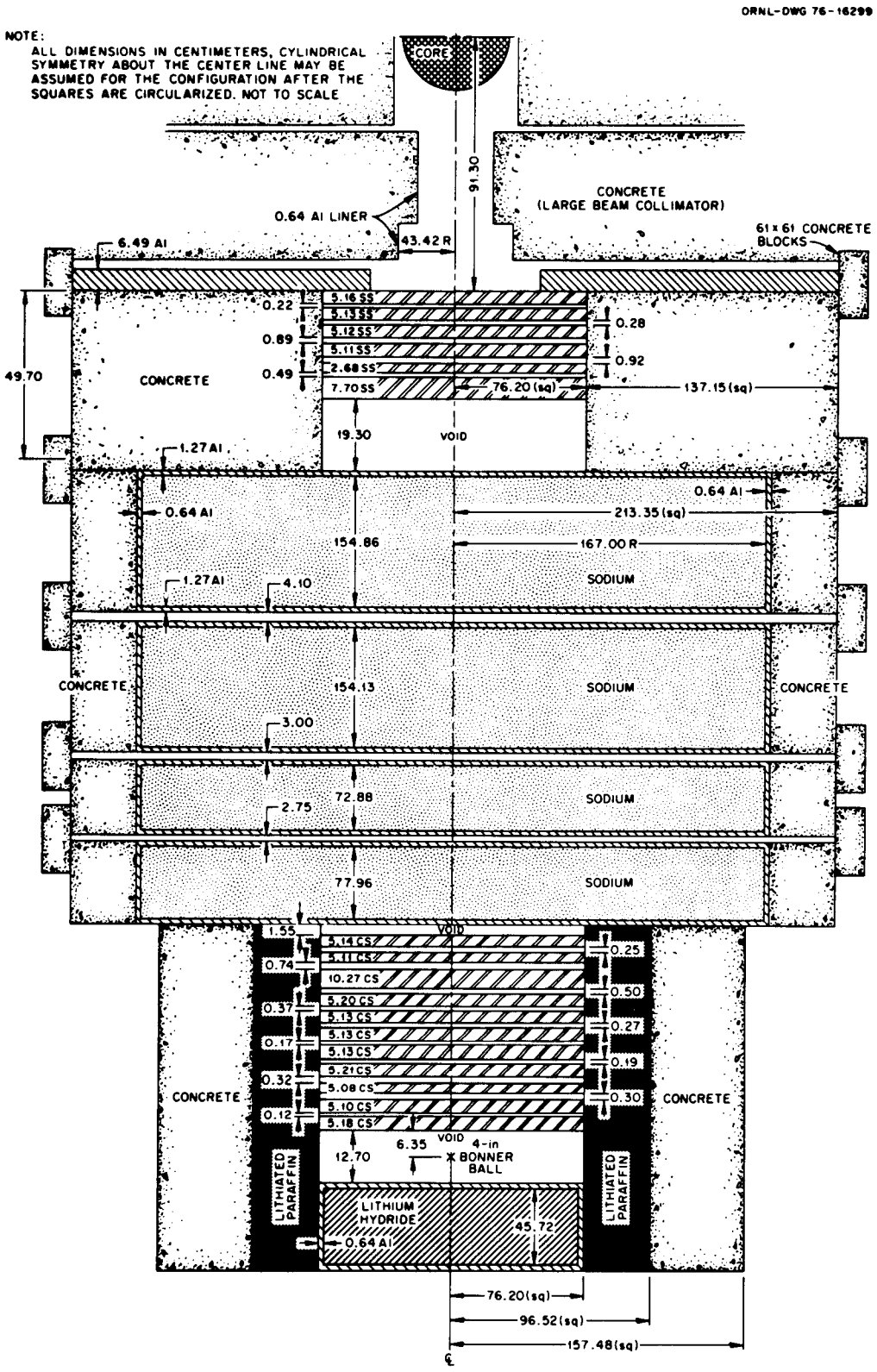

Fig. 29. Top view of the geometry of the measurements behind 30.90 cm. SS + 459.83 cm. Na + 61.68 cm. CS.

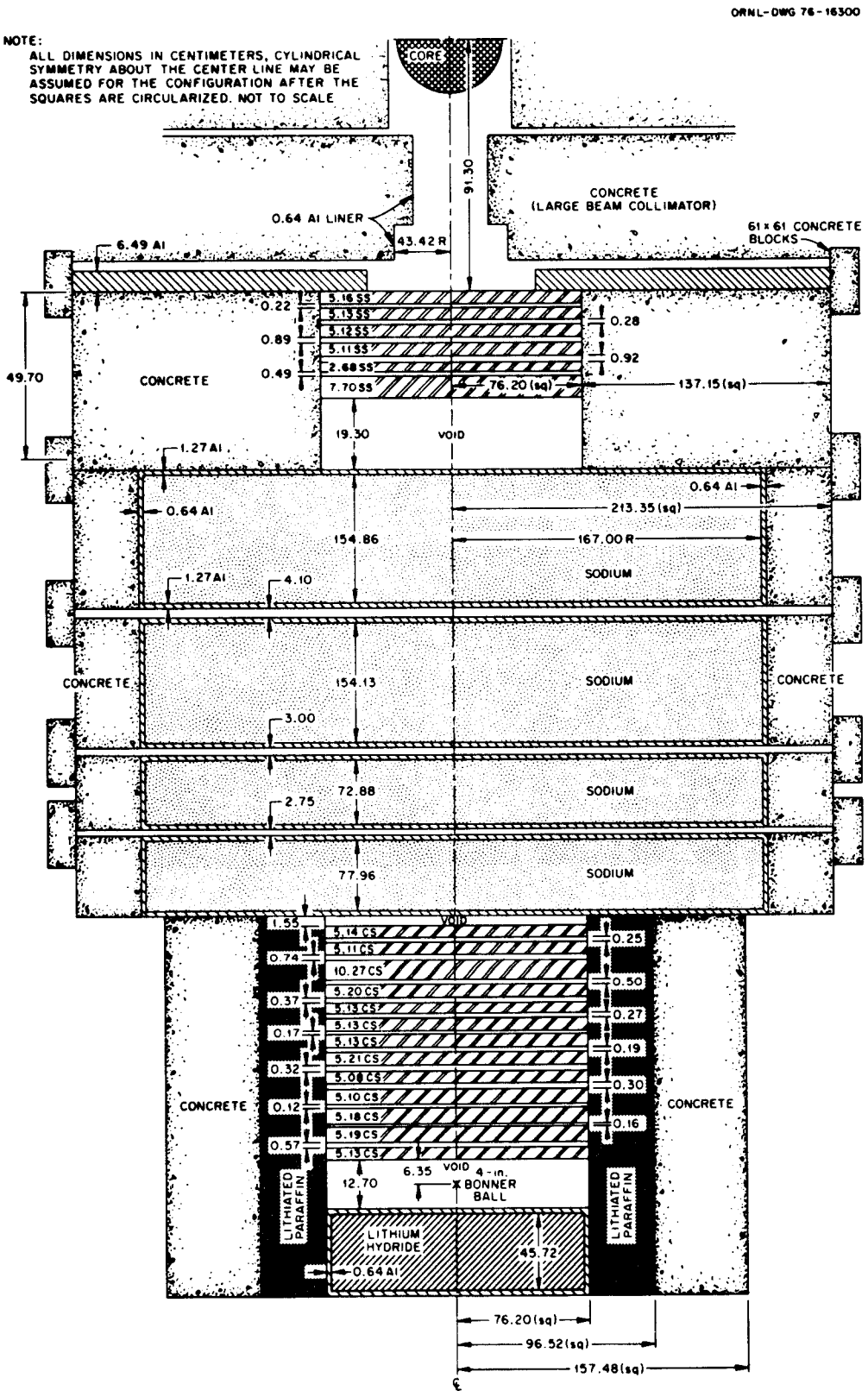

Fig. 30. Top view of the geometry of the measurements behind 30.90 cm. SS + 459.83 cm. Na + 72.00 cm. CS.

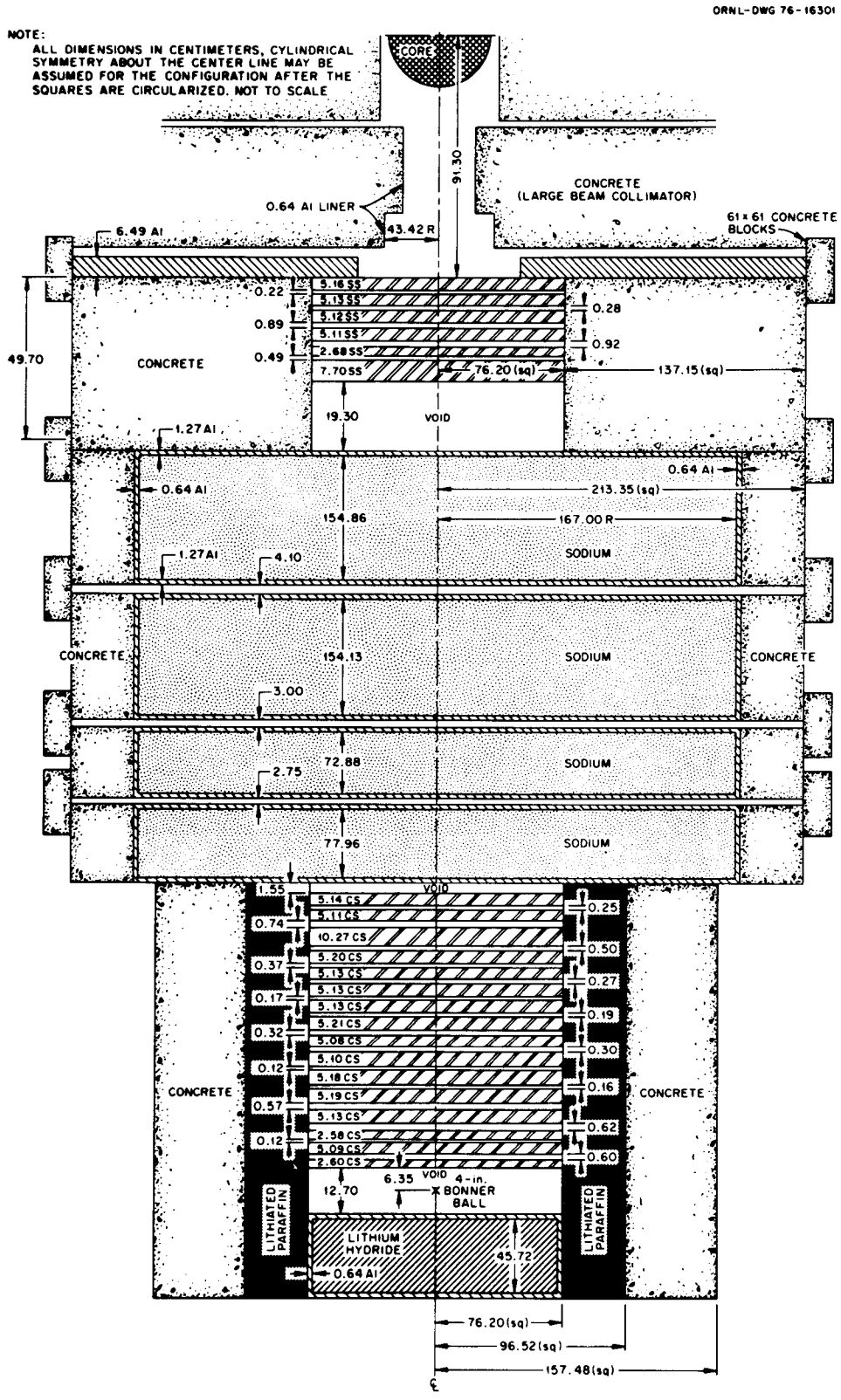

Fig. 31. Top view of the geometry of the measurements behind 30.90 cm. SS + 459.83 cm. Na + 82.27 cm. CS.

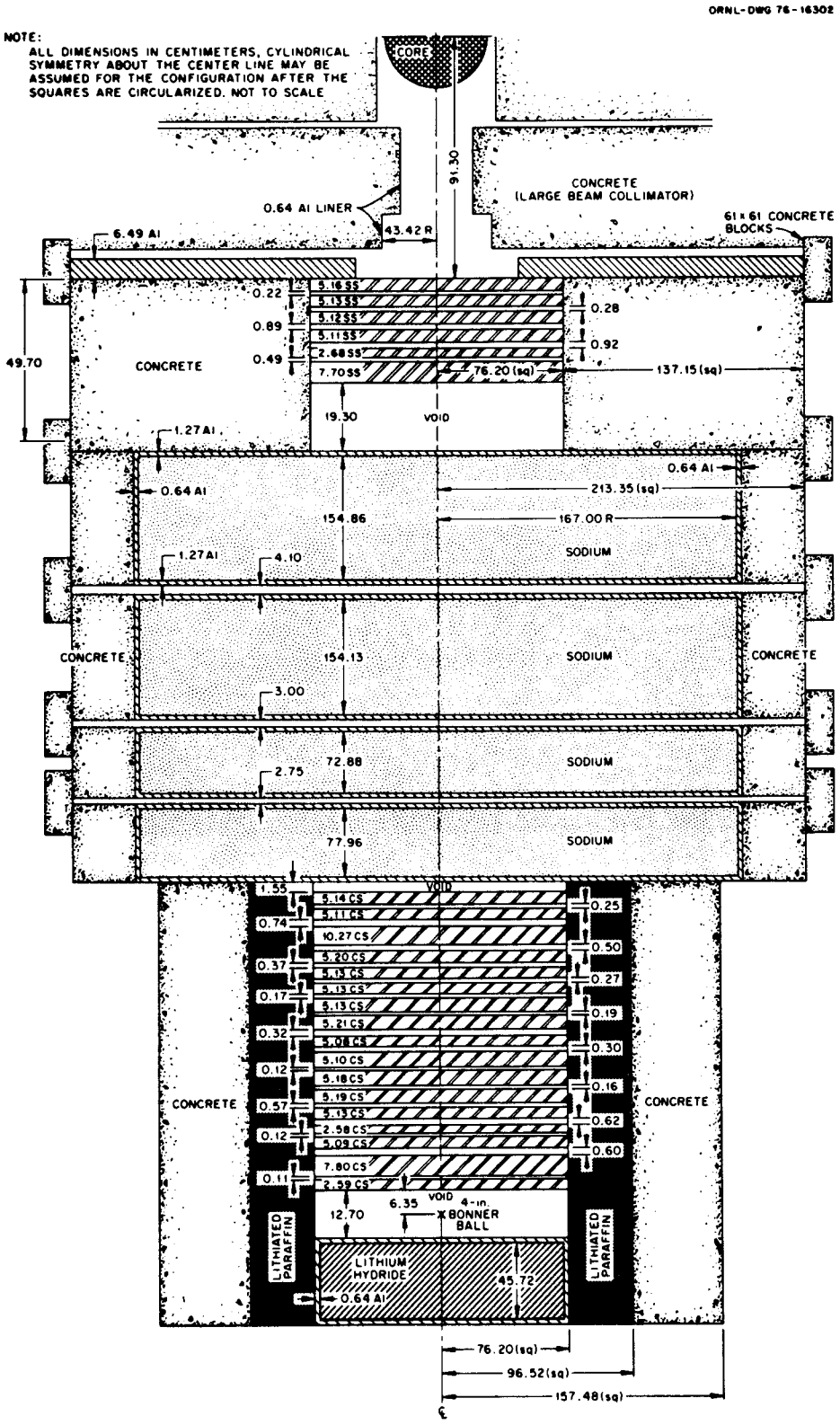

Fig. 32. Top view of the geometry of the measurements behind 30.90 cm. SS + 459.83 cm. Na + 90.06 cm. CS.

ORNL-DWG 76-16303

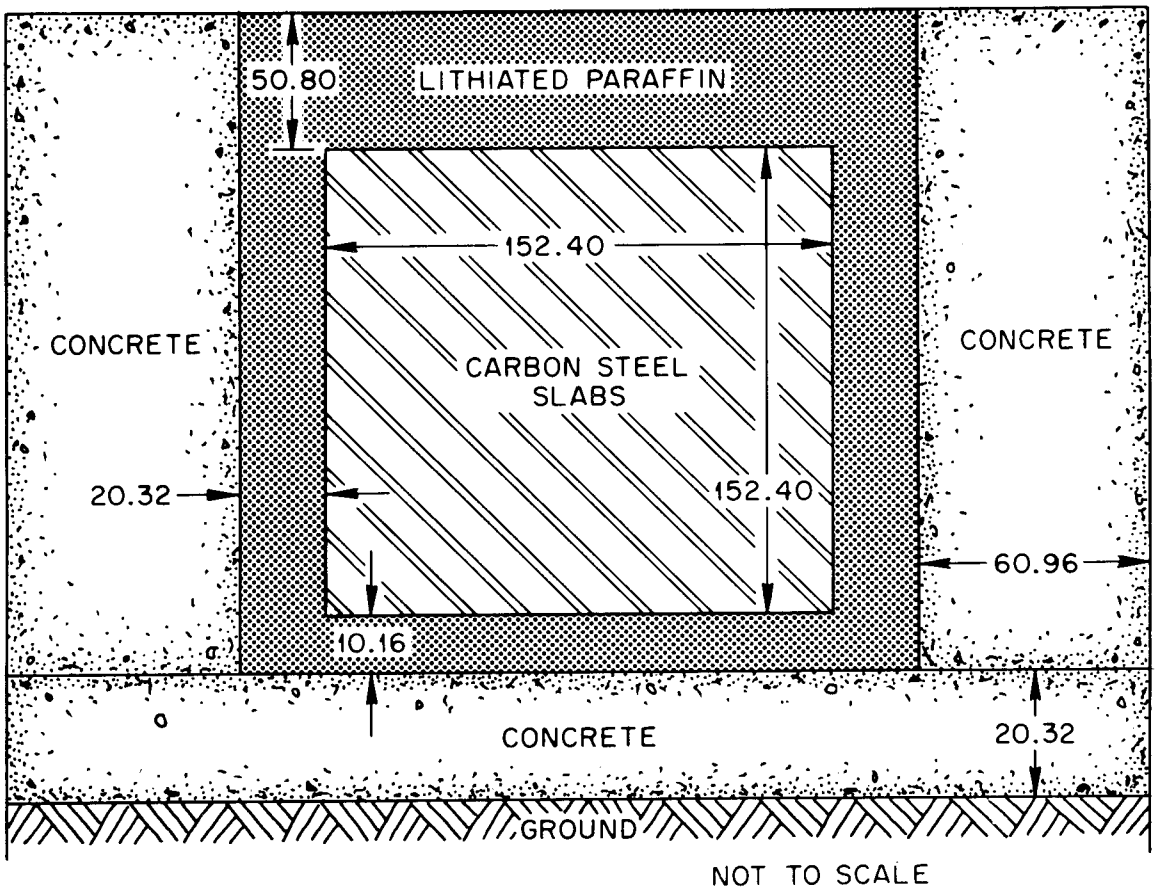

DIMENSIONS IN CENTIMETERS

Fig. 33. Front view of the peripheral shielding geometry for the carbon steel slabs.

steel slabs is unchanged for Figs. 10-19, and for Figs. 20-32. Notice that all the measurements made behind the stainless steel slab were performed without any lithium hydride placed behind the detector, whereas all other measurements were made in an air gap followed by lithium hydride immediately behind the configuration to ensure that there was minimum contribution to the measurement from air and ground scattering. Peripheral shielding in the form of lithiated paraffin and concrete bricks was used to further reduce effects of air scattering into the detector. Great care was taken to ensure that there were no streaming paths around the configurations. The thickness of each sodium tank given is an average sodium thickness between the end faces of each tank (the tanks were about 7.5 cm. thicker near the center than near the edges because of sodium creep), and since geometric effects may be important, the average void associated with each tank is taken as the difference between the measured centerline thickness and the average thickness. Thus, each tank is represented as a perfect cylinder both preceded and followed by one-half of the average void. The measured centerline gap between adjacent tanks is also included as an additional part of the void. For the slabs this centerline measurement is assumed to be the average void since the warp of each slab was not measured but is certainly far less than that of the sodium tanks. These geometric approximations to the configurations are probably more than adequate as long as the measured flux profile transverse to the beam is slowly varying, and previous measurements behind the sodium tanks have indicated that it is[1].

Three approximations must be made before the geometry is truly two-dimensional (i.e., cylindrical). First, the peripheral shielding around the carbon steel slabs is actually asymmetrical, as shown in Fig. 33. An adequate symmetric approximation to this shielding as indicated in Figs. 6-32 is 20.32 cm. of lithiated paraffin followed by 60.96 cm. of concrete. Second, the dimensions of the square slabs used in the experiment, as well as those of the peripheral shielding surrounding the entire configuration,

---

[1]See R. E. Maerker, "SDT12. The ORNL Benchmark Experiment for Neutron Transport Through Sodium," ORNL-TM-4223 (ENDF 189) (1974). Tables 23 and 24, pp. 31-32.

must be circularized in some fashion. The easiest way to accomplish this is to preserve the cross sectional area of the slabs, i.e., make the equivalent radius equal to $\frac{2}{\sqrt{\pi}}$ x 76.20 = 85.98 cm.. Thus, for most of the peripheral shielding, the equivalent radial thickness of the various materials would be equal to $\frac{2}{\sqrt{\pi}}$ x t, or 22.93 cm. (instead of 20.32 cm.) for the lithiated paraffin, 68.79 cm. (instead of 60.96 cm.) for the concrete surrounding the lithiated paraffin, and 154.76 cm. (instead of 137.15 cm.) for the concrete surrounding the stainless steel slabs. For the square concrete collar surrounding the circular sodium tanks, the equivalent outside radius is equal to $\frac{2}{\sqrt{\pi}}$ x 213.35 = 240.74 cm., leaving an equivalent radial thickness of 73.11 cm.. Third, the spherical surface of the pressure vessel must either be represented as a series of stepped cylindrical surfaces with axes coincident with the centerline of the shield geometry or, much simpler, as one cylindrical surface located about 15 cm. away from the source plane. Thus, in order to take into account the effect of multiple reflection between the stainless steel slabs at the mouth of the collimator, the concrete collimator, the pressure vessel and the surrounding stainless steel and water mixture, the simple geometry of Fig. 34 is recommended as being an adequate approximation.

C. MATERIALS

The nuclear densities of the materials used in this experiment were determined by either chemical or spectroscopic analysis together with direct measurement of the material densities, except for sodium. For the latter, concentrations of impurities were approximately those of commercial grade sodium, and the value of ρ_{Na} = 0.945 gm/cm^3 $\pm$ 1% was inferred from gamma-ray attenuation measurements through each of the sodium-filled tanks. Table 1 summarizes the results.

D. SOURCE

The angular and energy distribution of the steady state neutron flux leaking the pressure vessel was calculated with ANISN, using 51 groups, in spherical geometry. These differential leakage fluxes were then transformed to an equivalent disc source and used in a DOT calculation in the cylindrical

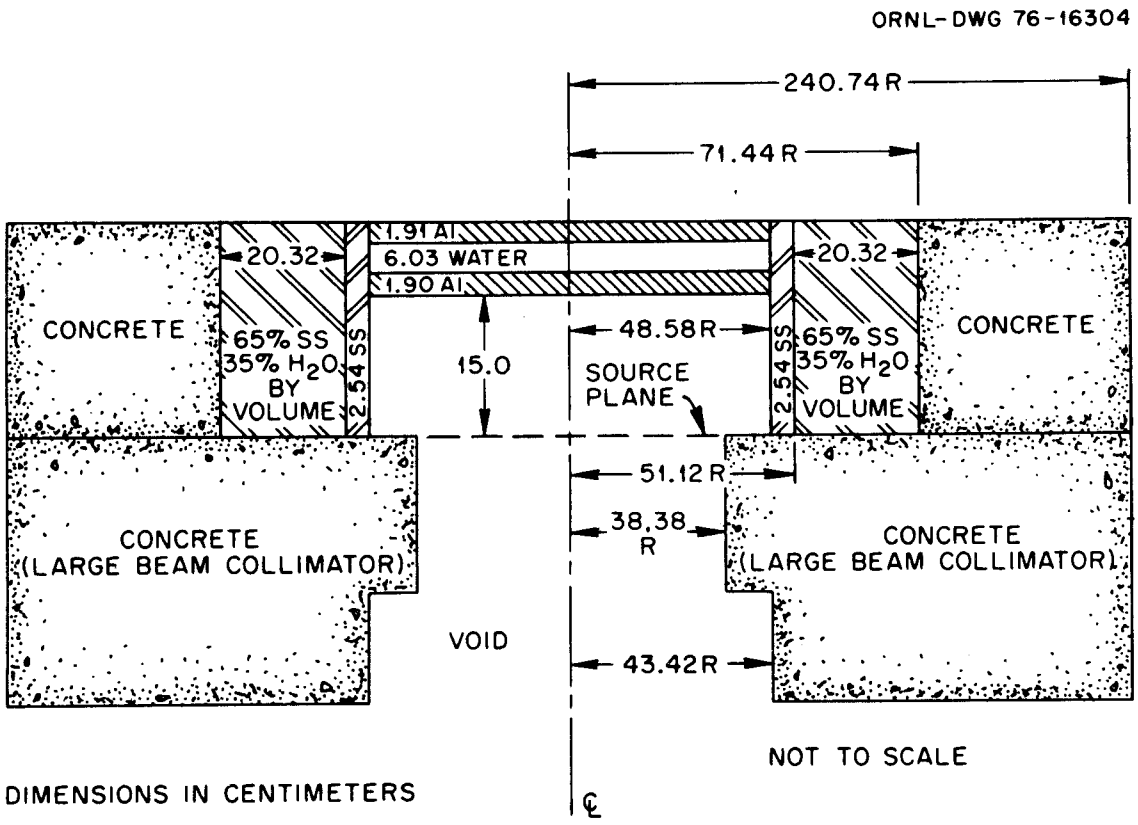

Fig. 34. Top view of an adequate cylindrical approximation to the collimator geometry.

TABLE 1. Nuclear Densities of the Materials Used in this Experiment in Atoms/Barn cm.

Material	Fe	Cr	Ni	Mn	C	H	O	Al	Na	Si	Ca	K	Li**
Stainless-304,SS	5.94(-2)*	1.69(-2)	7.9(-3)	1.2(-3)									
Aluminum	6.0(-4)							6.05(-2)					
Sodium						2.54(-5)†	3.6(-6)		2.476(-2)		5.7(-6)	2.2(-6)	
Carbon Steel,CS	8.37(-2)			5.15(-4)	9.82(-4)								
Concrete					1.07(-2)	7.3(-3)	4.47(-2)			3.8(-3)	1.22(-2)		
Lithiated Paraffin					3.34(-2)	5.93(-2)	1.125(-2)						7.50(-3)
Lithium Hydride						5.61(-2)							5.61(-2)
SS-304 + H_2O Mixture	3.86(-2)	1.10(-2)	5.14(-3)	7.8(-4)		2.34(-2)	1.17(-2)						

*Read as 5.94×10^{-2}.

**Natural lithium. For Li^6, multiply by 0.0756; for Li^7, multiply by 0.9244.

† Taken to be 75% of the upper limit of 60 ppm for commercial grade sodium.

geometry of Fig. 34 to calculate the effect of scattering from the shielding surrounding the pressure vessel and from the walls of the collimator at various locations beyond the collimator. Comparisons of the calculated scattered and direct fluxes were made with free-field measurements (i.e., in the open beam) and adjustments (typically of the order of 40%) made in the energy distribution of the ANISN fluxes to effect agreement on an absolute basis with the measurements. Thus the adjusted ANISN leakage flux, when transformed to an equivalent disc source and used in the geometry of Fig. 34, reproduces most of the free field measurements to within $\pm$ 10% on an absolute basis. The angular and energy distribution of the adjusted ANISN leakage flux is presented in Table 2 where θ_n is the angle between a normal to the sphere and the direction of the angular flux.

The transformation of the entries in Table 2 to angular distributions with respect to a plane located a centerline distance Z cm. from the core center, the equivalent disc source, is:

$$\phi_{g_p}(Z,R,\eta,\mu) = \phi_{g_h}(R_s,\cos\theta_n)\cos\theta_n/|\eta|\,,\quad 0\leq\cos\theta_n\leq 1,$$

where ϕ_{g_p} = group angular flux on the plane,

ϕ_{g_h} = group angular flux on the hemisphere of radius R_s = 48.58 cm. (i.e., entries in Table 2),

R = radius in cm. on the disc plane,

η,μ = cylindrical coordinate directions.

The relationship between the variables η, μ, and $\cos\theta_n$ is

$$\cos\theta_n = \frac{R^2+Z^2-R_s^2-A^2}{2R_sA}\,,$$

where $A \equiv |\eta|Z+\mu R-\sqrt{R_s^2+(|\eta|Z+\mu R)^2-(R^2+Z^2)}$.

It is recommended that the values Z = 53.66 and $0\leq R\leq 49.85$ (see Fig. 1) be used[2].

---

[2]For a description of the transformation code using slightly different values for both Z and the first nine rows in Table 2, see R. E. Maerker and F. J. Muckenthaler, "The Absolute Neutron Spectrum Emerging Through the Large Beam Collimator from the TSR-II Reactor at the Tower Shielding Facility," ORNL-TM-5183 (1976).

TABLE 2. Adjusted Angular Fluxes Leaking the Spherical Pressure Vessel

Group	E_u	Flux (neutrons·cm^{-2}·min^{-1}·watt^{-1}·unit weight^{-1})* for cosθ_n of							
		.0950124	.281603	.458017	.617876	.755404	.865631	.944574	.989401
1	14.92 MeV	2.91(2)**	9.65(2)	2.22(3)	6.99(3)	2.13(4)	3.62(4)	3.76(4)	3.70(4)
2	12.21	1.55(3)	4.73(3)	1.04(4)	3.09(4)	9.39(4)	1.62(5)	1.71(5)	1.71(5)
3	10.00	4.95(3)	1.49(4)	3.05(4)	8.66(4)	2.62(5)	4.51(5)	4.73(5)	4.75(5)
4	8.187	1.91(4)	5.27(4)	9.75(4)	2.43(5)	6.76(5)	1.16(6)	1.25(6)	1.28(6)
5	6.703	6.39(4)	1.60(5)	2.58(5)	5.44(5)	1.37(6)	2.30(6)	2.58(6)	2.68(6)
6	5.488	1.64(5)	3.78(5)	5.43(5)	9.92(5)	2.23(6)	3.62(6)	4.17(6)	4.40(6)
7	4.493	2.88(5)	6.28(5)	8.29(5)	1.34(6)	2.60(6)	4.15(6)	5.00(6)	5.44(6)
8	3.679	4.19(5)	8.92(5)	1.14(6)	1.70(6)	2.98(6)	4.55(6)	5.57(6)	6.10(6)
9	3.012	6.80(5)	1.39(6)	1.67(6)	2.38(6)	4.15(6)	6.25(6)	7.60(6)	8.27(6)
10	2.466	7.64(5)	1.56(6)	1.78(6)	2.35(6)	3.89(6)	5.69(6)	6.89(6)	7.53(6)
11	2.019	8.63(5)	1.68(6)	1.81(6)	2.26(6)	3.43(6)	4.81(6)	5.89(6)	6.47(6)
12	1.653	8.23(5)	1.59(6)	1.74(6)	2.13(6)	3.06(6)	4.17(6)	5.08(6)	5.59(6)
13	1.353	7.62(5)	1.43(6)	1.61(6)	1.96(6)	2.61(6)	3.38(6)	4.07(6)	4.46(6)
14	1.1080	7.96(5)	1.53(6)	1.61(6)	1.81(6)	2.28(6)	2.78(6)	3.28(6)	3.56(6)
15	0.9072	6.49(5)	1.16(6)	1.34(6)	1.63(6)	2.03(6)	2.52(6)	2.94(6)	3.21(6)
16	0.7427	7.32(5)	1.37(6)	1.50(6)	1.74(6)	2.15(6)	2.60(6)	3.02(6)	3.28(6)
17	0.6081	6.64(5)	1.19(6)	1.33(6)	1.53(6)	1.86(6)	2.21(6)	2.51(6)	2.70(6)
18	0.4978	4.68(5)	8.14(5)	9.04(5)	1.05(6)	1.19(6)	1.35(6)	1.48(6)	1.57(6)
19	0.4076	5.54(5)	1.06(6)	1.17(6)	1.31(6)	1.51(6)	1.71(6)	1.88(6)	1.97(6)
20	0.3337	3.67(5)	6.40(5)	7.48(5)	9.16(5)	1.07(6)	1.23(6)	1.36(6)	1.44(6)
21	0.2732	3.91(5)	7.73(5)	8.93(5)	1.02(6)	1.18(6)	1.32(6)	1.44(6)	1.53(6)
22	0.2237	3.29(5)	5.50(5)	6.30(5)	7.53(5)	8.58(5)	9.70(5)	1.06(6)	1.11(6)
23	0.1832	1.62(5)	2.49(5)	3.00(5)	3.88(5)	4.66(5)	5.47(5)	6.06(5)	6.44(5)
24	0.1500	5.25(5)	9.31(5)	1.02(6)	1.07(6)	1.14(6)	1.22(6)	1.27(6)	1.31(6)
25	0.12277	1.93(5)	3.15(5)	3.98(5)	5.39(5)	6.59(5)	7.70(5)	8.50(5)	8.97(5)
26	86.52 keV	6.76(5)	1.41(6)	1.61(6)	1.68(6)	1.85(6)	1.96(6)	2.07(6)	2.13(6)

TABLE 2. (Continued)

Group	E_u	Flux (neutrons·cm^{-2}·min^{-1}·watt^{-1}·unit weight^{-1})* for $\cos\theta_n$ of							
		.0950124	.281603	.458017	.617876	.755404	.865631	.944574	.989401
27	52.48	1.53(5)	2.90(5)	3.78(5)	4.84(5)	5.53(5)	6.19(5)	6.61(5)	6.93(5)
28	40.86	7.81(4)	1.08(5)	1.27(5)	1.57(5)	1.85(5)	2.16(5)	2.38(5)	2.52(5)
29	31.83	3.36(5)	9.63(5)	1.07(6)	8.61(5)	9.93(5)	9.79(5)	1.03(6)	1.04(6)
30	24.79	6.99(4)	2.25(5)	4.51(5)	5.52(5)	5.78(5)	6.48(5)	6.66(5)	6.94(5)
31	19.30	7.29(4)	2.04(5)	3.86(5)	4.90(5)	5.21(5)	5.87(5)	6.09(5)	6.31(5)
32	15.03	3.08(5)	7.70(5)	1.26(6)	1.60(6)	1.75(6)	1.95(6)	2.04(6)	2.11(6)
33	7.102	2.23(5)	5.17(5)	7.69(5)	9.80(5)	1.09(6)	1.21(6)	1.28(6)	1.33(6)
34	4.307	1.02(5)	2.46(5)	3.77(5)	4.79(5)	5.33(5)	5.96(5)	6.29(5)	6.55(5)
35	3.355	9.94(4)	2.38(5)	3.64(5)	4.63(5)	5.19(5)	5.80(5)	6.13(5)	6.40(5)
36	2.613	1.00(5)	2.37(5)	3.61(5)	4.59(5)	5.17(5)	5.78(5)	6.10(5)	6.38(5)
37	2.035	1.01(5)	2.37(5)	3.60(5)	4.56(5)	5.15(5)	5.77(5)	6.09(5)	6.36(5)
38	1.585	9.93(4)	2.34(5)	3.51(5)	4.49(5)	5.07(5)	5.66(5)	6.02(5)	6.29(5)
39	1.2341	9.79(4)	2.30(5)	3.46(5)	4.42(5)	5.00(5)	5.63(5)	5.95(5)	6.22(5)
40	961.1 eV	2.91(5)	6.83(5)	1.03(6)	1.32(6)	1.50(6)	1.67(6)	1.78(6)	1.85(6)
41	454.0	2.91(5)	6.82(5)	1.02(6)	1.30(6)	1.48(6)	1.67(6)	1.78(6)	1.85(6)
42	214.5	2.88(5)	6.75(5)	1.01(6)	1.29(6)	1.47(6)	1.65(6)	1.78(6)	1.83(6)
43	101.3	2.88(5)	6.78(5)	1.01(6)	1.29(6)	1.48(6)	1.67(6)	1.78(6)	1.85(6)
44	47.85	2.91(5)	6.82(5)	1.01(6)	1.30(6)	1.50(6)	1.68(6)	1.81(6)	1.86(6)
45	22.60	2.91(5)	6.83(5)	1.01(6)	1.30(6)	1.50(6)	1.68(6)	1.81(6)	1.88(6)
46	10.677	3.54(5)	8.29(5)	1.23(6)	1.58(6)	1.83(6)	2.06(6)	2.20(6)	2.30(6)
47	5.043	3.51(5)	8.18(5)	1.22(6)	1.55(6)	1.82(6)	2.06(6)	2.20(6)	2.28(6)
48	2.382	4.19(5)	9.80(5)	1.46(6)	1.89(6)	2.17(6)	2.45(6)	2.62(6)	2.73(6)
49	1.125	8.34(5)	1.96(6)	2.93(6)	3.79(6)	4.37(6)	4.93(6)	5.26(6)	5.50(6)
50	0.4140	1.40(6)	3.26(6)	4.93(6)	6.45(6)	7.42(6)	8.40(6)	9.02(6)	9.37(6)
51	0.1000	9.43(6)	2.18(7)	3.42(7)	4.60(7)	5.21(7)	5.92(7)	6.25(7)	6.54(7)

* To obtain angular currents per steradian, multiply the angular fluxes by $\frac{\cos\theta_n}{4\pi}$.

** Read as 2.91×10^2.

NOTE: To interpolate in this table, it is suggested that the angular fluxes be assumed to vary as $\cos\theta_n$ between entries, and hence the angular currents to vary as $\cos^2\theta_n$.

E. DETECTORS

Both the 2-in. by 2-in. NE-213 scintillator and 2-in. diameter hydrogen counter detectors produce pulse height distributions that are unfolded using the codes FERDOR[3] and SPEC4[4] respectively. For the NE-213, a modified Forte circuit was used to reduce the sensitivity to gamma rays, and the unfolded neutron spectrum, in the range $0.8 \leq E_n < 15$ MeV, consists of lower and upper bounds within which the true spectrum is expected to lie with a probability of 0.68. An additional uncertainty of $\pm$ 5% in determining the absolute power of the run producing the data should be added to the unfolded limits. The resolution function for the NE-213 detector is given in Table 3. For the hydrogen counter, two types were used. The first, at 10 atmospheres hydrogen pressure, was used without gamma-ray pulse discrimination to measure the neutron spectrum roughly in the range $0.50 \leq E_n \leq 1.4$ MeV. The second, a 3 atmosphere counter containing methane and a trace of nitrogen, was used without gamma-ray pulse discrimination to measure the neutron spectrum roughly in the range $0.20 \leq E_n \leq 0.60$ MeV, and with gamma-ray discrimination to measure in the approximate range 5 keV $\leq E_n \leq$ 300 keV, using two different gains. The overall range of the hydrogen counter is thus $\sim$ 5 keV - 1.4 MeV, and provides overlapping data with itself as well as with the NE-213. The resolution function for the hydrogen counter is assumed to be 10%, independent of energy, mode of operation, and composition of the counter. The unfolded spectra also have uncertainty estimates, which should be increased by 5% because of errors in the power determinations.

The 4-in. and 12-in. Bonner balls consist of 5.08 cm. diameter BF_3 detectors (96% enriched in B^{10}, filling pressure of 0.5 atmospheres) surrounded by radial thicknesses of 2.50 cm. and 12.42 cm. polyethylene (ρ = 0.951g/cm^3) respectively, and enclosed on the outside with a

---

[3]W. R. Burrus, "Utilization of a Priori Information in the Statistical Interpretation of Measured Distributions," Dissertation, The Ohio State University, ORNL-3743 (1964).

[4]P. W. Benjamin, C. D. Kenshall, and A. Brickstock, "The Analysis of Recoil Proton Spectra," AWRE-09/68 (1968).

TABLE 3. Energy Resolution of the NE-213 Spectrometer System*

E(MeV)	FWHM(%)	E(MeV)	FWHM(%)	E(MeV)	FWHM(%)
0.5	47.5	3.3	18.8	6.2	13.5
0.6	44	3.4	18.5	6.4	13.2
0.7	41	3.5	18.2	6.6	13.0
0.8	38.5	3.6	18.0	6.8	12.8
0.9	36	3.7	17.7	7.0	12.6
1.0	33.5	3.8	17.4	7.2	12.4
1.1	32.5	3.9	17.1	7.4	12.2
1.2	31	4.0	16.9	7.6	12.1
1.3	30	4.1	16.7	7.8	11.9
1.4	29	4.2	16.5	8.0	11.8
1.5	27.5	4.3	16.3	8.2	11.6
1.6	26.5	4.4	16.1	8.4	11.5
1.7	26	4.5	15.9	8.6	11.4
1.8	25	4.6	15.7	8.8	11.3
1.9	24.5	4.7	15.5	9.0	11.2
2.0	24	4.8	15.3	9.2	11.1
2.1	23.5	4.9	15.2	9.4	10.9
2.2	23	5.0	15.1	9.6	10.8
2.3	22.5	5.1	14.9	9.8	10.7
2.4	22	5.2	14.7	10.0	10.5
2.5	21.5	5.3	14.5	10.2	10.3
2.6	21.2	5.4	14.4	10.4	10.2
2.7	20.8	5.5	14.3	10.6	10.1
2.8	20.4	5.6	14.2	10.8	10.0
2.9	20.1	5.7	14.1	11.0	9.8
3.0	19.7	5.8	13.9	11.4	9.7
3.1	19.4	5.9	13.8	11.8	9.6
3.2	19.1	6.0	13.7	12.2	9.6

*Interpolation in this table should follow the formula:

$$a(E) = \frac{E_2 - E}{E_2 - E_1}\, a(E_1) + \frac{E - E_1}{E_2 - E_1}\, a(E_2)$$

where $E_1 \leq E \leq E_2$.

0.0762 cm. thick spherical shell of cadmium. The response functions for each Bonner ball were obtained by normalizing adjoint ANISN calculations to measured counting rates in a known spectrum[5,6]. The absolute response functions so obtained are, strictly speaking, good only for the same geometry that existed in the calibration procedure (i.e., far away from a point source with nothing behind the Bonner ball). For the geometry used in this experiment, there are two perturbations from this calibration geometry. The first is the presence of a backing material (i.e., lithium hydride) in all the measurements made in the 12.7 cm. voids, rendering a flux incident on both hemispheres of the Bonner ball. The second is that the angular distribution of the flux incident on either hemisphere for the measurements in the 12.7 cm. voids is obviously different from that of the calibration geometry, since the detector is placed very close to the back of the configurations. The effect of the backing material on the response function of the Bonner ball has not been calculated, but can be estimated from comparisons of measured and calculated counting rates, using the calibrated response functions, in different detector geometries[7]. From these comparisons, it appears that in the Bonner ball geometry using the 12.7 cm. voids backed by lithium hydride, there may be up to a 5% over-prediction of the counting rate if the flux at the center of the Bonner ball, calculated in the absence of the Bonner ball, is folded with the calibrated response functions, because of the neglect of the self-shielding effect on the Bonner ball. On the other hand, it can be shown[8] that the response function of the Bonner ball is independent of the incident angular distribution as long as it is constant over a hemisphere, a condition which is essentially satisfied in all these measurements. Thus, the expression:

---

[5]R. E. Maerker, F. J. Muckenthaler, J. J. Manning, J. L. Hull, J. N. Money, K. M. Henry, and R. M. Freestone, Jr., "Calibration of the Bonner Ball Neutron Detectors Used at the Tower Shielding Facility," ORNL-TM-3465 (1971).

[6]Slight revisions have been made to the original response functions appearing in R. E. Maerker, L. R. Williams, F. R. Mynatt, and N. M. Greene, "Response Functions for Bonner Ball Neutron Detectors," ORNL-TM-3451 (1971).

[7]R. E. Maerker, F. J. Muckenthaler, R. L. Childs, and M. L. Gritzner, "Final Report on a Benchmark Experiment for Neutron Transport in Thick Sodium," ORNL-4880 (1974), Table 33, pp. 69.

[8]F. R. Mynatt, private communication.

$$\text{calculated counting rate} = \int_{0.414\ \text{eV}}^{\infty} \phi_c(E)R(E)dE,$$

where $\phi_c(E)$ = calculated flux at a position corresponding to the geometric center of the Bonner ball, with the Bonner ball absent but with the lithium hydride present,

and $R(E)$ = the calibrated response function of the Bonner ball,

is probably accurate to within 5% for the 4-in. Bonner ball counting rate calculations in the voids followed by lithium hydride. This is in addition to the inaccuracy in R(E) itself, which is estimated to lie between 5 and 15%.

The calibrated response functions for the 4-in. and 12-in. Bonner balls are shown in Tables 4 and 5 respectively.

F. MEASURED RESULTS

Six separate sets of unfolded NE-213 spectra were obtained behind the stainless steel. The first three were repeats at the detector location shown in Fig. 3 (i.e., on the centerline, 168.60 cm. behind 46.56 cm. of SS-304). The last three were repeats at a detector location on the centerline, 161.61 cm. behind the 46.56 cm. of SS-304 (not shown in Fig. 3). The expected ratio of the spectra at the two locations is:

$$\frac{\phi(168.60)}{\phi(161.61)} = \left(\frac{161.61}{168.60}\right)^2 = 0.919$$

whereas the measured ratio of the 12-in. Bonner ball counting rates with the geometric center of the ball at the same locations was 0.886. Thus, the data in the second series of repeats should be multiplied by about 0.90 to conform to the location shown in Fig. 3. The individual NE-213 data are presented in Tables 6-8 for the first three repeats, and in Tables 9-11 for the last three repeats, where the latter data are not corrected to the first detector location. The six sets of data are reproducible up to about 4.0 MeV, but above this energy they disagree by factors of two to three and hence are unreliable, and consequently no data are presented above this energy. There is even reason to suspect the data above $\sim$ 2.5 MeV because the flux levels are so poorly calculated. At the present time, the reason for these higher fluxes in the NE-213 measurements is not known.

TABLE 4. Calibrated Response Function for 4.03-in. Diameter Bonner Sphere*

Group	Midpoint Energy (eV)	Response (Counts/Incident Neut/cm^2)
1	1.42E+07	3.71E-02
2	1.29E+07	4.20E-02
3	1.16E+07	4.74E-02
4	1.05E+07	5.46E-02
5	9.52E+06	6.15E-02
6	8.62E+06	6.91E-02
7	7.80E+06	7.93E-02
8	7.06E+06	8.58E-02
9	6.38E+06	1.02E-01
10	5.78E+06	1.11E-01
11	5.23E+06	1.20E-01
12	4.73E+06	1.27E-01
13	4.28E+06	1.41E-01
14	3.87E+06	1.56E-01
15	3.50E+06	1.71E-01
16	3.17E+06	1.88E-01
17	2.87E+06	2.05E-01
18	2.60E+06	2.25E-01
19	2.35E+06	2.46E-01
20	2.13E+06	2.66E-01
21	1.92E+06	2.88E-01
22	1.74E+06	3.11E-01
23	1.57E+06	3.34E-01
24	1.42E+06	3.57E-01
25	1.29E+06	3.81E-01
26	1.17E+06	4.06E-01
27	1.06E+06	4.30E-01
28	9.54E+05	4.55E-01
29	8.64E+05	4.80E-01
30	7.82E+05	5.04E-01
31	7.07E+05	5.29E-01
32	6.40E+05	5.52E-01
33	5.79E+05	5.76E-01
34	5.24E+05	5.99E-01
35	4.74E+05	6.21E-01
36	4.29E+05	6.42E-01
37	3.88E+05	6.63E-01
38	3.51E+05	6.81E-01
39	3.18E+05	7.00E-01
40	2.88E+05	7.18E-01
41	2.60E+05	7.34E-01
42	2.35E+05	7.50E-01
43	2.13E+05	7.65E-01
44	1.93E+05	7.79E-01
45	1.74E+05	7.92E-01
46	1.58E+05	8.04E-01
47	1.43E+05	8.16E-01
48	1.29E+05	8.27E-01
49	1.17E+05	8.38E-01
50	9.88E+04	8.54E-01

TABLE 4. (Continued)

Group	Midpoint Energy (eV)	Response (Counts/Incident Neut/cm^2)
51	7.69E+04	8.77E-01
52	5.99E+04	8.97E-01
53	4.67E+04	9.17E-01
54	3.63E+04	9.36E-01
55	2.83E+04	9.55E-01
56	2.20E+04	9.74E-01
57	1.72E+04	9.93E-01
58	1.34E+04	1.01E-00
59	1.04E+04	1.03E-00
60	8.11E+03	1.05E-00
61	6.32E+03	1.07E-00
62	4.92E+03	1.09E-00
63	3.83E+03	1.11E-00
64	2.98E+03	1.13E-00
65	2.32E+03	1.16E-00
66	1.81E+03	1.18E-00
67	1.41E+03	1.20E-00
68	1.10E+03	1.22E-00
69	8.55E+02	1.25E-00
70	6.66E+02	1.27E-00
71	5.18E+02	1.27E-00
72	4.04E+02	1.31E-00
73	3.14E+02	1.32E-00
74	2.45E+02	1.34E-00
75	1.91E+02	1.37E-00
76	1.49E+02	1.37E-00
77	1.16E+02	1.28E-00
78	9.01E+01	1.14E-00
79	7.02E+01	1.26E-00
80	5.46E+01	1.31E-00
81	4.26E+01	1.32E-00
82	3.31E+01	1.32E-00
83	2.58E+01	1.27E-00
84	2.01E+01	1.34E-00
85	1.57E+01	1.34E-00
86	1.22E+01	1.34E-00
87	9.50E-00	1.34E-00
88	7.40E-00	1.33E-00
89	5.76E-00	1.32E-00
90	4.49E-00	1.31E-00
91	3.49E-00	1.29E-00
92	2.72E-00	1.26E-00
93	2.12E-00	1.22E-00
94	1.65E-00	1.17E-00
95	1.29E-00	1.11E-00

TABLE 4. (Continued)

Group	Midpoint Energy (eV)	Response (Counts/Incident Neut/cm^2)
96	1.00E-00	1.01E-00
97	7.79E-01	8.68E-01
98	6.07E-01	6.70E-01
99	4.73E-01	3.82E-01
100	Thermal	Negligible

*Radial thickness of polyethylene = 2.50 cm.;
Density of polyethylene = 0.951 gram/cc.;
Estimated accuracy is $\pm$ 5% for groups 1-68 and $\pm$ 15% for groups 69-99.

TABLE 5. Calibrated Response Function for 11.84-in. Diameter Bonner Sphere*

Group	Midpoint Energy (eV)	Response (Counts/Incident Neut/cm^2)
1	1.42E+07	6.25E-01
2	1.29E+07	6.74E-01
3	1.16E+07	7.24E-01
4	1.05E+07	7.96E-01
5	9.52E+06	8.49E-01
6	8.62E+06	9.11E-01
7	7.80E+06	9.13E-01
8	7.06E+06	9.85E-01
9	6.38E+06	9.94E-01
10	5.78E+06	1.02E-00
11	5.23E+06	1.03E-00
12	4.73E+06	1.03E-00
13	4.28E+06	1.01E-00
14	3.87E+06	9.51E-01
15	3.50E+06	9.17E-01
16	3.17E+06	9.77E-01
17	2.87E+06	9.23E-01
18	2.60E+06	9.52E-01
19	2.35E+06	9.33E-01
20	2.13E+06	8.81E-01
21	1.92E+06	8.61E-01
22	1.74E+06	8.18E-01
23	1.57E+06	7.71E-01
24	1.42E+06	7.24E-01
25	1.29E+06	6.76E-01
26	1.17E+06	6.29E-01
27	1.06E+06	5.83E-01
28	9.54E+05	5.39E-01
29	8.64E+05	4.97E-01
30	7.82E+05	4.57E-01
31	7.07E+05	4.21E-01
32	6.40E+05	3.87E-01
33	5.79E+05	3.55E-01
34	5.24E+05	3.27E-01
35	4.74E+05	3.01E-01
36	4.29E+05	2.77E-01
37	3.88E+05	2.57E-01
38	3.51E+05	2.37E-01
39	3.18E+05	2.20E-01
40	2.88E+05	2.06E-01
41	2.60E+05	1.92E-01
42	2.35E+05	1.80E-01
43	2.13E+05	1.69E-01
44	1.93E+05	1.60E-01
45	1.74E+05	1.51E-01
46	1.58E+05	1.44E-01
47	1.43E+05	1.37E-01
48	1.29E+05	1.31E-01
49	1.17E+05	1.25E-01
50	9.88E+04	1.17E-01

TABLE 5. (Continued)

Group	Midpoint Energy (eV)	Response (Counts/Incident Neut/cm^2)
51	7.69E+04	1.08E-01
52	5.99E+04	1.00E-01
53	4.67E+04	9.45E-02
54	3.63E+04	8.97E-02
55	2.83E+04	8.57E-02
56	2.20E+04	8.24E-02
57	1.72E+04	7.94E-02
58	1.34E+04	7.68E-02
59	1.04E+04	7.47E-02
60	8.11E+03	7.28E-02
61	6.32E+03	7.09E-02
62	4.92E+03	6.91E-02
63	3.83E+03	6.75E-02
64	2.98E+03	6.60E-02
65	2.32E+03	6.46E-02
66	1.81E+03	6.33E-02
67	1.41E+03	6.20E-02
68	1.10E+03	6.06E-02
69	8.55E+02	5.93E-02
70	6.66E+02	5.79E-02
71	5.18E+02	5.57E-02
72	4.04E+02	5.54E-02
73	3.14E+02	5.40E-02
74	2.45E+02	5.25E-02
75	1.91E+02	5.17E-02
76	1.49E+02	5.01E-02
77	1.16E+02	4.96E-02
78	9.01E+01	4.73E-02
79	7.02E+01	5.06E-02
80	5.46E+01	5.08E-02
81	5.26E+01	4.95E-02
82	3.31E+01	4.90E-02
83	2.58E+01	4.85E-02
84	2.01E+01	5.40E-02
85	1.57E+01	5.24E-02
86	1.22E+01	5.08E-02
87	9.50E-00	4.93E-02
88	7.40E-00	4.76E-02
89	5.76E-00	4.59E-02
90	4.49E-00	4.42E-02
91	3.49E-00	4.24E-02
92	2.72E-00	4.06E-02
93	2.12E-00	3.81E-02
94	1.65E-00	3.61E-02
95	1.29E-00	3.34E-02

TABLE 5. (Continued)

Group	Midpoint Energy (eV)	Response (Counts/Incident Neut/cm^2)
96	1.00E-00	2.99E-02
97	7.79E-01	2.51E-02
98	6.07E-01	1.90E-02
99	4.73E-01	1.06E-02
100	Thermal	Negligible

*Radial thickness of polyethylene = 12.42 cm.;
Density of polyethylene = 0.951 gram/cc.;
Estimated accuracy is $\pm$ 5% for groups 1-68 and $\pm$ 25% for groups 69-99.

TABLE 6. Unfolded NE-213 Spectrum on the Centerline 168.60 cm. Behind 46.56 cm. of Stainless Steel

Energy (MeV)	FLUX (Neutrons/cm^2/MeV/min/W) Lower Bound	Upper Bound	Mean Value
0.80	0.236E 04	0.253E 04	0.245E 04
0.90	0.154E 04	0.172E 04	0.163E 04
1.00	0.123E 04	0.131E 04	0.127E 04
1.10	0.920E 03	0.962E 03	0.941E 03
1.20	0.655E 03	0.678E 03	0.667E 03
1.30	0.445E 03	0.462E 03	0.454E 03
1.40	0.305E 03	0.317E 03	0.311E 03
1.50	0.221E 03	0.231E 03	0.226E 03
1.60	0.162E 03	0.170E 03	0.166E 03
1.70	0.124E 03	0.129E 03	0.127E 03
1.80	0.103E 03	0.108E 03	0.105E 03
1.90	0.820E 02	0.855E 02	0.838E 02
2.00	0.627E 02	0.658E 02	0.643E 02
2.10	0.493E 02	0.520E 02	0.506E 02
2.20	0.376E 02	0.402E 02	0.389E 02
2.30	0.296E 02	0.318E 02	0.307E 02
2.40	0.236E 02	0.257E 02	0.247E 02
2.50	0.188E 02	0.207E 02	0.197E 02
2.60	0.165E 02	0.181E 02	0.173E 02
2.70	0.163E 02	0.179E 02	0.171E 02
2.80	0.167E 02	0.183E 02	0.175E 02
2.90	0.159E 02	0.173E 02	0.166E 02
3.00	0.137E 02	0.151E 02	0.144E 02
3.20	0.940E 01	0.107E 02	0.100E 02
3.40	0.679E 01	0.810E 01	0.745E 01
3.60	0.551E 01	0.677E 01	0.614E 01
3.80	0.399E 01	0.536E 01	0.468E 01
4.00	0.441E 01	0.579E 01	0.510E 01

TABLE 7. Repeat of Unfolded NE-213 Spectrum on the Centerline 168.60 cm. Behind 46.56 cm. of Stainless Steel

Energy (MeV)	FLUX (Neutrons/cm^2/MeV/min/W) Lower Bound	Upper Bound	Mean Value
0.80	0.212E 04	0.228E 04	0.220E 04
0.90	0.144E 04	0.161E 04	0.152E 04
1.00	0.116E 04	0.124E 04	0.120E 04
1.10	0.890E 03	0.930E 03	0.910E 03
1.20	0.630E 03	0.653E 03	0.641E 03
1.30	0.434E 03	0.451E 03	0.443E 03
1.40	0.306E 03	0.318E 03	0.312E 03
1.50	0.218E 03	0.228E 03	0.223E 03
1.60	0.160E 03	0.168E 03	0.164E 03
1.70	0.126E 03	0.131E 03	0.129E 03
1.80	0.101E 03	0.106E 03	0.104E 03
1.90	0.777E 02	0.812E 02	0.794E 02
2.00	0.579E 02	0.611E 02	0.595E 02
2.10	0.471E 02	0.498E 02	0.485E 02
2.20	0.392E 02	0.417E 02	0.405E 02
2.30	0.313E 02	0.335E 02	0.324E 02
2.40	0.247E 02	0.267E 02	0.257E 02
2.50	0.201E 02	0.220E 02	0.210E 02
2.60	0.175E 02	0.191E 02	0.183E 02
2.70	0.165E 02	0.181E 02	0.173E 02
2.80	0.164E 02	0.180E 02	0.172E 02
2.90	0.158E 02	0.173E 02	0.166E 02
3.00	0.144E 02	0.158E 02	0.151E 02
3.20	0.964E 01	0.109E 02	0.103E 02
3.40	0.559E 01	0.694E 01	0.627E 01
3.60	0.493E 01	0.623E 01	0.558E 01
3.80	0.521E 01	0.662E 01	0.591E 01
4.00	0.403E 01	0.546E 01	0.474E 01

TABLE 8. Second Repeat of Unfolded NE-213 Spectrum on the Centerline 168.60 cm. Behind 46.56 cm. of Stainless Steel

Energy (MeV)	FLUX (Neutrons/cm^2/MeV/min/W) Lower Bound	Upper Bound	Mean Value
0.80	0.217E 04	0.234E 04	0.225E 04
0.90	0.147E 04	0.166E 04	0.156E 04
1.00	0.118E 04	0.125E 04	0.122E 04
1.10	0.897E 03	0.938E 03	0.918E 03
1.20	0.652E 03	0.676E 03	0.664E 03
1.30	0.452E 03	0.469E 03	0.460E 03
1.40	0.307E 03	0.319E 03	0.313E 03
1.50	0.219E 03	0.229E 03	0.224E 03
1.60	0.165E 03	0.173E 03	0.169E 03
1.70	0.131E 03	0.137E 03	0.134E 03
1.80	0.100E 03	0.106E 03	0.103E 03
1.90	0.787E 02	0.829E 02	0.808E 02
2.00	0.636E 02	0.674E 02	0.655E 02
2.10	0.494E 02	0.525E 02	0.510E 02
2.20	0.370E 02	0.399E 02	0.385E 02
2.30	0.287E 02	0.311E 02	0.299E 02
2.40	0.241E 02	0.264E 02	0.253E 02
2.50	0.212E 02	0.234E 02	0.223E 02
2.60	0.184E 02	0.203E 02	0.194E 02
2.70	0.164E 02	0.183E 02	0.173E 02
2.80	0.156E 02	0.174E 02	0.165E 02
2.90	0.149E 02	0.165E 02	0.157E 02
3.00	0.136E 02	0.153E 02	0.144E 02
3.20	0.968E 01	0.112E 02	0.104E 02
3.40	0.643E 01	0.801E 01	0.722E 01
3.60	0.508E 01	0.663E 01	0.585E 01
3.80	0.374E 01	0.539E 01	0.457E 01
4.00	0.266E 01	0.436E 01	0.351E 01

TABLE 9. Unfolded NE-213 Spectrum on the Centerline 161.61 cm. Behind 46.56 cm. of Stainless Steel

Energy (MeV)	FLUX (Neutrons/cm^2/MeV/min/W) Lower Bound	Upper Bound	Mean Value
0.80	0.229E 04	0.242E 04	0.236E 04
0.90	0.158E 04	0.172E 04	0.165E 04
1.00	0.122E 04	0.129E 04	0.125E 04
1.10	0.903E 03	0.938E 03	0.920E 03
1.20	0.640E 03	0.661E 03	0.651E 03
1.30	0.453E 03	0.468E 03	0.461E 03
1.40	0.327E 03	0.337E 03	0.332E 03
1.50	0.236E 03	0.245E 03	0.241E 03
1.60	0.174E 03	0.181E 03	0.176E 03
1.70	0.134E 03	0.140E 03	0.137E 03
1.80	0.103E 03	0.107E 03	0.105E 03
1.90	0.789E 02	0.828E 02	0.808E 02
2.00	0.622E 02	0.654E 02	0.638E 02
2.10	0.502E 02	0.530E 02	0.516E 02
2.20	0.415E 02	0.441E 02	0.428E 02
2.30	0.343E 02	0.367E 02	0.355E 02
2.40	0.280E 02	0.303E 02	0.291E 02
2.50	0.240E 02	0.260E 02	0.250E 02
2.60	0.225E 02	0.242E 02	0.234E 02
2.70	0.218E 02	0.234E 02	0.220E 02
2.80	0.203E 02	0.219E 02	0.211E 02
2.90	0.178E 02	0.194E 02	0.186E 02
3.00	0.148E 02	0.162E 02	0.155E 02
3.20	0.916E 01	0.103E 02	0.975E 01
3.40	0.567E 01	0.681E 01	0.624E 01
3.60	0.422E 01	0.537E 01	0.479E 01
3.80	0.422E 01	0.542E 01	0.482E 01
4.00	0.448E 01	0.567E 01	0.507E 01

TABLE 10. Repeat of Unfolded NE-213 Spectrum on the Centerline 161.61 cm. Behind 46.56 cm. of Stainless Steel

Energy (MeV)	FLUX (Neutrons/cm^2/MeV/min/W) Lower Bound	Upper Bound	Mean Value
0.80	0.245E 04	0.259E 04	0.252E 04
0.90	0.170E 04	0.188E 04	0.178E 04
1.00	0.130E 04	0.137E 04	0.134E 04
1.10	0.944E 03	0.979E 03	0.962E 03
1.20	0.664E 03	0.684E 03	0.674E 03
1.30	0.455E 03	0.469E 03	0.462E 03
1.40	0.317E 03	0.327E 03	0.322E 03
1.50	0.227E 03	0.238E 03	0.232E 03
1.60	0.168E 03	0.175E 03	0.172E 03
1.70	0.133E 03	0.139E 03	0.136E 03
1.80	0.105E 03	0.111E 03	0.108E 03
1.90	0.823E 02	0.868E 02	0.844E 02
2.00	0.642E 02	0.681E 02	0.662E 02
2.10	0.496E 02	0.530E 02	0.513E 02
2.20	0.384E 02	0.418E 02	0.399E 02
2.30	0.306E 02	0.334E 02	0.320E 02
2.40	0.250E 02	0.275E 02	0.263E 02
2.50	0.218E 02	0.241E 02	0.230E 02
2.60	0.208E 02	0.228E 02	0.218E 02
2.70	0.205E 02	0.224E 02	0.215E 02
2.80	0.198E 02	0.217E 02	0.207E 02
2.90	0.181E 02	0.198E 02	0.189E 02
3.00	0.155E 02	0.171E 02	0.168E 02
3.20	0.961E 01	0.109E 02	0.103E 02
3.40	0.551E 01	0.887E 01	0.619E 01
3.60	0.364E 01	0.503E 01	0.433E 01
3.80	0.293E 01	0.440E 01	0.366E 01
4.00	0.247E 01	0.393E 01	0.320E 01

TABLE 11. Second Repeat of Unfolded NE-213 Spectrum on the Centerline 161.61 cm. Behind 46.56 cm. of Stainless Steel

Energy (MeV)	FLUX (Neutrons/cm^2/MeV/min/W) Lower Bound	Upper Bound	Mean Value
0.80	0.251E 04	0.266E 04	0.258E 04
0.90	0.173E 04	0.190E 04	0.181E 04
1.00	0.134E 04	0.141E 04	0.137E 04
1.10	0.966E 03	0.100E 04	0.985E 03
1.20	0.684E 03	0.706E 03	0.695E 03
1.30	0.484E 03	0.500E 03	0.402E 03
1.40	0.343E 03	0.354E 03	0.348E 03
1.50	0.246E 03	0.259E 03	0.251E 03
1.60	0.182E 03	0.100E 03	0.186E 03
1.70	0.143E 03	0.149E 03	0.146E 03
1.80	0.111E 03	0.116E 03	0.114E 03
1.90	0.822E 02	0.868E 02	0.844E 02
2.00	0.614E 02	0.654E 02	0.634E 02
2.10	0.487E 02	0.521E 02	0.504E 02
2.20	0.393E 02	0.425E 02	0.409E 02
2.30	0.319E 02	0.348E 02	0.334E 02
2.40	0.271E 02	0.299E 02	0.285E 02
2.50	0.254E 02	0.278E 02	0.266E 02
2.60	0.248E 02	0.268E 02	0.258E 02
2.70	0.234E 02	0.254E 02	0.244E 02
2.80	0.211E 02	0.232E 02	0.221E 02
2.90	0.183E 02	0.201E 02	0.192E 02
3.00	0.150E 02	0.167E 02	0.158E 02
3.20	0.834E 01	0.978E 01	0.904E 01
3.40	0.390E 01	0.536E 01	0.463E 01
3.60	0.390E 01	0.538E 01	0.464E 01
3.80	0.507E 01	0.663E 01	0.585E 01
4.00	0.435E 01	0.591E 01	0.513E 01

Two separate sets of unfolded hydrogen counter spectra were obtained behind the stainless steel at the detector location shown in Fig. 3 (i.e., at the same location as that of the first series of NE-213 measurements), and these data are seen to be reproducible. Furthermore, in the overlap regions between the various modes of use of the hydrogen counter as well as between the hydrogen counter and the NE-213, the consistency is considered satisfactory. The data are presented in Tables 12 and 13, along with suggestions for resolving the disagreements in the overlap regions.

The unfolded hydrogen counter spectra behind the stainless steel and first sodium tank (see Fig. 4) is shown in Table 14. Except in the vicinity of 1 MeV where the flux is very low, the data are acceptable statistically. No repeat of this particular measurement was performed.

The Bonner ball counting rates are presented in Table 15[9]. The 4-in. Bonner ball background in the geometry of the void and lithium hydride backing was measured by placing an 8-in.-thick lithiated paraffin slab behind the carbon steel in the configurations shown in Figs. 17, 19, and 30. These counting rates, obtained at 1 MW power, were essentially constant and were almost the same as those measured with the reactor shut down, which indicated that the background was probably due to cosmic rays. This background counting rate averaged 0.62 counts/minute, which is less than 10% of the lowest measured foreground counting rate (configuration shown in Fig. 19). Bonner ball background counting rates behind the stainless steel were measured with a lithium hydride slab placed behind the stainless steel and concrete. The measured 12-in. Bonner ball background was about 4% of the foreground, and the 4-in. Bonner ball background about 8% of the foreground. The net counting rates in Table 15 are estimated to be accurate to $\pm$ 10%. They are plotted in Fig. 35 for the three series of data involving carbon steel behind the sodium.

---

[9]There were several repeats of the 4-in. Bonner ball counting rates during the course of the measurements; the values in Table 15 are not necessarily averages of these repeats, but are the most accurate values in the judgement of the authors.

TABLE 12. Unfolded Hydrogen Counter Spectrum on the Centerline 168.60 cm. Behind 46.56 cm. of Stainless Steel

Energy Boundary (MeV)		Flux (Neutrons/cm^2/MeV/min/W)		Error (%)
0.0078	0.0090	0.4225E 05		15.39
0.0090	0.0107	0.6903E 05		8.20
0.0107	0.0124	0.7936E 05		8.12
0.0124	0.0145	0.7066E 05		8.15
0.0145	0.0174	0.6361E 05		7.15
0.0174	0.0204	0.8607E 05		6.04
0.0204	0.0237	0.1477E 06		3.31
0.0237	0.0279	0.1810E 06		2.19
0.0279	0.0330	0.5210E 05		6.57
0.0330	0.0389	0.2308E 05		14.05
0.0339	0.0391	0.2984E 05	Omit	6.18
0.0389	0.0460	0.4246E 05	} Average	6.87
0.0391	0.0460	0.4176E 05		3.84
0.0460	0.0547	0.4483E 05		3.27
0.0547	0.0634	0.4511E 05		3.72
0.0634	0.0755	0.5912E 05		2.20
0.0755	0.0877	0.6726E 05		2.14
0.0877	0.1033	0.4438E 05		2.65
0.1033	0.1224	0.5436E 05		1.88
0.1035	0.1229	0.5587E 05	Omit	1.00
0.1224	0.1450	0.6973E 05	Omit	1.24
0.1229	0.1450	0.5255E 05		0.98
0.1450	0.1698	0.3010E 05		1.62
0.1698	0.2002	0.2302E 05		1.85
0.2002	0.2361	0.2316E 05		1.67
0.2361	0.2775	0.3088E 05		1.12
0.2775	0.3244	0.2689E 05		1.10
0.3238	0.3785	0.1667E 05	Omit	0.79
0.3244	0.3824	0.1415E 05		1.57
0.3785	0.4815	0.7835E 04		1.25
0.3824	0.4515	0.6858E 04	Omit	2.73
0.4515	0.5244	0.7396E 04		1.41
0.5244	0.6156	0.8024E 04		0.99
0.6156	0.7251	0.4659E 04		1.25
0.7251	0.8528	0.2129E 04		2.10
0.8528	1.0078	0.1514E 04		2.20
1.0078	1.1902	0.8657E 03		2.76
1.1902	1.4000	0.3760E 03		4.54

TABLE 13. Repeat of Unfolded Hydrogen Counter Spectrum on the Centerline 168.60 cm. Behind 46.56 cm. of Stainless Steel

Energy Boundary (MeV)		Flux (Neutrons/cm^2/MeV/min/W)		Error (%)
0.0078	0.0090	0.4392E 05		15.00
0.0090	0.0107	0.7311E 05		7.84
0.0107	0.0124	0.8539E 05		7.63
0.0124	0.0145	0.7343E 05		7.93
0.0145	0.0174	0.5545E 05		8.30
0.0174	0.0204	0.9517E 05		5.53
0.0204	0.0237	0.1541E 06		3.21
0.0237	0.0279	0.1840E 06		2.18
0.0279	0.0330	0.4863E 05		7.12
0.0330	0.0389	0.2604E 05		12.62
0.0339	0.0391	0.3100E 05	Omit	6.95
0.0389	0.0460	0.4488E 05	} Average	6.57
0.0391	0.0460	0.4237E 05		4.42
0.0460	0.0547	0.4626E 05		3.70
0.0547	0.0634	0.4601E 05		4.25
0.0634	0.0755	0.6072E 05		2.50
0.0755	0.0877	0.6843E 05		2.46
0.0877	0.1033	0.4492E 05		3.06
0.1033	0.1224	0.5590E 05		2.12
0.1035	0.1229	0.5633E 05	Omit	1.18
0.1224	0.1450	0.6963E 05	Omit	1.44
0.1229	0.1450	0.5399E 05		1.14
0.1450	0.1698	0.3127E 05		1.86
0.1698	0.2002	0.2406E 05		2.10
0.2002	0.2361	0.2313E 05		1.98
0.2361	0.2775	0.3137E 05		1.31
0.2775	0.3244	0.2734E 05		1.28
0.3238	0.3785	0.1660E 05	Omit	0.72
0.3244	0.3824	0.1457E 05		1.81
0.3785	0.4515	0.7705E 04		1.16
0.3824	0.4515	0.6833E 04	Omit	3.25
0.4515	0.5244	0.7291E 04		1.30
0.5244	0.6156	0.7930E 04		0.91
0.6156	0.7251	0.4592E 04		1.15
0.7251	0.8528	0.2156E 04		1.89
0.8528	1.0078	0.1496E 04		2.01
1.0078	1.1902	0.8333E 03		2.61
1.1902	1.4000	0.3747E 03		4.17

TABLE 14. Unfolded Hydrogen Counter Spectrum at the Center of the 12.70 cm. Void Behind 46.56 cm. of Stainless Steel and the First Sodium Tank

Energy Boundary (MeV)		Flux (Neutrons/cm^2/MeV/min/W)		Error (%)
0.0087	0.0104	0.1477E 05		4.99
0.0104	0.0121	0.1475E 05		5.38
0.0121	0.0142	0.1312E 05		5.09
0.0142	0.0168	0.1072E 05		5.40
0.0168	0.0198	0.8894E 04		5.78
0.0198	0.0232	0.7396E 04		6.27
0.0232	0.0270	0.7020E 04		5.98
0.0270	0.0321	0.6684E 04		4.45
0.0321	0.0376	0.4215E 04		6.36
0.0322	0.0392	0.3648E 04	Average	3.66
0.0376	0.0444	0.1816E 04		11.84
0.0392	0.0444	0.2162E 04	Average	8.56
0.0444	0.0532	0.1775E 04		6.74
0.0532	0.0619	0.1593E 04		8.10
0.0619	0.0741	0.2313E 04		3.93
0.0741	0.0863	0.1463E 04		5.98
0.0863	0.1020	0.7649E 03		8.40
0.1020	0.1194	0.6764E 03		8.41
0.1034	0.1200	0.1319E 04	Omit	2.49
0.1194	0.1420	0.5243E 03		7.47
0.1200	0.1420	0.6305E 03		3.34
0.1420	0.1669	0.2812E 03		6.13
0.1669	0.1972	0.1616E 03		8.43
0.1972	0.2330	0.1000E 03		11.58
0.2000	0.2372	0.9317E 02	Average	0.80
0.2330	0.2744	0.1277E 03	Omit	7.66
0.2372	0.2744	0.6175E 02		1.10
0.2744	0.3209	0.3055E 02		1.60
0.3209	0.3767	0.1498E 02		2.50
0.3767	0.4512	0.9261E 01		2.83
0.4512	0.5256	0.5582E 01		4.57
0.5256	0.6186	0.2642E 01		7.50
0.6186	0.7302	0.1255E 01		13.84
0.7302	0.8605	0.9121E 00		17.99
0.8605	1.0093	0.2318E 00		70.08
1.0093	1.1860	0.4757E 00		32.89
1.1860	1.4000	0.1486E 01		8.79

TABLE 15. Foreground Less Background Counting Rates of the 4-in. Bonner Ball in counts/min/watt*

Configuration†	Figure	Counting Rate
46.56 cm. SS	3	1.64(4)**
46.56 cm. SS + 154.86 cm. Na	4	9.40(3)
46.56 cm. SS + 308.99 cm. Na	5	1.62(2)
46.56 cm. SS + 308.99 cm. Na + 15.38 cm. CS	6	2.06(0)
46.56 cm. SS + 308.99 cm. Na + 30.85 cm. CS	7	4.85(-2)
46.56 cm. SS + 308.99 cm. Na + 46.24 cm. CS	8	1.14(-2)
46.56 cm. SS + 308.99 cm. Na + 61.63 cm. CS	9	5.15(-3)
46.56 cm. SS + 459.83 cm. Na	10	1.31(0)
46.56 cm. SS + 459.83 cm. Na + 5.14 cm. CS	11	2.19(-1)
46.56 cm. SS + 459.83 cm. Na + 10.25 cm. CS	12	3.92(-2)
46.56 cm. SS + 459.83 cm. Na + 15.41 cm. CS	13	6.83(-3)
46.56 cm. SS + 459.83 cm. Na + 20.52 cm. CS	14	1.17(-3)
46.56 cm. SS + 459.83 cm. Na + 25.72 cm. CS	15	2.24(-4)
46.56 cm. SS + 459.83 cm. Na + 30.85 cm. CS	16	6.26(-5)††
46.56 cm. SS + 459.83 cm. Na + 41.11 cm. CS	17	2.22(-5)
46.56 cm. SS + 459.83 cm. Na + 51.40 cm. CS	18	1.18(-5)
46.56 cm. SS + 459.83 cm. Na + 61.68 cm. CS	19	6.52(-6)
30.90 cm. SS + 459.83 cm. Na	20	3.17(0)
30.90 cm. SS + 459.83 cm. Na + 5.14 cm. CS	21	5.51(-1)
30.90 cm. SS + 459.83 cm. Na + 10.25 cm. CS	22	1.04(-1)
30.90 cm. SS + 459.83 cm. Na + 15.41 cm. CS	23	1.91(-2)

TABLE 15. (Continued)

Configuration†	Figure	Counting Rate
30.90 cm. SS + 459.83 cm. Na + 20.52 cm. CS	24	3.67(-3)
30.90 cm. SS + 459.83 cm. Na + 25.72 cm. CS	25	8.60(-4)
30.90 cm. SS + 459.83 cm. Na + 30.85 cm. CS	26	3.19(-4)
30.90 cm. SS + 459.83 cm. Na + 41.11 cm. CS	27	1.19(-4)
30.90 cm. SS + 459.83 cm. Na + 51.40 cm. CS	28	6.57(-5)
30.90 cm. SS + 459.83 cm. Na + 61.68 cm. CS	29	3.86(-5)
30.90 cm. SS + 459.83 cm. Na + 72.00 cm. CS	30	2.20(-5)
30.90 cm. SS + 459.83 cm. Na + 82.27 cm. CS	31	1.31(-5)
30.90 cm. SS + 459.83 cm. Na + 90.06 cm. CS	32	9.09(-6)

* The net counting rate of the 12-in. Bonner ball behind 46.56 cm. of stainless steel was 3808 counts/min/watt.

† Neglecting voids and aluminum.

** Read as 1.64×10^4.

†† Subsequent analysis of this measurement indicates this value may be $\sim$ 40% too low.

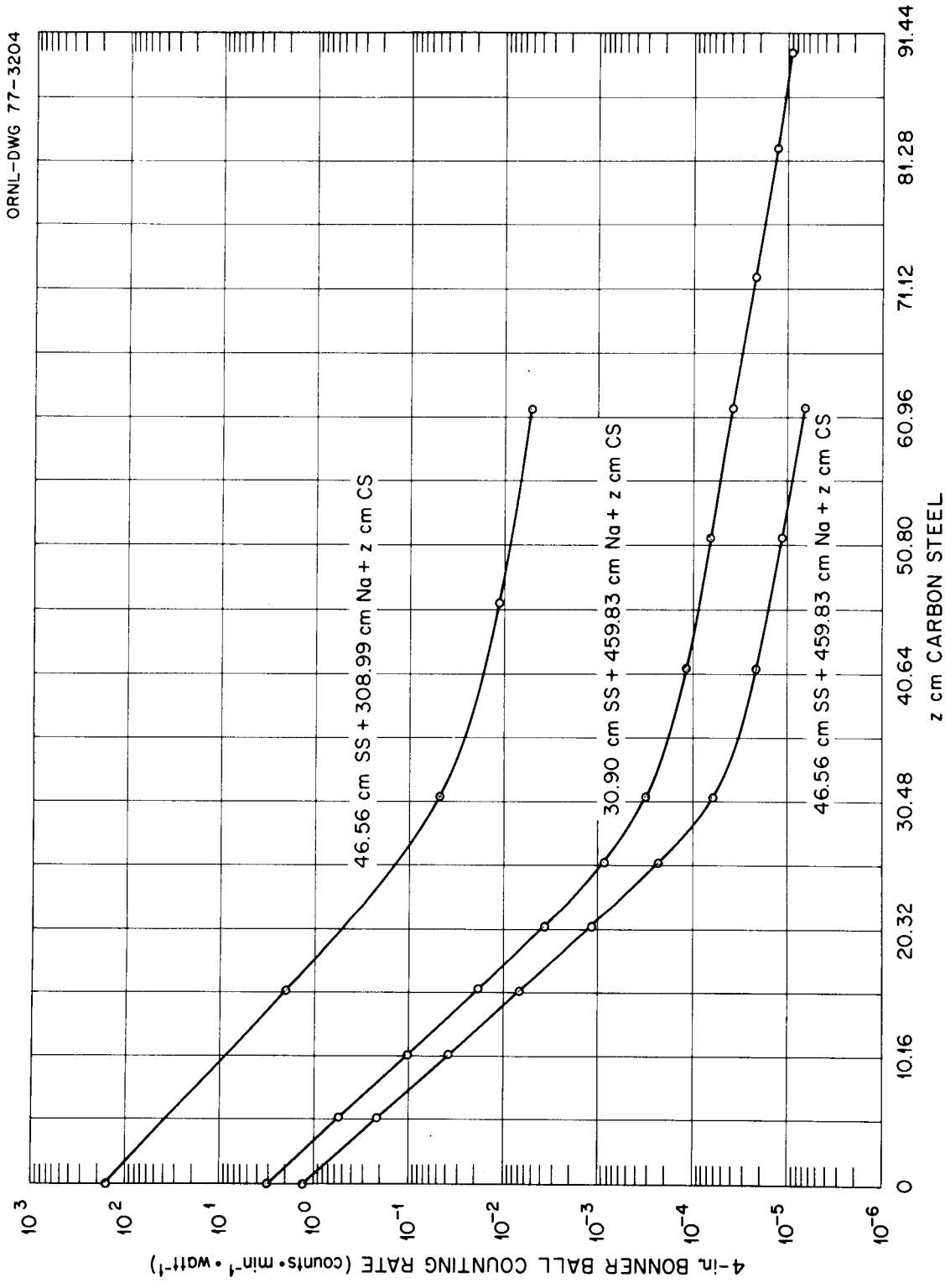

Fig. 35. Measured 4-in. Bonner ball counting rates as a function of carbon steel thickness for the three different stainless steel and sodium configurations.

II. Analysis

A. GENERAL

For the DOT-III[10] calculations, the disc source as described in a previous section was written as an interior boundary source tape for 38 radial intervals, 100 angles, and 49 groups. Zeroes appear on this tape for all backward angles, and for all forward angles for disc radii greater than 48.58 cm. (see Fig.34). The 100-angle quadrature set is a forward biased set containing 64 forward angles and appears in the appendix as part of the sample input. It was used instead of the 48-angle (S_8) set used in calculating earlier Tower experiments because the analytic first collision source calculation (GRTUNCLE) could no longer be made using the boundary source tape. In order to ensure the still significant forward bias of the neutrons leaking the large beam collimator, the 100-angle set was used to compensate for the missing first collision source calculation. The cross section set consisted of the first 49 neutron groups of the standard 51n-25γ (through P_3) set used at ORNL in its CRBR shield design studies and has already been presented in Table 2. Since the detectors used in the measurements had zero sensitivity to thermal neutrons, fluxes in the last two neutron groups were not calculated. The cross section set used throughout the calculations was based completely on ENDF/IV, and used consistent ($1/E\Sigma_{T_{SS}}$) weighting for SS-304 and ($1/E\Sigma_{T_{Fe}}$) weighting for carbon steel. The sodium, aluminum, and peripheral shielding materials were all weighted 1/E. It should be mentioned that the group structure used is based on simple lethargy intervals, and does not include any specially constructed groups that are centered around total cross section minima in any material. Consequently these 49-group calculations serve the purpose primarily of providing bias factors that can be used in the design calculations of the upper axial shield and the anticipated

---

[10] An updated version of the discrete ordinates DOT-III code was used, designated as DOT 3N5. It has accelerated convergence features compared with earlier versions. For a discussion of the earlier versions, see W. A. Rhoades and F. R. Mynatt, "The DOT-III Two-Dimensional Discrete Ordinates Transport Code," ORNL-TM-4280 (1973).

discrepancies with measurement should be assigned more to the course group structure employed (even with $1/E\Sigma_T$ weighting) than to inaccuracies in the basic ENDF/IV data from which the group constants are derived. Additional one-dimensional calculations can be (and were) made using a group structure tailored to the sodium and iron cross section minima and these calculations provide far more information regarding the accuracy of ENDF/IV. These latter ANISN scaling results using a 171-group set will also be presented.

B. METHOD OF CALCULATION

The 49-group DOT-III calculations started with the interior boundary disc source tape and the geometry of Fig. 34. A calculation of each measured result then preceded in a logical sequence of successive geometries presented in Figs. 3-32. A forward angular flux tape was often written during the calculation of a given configuration at an axial boundary located sufficiently inside the configuration that the fluxes were unperturbed by the lithium hydride. This tape then served as an external boundary source for the next configuration. This "bootstrapping" technique permitted most of the configurations to be calculated without having to start from the original interior boundary source each time, and saved many hours of computation. For example, the sequence of configurations shown in Figs. 10, 13, 16-19 were calculated by the scheme outlined in Table 16. Note that the configurations shown in Figs. 11, 12, 14, and 15 (as well as 21, 22, 24, and 25) were not calculated.

The radial grid used throughout the calculations is shown in the sample input, and is probably finer than necessary to calculate accurately the neutron transport to the detectors. However, the disc source must also be represented on the same grid, and making the mesh too course over the radius of the collimator could introduce errors into the calculation at the very start, so the grid was chosen conservatively. The axial grid was also conservative, especially for the carbon steel and lithium hydride. The situation is summarized in Table 17 for the series of calculations described in Table 16. Similar grids were used for the other two series of configurations. The axial grid intervals for the carbon steel and lithium hydride were based on the results of several ANISN calculations

TABLE 16. Calculational Scheme for the Sequence of Configurations 46.56 cm. SS + 459.83 cm. Na + z cm. CS

Run	Running Time*	Configuration Calculated	Source Tape	Source Axial Boundary	Axial Boundary for Ang. Flux Tape if written
1	116	Fig. 10 from top (Fig. 34) down through the 154.13 cm. sodium tank	Interior Boundary Disc Source	Top of large beam collimator (Fig. 34)	81.27 cm. above bottom of 154.13 cm. sodium tank
2	64	Fig. 10 from 81.27 cm. above bottom of 154.13 cm. sodium tank down through 12 cm. of LiH	Ang. Flux Tape from Run 1	81.27 cm. above bottom of 154.13 cm. sodium tank	9.93 cm. below top of 77.96 cm. sodium tank
3	56	Fig. 13 from 9.93 cm. below top of 77.96 cm. sodium tank down through 12 cm. of LiH	Ang. Flux Tape from Run 2	9.93 cm. below top of 77.96 cm. sodium tank	None
4	84	Fig. 16 from 9.93 cm. below top of 77.96 cm. sodium tank down through 12 cm. of LiH	Ang. Flux Tape from Run 2	9.93 cm. below top of 77.96 cm. sodium tank	None (there could have been one written at the top of the 5.14 cm. CS slab which would lead to alternate Runs 5, 6, and 7)
5	74	Fig. 17 from 9.93 cm. below top of 77.96 cm. sodium tank down through 12 cm. of LiH	Ang. Flux Tape from Run 2	9.93 cm. below top of 77.96 cm. sodium tank	None
5-Alternate		Fig. 17 from top of 5.14 cm. CS slab down through 12 cm. of LiH	Ang. Flux Tape from Run 4	Top of 5.14 cm. CS slab	None
6	73	Fig. 18 from 9.93 cm. below top of 77.96 cm. sodium tank down through 18 cm. LiH	Ang. Flux Tape from Run 2	9.93 cm. below top of 77.96 cm. sodium tank	None

TABLE 16. (Continued)

Run	Running Time*	Configuration Calculated	Source Tape	Source Axial Boundary	Axial Boundary for Ang. Flux Tape if written
6-Alternate		Fig. 18 from top of 5.14 cm. CS slab down through 18 cm. LiH	Ang. Flux Tape from Run 4	Top of 5.14 cm. CS slab	None
7	80	Fig. 19 from 9.93 cm. below top of 77.96 cm. sodium tank down through 18 cm. LiH	Ang. Flux Tape from Run 2	9.93 cm. below top of 77.96 cm. sodium tank	None
7-Alternate		Fig. 19 from top of 5.14 cm. CS slab down through 18 cm. LiH	Ang. Flux Tape from Run 4	Top of 5.14 cm. CS slab	None

*In CPU minutes on the IBM 360/195. Axial mesh used for the CS varied from run to run. (See Table 17).

TABLE 17. Axial Intervals Used in the Calculation of the Configurations
46.56 cm. SS + 459.83 cm. Na + z cm. CS

Material	Interval Size (cm.)
SS	$\sim$ 1.50
Na	$\sim$ 4.50
Al	0.64 for tanks nearest detector, 1.27 otherwise
LiH	$\sim$ 0.20 for first 2 cm. from top edge, $\sim$ 0.40 for next 2 cm., $\sim$ 0.67 for next 8 cm. for $0 \leq z \leq 42$, and $\sim$ 0.33 for first cm. from top edge, $\sim$ 0.50 for next 2 cm., $\sim$ 1.0 for next 9 cm., $\sim$ 2.0 for next 6 cm. for $z > 42$
CS	0.57 for $0 < z \leq 31$ and all depths 0 to z 0.86 for $31 < z \leq 42$ and all depths 0 to z 1.70 for $z > 42$ and all depths 0 to z
Void	$\sim$ 4.23 in detector voids, gap width in remaining voids

and increase in size as the thickness of carbon steel increases. This is because the spectrum at the detector becomes harder with increasing carbon steel penetration and the relaxation length changes from that of $\sim$ 1 eV neutrons at small penetration to that of 24 keV neutrons at large penetration (see Fig. 35).

A series of sample DOT-III problem inputs are presented in the Appendix. Results of the calculations will be presented after the following section.

C. ANISN SCALING CALCULATIONS

One-dimensional calculations of this experiment are very useful for several reasons. First, if attempts at establishment of a strong correlation between ANISN[11] and DOT results is successful, future calculations of this experiment need only be made with ANISN and knowledge of the "scaling factors" between DOT and ANISN results. Second, and this is really a corollary of the first, effects of using different cross section sets may easily be assessed by running ANISN. The advantage of the latter is that a set with a very large number of groups can be used in ANISN without the severe storage and computing time limitations that use in DOT would entail. Furthermore, the establishment of a strong one-dimensional correlation with this particular experiment, which is at the same time the most attenuating and most two-dimensional (i.e., broad source, presence of hydrogen in peripheral shielding, changes in cross sectional area between slabs and sodium tanks, etc.) of all the bulk shielding experiments performed at the Tower Shielding Facility in the past few years, would imply the existence of a similar correlation with all these other experiments performed earlier.

In order to establish a strong correlation between one- and two-dimensional calculations of this experiment, the following equation must be satisfied:

---

[11] W. W. Engle, Jr., "ANISN, A One-Dimensional Discrete Ordinates Transport Code with Anisotropic Scattering," K-1693 (1967). An updated version of this code (November, 1976) was used which converged more rapidly with mesh size. This version may be distinguished by the length of subroutine S833, which is 218A (hex) compared to the earlier length of 217E (hex).

$$\frac{DOT(A)}{DOT(B)} \approx \frac{ANISN(A)}{ANISN(B)} \qquad (1)$$

where A and B represent different problem parameters such as cross section sets, source spectra, etc., but the same source-detector separation, and the ratios are understood to be detector response ratios calculated by the two- and one-dimensional codes respectively. The one-dimensional problem (slab geometry was chosen for the calculations) should use the materials that appear along the centerline of the two-dimensional problem from source to detector and the same axial mesh, but the source description need only roughly approximate the one used in the two-dimensional calculation. It is not necessary to include the lithium hydride in the one-dimensional calculation, as will be seen, but some backing material should be present.

Three sets of comparisons in the form of Eq. (1) can be made from the results of earlier calculations of this experiment. The first two sets simultaneously changed the source, modified the cross section sets of SS and sodium slightly, and altered the CS and LiH axial mesh[12]. Thus, for the first two sets of comparisons, parameters A and B are summarized in Table 18.

The comparisons of the calculations using the parameter changes defined in Table 18 for the series 46.56 cm. SS + 308.99 cm. Na + z cm. CS is shown in Table 19 using both CS and LiH backing in the ANISN calculations.

The second set of comparisons involves the same parameter changes defined in Table 18, but for the series 46.56 cm. SS + 459.83 cm. Na + z cm. CS, and is shown in Table 20, again for both CS and LiH backing.

The column labeled "LiH backing" means that each of the five configurations in Table 19 and each of the six configurations in Table 20 were calculated with LiH following the z cm. of CS, similar to the DOT calculations, and there were thus eleven separate calculations for the two tables combined. The column labeled "CS backing" means that only the geometry of the last configuration in each table was used to which 10.16 cm.

---

[12]It is well known that the convergence as a function of axial mesh is more rapid for two-dimensional calculations than for analogous one-dimensional calculations. Thus there is some error involved when the parameters A and B involve different mesh sizes, as in the first two sets of comparisons, even though the more rapidly converging version of ANISN was used. Consequently, the ANISN results in Tables 19 and 20 are not as conclusive as those in Table 21, where A and B did not involve a change in mesh.

TABLE 18. Problem Parameter Changes for the First Two Sets of Comparisons Between ANISN and DOT Calculated Ratios

Parameters	A	B
Cross-Section Set	Standard 51 group used for all final DOT results	Added 2.2×10^{-3} atoms/barn cm. C to SS, Weighted SS as $(1/E\Sigma_T)$ ENDF/III, Increased H in Na by 0.85×10^{-5} atoms/barn cm.
Source	Standard disc source used for all final DOT results	∿ 17% decrease from 3 to 10 MeV, ∿ 33% decrease above 10 MeV
Axial Mesh	Standard mesh used for all final DOT results*	∿1.70 cm. for all CS, 1.50 cm. for first 7.5 cm. LiH nearest detector, 3.29 cm. for remaining 23 cm. LiH, 1.27 cm. for Al

*See Table 17.

TABLE 19. First Set of Comparisons of ANISN and DOT Calculated 4-in. Bonner Ball Ratios (behind 46.56 cm. SS + 308.99 cm. Na + z cm. CS)

	DOT(A)/DOT(B)	ANISN(A)/ANISN(B)		DOT(A)/DOT(B) / ANISN(A)/ANISN(B)
z(cm.)	LiH backing	LiH backing	CS backing*	Average
0	1.24	1.48	1.44	0.85
15.38	1.24	1.65	1.60	0.76
30.85	1.24	1.62	1.60	0.77
46.24	1.21	1.48	1.48	0.82
61.63	1.19	1.44	1.45	0.82

*The LiH was removed and 10.16 cm. CS were added behind the 61.63 cm. CS.

TABLE 20. Second Set of Comparisons of ANISN and DOT Calculated 4-in. Bonner Ball Ratios (behind 46.56 cm. SS + 459.83 cm. Na + z cm. CS)

	$\frac{DOT(A)}{DOT(B)}$	$\frac{ANISN(A)}{ANISN(B)}$		$\frac{DOT(A)/DOT(B)}{ANISN(A)/ANISN(B)}$
z(cm.)	LiH backing	LiH backing	CS backing*	Average
0	1.32	1.53	1.52	0.87
15.41	1.31	1.68	1.65	0.79
30.85	1.27	1.81	1.81	0.70
41.11	1.15	1.53	1.55	0.75
51.40	1.22	1.37	1.39	0.88
61.68	1.22	1.38	1.36	0.89

*The LiH was removed and 10.16 cm. CS were added behind the 61.68 cm. CS.

CS were added behind the last carbon steel, and there were thus only two calculations for the two tables combined. Detector counting rates were calculated in suitably positioned voids throughout the configuration.

The third set of comparisons involves the ratios behind the configurations (30.90 cm. SS + 459.83 cm. Na + z cm. CS) and (46.56 cm. SS + 459.83 cm. Na + z cm. CS). These two series of configurations may be compared because the detector remained at the same position for a given value of z; the 15.66 cm. of SS which changes the configuration was simply removed from the rear of the 46.56 cm. of SS leaving a void which was allowed to remain (see Fig. 10 and Fig. 20). Consequently, the two-dimensional effects of the two configurations are very closely the same, and attempts at one-dimensional scaling of these configurations are legitimate. For these comparisons, the change in parameters A and B is effectively a cross section change for the last 15.66 cm. of SS. Parameter B is now the standard 51 group set used to calculate all the final DOT results and parameter A is a modification to this set which sets all the cross sections for the final 15.66 cm. of SS equal to zero. The third set of comparisons is shown in Table 21, where B represents the series (46.56 cm. SS + 459.83 cm. Na + z cm. CS) and A the series (30.90 cm. SS + 459.83 cm. Na + z cm. CS).

An inspection of Tables 19-21 shows several interesting things. First, the lithium hydride backing may be replaced with carbon steel with negligible error in the ANISN ratios. This is a great simplification because this means only one ANISN run is necessary for each series of configurations characterized by different thicknesses of carbon steel following the sodium. Second, it appears that the ANISN ratios rather consistently overestimate the effects of cross section and other changes by about 20% compared with other DOT ratios, over a wide range of ratios.

This may be due to neglect of the effect of the peripheral shielding such as the concrete and lithiated paraffin, and to the limitation of the source in one dimension to the most forward angle in the ANISN mock-ups[13].

[13]In these simulations, the source spectrum used in ANISN is identical in shape to that leaking the pressure vessel at the angle closest to the normal, presented in the last column of Table 2. If the ANISN source were given an angular distribution identical to that given in Table 2 (i.e., non-zero for angles 10-17 in S_8 quadrature), the carbon steel backed ANISN ratios in Table 21 would become 2.91, 3.12, 4.47, 11.26, 16.6, and 17.3, yielding entries in the last column of 0.87, 0.88, 0.86, 0.85, 0.86 and 0.86. Thus, improving the source has bettered the correlation with DOT and in a more consistent fashion. Further improvements in the source by averaging over the disc source can undoubtedly be made to improve the correlation even more.

TABLE 21. Third Set of Comparisons of ANISN and DOT Calculated 4-in. Bonner Ball Ratios

	$\frac{DOT(A)}{DOT(B)}$	$\frac{ANISN(A)}{ANISN(B)}$		$\frac{DOT(A)/DOT(B)}{ANISN(A)/ANISN(B)}$
z(cm.)	LiH backing	LiH backing†	CS backing*	Average
0	2.53	2.87	2.92	0.87
15.41	2.74	3.14	3.17	0.87
30.85	3.87	4.99	5.01	0.77
41.11	9.55	12.8	12.6	0.75
51.40	14.3	16.95	17.1	0.84
61.68	14.9	17.5	17.7	0.85

†All mesh sizes in the ANISN runs were the same as those in the DOT runs.

*The LiH was removed and 10.16 cm. CS were added behind the 61.68 cm. CS. A constant mesh size of $\sim$ 0.85 cm. was used throughout the 71.84 cm. of carbon steel.

There does appear to be an adequate correlation between the ANISN ratios and the DOT ratios, however, and the relationship

$$\frac{DOT(A)}{DOT(B)} = K \frac{ANISN(A)}{ANISN(B)}$$

where $K \simeq 0.8$,
is accurate to about $\pm$ 10% over ranges of the ANISN ratio from $\sim$ 1.4 to 18. It should be noted that when A = B, the two ratios must obviously agree; thus an estimated extrapolation to values of the ANISN ratio from 1.0 to 1.4 would yield

$$\frac{DOT(A)}{DOT(B)} = K \frac{ANISN(A)}{ANISN(B)} \qquad (2)$$

where $K \simeq 0.8$ for $ANISN(A)/ANISN(B) > 1.4$,
$K \simeq 0.9$ for $1.2 \leq ANISN(A)/ANISN(B) \leq 1.4$,
and $K \simeq 1.0$ for $1.0 \leq ANISN(A)/ANISN(B) < 1.2$,
and the overall estimated accuracy is $\pm$ 10%[14].

By rewriting Eq. (2) as:

$$DOT(A) = K \cdot DOT(B) \cdot ANISN(A)/ANISN(B),$$
$$\text{then} \quad DOT(A) = K \cdot SF(B) \cdot ANISN(A), \qquad (3a)$$

where we have introduced the "scaling factor"

$$SF(B) = DOT(B)/ANISN(B). \qquad (3b)$$

The input for the four ANISN problems calculated without lithium hydride backing (i.e., 46.56 cm. SS, 46.56 cm. SS + 308.99 cm. Na + 71.79 cm. CS, 46.56 cm. SS + 459.83 cm. Na + 71.84 cm. CS, and 30.90 cm. SS + 459.83 cm. Na + 100.22 cm. CS) is shown in the Appendix and the scaling factors along with the DOT calculated results are shown in the tables presented in the next section.

---

[14]The ratio ANISN(A)/ANISN(B) must be set up so that its value is always ≥ 1.

In order to calculate the ANISN(A) results with a different cross section set, such cross section dependent parameters as ISCT, IGM, IHT, IHS, IHM, MS, MCR, MTP, MT, and ID2 in the 15$$ array are in general different from those given in the Appendix, but the remaining parameters must not be changed. The only other ANISN data that should be changed are the source spectrum in the 18** array, which must conform to the new group structure, and perhaps the 9$$ and 19$$ arrays. If AXMIX is used preparatory to ANISN, the 4-in. Bonner ball response function, the 14** array, must also conform to the new group structure. The source spectrum in the new group structure must be calculated from interpolation of the spectrum in the 51 group structure. Interpolation based on a 1/E law is probably adequate. The integral over the entire energy range (including thermal) before normalization must be 1.93768×10^6.

D. CALCULATED RESULTS AND COMPARISONS WITH EXPERIMENT

The calculated results using DOT-III and comparisons with the measurements are shown in Tables 22-34. Also shown are the scaling factors, defined by Eq. (3b), in many cases for both in situ and lithium hydride backing. Although the in situ backing (carbon steel in all cases except behind 46.56 cm. of SS where there was no backing and behind 46.56 cm. SS + 154.86 cm. Na where there was sodium backing) has been seen to represent an adequate scaling geometry, the lithium hydride backed results are presented for all but these two configurations in order to show the changes in the LiH reflected spectra that occur between the one- and two-dimensional treatments. Obviously, if the two spectral shapes were identical, the scaling factors would be constant, independent of energy. Their deviation from constancy for a given configuration is thus an indication of the failure of the one-dimensional approximation to mock up properly the true geometry[15].

E. DISCUSSION OF COMPARISONS

From the comparisons shown in the preceding section, it may be concluded that the calculations agree with the measurements to within about 30% behind

[15]Large deviations occur in the vicinity of group 6 for large z in Table 33, for example.

TABLE 22. Spectral Comparisons Behind 46.56 cm SS in Neutrons $cm^{-2}min^{-1}watt^{-1}$

Group	Calculated, unsmoothed	Calculated, smoothed*		Measured†		Calc./meas.		Scaling factor*	
		NE-213	HC	NE-213	HC	NE-213	HC	NE-213	HC
1	9.95(-2)††							4.16(5)	
2	3.03(-1)							3.99(5)	
3	5.86(-1)							3.88(5)	
4	9.14(-1)	9.14(-1)		1.40(0)**		0.65**		3.73(5)	
5	1.16(0)	1.16(0)		1.57(0)**		0.74**		3.68(5)	
6	1.35(0)	1.38(0)		2.37(0)**		0.58**		3.82(5)	
7	1.77(0)	1.95(0)		3.57(0)**		0.55**		3.76(5)	
8	3.11(0)	3.44(0)		5.32(0)**		0.65**		3.68(5)	
9	6.00(0)	6.60(0)		1.00(1)**		0.66**		3.71(5)	
10	1.09(1)	1.30(1)		1.65(1)		0.79		4.06(5)	
11	2.59(1)	2.57(1)		3.50(1)		0.73		3.35(5)	
12	3.47(1)	5.47(1)		6.90(1)		0.79		5.02(5)	
13	1.15(2)	1.37(2)	1.21(2)	1.40(2)	1.31(2)	0.98	0.92	3.85(5)	3.40(5)
14	2.72(2)	2.55(2)	2.59(2)	2.39(2)	2.37(2)	1.07	1.09	2.94(5)	2.98(5)
15	2.72(2)		3.20(2)		3.18(2)		1.01		3.50(5)
16	8.43(2)		8.19(2)		6.04(2)		1.36		2.99(5)
17	1.06(3)		1.00(3)		8.62(2)		1.16		2.90(5)
18	5.90(2)		6.49(2)		6.82(2)		0.95		3.21(5)
19	1.04(3)		1.03(3)		8.95(2)		1.15		2.99(5)
20	1.45(3)		1.43(3)		1.54(3)		0.93		3.03(5)
21	1.22(3)		1.17(3)		1.44(3)		0.81		2.94(5)
22	6.97(2)		7.44(2)		9.44(2)		0.79		3.22(5)
23	8.49(2)		8.62(2)		9.23(2)		0.93		3.13(5)
24	1.20(3)		1.14(3)		1.34(3)		0.85		2.96(5)
25	1.07(3)		1.13(3)		1.85(3)		0.61		3.27(5)
26	1.79(3)		1.74(3)		1.97(3)		0.88		3.12(5)
27	5.64(2)		5.61(2)		5.15(2)		1.09		3.17(5)
28	3.32(2)		3.43(2)		2.88(2)		1.19		3.33(5)

TABLE 22 (Continued)

Group	Calculated, unsmoothed	Calculated, smoothed*		Measured†		Calc./meas.		Scaling factor*	
		NE-213	HC	NE-213	HC	NE-213	HC	NE-213	HC
29	2.80(2)		3.54(2)		1.56(3)		1.02		4.14(5)
30	1.38(3)		1.25(3)						3.00(5)
31	3.73(2)		4.20(2)		3.13(2)		1.34		3.62(5)
32	6.00(2)		6.07(2)		5.25(2)		1.16		3.45(5)
33	2.20(2)							3.54(5)	
34	1.19(2)							3.58(5)	
35	1.49(2)							3.53(5)	
36	9.11(1)							3.59(5)	
37	1.62(2)							3.56(5)	
38	1.72(2)							3.54(5)	
39	1.12(2)							3.57(5)	
40	3.70(2)							3.63(5)	
41	1.46(2)							4.00(5)	
42	2.30(2)							3.83(5)	
43	2.09(2)							3.89(5)	
44	1.82(2)							4.01(5)	
45	1.48(2)							4.13(5)	
46	1.13(2)							4.35(5)	
47	8.00(1)							4.76(5)	
48	5.32(1)							5.69(5)	
49	4.23(1)							9.02(5)	
Totals		5.008(2)	1.595(4)	5.237(2)	1.694(4)	0.96	0.94		

*The calculations were smoothed with the resolution function of the NE-213 for groups 4-14 and of the hydrogen counter for groups 13-32. The remaining groups are unsmoothed. The scaling factors were calculated with nothing backing the stainless steel.

†The measurements are averaged over all six NE-213 and two hydrogen counter runs except for groups 4-6, where only the first three NE-213 runs were used.

††Read as 9.95×10^{-2}, etc.

**These measured values are questionable. See text.

TABLE 23. Bonner Ball Comparisons Behind 46.56 cm SS in Counts $min^{-1}watt^{-1}$

Bonner Ball	Calculated*	Measured	Calc./meas.	Scaling factor
4-in.	1.64(4)	1.64(4)	1.00	3.40(5)
12-in.	3.60(3)	3.81(3)	0.94	3.44(5)

*The calculated spectrum at the 4-in. Bonner ball location is closely approximated by multiplying the unsmoothed spectrum in Table 22 by 1.035. The calculated spectrum at the 12-in. Bonner ball location is closely approximated by multiplying the unsmoothed spectrum in Table 22 by 1.105.

TABLE 24. Spectral Comparisons Behind 46.56 cm SS + 154.86 cm Na in Neutrons $cm^{-2}min^{-1}watt^{-1}$

Group	Calculated, unsmoothed	Calculated, smoothed	Measured (HC)	Calc./meas.	Scaling factor[†]
1	1.24(-3)				8.16(5)
2	2.97(-3)				8.63(5)
3	5.57(-3)				8.80(5)
4	8.39(-3)				8.50(5)
5	9.47(-3)				8.16(5)
6	1.31(-2)				7.84(5)
7	1.41(-2)				7.38(5)
8	2.55(-2)				7.41(5)
9	3.52(-2)				7.26(5)
10	4.06(-2)				6.95(5)
11	1.01(-1)				7.59(5)
12	1.84(-1)				7.57(5)
13	1.74(-1)	1.75(-1)	2.85(-1)	0.61	7.20(5)
14	1.72(-1)	1.71(-1)	—	—	6.68(5)
15	1.60(-1)	1.60(-1)	1.18(-1)	1.44	6.78(5)
16	1.47(-1)	1.81(-1)	1.79(-1)	1.01	7.42(5)
17	5.30(-1)	5.40(-1)	3.73(-1)	1.45	8.36(5)
18	1.01(0)	1.05(0)	6.65(-1)	1.58	9.91(5)
19	1.96(0)	2.05(0)	9.30(-1)	2.20	9.40(5)
20	3.89(0)	3.71(0)	1.69(0)	2.20	9.64(5)
21	3.54(0)	3.67(0)	3.53(0)	1.04	8.72(5)
22	4.74(0)	4.78(0)	4.82(0)	0.99	8.72(5)
23	6.41(0)	7.04(0)	7.39(0)	0.95	1.20(6)
24	1.50(1)	1.44(1)	1.33(1)	1.08	8.09(5)
25	2.62(1)	2.60(1)	2.56(1)	1.02	1.02(6)
26	2.53(1)	2.71(1)	6.14(1)	0.44	7.00(5)
27	2.44(1)	2.33(1)	2.14(1)	1.09	6.98(5)
28	2.06(1)	2.37(1)	3.15(1)	0.75	1.02(6)
29	5.89(1)	5.57(1)	4.78(1)	1.17	6.11(5)
30	4.84(1)	4.91(1)	4.08(1)	1.20	6.22(5)
31	4.82(1)	4.82(1)	4.12(1)	1.17	5.81(5)
32	1.14(2)	1.12(2)	1.12(2)	1.00	5.00(5)
33	3.29(1)				4.41(5)
34	7.54(0)				5.35(5)
35	4.60(0)				1.32(6)
36	1.03(1)				4.81(5)
37	2.74(1)				4.31(5)
38	5.67(1)				5.02(5)
39	8.65(1)				5.37(5)
40	4.64(2)				4.87(5)

TABLE 24. (Continued)

Group	Calculated, unsmoothed	Calculated, smoothed	Measured (HC)	Calc./meas.	Scaling factor†
41	6.07(2)				4.24(5)
42	7.03(2)				3.72(5)
43	7.48(2)				3.30(5)
44	7.54(2)				2.95(5)
45	7.25(2)				2.66(5)
46	6.68(2)				2.44(5)
47	5.81(2)				2.23(5)
48	4.74(2)				2.04(5)
49	4.43(2)				1.89(5)
Totals		4.03(2)	4.15(2)	0.97	

†The scaling factor is based on the calculated unsmoothed values for groups 1-12 and 33-49, and on the calculated smoothed values for groups 13-32. Sodium was used as the backing material.

TABLE 25. 4-in. Bonner Ball Comparisons Behind 46.56 cm SS + 154.86 cm Na in Counts $min^{-1}watt^{-1}$

Calculated*	Measured	Calc./meas.	Scaling factor
8.48(3)	9.40(3)	0.90	3.05(5)

*The calculated spectrum at the center of detection of the Bonner ball is closely approximated by multiplying the unsmoothed spectrum in Table 24 by 1.02.

TABLE 26. Calculated Spectra Behind 46.56 cm SS + 308.99 cm Na + z cm CS at the Center of Detection of the 4-in. Bonner Ball in Neutrons $cm^{-2}min^{-1}watt^{-1}$

Group	z = 0	z = 15.38	z = 30.85	z = 46.24	z = 61.63
1	4.15(-6)	3.67(-7)	2.96(-8)	2.32(-9)	1.89(-10)
2	8.04(-6)	6.77(-7)	4.98(-8)	3.58(-9)	2.77(-10)
3	1.45(-5)	1.13(-6)	7.39(-8)	4.78(-9)	3.49(-10)
4	2.02(-5)	1.33(-6)	7.74(-8)	4.63(-9)	3.44(-10)
5	1.99(-5)	1.13(-6)	6.33(-8)	3.90(-9)	3.25(-10)
6	2.82(-5)	1.32(-6)	6.76(-8)	4.09(-9)	3.60(-10)
7	2.85(-5)	1.46(-6)	8.11(-8)	5.02(-9)	4.21(-10)
8	4.74(-5)	2.61(-6)	1.49(-7)	8.92(-9)	6.53(-10)
9	5.88(-5)	3.98(-6)	2.55(-7)	1.62(-8)	1.15(-9)
10	6.25(-5)	5.58(-6)	4.16(-7)	2.93(-8)	2.13(-9)
11	1.18(-4)	1.21(-5)	1.07(-6)	8.87(-8)	7.27(-9)
12	1.90(-4)	1.84(-5)	1.66(-6)	1.44(-7)	1.22(-8)
13	1.63(-4)	3.07(-5)	4.39(-6)	5.88(-7)	7.54(-8)
14	1.50(-4)	4.36(-5)	9.02(-6)	1.74(-6)	3.17(-7)
15	1.29(-4)	4.07(-5)	8.83(-6)	1.78(-6)	3.37(-7)
16	1.19(-4)	8.81(-5)	3.34(-5)	1.12(-5)	3.44(-6)
17	2.53(-4)	9.75(-5)	3.26(-5)	1.08(-5)	3.41(-6)
18	3.09(-4)	8.35(-5)	2.46(-5)	7.85(-6)	2.44(-6)
19	4.75(-4)	1.83(-4)	6.02(-5)	2.04(-5)	6.50(-6)
20	7.23(-4)	3.12(-4)	1.18(-4)	4.36(-5)	1.51(-5)
21	6.45(-4)	2.51(-4)	9.65(-5)	3.69(-5)	1.30(-5)
22	8.09(-4)	2.31(-4)	8.12(-5)	3.05(-5)	1.08(-5)
23	1.05(-3)	3.97(-4)	1.41(-4)	5.35(-5)	1.92(-5)
24	2.53(-3)	8.31(-4)	2.88(-4)	1.06(-4)	3.80(-5)
25	5.32(-3)	8.24(-4)	2.06(-4)	6.95(-5)	2.43(-5)
26	5.30(-3)	1.59(-3)	4.76(-4)	1.56(-4)	5.22(-5)
27	5.48(-3)	4.67(-4)	1.23(-4)	3.99(-5)	1.32(-5)
28	5.22(-3)	3.02(-4)	7.44(-5)	2.40(-5)	7.91(-6)
29	1.70(-2)	1.17(-3)	1.91(-4)	5.59(-5)	1.81(-5)
30	1.61(-2)	1.13(-2)	4.96(-3)	2.25(-3)	9.76(-4)
31	1.81(-2)	5.93(-3)	2.16(-3)	8.99(-4)	3.76(-4)
32	5.44(-2)	6.94(-3)	1.81(-3)	6.94(-4)	2.83(-4)
33	1.51(-2)	3.93(-3)	1.02(-3)	3.75(-4)	1.51(-4)
34	3.21(-3)	1.98(-3)	5.22(-4)	1.90(-4)	7.61(-5)
35	2.04(-3)	1.77(-3)	4.87(-4)	1.76(-4)	7.05(-5)
36	4.17(-3)	1.49(-3)	4.29(-4)	1.57(-4)	6.27(-5)
37	1.31(-2)	1.63(-3)	4.76(-4)	1.71(-4)	6.84(-5)
38	3.20(-2)	1.59(-3)	4.66(-4)	1.67(-4)	6.66(-5)
39	6.05(-2)	1.37(-3)	4.02(-4)	1.46(-4)	5.84(-5)
40	8.90(-1)	1.05(-2)	1.26(-3)	4.42(-4)	1.76(-4)

TABLE 26. (Continued)

Group	z = 0	z = 15.38	z = 30.85	z = 46.24	z = 61.63
41	2.32(0)	1.43(-2)	1.12(-3)	3.92(-4)	1.55(-4)
42	4.51(0)	4.24(-2)	1.33(-3)	3.88(-4)	1.52(-4)
43	7.29(0)	9.14(-2)	1.79(-3)	3.73(-4)	1.44(-4)
44	1.04(1)	1.61(-1)	2.66(-3)	3.53(-4)	1.31(-4)
45	1.35(1)	2.40(-1)	3.91(-3)	3.28(-4)	1.15(-4)
46	1.58(1)	3.03(-1)	5.16(-3)	2.99(-4)	9.57(-5)
47	1.70(1)	3.27(-1)	5.82(-3)	2.58(-4)	7.51(-5)
48	1.67(1)	2.94(-1)	5.40(-3)	2.04(-4)	5.45(-5)
49	1.86(1)	2.58(-1)	4.76(-3)	1.71(-4)	4.37(-5)

TABLE 27. Spectral Scaling Factors for ANISN Calculations Behind 46.56 cm SS + 308.99 cm Na + z cm CS for (a) Carbon Steel Backing and (b) Lithium Hydride Backing

Group	z = 0		z = 15.38		z = 30.85		z = 46.24		z = 61.63	
	(a)	(b)	(a)	(b)	(a)	(b)	(a)	(b)	(a)	(b)
1	4.33(5)	4.37(5)	4.45(5)	4.56(5)	4.32(5)	4.42(5)	4.04(5)	4.30(5)	3.93(5)	4.24(5)
2	4.67(5)	4.75(5)	4.87(5)	4.94(5)	4.74(5)	4.78(5)	4.48(5)	4.73(5)	4.56(5)	4.87(5)
3	4.83(5)	4.89(5)	5.07(5)	5.10(5)	4.92(5)	4.92(5)	4.69(5)	4.92(5)	5.01(5)	5.31(5)
4	4.75(5)	4.80(5)	4.99(5)	5.00(5)	4.93(5)	4.88(5)	4.87(5)	5.09(5)	5.86(5)	6.15(5)
5	4.66(5)	4.70(5)	4.91(5)	4.87(5)	4.98(5)	4.88(5)	5.27(5)	5.45(5)	7.25(5)	7.54(5)
6	4.59(5)	4.66(5)	4.83(5)	4.84(5)	4.95(5)	4.89(5)	5.46(5)	5.74(5)	8.16(5)	8.64(5)
7	4.34(5)	4.53(5)	4.52(5)	4.69(5)	4.62(5)	4.78(5)	4.93(5)	5.44(5)	6.78(5)	7.59(5)
8	4.19(5)	4.52(5)	4.26(5)	4.62(5)	4.25(5)	4.60(5)	4.27(5)	4.93(5)	5.11(5)	6.00(5)
9	3.89(5)	4.49(5)	3.93(5)	4.56(5)	3.89(5)	4.50(5)	3.84(5)	4.70(5)	4.25(5)	5.28(5)
10	3.61(5)	4.42(5)	3.74(5)	4.51(5)	3.70(5)	4.42(5)	3.63(5)	4.52(5)	3.80(5)	4.78(5)
11	3.67(5)	4.60(5)	3.73(5)	4.58(5)	3.68(5)	4.43(5)	3.55(5)	4.41(5)	3.52(5)	4.39(5)
12	3.69(5)	4.72(5)	3.64(5)	4.61(5)	3.53(5)	4.43(5)	3.41(5)	4.40(5)	3.35(5)	4.34(5)
13	3.24(5)	4.66(5)	3.41(5)	4.58(5)	3.38(5)	4.39(5)	3.32(5)	4.34(5)	3.27(5)	4.22(5)
14	2.96(5)	4.56(5)	3.23(5)	4.48(5)	3.21(5)	4.29(5)	3.19(5)	4.23(5)	3.17(5)	4.10(5)
15	2.69(5)	4.58(5)	2.82(5)	4.40(5)	2.76(5)	4.18(5)	2.73(5)	4.13(5)	2.74(5)	3.99(5)
16	1.82(5)	4.48(5)	2.36(5)	4.36(5)	2.44(5)	4.12(5)	2.48(5)	4.00(5)	2.58(5)	3.82(5)
17	2.44(5)	4.83(5)	2.37(5)	4.41(5)	2.24(5)	4.06(5)	2.20(5)	3.91(5)	2.32(5)	3.73(5)
18	2.62(5)	4.96(5)	2.17(5)	4.46(5)	1.95(5)	4.05(5)	1.89(5)	3.88(5)	1.99(5)	3.66(5)
19	2.46(5)	5.09(5)	2.28(5)	4.67(5)	2.09(5)	4.17(5)	2.08(5)	4.05(5)	2.19(5)	3.79(5)
20	2.77(5)	5.60(5)	2.46(5)	4.92(5)	2.30(5)	4.39(5)	2.27(5)	4.14(5)	2.40(5)	3.85(5)
21	2.59(5)	5.46(5)	2.22(5)	4.85(5)	2.05(5)	4.30(5)	2.03(5)	4.09(5)	2.16(5)	3.78(5)
22	2.86(5)	5.67(5)	2.21(5)	4.88(5)	1.95(5)	4.27(5)	1.89(5)	4.02(5)	2.03(5)	3.70(5)
23	3.10(5)	6.23(5)	2.42(5)	5.33(5)	2.10(5)	4.56(5)	2.03(5)	4.26(5)	2.18(5)	3.88(5)
24	3.56(5)	6.07(5)	3.10(5)	5.43(5)	2.68(5)	4.69(5)	2.51(5)	4.27(5)	2.64(5)	3.85(5)
25	3.91(5)	7.06(5)	2.47(5)	6.02(5)	1.84(5)	4.92(5)	1.65(5)	4.40(5)	1.73(5)	3.92(5)

TABLE 27. (Continued)

Group	z = 0		z = 15.38		z = 30.85		z = 46.24		z = 61.63	
	(a)	(b)	(a)	(b)	(a)	(b)	(a)	(b)	(a)	(b)
26	2.92(5)	6.17(5)	2.31(5)	5.96(5)	1.94(5)	5.12(5)	1.74(5)	4.62(5)	1.83(5)	4.06(5)
27	3.58(5)	7.14(5)	1.98(5)	6.02(5)	1.56(5)	5.06(5)	1.40(5)	4.54(5)	1.46(5)	3.98(5)
28	3.87(5)	7.19(5)	1.85(5)	6.08(5)	1.40(5)	5.10(5)	1.26(5)	4.57(5)	1.31(5)	3.99(5)
29	3.84(5)	6.95(5)	2.71(5)	6.54(5)	1.79(5)	5.20(5)	1.52(5)	4.55(5)	1.58(5)	3.95(5)
30	2.78(5)	7.49(5)	3.51(5)	6.98(5)	3.24(5)	6.14(5)	3.15(5)	5.72(5)	3.28(5)	5.16(5)
31	3.33(5)	7.56(5)	2.78(5)	6.90(5)	2.35(5)	6.04(5)	2.19(5)	5.59(5)	2.34(5)	5.02(5)
32	3.16(5)	7.46(5)	2.10(5)	6.47(5)	1.58(5)	5.36(5)	1.43(5)	4.89(5)	1.55(5)	4.36(5)
33	2.25(5)	6.52(5)	1.89(5)	6.29(5)	1.50(5)	5.27(5)	1.34(5)	4.70(5)	1.47(5)	4.16(5)
34	1.68(5)	5.43(5)	1.87(5)	6.29(5)	1.53(5)	5.29(5)	1.37(5)	4.73(5)	1.51(5)	4.18(5)
35	2.11(5)	5.51(5)	1.86(5)	6.19(5)	1.59(5)	5.26(5)	1.43(5)	4.69(5)	1.60(5)	4.15(5)
36	2.11(5)	5.20(5)	1.70(5)	6.01(5)	1.52(5)	5.15(5)	1.40(5)	4.60(5)	1.56(5)	4.06(5)
37	2.68(5)	6.56(5)	1.73(5)	6.13(5)	1.56(5)	5.29(5)	1.42(5)	4.71(5)	1.61(5)	4.17(5)
38	3.45(5)	7.30(5)	1.77(5)	6.12(5)	1.60(5)	5.30(5)	1.47(5)	4.72(5)	1.67(5)	4.18(5)
39	3.88(5)	7.41(5)	1.88(5)	6.01(5)	1.72(5)	5.22(5)	1.61(5)	4.66(5)	1.85(5)	4.13(5)
40	3.12(5)	6.68(5)	2.44(5)	6.56(5)	1.83(5)	5.29(5)	1.73(5)	4.70(5)	2.00(5)	4.19(5)
41	2.64(5)	6.07(5)	2.22(5)	6.41(5)	1.93(5)	5.24(5)	1.89(5)	4.41(5)	2.20(5)	4.23(5)
42	2.37(5)	5.61(5)	2.33(5)	6.11(5)	2.07(5)	5.41(5)	1.98(5)	4.56(5)	2.32(5)	4.25(5)
43	2.13(5)	5.22(5)	2.13(5)	5.75(5)	2.11(5)	5.50(5)	2.01(5)	4.54(5)	2.38(5)	4.32(5)
44	1.93(5)	4.89(5)	1.95(5)	5.42(5)	2.08(5)	5.46(5)	2.05(5)	4.56(5)	2.42(5)	4.35(5)
45	1.79(5)	4.62(5)	1.82(5)	5.15(5)	2.01(5)	5.33(5)	2.09(5)	4.60(5)	2.49(5)	4.39(5)
46	1.67(5)	4.35(5)	1.72(5)	4.89(5)	1.93(5)	5.17(5)	2.15(5)	4.66(5)	2.61(5)	4.38(5)
47	1.59(5)	4.16(5)	1.65(5)	4.68(5)	1.86(5)	5.01(5)	2.22(5)	5.05(5)	2.83(5)	4.27(5)
48	1.54(5)	3.99(5)	1.61(5)	4.49(5)	1.83(5)	4.86(5)	2.33(5)	5.53(5)	3.22(5)	4.08(5)
49	1.52(5)	3.82(5)	1.63(5)	4.29(5)	1.85(5)	4.71(5)	2.65(5)	5.55(5)	4.22(5)	4.16(5)

TABLE 28. 4-in. Bonner Ball Comparisons Behind 46.56 cm SS + 308.99 cm Na + z cm CS in Counts $min^{-1}watt^{-1}$

z	Calculated	Measured	Calc./meas.	Scaling factor	
				(a)	(b)
0	1.27(2)	1.62(2)	0.78	1.73(5)	4.43(5)
15.38	2.14(0)	2.06(0)	1.04	1.77(5)	4.93(5)
30.85	5.46(-2)	4.85(-2)	1.13	1.96(5)	5.24(5)
46.24	9.94(-3)	1.14(-2)	0.87	1.98(5)	4.95(5)
61.63	3.87(-3)	5.15(-3)	0.75	2.22(5)	4.49(5)

TABLE 29. Calculated Spectra Behind 46.56 cm SS + 459.83 cm Na + z cm CS at the Center of Detection of the 4-in. Bonner Ball in Neutrons $cm^{-2}min^{-1}watt^{-1}$

Group	z = 0	z = 15.41	z = 30.85	z = 41.11	z = 51.40	z = 61.68
1	1.48(-8)	1.29(-9)	1.06(-10)	1.99(-11)	3.61(-12)	6.82(-13)
2	2.35(-8)	1.96(-9)	1.47(-10)	2.63(-11)	4.62(-12)	8.71(-13)
3	4.10(-8)	3.14(-9)	2.10(-10)	3.52(-11)	5.84(-12)	1.07(-12)
4	5.28(-8)	3.44(-9)	2.07(-10)	3.31(-11)	5.46(-12)	1.05(-12)
5	4.81(-8)	2.74(-9)	1.62(-10)	2.67(-11)	4.73(-12)	9.99(-13)
6	6.80(-8)	3.20(-9)	1.74(-10)	2.81(-11)	5.05(-12)	1.11(-12)
7	6.88(-8)	3.59(-9)	2.10(-10)	3.45(-11)	6.10(-12)	1.28(-12)
8	1.10(-7)	6.18(-9)	3.71(-10)	5.97(-11)	9.91(-12)	1.88(-12)
9	1.32(-7)	9.24(-9)	6.21(-10)	1.04(-10)	1.73(-11)	3.16(-12)
10	1.40(-7)	1.29(-8)	1.00(-9)	1.79(-10)	3.08(-11)	5.59(-12)
11	2.40(-7)	2.59(-8)	2.38(-9)	4.73(-10)	8.94(-11)	1.71(-11)
12	3.47(-7)	3.64(-8)	3.47(-9)	7.09(-10)	1.40(-10)	2.74(-11)
13	2.97(-7)	6.00(-8)	8.91(-9)	2.39(-9)	6.16(-10)	1.57(-10)
14	2.72(-7)	8.49(-8)	1.81(-8)	6.11(-9)	2.00(-9)	6.41(-10)
15	2.31(-7)	7.92(-8)	1.77(-8)	6.16(-9)	2.08(-9)	6.81(-10)
16	2.14(-7)	1.69(-7)	6.56(-8)	3.20(-8)	1.51(-8)	6.83(-9)
17	4.24(-7)	1.78(-7)	6.23(-8)	3.02(-8)	1.45(-8)	6.69(-9)
18	4.74(-7)	1.46(-7)	4.61(-8)	2.19(-8)	1.04(-8)	4.75(-9)
19	6.70(-7)	2.93(-7)	1.06(-7)	5.26(-8)	2.57(-8)	1.22(-8)
20	8.16(-7)	4.25(-7)	1.79(-7)	9.70(-8)	5.11(-8)	2.58(-8)
21	7.10(-7)	3.29(-7)	1.42(-7)	7.82(-8)	4.21(-8)	2.16(-8)
22	8.11(-7)	2.87(-7)	1.16(-7)	6.36(-8)	3.43(-8)	1.76(-8)
23	8.40(-7)	4.19(-7)	1.80(-7)	1.02(-7)	5.62(-8)	2.97(-8)
24	1.75(-6)	7.22(-7)	3.05(-7)	1.72(-7)	9.73(-8)	5.25(-8)
25	2.35(-6)	5.47(-7)	1.95(-7)	1.08(-7)	6.01(-8)	3.24(-8)
26	2.40(-6)	9.32(-7)	3.68(-7)	2.04(-7)	1.14(-7)	6.17(-8)
27	2.11(-6)	2.62(-7)	9.44(-8)	5.20(-8)	2.89(-8)	1.55(-8)
28	1.71(-6)	1.67(-7)	5.73(-8)	3.14(-8)	1.74(-8)	9.34(-9)
29	5.27(-6)	5.12(-7)	1.32(-7)	6.95(-8)	3.83(-8)	2.06(-8)
30	4.77(-6)	3.78(-6)	1.85(-6)	1.16(-6)	7.29(-7)	4.40(-7)
31	5.32(-6)	1.92(-6)	7.72(-7)	4.54(-7)	2.77(-7)	1.65(-7)
32	1.66(-5)	2.31(-6)	6.78(-7)	3.75(-7)	2.21(-7)	1.29(-7)
33	4.76(-6)	1.32(-6)	3.84(-7)	2.08(-7)	1.21(-7)	7.00(-8)
34	1.06(-6)	6.66(-7)	1.97(-7)	1.05(-7)	6.11(-8)	3.53(-8)
35	7.31(-7)	6.00(-7)	1.84(-7)	9.84(-8)	5.69(-8)	3.28(-8)
36	1.30(-6)	5.12(-7)	1.65(-7)	8.88(-8)	5.14(-8)	2.96(-8)
37	4.07(-6)	5.56(-7)	1.81(-7)	9.62(-8)	5.55(-8)	3.20(-8)
38	1.01(-5)	5.43(-7)	1.77(-7)	9.39(-8)	5.41(-8)	3.11(-8)
39	1.99(-5)	4.73(-7)	1.54(-7)	8.29(-8)	4.78(-8)	2.75(-8)
40	7.75(-4)	6.64(-6)	5.04(-7)	2.52(-7)	1.44(-7)	8.26(-8)

TABLE 29. (Continued)

Group	z = 0	z = 15.41	z = 30.85	z = 41.11	z = 51.40	z = 61.68
41	3.83(-3)	1.29(-5)	4.73(-7)	2.24(-7)	1.28(-7)	7.37(-8)
42	1.19(-2)	7.00(-5)	7.83(-7)	2.30(-7)	1.26(-7)	7.19(-8)
43	2.79(-2)	2.16(-4)	1.80(-6)	2.52(-7)	1.19(-7)	6.74(-8)
44	5.44(-2)	5.05(-4)	4.31(-6)	3.29(-7)	1.11(-7)	6.13(-8)
45	9.20(-2)	9.48(-4)	8.83(-6)	4.94(-7)	1.03(-7)	5.38(-8)
46	1.36(-1)	1.47(-3)	1.48(-5)	7.36(-7)	9.70(-8)	4.52(-8)
47	1.78(-1)	1.89(-3)	1.99(-5)	9.60(-7)	8.96(-8)	3.59(-8)
48	2.07(-1)	1.97(-3)	2.11(-5)	1.01(-6)	7.68(-8)	2.65(-8)
49	2.75(-1)	1.99(-3)	2.07(-5)	9.98(-7)	6.93(-8)	2.17(-8)

TABLE 30. Spectral Scaling Factors for ANISN Calculations Behind 46.56 cm SS + 459.83 cm Na + z cm CS for (a) Carbon Steel Backing and (b) Lithium Hydride Backing

Group	z = 0		z = 15.41		z = 30.85		z = 41.11		z = 51.40		z = 61.68	
	(a)	(b)	(a)	(b)	(a)	(b)	(a)	(b)	(a)	(b)	(a)	(b)
1	2.66(5)	2.74(5)	2.76(5)	2.83(5)	2.72(5)	2.78(5)	2.66(5)	2.74(5)	2.54(5)	2.70(5)	2.51(5)	2.70(5)
2	2.97(5)	3.01(5)	3.09(5)	3.12(5)	3.02(5)	3.04(5)	3.00(5)	3.03(5)	2.93(5)	3.09(5)	3.08(5)	3.26(5)
3	3.13(5)	3.15(5)	3.23(5)	3.24(5)	3.17(5)	3.16(5)	3.18(5)	3.18(5)	3.17(5)	3.30(5)	3.47(5)	3.63(5)
4	3.07(5)	3.09(5)	3.18(5)	3.18(5)	3.19(5)	3.15(5)	3.28(5)	3.25(5)	3.47(5)	3.58(5)	4.22(5)	4.37(5)
5	3.01(5)	3.02(5)	3.14(5)	3.10(5)	3.23(5)	3.15(5)	3.48(5)	3.40(5)	3.98(5)	4.06(5)	5.32(5)	5.44(5)
6	2.96(5)	3.00(5)	3.08(5)	3.08(5)	3.22(5)	3.18(5)	3.53(5)	3.51(5)	4.20(5)	4.38(5)	5.90(5)	6.19(5)
7	2.81(5)	2.94(5)	2.90(5)	3.02(5)	2.99(5)	3.11(5)	3.21(5)	3.37(5)	3.65(5)	4.02(5)	4.81(5)	5.35(5)
8	2.72(5)	2.94(5)	2.74(5)	2.98(5)	2.75(5)	2.99(5)	2.83(5)	3.11(5)	2.99(5)	3.46(5)	3.57(5)	4.16(5)
9	2.51(5)	2.91(5)	2.52(5)	2.94(5)	2.52(5)	2.93(5)	2.56(5)	3.00(5)	2.61(5)	3.20(5)	2.93(5)	3.61(5)
10	2.32(5)	2.87(5)	2.40(5)	2.91(5)	2.39(5)	2.87(5)	2.42(5)	2.91(5)	2.41(5)	3.01(5)	2.56(5)	3.21(5)
11	2.30(5)	2.91(5)	2.36(5)	2.91(5)	2.34(5)	2.84(5)	2.34(5)	2.83(5)	2.29(5)	2.85(5)	2.30(5)	2.86(5)
12	2.26(5)	2.94(5)	2.27(5)	2.91(5)	2.23(5)	2.82(5)	2.22(5)	2.80(5)	2.19(5)	2.83(5)	2.18(5)	2.82(5)
13	1.97(5)	2.90(5)	2.12(5)	2.87(5)	2.13(5)	2.78(5)	2.13(5)	2.76(5)	2.10(5)	2.75(5)	2.10(5)	2.70(5)
14	1.79(5)	2.85(5)	2.02(5)	2.82(5)	2.04(5)	2.73(5)	2.03(5)	2.69(5)	2.02(5)	2.67(5)	2.02(5)	2.62(5)
15	1.61(5)	2.85(5)	1.76(5)	2.77(5)	1.75(5)	2.66(5)	1.74(5)	2.62(5)	1.73(5)	2.61(5)	1.75(5)	2.54(5)
16	1.09(5)	2.80(5)	1.47(5)	2.74(5)	1.55(5)	2.61(5)	1.56(5)	2.55(5)	1.59(5)	2.52(5)	1.65(5)	2.44(5)
17	1.43(5)	2.95(5)	1.45(5)	2.74(5)	1.41(5)	2.56(5)	1.39(5)	2.49(5)	1.41(5)	2.46(5)	1.48(5)	2.37(5)
18	1.48(5)	2.96(5)	1.31(5)	2.74(5)	1.21(5)	2.54(5)	1.19(5)	2.47(5)	1.20(5)	2.44(5)	1.26(5)	2.33(5)
19	1.34(5)	2.96(5)	1.32(5)	2.78(5)	1.28(5)	2.59(5)	1.27(5)	2.52(5)	1.28(5)	2.47(5)	1.37(5)	2.39(5)
20	1.36(5)	3.04(5)	1.33(5)	2.79(5)	1.31(5)	2.57(5)	1.32(5)	2.50(5)	1.35(5)	2.44(5)	1.45(5)	2.35(5)
21	1.27(5)	2.97(5)	1.19(5)	2.72(5)	1.16(5)	2.51(5)	1.16(5)	2.43(5)	1.19(5)	2.38(5)	1.30(5)	2.28(5)
22	1.37(5)	3.00(5)	1.17(5)	2.69(5)	1.09(5)	2.47(5)	1.08(5)	2.38(5)	1.11(5)	2.33(5)	1.21(5)	2.22(5)
23	1.35(5)	3.11(5)	1.18(5)	2.80(5)	1.12(5)	2.54(5)	1.12(5)	2.46(5)	1.15(5)	2.39(5)	1.27(5)	2.29(5)
24	1.51(5)	2.96(5)	1.42(5)	2.71(5)	1.32(5)	2.45(5)	1.29(5)	2.33(5)	1.33(5)	2.28(5)	1.47(5)	2.18(5)
25	1.55(5)	3.25(5)	1.02(5)	2.83(5)	8.65(4)	2.49(5)	8.41(4)	2.38(5)	8.55(4)	2.30(5)	9.59(4)	2.19(5)

TABLE 30. (Continued)

Group	z = 0		z = 15.41		z = 30.85		z = 41.11		z = 51.40		z = 61.68	
	(a)	(b)	(a)	(b)	(a)	(b)	(a)	(b)	(a)	(b)	(a)	(b)
26	1.20(5)	2.90(5)	9.63(4)	2.76(5)	8.56(4)	2.46(5)	8.31(4)	2.35(5)	8.49(4)	2.28(5)	9.65(4)	2.17(5)
27	1.45(5)	3.31(5)	8.29(4)	2.76(5)	6.97(4)	2.42(5)	6.74(4)	2.32(5)	6.84(4)	2.25(5)	7.75(4)	2.12(5)
28	1.54(5)	3.36(5)	7.80(4)	2.82(5)	6.36(4)	2.46(5)	6.11(4)	2.35(5)	6.19(4)	2.27(5)	7.04(4)	2.15(5)
29	1.61(5)	3.33(5)	1.07(5)	2.92(5)	7.71(4)	2.42(5)	7.23(4)	2.28(5)	7.31(4)	2.20(5)	8.37(4)	2.09(5)
30	1.16(5)	3.76(5)	1.46(5)	3.29(5)	1.35(5)	2.87(5)	1.32(5)	2.70(5)	1.36(5)	2.58(5)	1.46(5)	2.40(5)
31	1.51(5)	3.96(5)	1.23(5)	3.35(5)	1.01(5)	2.84(5)	9.53(4)	2.63(5)	9.60(4)	2.51(5)	1.06(5)	2.33(5)
32	1.63(5)	4.21(5)	1.03(5)	3.22(5)	7.43(4)	2.54(5)	6.77(4)	2.32(5)	6.68(4)	2.18(5)	7.49(4)	2.02(5)
33	1.20(5)	3.80(5)	9.57(4)	3.15(5)	7.23(4)	2.48(5)	6.54(4)	2.25(5)	6.43(4)	2.11(5)	7.27(4)	1.94(5)
34	9.36(4)	3.20(5)	9.53(4)	3.16(5)	7.45(4)	2.52(5)	6.70(4)	2.27(5)	6.61(4)	2.13(5)	7.51(4)	1.95(5)
35	1.25(5)	3.11(5)	9.62(4)	3.12(5)	7.82(4)	2.51(5)	7.11(4)	2.27(5)	6.99(4)	2.12(5)	8.00(4)	1.94(5)
36	1.10(5)	3.39(5)	8.95(4)	3.01(5)	7.63(4)	2.46(5)	7.02(4)	2.22(5)	6.93(4)	2.08(5)	7.95(4)	1.90(5)
37	1.43(5)	4.06(5)	9.08(4)	3.08(5)	7.80(4)	2.53(5)	7.13(4)	2.28(5)	7.04(4)	2.13(5)	8.14(4)	1.95(5)
38	1.91(5)	4.51(5)	9.33(4)	3.08(5)	8.04(4)	2.54(5)	7.38(4)	2.29(5)	7.30(4)	2.14(5)	8.45(4)	1.96(5)
39	2.27(5)	4.73(5)	1.01(5)	3.03(5)	8.77(4)	2.49(5)	8.19(4)	2.26(5)	8.14(4)	2.11(5)	9.46(4)	1.94(5)
40	2.25(5)	4.97(5)	1.69(5)	4.30(5)	9.73(4)	2.62(5)	8.84(4)	2.30(5)	8.80(4)	2.14(5)	1.03(5)	1.96(5)
41	2.00(5)	4.65(5)	1.59(5)	4.37(5)	1.07(5)	2.66(5)	9.70(4)	2.28(5)	9.74(4)	2.11(5)	1.15(5)	1.95(5)
42	1.85(5)	4.32(5)	1.72(5)	4.31(5)	1.31(5)	3.16(5)	1.04(5)	2.37(5)	1.03(5)	2.16(5)	1.22(5)	1.98(5)
43	1.67(5)	4.03(5)	1.59(5)	4.11(5)	1.46(5)	3.60(5)	1.10(5)	2.53(5)	1.04(5)	2.18(5)	1.24(5)	1.99(5)
44	1.54(5)	3.78(5)	1.48(5)	3.92(5)	1.48(5)	3.73(5)	1.20(5)	2.82(5)	1.06(5)	2.20(5)	1.27(5)	1.99(5)
45	1.43(5)	3.55(5)	1.39(5)	3.71(5)	1.44(5)	3.68(5)	1.29(5)	3.14(5)	1.09(5)	2.24(5)	1.31(5)	1.99(5)
46	1.34(5)	3.36(5)	1.31(5)	3.54(5)	1.38(5)	3.59(5)	1.33(5)	3.32(5)	1.14(5)	2.35(5)	1.38(5)	2.00(5)
47	1.27(5)	3.20(5)	1.26(5)	3.39(5)	1.34(5)	3.48(5)	1.33(5)	3.38(5)	1.20(5)	2.47(5)	1.50(5)	2.02(5)
48	1.23(5)	3.07(5)	1.23(5)	3.25(5)	1.31(5)	3.39(5)	1.33(5)	3.36(5)	1.28(5)	2.59(5)	1.70(5)	2.04(5)
49	1.21(5)	2.94(5)	1.23(5)	3.10(5)	1.31(5)	3.28(5)	1.35(5)	3.30(5)	1.42(5)	2.79(5)	2.19(5)	2.13(5)

TABLE 31. 4-in. Bonner Ball Comparisons Behind 46.56 cm SS + 459.83 cm Na + z cm CS in Counts $min^{-1}watt^{-1}$

z	Calculated	Measured	Calc./meas.	Scaling factor	
				(a)	(b)
0	1.10(0)	1.31(0)	0.84	1.31(5)	3.25(5)
15.41	1.05(-2)	6.83(-3)	1.54	1.30(5)	3.44(5)
30.85	1.14(-4)	6.26(-5)	1.82	1.32(5)	3.41(5)
41.11	1.02(-5)	2.22(-5)	0.46	1.10(5)	2.80(5)
51.40	3.54(-6)	1.18(-5)	0.30	9.71(4)	2.31(5)
61.68	1.96(-6)	6.52(-6)	0.30	1.10(5)	2.11(5)

TABLE 32. Calculated Spectra Behind 30.90 cm SS + 459.83 cm Na + z cm CS at the Center of Detection of the 4-in. Bonner Ball in Neutrons $cm^{-2}min^{-1}watt^{-1}$

Group	z = 0	z = 15.41	z = 30.85	z = 41.11	z = 51.40	z = 61.68	z = 72.00	z = 82.27	z = 90.06
1	1.73(-7)	1.52(-8)	1.24(-9)	2.33(-10)	4.23(-11)	8.03(-12)	1.56(-12)	3.27(-13)	1.02(-13)
2	3.06(-7)	2.56(-8)	1.95(-9)	3.42(-10)	6.36(-11)	1.30(-11)	2.92(-12)	7.54(-13)	2.93(-13)
3	5.94(-7)	4.59(-8)	3.10(-9)	5.06(-10)	9.12(-11)	1.86(-11)	4.42(-12)	1.21(-12)	4.99(-13)
4	8.45(-7)	5.53(-8)	3.38(-9)	5.16(-10)	9.96(-11)	2.25(-11)	6.03(-12)	1.81(-12)	7.87(-13)
5	7.93(-7)	4.53(-8)	2.79(-9)	4.21(-10)	9.64(-11)	2.47(-11)	7.32(-12)	2.31(-12)	1.03(-12)
6	1.14(-6)	5.38(-8)	3.06(-9)	4.45(-10)	1.10(-10)	2.98(-11)	9.18(-12)	2.94(-12)	1.33(-12)
7	1.15(-6)	5.95(-8)	3.65(-9)	5.43(-10)	1.27(-10)	3.38(-11)	1.00(-11)	3.17(-12)	1.42(-12)
8	1.85(-6)	1.03(-7)	6.32(-9)	9.47(-10)	1.94(-10)	4.44(-11)	1.20(-11)	3.57(-12)	1.56(-12)
9	2.23(-6)	1.55(-7)	1.06(-8)	1.66(-9)	3.22(-10)	6.89(-11)	1.70(-11)	4.81(-12)	2.03(-12)
10	2.38(-6)	2.16(-7)	1.69(-8)	2.87(-9)	5.49(-10)	1.11(-10)	2.49(-11)	6.44(-12)	2.57(-12)
11	4.09(-6)	4.35(-7)	4.00(-8)	7.74(-9)	1.53(-9)	3.03(-10)	6.20(-11)	1.37(-11)	4.66(-12)
12	5.92(-6)	6.13(-7)	5.83(-8)	1.17(-8)	2.34(-9)	4.70(-10)	9.53(-11)	2.02(-11)	6.61(-12)
13	5.09(-6)	1.02(-6)	1.50(-7)	3.97(-8)	1.04(-8)	2.63(-9)	6.62(-10)	1.66(-10)	5.85(-11)
14	4.65(-6)	1.43(-6)	3.03(-7)	1.02(-7)	3.36(-8)	1.08(-8)	3.39(-9)	1.06(-9)	4.38(-10)
15	3.96(-6)	1.34(-6)	2.98(-7)	1.03(-7)	3.48(-8)	1.15(-8)	3.67(-9)	1.17(-9)	4.92(-10)
16	3.69(-6)	2.85(-6)	1.11(-6)	5.37(-7)	2.54(-7)	1.16(-7)	5.10(-8)	2.21(-8)	1.19(-8)
17	7.28(-6)	3.01(-6)	1.05(-6)	5.07(-7)	2.43(-7)	1.13(-7)	5.08(-8)	2.30(-8)	1.22(-8)
18	8.15(-6)	2.47(-6)	7.79(-7)	3.66(-7)	1.74(-7)	8.01(-8)	3.65(-8)	1.64(-8)	8.78(-9)
19	1.15(-5)	4.97(-6)	1.79(-6)	8.83(-7)	4.34(-7)	2.05(-7)	9.55(-8)	4.37(-8)	2.40(-8)
20	1.40(-5)	7.19(-6)	3.02(-6)	1.64(-6)	8.61(-7)	4.36(-7)	2.14(-7)	1.03(-7)	5.86(-8)
21	1.21(-5)	5.57(-6)	2.40(-6)	1.31(-6)	7.08(-7)	3.65(-7)	1.82(-7)	8.84(-8)	5.11(-8)
22	1.37(-5)	4.84(-6)	1.95(-6)	1.07(-6)	5.75(-7)	2.99(-7)	1.50(-7)	7.33(-8)	4.25(-8)
23	1.39(-5)	7.04(-6)	3.04(-6)	1.70(-6)	9.45(-7)	5.03(-7)	2.58(-7)	1.29(-7)	7.58(-8)
24	2.97(-5)	1.20(-5)	5.11(-6)	2.89(-6)	1.63(-6)	8.85(-7)	4.65(-7)	2.38(-7)	1.43(-7)
25	3.75(-5)	8.92(-6)	3.26(-6)	1.79(-6)	1.01(-6)	5.46(-7)	2.90(-7)	1.48(-7)	8.93(-8)
26	3.92(-5)	1.51(-5)	6.07(-6)	3.36(-6)	1.89(-6)	1.03(-6)	5.51(-7)	2.86(-7)	1.74(-7)
27	3.27(-5)	4.21(-6)	1.55(-6)	8.53(-7)	4.79(-7)	2.60(-7)	1.39(-7)	7.12(-8)	4.34(-8)
28	2.43(-5)	2.68(-6)	9.46(-7)	5.17(-7)	2.89(-7)	1.56(-7)	8.28(-8)	4.26(-8)	2.61(-8)
29	7.54(-5)	7.88(-6)	2.16(-6)	1.14(-6)	6.36(-7)	3.44(-7)	1.83(-7)	9.48(-8)	5.79(-8)
30	6.22(-5)	5.24(-5)	2.65(-5)	1.68(-5)	1.08(-5)	6.57(-6)	3.93(-6)	2.30(-6)	1.55(-6)
31	6.45(-5)	2.50(-5)	1.07(-5)	6.45(-6)	4.03(-6)	2.44(-6)	1.44(-6)	8.46(-7)	5.69(-7)
32	1.75(-4)	2.83(-5)	9.39(-6)	5.36(-6)	3.18(-6)	1.88(-6)	1.10(-6)	6.37(-7)	4.25(-7)
33	5.18(-5)	1.61(-5)	5.30(-6)	2.97(-6)	1.74(-6)	1.02(-6)	5.96(-7)	3.42(-7)	2.28(-7)
34	1.22(-5)	8.09(-6)	2.70(-6)	1.50(-6)	8.77(-7)	5.15(-7)	3.01(-7)	1.73(-7)	1.15(-7)
35	8.30(-6)	7.32(-6)	2.53(-6)	1.41(-6)	8.18(-7)	4.79(-7)	2.80(-7)	1.60(-7)	1.07(-7)
36	1.71(-5)	6.35(-6)	2.28(-6)	1.27(-6)	7.41(-7)	4.33(-7)	2.53(-7)	1.44(-7)	9.59(-8)
37	4.35(-5)	6.85(-6)	2.48(-6)	1.37(-6)	7.99(-7)	4.68(-7)	2.73(-7)	1.56(-7)	1.04(-7)
38	9.63(-5)	6.68(-6)	2.42(-6)	1.33(-6)	7.79(-7)	4.55(-7)	2.66(-7)	1.52(-7)	1.01(-7)
39	1.69(-4)	5.86(-6)	2.13(-6)	1.18(-6)	6.91(-7)	4.03(-7)	2.35(-7)	1.35(-7)	8.95(-8)
40	3.26(-3)	3.96(-5)	6.56(-6)	3.56(-6)	2.08(-6)	1.21(-6)	7.06(-7)	4.03(-7)	2.68(-7)
41	1.29(-2)	5.93(-5)	5.91(-6)	3.18(-6)	1.85(-6)	1.08(-6)	6.33(-7)	3.61(-7)	2.39(-7)
42	3.61(-2)	2.39(-4)	6.82(-6)	3.14(-6)	1.81(-6)	1.05(-6)	6.16(-7)	3.51(-7)	2.34(-7)
43	7.95(-2)	6.64(-4)	9.68(-6)	3.07(-6)	1.70(-6)	9.91(-7)	5.77(-7)	3.29(-7)	2.20(-7)
44	1.49(-1)	1.47(-3)	1.67(-5)	3.09(-6)	1.55(-6)	9.01(-7)	5.24(-7)	2.99(-7)	1.99(-7)
45	2.43(-1)	2.68(-3)	2.94(-5)	3.29(-6)	1.37(-6)	7.86(-7)	4.58(-7)	2.61(-7)	1.74(-7)
46	3.50(-1)	4.04(-3)	4.56(-5)	3.66(-6)	1.16(-6)	6.56(-7)	3.81(-7)	2.18(-7)	1.45(-7)
47	4.47(-1)	5.08(-3)	5.87(-5)	3.92(-6)	9.45(-7)	5.14(-7)	2.99(-7)	1.71(-7)	1.13(-7)
48	5.10(-1)	5.21(-3)	6.07(-5)	3.72(-6)	7.16(-7)	3.74(-7)	2.17(-7)	1.24(-7)	8.19(-8)
49	6.64(-1)	5.19(-3)	5.84(-5)	3.48(-6)	5.96(-7)	3.00(-7)	1.74(-7)	9.89(-8)	6.56(-8)

TABLE 33. Spectral Scaling Factors for ANISN Calculations Behind 30.90 cm SS + 459.83 cm Na + z cm CS for (a) Carbon Steel Backing and (b) Lithium Hydride Backing

Group	z = 0		z = 15.41		z = 30.85		z = 41.11		z = 51.40		z = 61.68		z = 72.00		z = 82.27		z = 90.06	
	(a)	(b)	(a)	(b)	(a)	(b)	(a)	(b)	(a)	(b)	(a)	(b)	(a)	(b)	(a)	(b)	(a)	(b)
1	2.53(5)	2.61(5)	2.65(5)	2.71(5)	2.59(5)	2.65(5)	2.54(5)	2.61(5)	2.42(5)	2.59(5)	2.41(5)	2.59(5)	2.46(5)	2.53(5)	2.70(5)	2.78(5)	2.96(5)	2.71(5)
2	2.83(5)	2.87(5)	2.95(5)	2.99(5)	2.95(5)	2.97(5)	2.87(5)	2.91(5)	2.98(5)	3.16(5)	3.40(5)	3.62(5)	4.28(5)	4.32(5)	6.13(5)	6.18(5)	8.73(5)	7.80(5)
3	2.96(5)	2.99(5)	3.10(5)	3.11(5)	3.09(5)	3.09(5)	3.03(5)	3.04(5)	3.30(5)	3.47(5)	4.04(5)	4.29(5)	5.79(5)	5.76(5)	9.42(5)	9.33(5)	1.50(6)	1.30(6)
4	2.88(5)	2.91(5)	3.03(5)	3.04(5)	3.13(5)	3.11(5)	3.12(5)	3.10(5)	3.91(5)	4.09(5)	5.66(5)	5.96(5)	9.69(5)	9.48(5)	1.82(6)	1.77(6)	3.16(6)	2.68(6)
5	2.79(5)	2.81(5)	2.98(5)	2.95(5)	3.29(5)	3.22(5)	3.31(5)	3.25(5)	5.01(5)	5.18(5)	8.30(5)	8.61(5)	1.57(6)	1.52(6)	3.08(6)	2.96(6)	5.44(6)	4.58(6)
6	2.71(5)	2.75(5)	2.91(5)	2.91(5)	3.31(5)	3.27(5)	3.37(5)	3.35(5)	5.68(5)	5.97(5)	1.01(6)	1.07(6)	2.00(6)	1.97(6)	3.98(6)	3.92(6)	7.07(6)	6.13(6)
7	2.60(5)	2.71(5)	2.75(5)	2.86(5)	3.09(5)	3.20(5)	3.09(5)	3.22(5)	4.77(5)	5.28(5)	8.17(5)	9.15(5)	1.53(6)	1.60(6)	2.98(6)	3.12(6)	5.23(6)	4.83(6)
8	2.51(5)	2.71(5)	2.58(5)	2.80(5)	2.73(5)	2.96(5)	2.68(5)	2.93(5)	3.58(5)	4.16(5)	5.25(5)	6.18(5)	9.05(5)	9.94(5)	1.67(6)	1.84(6)	2.90(6)	2.81(6)
9	2.32(5)	2.69(5)	2.39(5)	2.77(5)	2.48(5)	2.88(5)	2.41(5)	2.80(5)	2.92(5)	3.59(5)	3.89(5)	4.84(5)	6.00(5)	6.98(5)	1.05(6)	1.22(6)	1.75(6)	1.79(6)
10	2.16(5)	2.66(5)	2.26(5)	2.72(5)	2.32(5)	2.77(5)	2.26(5)	2.70(5)	2.53(5)	3.17(5)	3.03(5)	3.83(5)	4.08(5)	4.85(5)	6.31(5)	7.49(5)	9.81(5)	1.02(6)
11	2.12(5)	2.68(5)	2.19(5)	2.69(5)	2.20(5)	2.66(5)	2.17(5)	2.61(5)	2.23(5)	2.78(5)	2.33(5)	2.92(5)	2.56(5)	3.04(5)	3.03(5)	3.60(5)	3.72(5)	3.90(5)
12	2.08(5)	2.70(5)	2.09(5)	2.68(5)	2.08(5)	2.62(5)	2.05(5)	2.58(5)	2.06(5)	2.68(5)	2.11(5)	2.75(5)	2.22(5)	2.76(5)	2.45(5)	3.03(5)	2.83(5)	3.09(5)
13	1.82(5)	2.67(5)	1.97(5)	2.66(5)	1.97(5)	2.58(5)	1.96(5)	2.53(5)	1.96(5)	2.57(5)	1.92(5)	2.52(5)	1.90(5)	2.41(5)	1.88(5)	2.37(5)	1.89(5)	2.14(5)
14	1.65(5)	2.61(5)	1.85(5)	2.59(5)	1.87(5)	2.50(5)	1.86(5)	2.46(5)	1.86(5)	2.46(5)	1.83(5)	2.42(5)	1.79(5)	2.32(5)	1.75(5)	2.25(5)	1.74(5)	2.03(5)
15	1.49(5)	2.62(5)	1.63(5)	2.55(5)	1.62(5)	2.45(5)	1.60(5)	2.40(5)	1.59(5)	2.40(5)	1.57(5)	2.36(5)	1.52(5)	2.24(5)	1.48(5)	2.17(5)	1.49(5)	1.97(5)
16	1.02(5)	2.58(5)	1.35(5)	2.51(5)	1.42(5)	2.41(5)	1.43(5)	2.33(5)	1.44(5)	2.32(5)	1.42(5)	2.26(5)	1.38(5)	2.15(5)	1.34(5)	2.05(5)	1.39(5)	1.90(5)
17	1.33(5)	2.72(5)	1.33(5)	2.50(5)	1.29(5)	2.35(5)	1.26(5)	2.28(5)	1.26(5)	2.25(5)	1.24(5)	2.19(5)	1.20(5)	2.08(5)	1.19(5)	2.02(5)	1.22(5)	1.82(5)
18	1.37(5)	2.73(5)	1.20(5)	2.50(5)	1.11(5)	2.33(5)	1.08(5)	2.24(5)	1.07(5)	2.22(5)	1.04(5)	2.14(5)	1.01(5)	2.05(5)	9.99(4)	1.97(5)	1.04(5)	1.79(5)
19	1.23(5)	2.69(5)	1.21(5)	2.54(5)	1.17(5)	2.36(5)	1.15(5)	2.29(5)	1.14(5)	2.26(5)	1.11(5)	2.18(5)	1.09(5)	2.08(5)	1.07(5)	1.99(5)	1.13(5)	1.82(5)
20	1.25(5)	2.81(5)	1.21(5)	2.53(5)	1.19(5)	2.34(5)	1.19(5)	2.27(5)	1.19(5)	2.22(5)	1.17(5)	2.15(5)	1.15(5)	2.04(5)	1.14(5)	1.94(5)	1.19(5)	1.78(5)
21	1.15(5)	2.68(5)	1.08(5)	2.47(5)	1.05(5)	2.28(5)	1.04(5)	2.19(5)	1.05(5)	2.16(5)	1.03(5)	2.09(5)	1.00(5)	1.98(5)	9.91(4)	1.87(5)	1.06(5)	1.73(5)
22	1.25(5)	2.72(5)	1.06(5)	2.44(5)	9.86(4)	2.23(5)	9.73(4)	2.16(5)	9.65(4)	2.11(5)	9.48(4)	2.04(5)	9.24(4)	1.93(5)	9.12(4)	1.82(5)	9.81(4)	1.68(5)
23	1.23(5)	2.90(5)	1.06(5)	2.52(5)	1.01(5)	2.30(5)	9.93(4)	2.21(5)	9.97(4)	2.17(5)	9.82(4)	2.09(5)	9.59(4)	1.99(5)	9.55(4)	1.88(5)	1.03(5)	1.73(5)
24	1.35(5)	2.63(5)	1.27(5)	2.42(5)	1.18(5)	2.21(5)	1.15(5)	2.11(5)	1.15(5)	2.06(5)	1.13(5)	1.98(5)	1.10(5)	1.87(5)	1.09(5)	1.76(5)	1.18(5)	1.63(5)
25	1.39(5)	2.98(5)	9.01(4)	2.50(5)	7.76(4)	2.24(5)	7.41(4)	2.13(5)	7.36(4)	2.09(5)	7.14(4)	1.99(5)	7.00(4)	1.89(5)	6.92(4)	1.77(5)	7.59(4)	1.64(5)
26	1.05(5)	2.54(5)	8.46(4)	2.43(5)	7.59(4)	2.19(5)	7.27(4)	2.09(5)	7.16(4)	2.05(5)	6.94(4)	1.96(5)	6.78(4)	1.84(5)	6.77(4)	1.73(5)	7.52(4)	1.60(5)
27	1.26(5)	2.91(5)	7.25(4)	2.42(5)	6.16(4)	2.15(5)	5.86(4)	2.05(5)	5.76(4)	2.02(5)	5.56(4)	1.92(5)	5.42(4)	1.80(5)	5.33(4)	1.68(5)	5.96(4)	1.55(5)
28	1.32(5)	2.98(5)	6.81(4)	2.47(5)	5.65(4)	2.20(5)	5.35(4)	2.09(5)	5.23(4)	2.04(5)	5.01(4)	1.94(5)	4.85(4)	1.75(5)	4.79(4)	1.64(5)	5.40(4)	1.53(5)
29	1.31(5)	2.75(5)	9.09(4)	2.50(5)	6.79(4)	2.15(5)	6.30(4)	2.02(5)	6.16(4)	1.98(5)	5.90(4)	1.88(5)	5.71(4)	1.76(5)	5.68(4)	1.65(5)	6.40(4)	1.53(5)
30	8.87(4)	3.66(5)	1.16(5)	2.68(5)	1.09(5)	2.37(5)	1.06(5)	2.23(5)	1.06(5)	2.18(5)	1.01(5)	2.03(5)	9.81(4)	1.86(5)	9.66(4)	1.71(5)	1.03(5)	1.58(5)
31	1.12(5)	3.10(5)	9.49(4)	2.64(5)	8.03(4)	2.31(5)	7.52(4)	2.16(5)	7.33(4)	2.11(5)	6.99(4)	1.98(5)	6.66(4)	1.78(5)	6.62(4)	1.65(5)	7.28(4)	1.52(5)
32	1.18(5)	3.15(5)	7.76(4)	2.48(5)	5.95(4)	2.06(5)	5.40(4)	1.91(5)	5.03(4)	1.85(5)	4.69(4)	1.72(5)	4.43(4)	1.52(5)	4.36(4)	1.40(5)	4.89(4)	1.29(5)
33	8.95(4)	2.88(5)	7.29(4)	2.42(5)	5.81(4)	2.02(5)	5.23(4)	1.85(5)	4.83(4)	1.77(5)	4.47(4)	1.64(5)	4.22(4)	1.45(5)	4.13(4)	1.33(5)	4.69(4)	1.23(5)
34	7.52(4)	2.55(5)	7.29(4)	2.43(5)	5.96(4)	2.04(5)	5.36(4)	1.87(5)	4.95(4)	1.78(5)	4.59(4)	1.65(5)	4.34(4)	1.46(5)	4.26(4)	1.34(5)	4.85(4)	1.24(5)
35	1.05(5)	2.54(5)	7.43(4)	2.40(5)	6.29(4)	2.03(5)	5.72(4)	1.87(5)	5.25(4)	1.77(5)	4.86(4)	1.63(5)	4.59(4)	1.46(5)	4.48(4)	1.33(5)	5.16(4)	1.23(5)
36	9.20(4)	2.60(5)	7.04(4)	2.34(5)	6.19(4)	2.00(5)	5.64(4)	1.83(5)	5.21(4)	1.73(5)	4.82(4)	1.60(5)	4.55(4)	1.43(5)	4.43(4)	1.30(5)	5.10(4)	1.20(5)
37	1.06(5)	3.05(5)	7.13(4)	2.38(5)	6.29(4)	2.05(5)	5.71(4)	1.87(5)	5.29(4)	1.77(5)	4.91(4)	1.64(5)	4.62(4)	1.46(5)	4.53(4)	1.34(5)	5.24(4)	1.23(5)
38	1.34(5)	3.28(5)	7.32(4)	2.39(5)	6.48(4)	2.05(5)	5.88(4)	1.87(5)	5.48(4)	1.78(5)	5.07(4)	1.64(5)	4.79(4)	1.47(5)	4.70(4)	1.34(5)	5.44(4)	1.24(5)
39	1.55(5)	3.41(5)	8.02(4)	2.36(5)	7.16(4)	2.03(5)	6.57(4)	1.86(5)	6.13(4)	1.76(5)	5.67(4)	1.62(5)	5.34(4)	1.45(5)	5.27(4)	1.34(5)	6.10(4)	1.23(5)
40	1.71(5)	3.90(5)	1.12(5)	2.94(5)	7.71(4)	2.07(5)	7.07(4)	1.88(5)	6.62(4)	1.78(5)	6.11(4)	1.64(5)	5.77(4)	1.47(5)	5.67(4)	1.34(5)	6.63(4)	1.24(5)
41	1.63(5)	3.88(5)	1.15(5)	3.16(5)	8.42(4)	2.07(5)	7.83(4)	1.87(5)	7.34(4)	1.81(5)	6.81(4)	1.65(5)	6.45(4)	1.47(5)	6.35(4)	1.35(5)	7.42(4)	1.24(5)
42	1.55(5)	3.71(5)	1.37(5)	3.46(5)	9.25(4)	2.21(5)	8.22(4)	1.91(5)	7.71(4)	1.82(5)	7.12(4)	1.66(5)	6.77(4)	1.49(5)	6.67(4)	1.36(5)	7.88(4)	1.26(5)
43	1.43(5)	3.50(5)	1.31(5)	3.42(5)	1.02(5)	2.48(5)	8.41(4)	1.95(5)	7.80(4)	1.85(5)	7.27(4)	1.68(5)	6.86(4)	1.50(5)	6.78(4)	1.37(5)	8.06(4)	1.27(5)
44	1.33(5)	3.32(5)	1.25(5)	3.33(5)	1.11(5)	2.76(5)	8.73(4)	2.02(5)	7.90(4)	1.88(5)	7.39(4)	1.70(5)	6.98(4)	1.50(5)	6.91(4)	1.37(5)	8.21(4)	1.27(5)
45	1.24(5)	3.13(5)	1.19(5)	3.22(5)	1.16(5)	2.94(5)	9.26(4)	2.14(5)	8.12(4)	1.91(5)	7.60(4)	1.70(5)	7.20(4)	1.50(5)	7.13(4)	1.37(5)	8.51(4)	1.27(5)
46	1.16(5)	2.98(5)	1.14(5)	3.08(5)	1.16(5)	2.99(5)	9.95(4)	2.30(5)	8.47(4)	1.94(5)	8.02(4)	1.72(5)	7.60(4)	1.50(5)	7.57(4)	1.38(5)	9.04(4)	1.27(5)
47	1.11(5)	2.83(5)	1.10(5)	2.97(5)	1.15(5)	2.96(5)	1.05(5)	2.43(5)	9.15(4)	1.98(5)	8.73(4)	1.73(5)	8.31(4)	1.51(5)	8.30(4)	1.38(5)	9.86(4)	1.27(5)
48	1.07(5)	2.71(5)	1.08(5)	2.87(5)	1.14(5)	2.92(5)	1.10(5)	2.52(5)	1.03(5)	1.87(5)	1.00(5)	1.68(5)	9.57(4)	1.52(5)	9.55(4)	1.39(5)	1.14(5)	1.28(5)
49	1.05(5)	2.60(5)	1.08(5)	2.75(5)	1.15(5)	2.84(5)	1.18(5)	2.55(5)	1.29(5)	1.81(5)	1.32(5)	1.66(5)	1.28(5)	1.56(5)	1.27(5)	1.41(5)	1.52(5)	1.30(5)

TABLE 34. 4-in. Bonner Ball Comparisons Behind 30.90 cm SS + 459.83 cm Na + z cm CS in Counts $min^{-1}watt^{-1}$

z	Calculated	Measured	Calc./meas.	Scaling factor	
				(a)	(b)
0	2.78(0)	3.17(0)	0.88	1.13(5)	2.85(5)
15.41	2.88(-2)	1.91(-2)	1.51	1.12(5)	3.00(5)
30.85	4.41(-4)	3.19(-4)	1.38	1.02(5)	2.65(5)
41.11	9.74(-5)	1.19(-4)	0.82	8.10(4)	2.09(5)
51.40	5.07(-5)	6.57(-5)	0.77	7.47(4)	1.96(5)
61.68	2.93(-5)	3.86(-5)	0.76	7.03(4)	1.81(5)
72.00	1.70(-5)	2.20(-5)	0.77	6.72(4)	1.63(5)
82.27	9.61(-6)	1.31(-5)	0.73	6.58(4)	1.50(5)
90.06	6.33(-6)	9.09(-6)	0.70	7.43(4)	1.38(5)

all the configurations except for those involving 46.56 cm. SS + 459.83 cm. Na + z cm. CS. For these latter configurations, the disagreement ranges from a factor of two overprediction for z = 30.85 cm. to a factor of three underprediction for z = 51.40 cm. and 61.68 cm.. The reason for these relatively severe disagreements may be traced to the group structure of the cross section set. From recent sensitivity studies of this experiment[16], together with the results of fine-group calculations described in a subsequent section of this report, it may be concluded that there are at least two glaring deficiencies in the 51 group structure.

The first deficiency is the course group structure below 1 keV, where the cross section weighting is 1/E. An inspection of the calculated spectra for groups 40-49 in Tables 26, 29, and 32 indicates that the spectrum approximates a 1/E shape only when $z \gtrsim 40$ cm.. For the thinner carbon steel penetrations, the spectrum approximates a $1/E^2$ dependence due to the sodium transport. The effect of the improper weighting in such a course group structure does not involve the total cross section, however, for it is essentially constant over this energy range for both sodium and iron. The effect is more subtle in that it alters the downscattering matrix, and in such a complex manner that it forbids an intuitive prediction of the changes in the group fluxes in this energy region. Thus, to calculate accurately the fluxes below 1 keV, for carbon steel thicknesses less than 40 cm., either a finer group structure than that of the 51 group set with 1/E weighting or the same 51 group structure but with a different weighting is required.

The second obvious deficiency in the 51 group structure is the courseness around the $\sim$ 300 keV minimum in the total cross section of sodium and to a less extent around the 24 keV minimum in iron. The 51 group structure is such that it does not even sense the former minimum because the minimum is confined to such a small energy region; even a $1/E\Sigma_T$ weighting (instead of 1/E) would not properly treat this minimum. The group structure does sense the iron window much more adequately, but a refinement in the energy structure in this region is probably still desirable. The effect of not

---

[16]E. M. Oblow, et al., to be published. Most of the total sensitivity tables from this analysis are shown in the Appendix of this report.

adequately treating these two minima is to make the calculated counting rates low behind the larger thicknesses of carbon steel following the sodium. Thus, to calculate accurately the fluxes below 24 keV for carbon steel thicknesses greater than about 40 cm., a finer group structure than that presently used is necessary in the vicinity of 300 keV and desirable in the vicinity of 24 keV.

Correcting these deficiencies in the 51 group structure should improve not only the agreement behind the configurations 46.56 cm. SS + 459.83 cm. Na + z cm. CS, but behind the others as well. Scaling calculations with a cross section set in an adequate group structure consisting of 171 groups were made and the results are presented in a subsequent section.

The DOT calculations based on the 51 group structure successfully predict a basic feature of the measurements - the changes in slope observed in Fig. 35 at about 40 cm. of carbon steel penetration. At shallower penetrations, the carbon steel is simply attenuating the low energy neutrons (E_n < 1 keV) leaking the sodium. At deeper penetrations the carbon steel is attenuating a quasi-equilibrium spectrum of neutrons that exists from 24 keV on down to thermal energies (see Tables 26, 29, and 32). The relaxation length through carbon steel of the very soft neutrons is considerably less than that of the neutrons penetrating at energies near the 24 keV iron window and the subsequent slowing down of these 24 keV neutrons approaches equilibrium with the 24 keV neutrons. The magnitude of the flux in the vicinity of 24 keV through the carbon steel in turn is dependent on the 300 keV window in the preceding sodium and this sensitivity increases with increasing thickness of both the stainless steel and the sodium as well as of the carbon steel[16,17].

F. 171 GROUP ANISN SCALING CALCULATIONS

A cross section set based on a group structure that more than satisfies the criteria outlined in the previous section was readily assembled to test more stringently the basic data in ENDF/IV. This set contained 171 groups

---

[17]The slope of the measured curves in Fig. 35 for z $\geq$ 50 cm. is adequately calculated by the 51 group set as shown in Tables 31 and 34. This probably indicates that the iron window is fairly well represented and that the neglect of the sodium window is responsible for the underprediction of the absolute counting rates.

with expansion through P_3, and was a fine group library processed with the MINX/SPHINX code system for DRDD and DMFE[18].

The 171 group structure contains several groups in the vicinity of the sodium and iron windows as well as three times as many groups below 1 keV as does the 51 group structure (see Appendix). The set used in the present analysis consisted of SS-304 weighted essentially as $1/E\Sigma_{T_{SS}}$, carbon steel weighted as $1/E\Sigma_{T_{Fe}}$, and sodium weighted $1/E\Sigma_{T_{Na}}$. The composition of the carbon steel did not include carbon, but the remaining elemental atomic densities in the three materials were essentially identical to those presented in Table 1. Since no aluminum cross sections were used, the scaling factors presented in the earlier tables for carbon steel backing could not be employed. Instead, ANISN calculations using both the 51 group set and the 171 group set with identical compositions were made for each of the four configurations, (46.56 cm. SS), (46.56 cm. SS + 308.99 cm. Na + 71.79 cm. CS), (46.56 cm. SS + 459.83 cm. Na + 71.84 cm. CS), and (30.90 cm. SS + 459.83 cm. Na + 100.22 cm. CS), using the source limited to the most forward angle, and the results scaled according to Eq. (2) on page 78:

$$\frac{\text{DOT(171)}}{\text{DOT(51)}} = K \cdot \frac{\text{ANISN(171)}}{\text{ANISN(51)}} \quad .$$

For those cases where ANISN(171)/ANISN(51) was < 1, the equation was amended to give:

$$\frac{\text{DOT(51)}}{\text{DOT(171)}} = K \cdot \frac{\text{ANISN(51)}}{\text{ANISN(171)}} \quad .$$

Finally, values of

$$\frac{\text{DOT(171)}}{\text{Meas.}} = \frac{\text{DOT(51)}}{\text{Meas.}} \cdot \frac{\text{DOT(171)}}{\text{DOT(51)}}$$

---

[18] C. R. Weisbin, R. W. Roussin, J. E. White, N. M. Greene, R. Q. Wright, and J. B. Wright, "The CTR Processed Multigroup Cross Section Library for Neutronics Studies," ORNL/RSIC-37 (1977).

were calculated, leading to the entries in Table 35.

If the source be given the full angular distribution in the forward hemisphere, as described earlier in footnote 13, then the ANISN ratios change slightly and yield the values appearing in Table 36. For this case,

$K \simeq 0.865$ for ANISN(A)/ANISN(B) > 1.4,

$K \simeq 0.9$ for $1.2 \leq$ ANISN(A)/ANISN(B) ≤ 1.4,

and $K \simeq 1.0$ for $1.0 \leq$ ANISN(A)/ANISN(B) < 1.2.

Comparison of the last columns in Tables 35 or 36 with the DOT(51)/meas. values presented earlier in Tables 23, 25, 28, 31, and 34 shows that the agreement with measurement is improved in almost every instance. There are still overpredictions centered around 30 cm. of carbon steel and less severe underpredictions immediately behind the sodium, but the most serious remaining disagreement is an underprediction by a factor of about 1.5 behind the larger thicknesses of carbon steel in the configurations preceded by 46.56 cm. SS + 459.83 cm. Na. For the latter case, earlier sensitivity studies indicated that recent measurements of the total cross section in the vicinity of the 300 keV window in sodium[19] would increase these counting rates by about a factor of about 1.75[20]. A more or less general increase in the sodium total cross section above 2 MeV of about 5% over ENDF/IV was also indicated in these same measurements[21], which would decrease the counting rates by a factor of about 0.75. The net increase from these two adjustments, a factor of about 1.3, would yield calc./meas. ratios in the vicinity of 0.9. A complete set of predictions using ENDF/V instead of those using ENDF/IV shown in Tables 35 or 36 will have to await the general release of ENDF/V. However, the use of the recently calculated total sensitivity tables in conjunction with knowledge of approximate changes to be incorporated in ENDF/V allows estimates to be made of the calc./meas. values using ENDF/V.

---

[19]D. C. Larson, J. A. Harvey, and N. W. Hill, "Measurement of the Neutron Total Cross Section of Sodium from 32 keV to 37 MeV," ORNL-TM-5614 (1976).

[20]E. M. Oblow, private communication.

[21]This was originally suggested from analysis of the sodium "broomstick" measurements. See R. E. Maerker and F. J. Muckenthaler, "Neutron Total Cross Section Checks for Iron, Chromium, Nickel, Stainless Steel, Sodium and Carbon," ORNL-5013 (1976).

TABLE 35. 171-Group vs. 51-Group Comparisons of the Bonner Ball Counting Rates using the Source limited to the Most Forward Angle†

Configuration	ANISN(171)/ ANISN(51)	DOT(171)/ DOT(51)††	DOT(171)/ meas.*
46.56 cm SS**	1.03	1.03	0.97
46.56 cm SS	1.07	1.07	1.07
46.56 cm SS + 154.86 cm Na	1.16	1.16	1.04
46.56 cm SS + 308.99 cm Na	1.07	1.07	0.83
46.56 cm SS + 308.99 cm Na + 15.38 cm CS	0.91	0.91	0.94
46.56 cm SS + 308.99 cm Na + 30.85 cm CS	1.28	1.15	1.30
46.56 cm SS + 308.99 cm Na + 46.24 cm CS	1.96	1.57	1.37
46.56 cm SS + 308.99 cm Na + 61.63 cm CS	2.03	1.62	1.22
46.56 cm SS + 459.83 cm Na	0.79	0.87	0.73
46.56 cm SS + 459.83 cm Na + 15.41 cm CS	0.54	0.68	1.04
46.56 cm SS + 459.83 cm Na + 30.85 cm CS	0.70	0.78	1.41
46.56 cm SS + 459.83 cm Na + 41.11 cm CS	1.91	1.53	0.70
46.56 cm SS + 459.83 cm Na + 51.40 cm CS	2.45	1.96	0.59
46.56 cm SS + 459.83 cm Na + 61.68 cm CS	2.52	2.02	0.60
30.90 cm SS + 459.83 cm Na	0.83	0.92	0.81
30.90 cm SS + 459.83 cm Na + 15.41 cm CS	0.63	0.79	1.19
30.90 cm SS + 459.83 cm Na + 30.85 cm CS	1.09	1.09	1.51
30.90 cm SS + 459.83 cm Na + 41.11 cm CS	1.67	1.34	1.10
30.90 cm SS + 459.83 cm Na + 51.40 cm CS	1.77	1.42	1.10
30.90 cm SS + 459.83 cm Na + 61.68 cm CS	1.80	1.44	1.10
30.90 cm SS + 459.83 cm Na + 72.00 cm CS	1.82	1.46	1.12
30.90 cm SS + 459.83 cm Na + 82.27 cm CS	1.85	1.48	1.08
30.90 cm SS + 459.83 cm Na + 90.06 cm CS	1.87	1.49	1.05

†All ratios are for the 4-in. Bonner ball except where otherwise noted.

††Estimated ratios, which should be accurate to about ±10%.

*Estimated ratios, which should be accurate to about ± 15% considering uncertainties in the measurements.

**12-in. Bonner ball.

TABLE 36. 171-Group vs. 51-Group Comparisons of the 4-in. Bonner Ball Counting Rates Using the Angular Distributed Source

Configuration	ANISN(171)/ ANISN(51)	DOT(171)/ DOT(51)†	DOT(171)/ Meas.*
46.56 cm. SS + 154.86 cm. Na	1.16	1.16	1.05
46.56 cm. SS + 308.99 cm. Na	1.07	1.07	0.84
46.56 cm. SS + 308.99 cm. Na + 15.38 cm. CS	0.90	0.90	0.94
46.56 cm. SS + 308.99 cm. Na + 30.85 cm. CS	1.27	1.14	1.29
46.56 cm. SS + 308.99 cm. Na + 46.24 cm. CS	2.02	1.75	1.52
46.56 cm. SS + 308.99 cm. Na + 61.63 cm. CS	2.10	1.82	1.37
46.56 cm. CS + 459.83 cm. Na	0.78	0.87	0.73
46.56 cm. SS + 459.83 cm. Na + 15.41 cm. CS	0.54	0.63	0.95
46.56 cm. SS + 459.83 cm. Na + 30.85 cm. CS	0.66	0.76	1.38
46.56 cm. SS + 459.83 cm. Na + 41.11 cm. CS	2.01	1.74	0.80
46.56 cm. SS + 459.83 cm. Na + 51.40 cm. CS	2.79	2.41	0.72
46.56 cm. SS + 459.83 cm. Na + 61.68 cm. CS	2.89	2.50	0.75
30.90 cm. SS + 459.83 cm. Na	0.83	0.92	0.80
30.90 cm. SS + 459.83 cm. Na + 15.41 cm. CS	0.61	0.71	1.07
30.90 cm. SS + 459.83 cm. Na + 30.85 cm. CS	1.03	1.03	1.42
30.90 cm. SS + 459.83 cm. Na + 41.11 cm. CS	1.75	1.51	1.24
30.90 cm. SS + 459.83 cm. Na + 51.40 cm. CS	1.89	1.64	1.26
30.90 cm. SS + 459.83 cm. Na + 61.68 cm. CS	1.92	1.66	1.26
30.90 cm. SS + 459.83 cm. Na + 72.00 cm. CS	1.94	1.68	1.30
30.90 cm. SS + 459.83 cm. Na + 82.27 cm. CS	1.97	1.70	1.25
30.90 cm. SS + 459.83 cm. Na + 90.06 cm. CS	1.99	1.72	1.20

†Estimated ratios, which should be accurate to about ± 10%.

*Estimated ratios, which should be accurate to about ± 15%.

For example, the net effect on the counting rates behind the larger thicknesses of carbon steel preceded by 30.90 cm. SS + 459.83 cm. Na is a decrease of about 25%, again yielding calc./meas. ratios in the vicinity of 0.9[22].

G. CONCLUSIONS

The first objective of a benchmark experiment is that it serve as a basis of comparison with the results of calculations using a standard design cross section set and a standard transport method, however poor the standards might be. The present experiment can be calculated well enough with the 51 group cross section set based on ENDF/IV that "bias" factors not too different from unity can be incorporated into design calculations of the upper axial shield. The 51 group calculations predict the measured neutron transmissions within about 30% for the vast majority of the configurations, failing only in the configurations containing both $\sim$ 46 cm. of stainless steel and $\sim$ 460 cm. of sodium, where the calculations overpredict the measurements by factors of up to 1.8 behind 30 cm. of carbon steel and underpredict the measurements by factors of 3.3 behind 50 cm. and 60 cm. of carbon steel, due primarily to the course group structure. Since in the present design the neutrons streaming around the upper axial shield dominate the dose on the top deck, producing of the order of ten times the dose actually penetrating the shield[23], the incorporation of a bias factor of at most 3.3 in the dose penetrating the upper axial shield would not alter the conclusion that the streaming is still dominant and would only increase the dose on the top deck by at most 20%.

---

[22]An adjustment analysis based on all the measurements and involving only the total cross sections of sodium and iron was performed by one of the authors (R. E. Maerker) by hand using the recently calculated sensitivities. The results of this analysis agree surprisingly well with those calculated by Oblow, et al., using a more sophisticated method, but disagree in several respects with the recent measurements of Larson, et al.. The adjustments for sodium indicate no correction above 3.2 MeV, a 4% increase in the region 0.30-3.2 MeV, an 18% decrease in the region that includes the window, 250-300 keV, a 7% increase in the region 4-250 keV, and a 5% decrease in the region below 1 keV. These adjustments provide agreement within $\sim$ 10% with all the experiments except for the one indicated in Table 15.

[23]W. W. Engle, Jr., private communication.

The second objective of any benchmark experiment is that it serve as a basis of comparison with the results of accurate transport calculations using as much detail in the ENDF cross sections as the results of a sensitivity analysis deem necessary. This comparison impacts directly on the basic point data, and together with a sensitivity analysis and an adjustment analysis indicates regions in the point data which are probably deficient and must be remeasured. From scaled one-dimensional calculations using a 171 group structure, still based on ENDF/IV, the general conclusion can be drawn that the agreement with experiment is improved over that provided by the 51 group structure. The agreement is within about 40% everywhere. The largest overpredictions occur behind 30 cm. of carbon steel for all sodium and stainless steel thicknesses and behind the larger thicknesses of carbon steel preceded by 46.56 cm. SS + 308.99 cm. Na. The largest underpredictions occur immediately behind the two largest thicknesses of sodium and behind the larger thicknesses of carbon steel preceded by 46.56 cm. SS + 459.83 cm. Na. This lattermost disagreement is due in large part to a poor representation of the 300 keV sodium window in ENDF/IV, for if the results of recent sodium total cross section measurements were used in this region[24], the disagreement with experiment would be greatly reduced.

---

[24]It is anticipated that these recent total cross section measurements for sodium will be incorporated into ENDF/V.

APPENDIX

TABLE A1. Listing of DOT Input for Calculation of Fluxes Through 46.56 cm. SS + 228.99 cm. Na Backed by 80 cm. Na, Starting from Interior Boundary Source

```
18 IN. SS + 10 FT. SODIUM USING XSCT 029300,IBSO 020561,BOOT 013752.
   0
61$$   0   3   11   38   135   49   5   6   81   13   0   0   64   1
   100   1   1   0   0   0   1   13   13   3   5   2   0   0   0   1
   6R0   -127   0   -18   0   1   9R0  2   1   1   6R0  8   0
62$$   1   4   3   14   1   16   1   12   1   1   8   90000   0   0
63**   0   1-3   F0   T
7* 0 -25298- 6 0 -16595- 6 0 &16595- 6 0 -57248- 6 0 -37554- 6 0 &37554- 6
   0 -89576- 6 0 -58760- 6 0 &58760- 6 0 -12192- 5 0 -79977- 6 0 &79977- 6
   0 -15413- 5 0 -10111- 5 0 &10111- 5 0 -18621- 5 0 -12215- 5 0 &12215- 5
   0 -21808- 5 0 -14306- 5 0 &14306- 5 0 -24971- 5 0 -16381- 5 0 &16381- 5
   0 -28110- 5 0 -18439- 5 0 &18439- 5 0 -31216- 5 0 -20477- 5 0 &20477- 5
   0 -34291- 5 0 -22494- 5 0 &22494- 5 0 -50167- 5 0 -43340- 5 0 -14888- 5
   0 &14888- 5 0 &43340- 5 0 -73377- 5 0 -67942- 5 0 -43340- 5 0 -14888- 5
   0 &14888- 5 0 &43340- 5 0 &67942- 5 0 -90121- 5 0 -86507- 5 0 -67941- 5
   0 -43340- 5 0 -14887- 5 0 &14887- 5 0 &43340- 5 0 &67941- 5 0 &86507- 5
   0 -98886- 5 0 -97391- 5 0 -86506- 5 0 -67941- 5 0 -43340- 5 0 -14887- 5
   0 &14887- 5 0 &43340- 5 0 &67941- 5 0 &86506- 5 0 &97391- 5 0 -22698- 5
   0 -14889- 5 0 &14889- 5 0 -50167- 5 0 -43340- 5 0 -14888- 5 0 &14888- 5
   0 &43340- 5 0 -73377- 5 0 -67942- 5 0 -43340- 5 0 -14888- 5 0 &14888- 5
   0 &43340- 5 0 &67942- 5 0 -90121- 5 0 -86507- 5 0 -67941- 5 0 -43340- 5
   0 -14887- 5 0 &14887- 5 0 &43340- 5 0 &67941- 5 0 &86507- 5 0 -98886- 5
   0 -97391- 5 0 -86506- 5 0 -87941- 5 0 -43340- 5 0 -14887- 5 0 &14887- 5
   0 &43340- 5 0 &67941- 5 0 &86506- 5 0 &97391- 5
   3R-99968- 5 3R-99836- 5 3R-99598- 5 3R-99254- 5 3R-98805- 5 3R-98251- 5
   3R-97593- 5 3R-96832- 5 3R-95968- 5 3R-95003- 5 3R-93937- 5 5R-86506- 5
   7R-67940- 5 9R-43339- 511R-14887- 5 3R&97390- 5 5R&86506- 5 7R&67940- 5
   9R&43339- 511R&14887- 5
   T
6* 0 &    0& 0 2R&19755- 8 0 &    0& 0 2R&46261- 8 0 &    0& 0 2R&72768- 8
   0 &    0& 0 2R&99024- 8 0 &    0& 0 2R&12528- 7 0 &    0& 0 2R&15129- 7
   0 &    0& 0 2R&17729- 7 0 &    0& 0 2R&20305- 7 0 &    0& 0 2R&22856- 7
   0 &    0& 0 2R&25406- 7 0 &    0& 0 2R&27907- 7 0 &    0& 0 0 &24447- 6
   2R&12924- 6 0 &24447- 6 0 &    0& 0 0 &27017- 6 0 &85519- 7 2R&19214- 6
   0 &85519- 7 0 &27017- 6 0 &    0& 0 0 &24447- 6 0 &85519- 7 0 &27474- 6
   2R&68585- 7 0 &27474- 6 0 &85519- 7 0 &24447- 6 0 &    0& 0 0 &16672- 6
   0 &12924- 6 0 &19215- 6 0 &68586- 7 2R&18229- 6 0 &68586- 7 0 &19215- 6
   0 &12924- 6 0 &16672- 6 0 &    0& 0 2R&16672- 6 0 &    0& 0 0 &24447- 6
   2R&12924- 6 0 &24447- 6 0 &    0& 0 0 &27017- 6 0 &85519- 7 2R&19214- 6
   0 &85519- 7 0 &27017- 6 0 &    0& 0 0 &24447- 6 0 &85519- 7 0 &27474- 6
   2R&68585- 7 0 &27474- 6 0 &85519- 7 0 &24447- 6 0 &    0& 0 0 &16672- 6
   0 &12924- 6 0 &19215- 6 0 &68586- 7 2R&18229- 6 0 &68586- 7 0 &19215- 6
   0 &12924- 6 0 &16672- 6
   T
```

TABLE A1. (Continued)

```
3**   F0   T
1**   F0
2**   16I   0.   16I   80.   154.13   155.40   159.50   34I   160.77
   315.63   316.90   3I   320.10   325.25   1I   325.38   327.97
   1I   328.10   330.78   2I   330.91   336.07   5I   336.20   343.90
   1I   344.39   347.07   2I   347.99   353.10   2I   353.99   359.11
   2I   359.39   364.52   2I   364.74   1I   369.90   374.54
   8I   375.49   3I   405.70   1I   421.66   2I   424.20   430.23
4**   9I   0.   48.26   1I   51.12   1I   71.44   1I   82.0   2I   86.
   1I   92.   1I   102.   1I   108.91   4I   115.   1I   160.
   1I   167.   2I   177.7   200.
5**   F1
8$$   33R1   5R2   12Q38   33R5   5R2   7Q38   33R1   5R2   12Q38
   33R3   5R2   38R4   33R3   5R2   33R1   5R2   34Q38   33R3   5R2
   17R4   21R2   17R6   21R2   3Q38   17R4   21R2   17R6   21R2   Q38
   17R4   21R2   17R6   21R2   Q38   17R4   21R2   17R6   21R2   2Q38
   17R4   21R2   17R6   21R2   5Q38   17R4   21R2   17R6   21R2   Q38
   17R4   21R2   17R6   21R2   2Q38   17R4   21R2   17R6   21R2   2Q38
   17R4   21R2   17R6   21R2   2Q38   17R4   21R2   17R6   21R2   2Q38
   12R7   26R3   Q38   38R7   9R7   29R2   2Q38   8R7   30R2   5Q38
   10R7   8   2R9   25R2   3Q38   10R10   8   2R9   25R2   Q38
   10R11   8   2R9   25R2   2Q38
9$$   -13   -1   -9   49   -13   -5   49   -5   -57   -9   -61
10$$   57   58   59   60   2Q4   49
11$$   4R0   5   6   7   8   61   62   63   64   0
12**   4R0   4R.65   4R.35   0
32$$   5   T
```

TABLE A2. Listing of DOT Input for Follow-Up Calculation From Previous Problem of Fluxes Behind 46.56 cm. SS + 459.83 cm. Na Backed by Lithium Hydride

```
18 IN. SS + 15 FT. SODIUM USING XSCT 029300,EBSO 013752, BOOT 001574.
   0
61$$   0   3   8   38   89   49   5   6   81   1   0   0   57   1
   100   1   1   0   0   6   1   13   13   3   5   2   3R0   1   8R0
   -49   0   1   9R0   2   1   1   6R0   8   0
62$$   1   4   3   14   1   16   1   12   1   1   8   90000   0   0
63**   0   1-3   F0   T
7*   (SAME AS PREVIOUS PROBLEM)
6*   (SAME AS PREVIOUS PROBLEM)
3**   F0   T
1**   F0
2**   7I   -189.83   5I   -181.83   11I   -179.83   -177.83
   2I   -177.19   1I   -162.94   17I   -161.67   -83.71   -82.44   -79.69
   15I   -78.42   -5.54   -4.27   -1.27   16I   0.0   80.0
4**   9I   0.   48.26   1I   51.12   1I   71.44   1I   82.   2I   86.
   1I   92.   1I   102.   1I   108.91   4I   115.   1I   160.
   1I   167.   2I   177.7   200.
5**   F1
8$$   17R1   7R2   11R3   3R4   25Q38   17R5   7R2   11R3   3R4
   17R6   7R2   11R3   3R4   2Q38   33R5   5R3   Q38
   33R7   5R3   17Q38   33R5   5R3   38R4   33R5   5R3
   33R8   5R3   15Q38   33R5   5R3   38R4   33R5   5R3
   33R8   5R3   16Q38
9$$   -53   -45   -1   57   -9   57   -13   -13
10$$   57
11$$   0
12**   0
32$$   7   T
```

TABLE A3. Listing of DOT Input for Follow-Up Calculation From Previous Problem of Fluxes Behind 46.56 cm. SS + 459.83 cm. Na + 15.41 cm. CS Backed by Lithium Hydride

```
18 IN. SS + 15 FT. SODIUM + 6 IN. CS USING XSCT 029300,EBS0 001574.
   0
61$$   0   3   9   38   79   49   5   6   81   1   0   0   57   1
   100   1   1   0   0   6   1   13   13   3   5   2   0   0   0   1
   10R0   1   9R0   2   1   1   6R0   8   0
62$$   1   4   3   14   1   16   4R1   8   90000   0   0
63**   0   1-3   F0   T
7*   (SAME AS TABLE A1)
6*   (SAME AS TABLE A1)
3**   F0   T
1**   F0
2**   11I   -113.86   4I   -105.86   9I   -103.86   -101.86
   2I   -101.22   8I   -88.52   -83.36   8I   -82.62   -77.51
   8I   -77.26   -72.12   1I   -70.57   15I   -69.30   0.0
4**   9I   0.   48.26   1I   51.12   1I   71.44   1I   82.   2I   86.
   1I   92.   1I   102.   1I   108.91   4I   115.   1I   160.
   1I   167.   2I   177.7   200.
5**   F1
8$$   17R1   7R2   11R3   3R4   26Q38   17R5   7R2   11R3   3R4
   17R6   7R2   11R3   3R4   2Q38
   17R9   7R2   11R3   3R4   8Q38   17R4   7R2   11R3   3R4
   17R7   7R2   11R3   3R4   8Q38   17R4   7R2   11R3   3R4
   17R7   7R2   11R3   3R4   8Q38   17R4   7R2   11R3   3R4
   33R5   5R3   Q38   33R8   5R3   15Q38
9$$   -53   -45   -1   57   -9   57   -37   -13   -37
10$$   57
11$$   0
12**   0
32$$   9   T
```

TABLE A4. Listing of ANISN Input for 51-Group Calculation of Fluxes and 4-in. Bonner Ball Counting Rate Behind 46.56 cm. SS

```
18 IN. SS,FINE MESH,USING 029300,GENERAL SCALING.
   0
15$$   1   0   3   16   1   0   0   3   62   0   51   5   6   81   0
   0   6   6   3R0   2R1   20   0   2R1   0   2R1   2R0   3   2R1   0
16**   0   0   1-4   4R0   1.   2R0   1-4   F0   T
18**   16Z   2.85+4   16Z   1.29+5   16Z   3.65+5   16Z   9.80+5
   16Z   2.06+6   16Z   3.39+6   16Z   4.19+6   16Z   4.69+6
   16Z   6.36+6   16Z   5.79+6   16Z   4.98+6   16Z   4.30+6
   16Z   3.43+6   16Z   2.74+6   16Z   2.47+6   16Z   2.52+6
   16Z   2.08+6   16Z   1.21+6   16Z   1.52+6   16Z   1.11+6
   16Z   1.17+6   16Z   8.56+5   16Z   4.95+5   16Z   1.01+6
   16Z   6.90+5   16Z   1.64+6   16Z   5.33+5   16Z   1.94+5
   16Z   7.97+5   16Z   5.34+5   16Z   4.86+5   16Z   1.63+6
   16Z   1.03+6   16Z   5.04+5   16Z   4.92+5   16Z   4.91+5
   16Z   4.89+5   16Z   4.84+5   16Z   4.78+5   16Z   1.42+6
   16Z   1.42+6   16Z   1.41+6   16Z   1.42+6   16Z   1.43+6
   16Z   1.44+6   16Z   1.77+6   16Z   1.76+6   16Z   2.10+6
   16Z   4.23+6   16Z   7.21+6   16Z   5.03+7   T
3**   F0   T
1**   F0
4**   0   59I   1.   47.56   48.56
6*          0.0          .01357623   .03112676   .04757925   .06231448
  .07479799   .08457826   .09130171   .09472531   .09472531   .09130171
  .08457826   .07479799   .06231448   .04757925   .03112676   .01357623
7*          -1.0         -.9894009   -.944575    -.8656312   -.7554044
  -.6178762   -.4580168   -.2816036   -.0950125   .0950125    .2816036
   .4580168    .6178762    .7554044    .8656312    .944575    .9894009
8$$   1   60R2   3
9$$   6   2   6
19$$   0   3   0
22$$   -1
23$$   1   T
```

TABLE A5. Listing of ANISN Input for 51-Group Calculation of Fluxes and 4-in. Bonner Ball Counting Rates Throughout the Configuration 46.56 cm. SS + 308.99 cm. Na + 71.79 cm. CS

```
18 IN. SS + 10 FT. SODIUM + 28 IN. CS,ADEQUATE MESH,USING 029300.
   0
15$$   1   0   3   16   1   0   0   11   196   0   51   5   6   81   0
   0   22   22   3R0   2R1   20   0   2R1   0   2R1   2R0   3   2R1   0
16**   0   0   1-4   4R0   1.   2R0   1-4   F0   T
18**   (SAME AS PREVIOUS PROBLEM)
3**   F0   T
1**   F0
4**   0   30I   1.   47.56   34I   48.83   203.69   204.96   205.96
   16I   207.23   16I   281.36   1I   361.36   362.63   5I   363.63
   5I   368.77   5I   373.88   379.01   5I   380.01   5I   385.17
   5I   390.28   395.48   5I   396.48   5I   401.61   5I   406.74
   411.87   5I   412.87   5I   417.97   5I   423.05   428.26
   11I   429.26   439.42
6*   (SAME AS PREVIOUS PROBLEM)
7*   (SAME AS PREVIOUS PROBLEM)
8$$   1   31R2   3   35R4   3   5   3   34R4   2R3   6   18R7   8
   18R7   9   18R7   10   18R7   11   12R7
9$$   22   2   6   10   22   22   14   4R22
19$$   0   3R3   2R0   3   4R0
22$$   -1
23$$   1   T
```

TABLE A6. Listing of ANISN Input for 51-Group Calculation of Fluxes and 4-in. Bonner Ball Counting Rates Throughout the Configuration 46.56 cm. SS + 459.83 cm. Na + 71.84 cm. CS

```
18 IN. SS + 15 FT. SODIUM + 28 IN. CS,ADEQUATE MESH,USING 029300.
   0
15$$   1   0   3   16   1   0   0   11   234   0   51   5   6   81   0
   0   22   22   3R0   2R1   20   0   2R1   0   2R1   2R0   3   2R1   0
16**   0   0   1-4   4R0   1.   2R0   1-4   F0   T
18**   (SAME AS TABLE A4)
3**   F0   T
1**   F0
4**   0   30I   1.   47.56   34I   48.83   203.69   204.96
   16I   206.23   16I   280.36   360.36   361.63   15I   362.90
   435.78   437.05   17I   438.32   1I   516.28   517.55
   5I   518.55   5I   523.69   5I   528.80   533.96
   11I   534.96   5I   545.27   550.40
   11I   551.40   561.66
   5I   562.66   5I   567.87   572.95
   5I   573.95   5I   579.09   584.23
   11I   585.23   595.39
6*   (SAME AS TABLE A4)
7*   (SAME AS TABLE A4)
8$$   1   31R2   3   35R4   2R3   34R4   2R3   16R4   2R3   18R4   2R3
   5   18R6   7   18R6   8   12R6   9   12R6   10   12R6   11   12R6
9$$   22   2   6   10   22   14   5R22
19$$   0   3R3   0   3   5R0
22$$   -1
23$$   1   T
```

TABLE A7. Listing of ANISN Input for 51-Group Calculation of Fluxes and 4-in. Bonner Ball Counting Rates Throughout the Configuration 30.90 cm. SS + 459.83 cm. Na + 100.22 cm. CS

```
12 IN. SS + 15 FT. SODIUM + 39 IN. CS,ADEQUATE MESH,USING 029300.
   0
15$$   1   0   3   16   1   0   0   14   259   0   51   5   6   81   0
   0   22   22   3R0   2R1   20   0   2R1   0   2R1   2R0   3   2R1   0
16**   0   0   1-4   4R0   1.   2R0   1-4   F0   T
18**   (SAME AS TABLE A4)
3**   F0   T
1**   F0
4**   0   2I   1.   2I   6.16   2I   11.29   2I   16.41   1I   21.52
   2I   24.2   2I   29.31   31.9   34I   33.17   1I   188.03
   34I   190.57   1I   344.70   15I   347.24   2I   420.12
   16I   422.66   500.62   501.89
   5I   502.89   5I   508.03   5I   513.14   518.30
   5I   519.30   5I   524.41   5I   529.61   534.74
   5I   535.74   5I   540.87   546.00   5I   547.00   5I   552.21
   557.29   5I   558.29   5I   563.39   568.57   5I   569.57
   5I   574.76   579.89   2I   580.89   5I   583.47   2I   588.56
   591.16   5I   592.16   2I   597.36   599.95   11I   600.95   611.11
6*   (SAME AS TABLE A4)
7*   (SAME AS TABLE A4)
8$$   1   20R2   3   35R4   2R3   35R4   2R3   16R4   3R3   17R4   3   5
   18R6   7   18R6   8   12R6   9   12R6   10   12R6   11   12R6   12   12R6   13
   9R6   14   12R6
9$$   22   2   6   10   22   14   8R22
19$$   0   3R3   0   3   8R0
22$$   -1
23$$   1   T
```

TABLE A8. Zones in ANISN Calculations for Desired Detector Responses

Configuration	Table A4	Table A5	Table A6	Table A7
46.56 cm. SS	3			
46.56 cm. SS+154.86 cm. Na		5		
46.56 cm. SS+308.99 cm. Na		6		
46.56 cm. SS+308.99 cm. Na+15.38 cm. CS		8		
46.56 cm. SS+308.99 cm. Na+30.85 cm. CS		9		
46.56 cm. SS+308.99 cm. Na+46.24 cm. CS		10		
46.56 cm. SS+308.99 cm. Na+61.63 cm. CS		11		
46.56 cm. SS+459.83 cm. Na			5	
46.56 cm. SS+459.83 cm. Na+15.41 cm. CS			7	
46.56 cm. SS+459.83 cm. Na+30.85 cm. CS			8	
46.56 cm. SS+459.83 cm. Na+41.11 cm. CS			9	
46.56 cm. SS+459.83 cm. Na+51.40 cm. CS			10	
46.56 cm. SS+459.83 cm. Na+61.68 cm. CS			11	
30.90 cm. SS+459.83 cm. Na				5
30.90 cm. SS+459.83 cm. Na+15.41 cm. CS				7
30.90 cm. SS+459.83 cm. Na+30.85 cm. CS				8
30.90 cm. SS+459.83 cm. Na+41.11 cm. CS				9
30.90 cm. SS+459.83 cm. Na+51.40 cm. CS				10
30.90 cm. SS+459.83 cm. Na+61.68 cm. CS				11
30.90 cm. SS+459.83 cm. Na+72.00 cm. CS				12
30.90 cm. SS+459.83 cm. Na+82.27 cm. CS				13
30.90 cm. SS+459.83 cm. Na+90.06 cm. CS				14

TABLE A9. Listing of AXMIX Input Preceding ANISN Input*

```
51 GROUP XSECTS,029300.
   0
1$$   51   81   81   1   0   56   0   0   1   58   0   0
2$$   1   6R0   3   T
10$$   58
11$$   0
12**   0
17$$   1   4R0   12R1   20R0   4R1   12R0   5R1   T
14**   .03953   80Z   .05098   80Z   .06531   80Z   .08255   80Z
   .1067   80Z   .1232   80Z   .1485   80Z   .1794   80Z   .2154   80Z
   .2558   80Z   .2993   80Z   .3454   80Z   .3935   80Z   .4428   80Z
   .4922   80Z   .5404   80Z   .5871   80Z   .6313   80Z   .6720   80Z
   .7090   80Z   .7420   80Z   .7717   80Z   .7853   80Z   .8218   80Z
   .8460   80Z   .8869   80Z   .9166   80Z   .9361   80Z   .9548   80Z
   .9742   80Z   .9927   80Z   1.032   80Z   1.082   80Z   1.112   80Z
   1.133   80Z   1.156   80Z   1.179   80Z   1.202   80Z   1.223   80Z
   1.259   80Z   1.290   80Z   1.273   80Z   1.236   80Z   1.303   80Z
   1.343   80Z   1.332   80Z   1.284   80Z   1.169   80Z   .7334   242Z
   T
```

---

*The purpose of using AXMIX is to produce the void cross sections and to incorporate the 4-in. Bonner ball response functions (14**) onto the cross section disc so that the counting rates could be calculated by ANISN. For the calculations described in Table A4 (behind 46.56 cm. SS) superfluous cross sections were not carried over onto the disc and the input was altered in the following arrays to:

```
 1$$   51   81   81   1   0   8   0   0   1   10   0   0
10$$   10
17$$   1   4R0   5R1   T
```

TABLE A10. Group Integrated Total Sensitivity Functions for the 4-in. Bonner Ball Behind 46.56 cm. SS + 308.99 cm. Na + z cm. CS*

		z=0		z=15.38		z=30.85		z=46.24		z=61.63	
Group	Eu	Fe	Na	Fe†	Na	Fe†	Na	Fe†	Na	Fe†	Na
1	17.333 MeV	3.80(-5)**	1.70(-6)	9.14(-5)	1.93(-5)	5.47(-4)	2.10(-4)	8.29(-4)	3.46(-4)	9.43(-4)	4.07(-4)
2	16.487	4.84(-5)	2.67(-6)	1.18(-4)	3.12(-5)	7.17(-4)	3.43(-4)	1.09(-3)	5.66(-4)	1.24(-3)	6.67(-4)
3	15.683	5.14(-5)	2.39(-6)	1.20(-4)	2.89(-5)	7.08(-4)	3.21(-4)	1.07(-3)	5.31(-4)	1.22(-3)	6.28(-4)
4	14.918	3.74(-5)	2.12(-6)	9.13(-5)	2.43(-5)	5.49(-4)	2.66(-4)	8.32(-4)	4.38(-4)	9.46(-4)	5.16(-4)
5	14.550	4.19(-5)	2.43(-6)	1.02(-4)	2.81(-5)	6.08(-4)	3.07(-4)	9.19(-4)	5.06(-4)	1.04(-3)	5.96(-4)
6	14.191	5.11(-5)	3.01(-6)	1.25(-4)	3.44(-5)	7.45(-4)	3.75(-4)	1.13(-3)	6.17(-4)	1.28(-3)	7.27(-4)
7	13.840	6.08(-5)	3.59(-6)	1.48(-4)	4.03(-5)	8.79(-4)	4.36(-4)	1.32(-3)	7.15(-4)	1.50(-3)	8.41(-4)
8	13.499	1.62(-4)	9.79(-6)	3.94(-4)	1.08(-4)	2.31(-3)	1.15(-3)	3.47(-3)	1.88(-3)	3.92(-3)	2.21(-3)
9	12.840	2.09(-4)	1.11(-5)	4.95(-4)	1.19(-4)	2.82(-3)	1.26(-3)	4.20(-3)	2.05(-3)	4.73(-3)	2.40(-3)
10	12.214	3.22(-4)	1.44(-5)	7.26(-4)	1.49(-4)	3.94(-3)	1.55(-3)	5.83(-3)	2.52(-3)	6.55(-3)	2.94(-3)
11	11.618	4.25(-4)	1.88(-5)	9.41(-4)	1.92(-4)	5.02(-3)	2.00(-3)	7.41(-3)	3.24(-3)	8.32(-3)	3.78(-3)
12	11.052	5.62(-4)	2.39(-5)	1.22(-3)	2.43(-4)	6.39(-3)	2.52(-3)	9.40(-3)	4.08(-3)	1.05(-2)	4.76(-3)
13	10.513	7.40(-4)	2.88(-5)	1.56(-3)	2.89(-4)	7.93(-3)	2.98(-3)	1.16(-2)	4.81(-3)	1.30(-2)	5.60(-3)
14	10.000	9.25(-4)	3.39(-5)	1.93(-3)	3.41(-4)	9.70(-3)	3.51(-3)	1.42(-2)	5.67(-3)	1.59(-2)	6.61(-3)
15	9.5123	1.16(-3)	4.21(-5)	2.39(-3)	4.29(-4)	1.19(-2)	4.44(-3)	1.74(-2)	7.18(-3)	1.95(-2)	8.37(-3)
16	9.0484	1.45(-3)	5.07(-5)	2.87(-3)	5.15(-4)	1.38(-2)	5.31(-3)	2.01(-2)	8.58(-3)	2.24(-2)	1.00(-2)
17	8.6071	1.76(-3)	5.65(-5)	3.32(-3)	5.63(-4)	1.50(-2)	5.77(-3)	2.16(-2)	9.30(-3)	2.40(-2)	1.08(-2)
18	8.1873	2.16(-3)	5.92(-5)	3.87(-3)	5.69(-4)	1.64(-2)	5.74(-3)	2.34(-2)	9.21(-3)	2.59(-2)	1.07(-2)
19	7.7880	2.67(-3)	6.52(-5)	4.60(-3)	6.13(-4)	1.85(-2)	6.13(-3)	2.63(-2)	9.82(-3)	2.91(-2)	1.14(-2)
20	7.4082	3.31(-3)	7.56(-5)	5.55(-3)	7.22(-4)	2.17(-2)	7.26(-3)	3.06(-2)	1.16(-2)	3.39(-2)	1.35(-2)
21	7.0469	4.08(-3)	8.69(-5)	6.65(-3)	8.39(-4)	2.48(-2)	8.48(-3)	3.49(-2)	1.36(-2)	3.85(-2)	1.58(-2)
22	6.7032	1.40(-3)	2.71(-5)	2.20(-3)	2.51(-4)	7.75(-3)	2.49(-3)	1.08(-2)	3.97(-3)	1.18(-2)	4.59(-3)
23	6.5924	2.92(-3)	5.45(-5)	4.51(-3)	5.05(-4)	1.52(-2)	5.01(-3)	2.09(-2)	7.99(-3)	2.29(-2)	9.25(-3)
24	6.3763	5.07(-3)	7.99(-5)	7.60(-3)	7.09(-4)	2.42(-2)	6.90(-3)	3.30(-2)	1.09(-2)	3.60(-2)	1.26(-2)
25	6.0653	5.89(-3)	9.08(-5)	8.55(-3)	8.25(-4)	2.57(-2)	8.10(-3)	3.48(-2)	1.29(-2)	3.79(-2)	1.49(-2)
26	5.7695	7.01(-3)	9.05(-5)	9.77(-3)	7.88(-4)	2.69(-2)	7.59(-3)	3.58(-2)	1.20(-2)	3.87(-2)	1.38(-2)
27	5.4881	6.79(-3)	8.60(-5)	9.25(-3)	7.32(-4)	2.41(-2)	6.98(-3)	3.17(-2)	1.10(-2)	3.41(-2)	1.27(-2)
28	5.2205	7.53(-3)	9.85(-5)	1.01(-2)	8.65(-4)	2.52(-2)	8.37(-3)	3.29(-2)	1.32(-2)	3.54(-2)	1.53(-2)
29	4.9659	8.46(-3)	9.72(-5)	1.11(-2)	8.38(-4)	2.62(-2)	8.03(-3)	3.37(-2)	1.27(-2)	3.61(-2)	1.46(-2)
30	4.7237	1.00(-2)	1.11(-4)	1.30(-2)	9.39(-4)	3.00(-2)	8.91(-3)	3.83(-2)	1.40(-2)	4.08(-2)	1.61(-2)

TABLE A10. (Continued)

Group	Eu	z=0		z=15.38		z=30.85		z=46.24		z=61.63	
		Fe	Na	Fe^{+}	Na	Fe^{+}	Na	Fe^{+}	Na	Fe^{+}	Na
31	4.4933	1.85(-2)	2.18(-4)	2.40(-2)	1.71(-3)	5.41(-2)	1.57(-2)	6.85(-2)	2.45(-2)	7.29(-2)	2.80(-2)
32	4.0657	2.24(-2)	2.28(-4)	2.85(-2)	1.69(-3)	6.10(-2)	1.52(-2)	7.63(-2(	2.35(-2)	8.08(-2)	2.69(-2)
33	3.6788	2.29(-2)	3.04(-4)	3.04(-2)	2.17(-3)	7.19(-2)	1.91(-2)	9.14(-2)	2.96(-2)	9.72(-2)	3.37(-2)
34	3.3287	1.23(-2)	1.88(-4)	1.65(-2)	1.39(-3)	4.03(-2)	1.24(-2)	5.15(-2)	1.92(-2)	5.48(-2)	2.19(-2)
35	3.1664	1.29(-2)	3.16(-4)	1.77(-2)	2.72(-3)	4.53(-2)	2.60(-2)	5.85(-2)	4.09(-2)	6.24(-2)	4.70(-2)
36	3.0119	1.48(-2)	2.67(-4)	1.99(-2)	1.95(-3)	4.70(-2)	1.72(-2)	5.89(-2)	2.66(-2)	6.20(-2)	3.02(-2)
37	2.8650	1.53(-2)	2.80(-4)	2.06(-2)	1.92(-3)	4.77(-2)	1.64(-2)	5.92(-2)	2.50(-2)	6.20(-2)	2.83(-2)
38	2.7253	1.64(-2)	3.80(-4)	2.24(-2)	2.60(-3)	5.12(-2)	2.20(-2)	6.29(-2)	3.36(-2)	6.57(-2)	3.79(-2)
39	2.5924	1.63(-2)	2.98(-4)	2.10(-2)	1.91(-3)	4.02(-2)	1.56(-2)	4.72(-2)	2.36(-2)	4.86(-2)	2.65(-2)
40	2.4660	1.06(-2)	1.76(-4)	1.39(-2)	1.05(-3)	2.65(-2)	8.31(-3)	3.10(-2)	1.24(-2)	3.18(-2)	1.39(-2)
41	2.3852	3.65(-3)	6.70(-5)	4.98(-3)	3.90(-4)	1.04(-2)	3.02(-3)	1.25(-2)	4.49(-3)	1.29(-2)	5.00(-3)
42	2.3653	4.17(-3)	9.23(-5)	5.83(-3)	5.15(-4)	1.29(-2)	3.89(-3)	1.57(-2)	5.74(-3)	1.62(-2)	6.38(-3)
43	2.3457	6.18(-3)	1.48(-4)	8.04(-3)	8.65(-4)	1.52(-2)	6.70(-3)	1.78(-2)	9.96(-3)	1.83(-2)	1.11(-2)
44	2.3069	1.43(-2)	3.29(-4)	1.89(-2)	1.79(-3)	3.72(-2)	1.33(-2)	4.38(-2)	1.95(-2)	4.51(-2)	2.17(-2)
45	2.2313	1.95(-2)	4.27(-4)	2.49(-2)	2.29(-3)	4.56(-2)	1.68(-2)	5.31(-2)	2.46(-2)	5.45(-2)	2.72(-2)
46	2.1225	1.67(-2)	3.72(-4)	2.06(-2)	2.01(-3)	3.58(-2)	1.48(-2)	4.13(-2)	2.17(-2)	4.24(-2)	2.40(-2)
47	2.0190	1.71(-2)	5.53(-4)	2.19(-2)	3.06(-3)	4.30(-2)	2.28(-2)	5.12(-2)	3.36(-2)	5.28(-2)	3.73(-2)
48	1.9205	1.80(-2)	1.26(-3)	2.50(-2)	7.90(-3)	5.97(-2)	6.34(-2)	7.38(-2)	9.51(-2)	7.70(-2)	1.06(-1)
49	1.8268	1.52(-2)	8.68(-4)	2.07(-2)	4.18(-3)	4.45(-2)	2.86(-2)	5.28(-2)	4.12(-2)	5.42(-2)	4.53(-2)
50	1.7377	1.40(-2)	1.18(-3)	1.99(-2)	5.81(-3)	4.51(-2)	4.02(-2)	5.38(-2)	5.81(-2)	5.52(-2)	6.38(-2)
51	1.6530	1.16(-2)	9.04(-4)	1.62(-2)	4.28(-3)	3.47(-2)	2.88(-2)	4.09(-2)	4.13(-2)	4.18(-2)	4.53(-2)
52	1.5724	9.46(-3)	1.43(-3)	1.39(-2)	7.89(-3)	3.19(-2)	5.85(-2)	3.81(-2)	8.58(-2)	3.90(-2)	9.49(-2)
53	1.4957	1.13(-2)	1.30(-3)	1.54(-2)	6.74(-3)	2.88(-2)	4.79(-2)	3.27(-2)	6.95(-2)	3.30(-2)	7.65(-2)
54	1.4227	2.16(-2)	1.75(-3)	2.91(-2)	7.49(-3)	5.20(-2)	4.68(-2)	5.80(-2)	6.61(-2)	5.82(-2)	7.18(-2)
55	1.3534	1.57(-2)	1.41(-3)	2.03(-2)	5.50(-3)	3.28(-2)	3.21(-2)	3.45(-2)	4.46(-2)	3.44(-2)	4.81(-2)
56	1.2873	1.46(-2)	1.35(-3)	1.88(-2)	5.05(-3)	2.95(-2)	2.84(-2)	3.18(-2)	3.92(-2)	3.16(-2)	4.21(-2)
57	1.2246	3.28(-2)	2.68(-3)	4.40(-2)	8.24(-3)	7.21(-2)	3.86(-2)	7.79(-2)	5.11(-2)	7.74(-2)	5.40(-2)
58	1.1648	3.11(-2)	2.71(-3)	4.07(-2)	8.10(-3)	6.29(-2)	3.66(-2)	6.70(-2)	4.81(-2)	6.64(-2)	5.05(-2)
59	1.1080	5.65(-2)	5.09(-3)	7.28(-2)	1.44(-2)	1.08(-1)	6.14(-2)	1.14(-1)	7.95(-2)	1.12(-1)	8.31(-2)
60	1.0026	2.22(-2)	2.50(-3)	2.85(-2)	7.50(-3)	4.06(-2)	3.33(-2)	4.23(-2)	4.35(-2)	4.17(-2)	4.56(-2)
61	961.64 keV	5.22(-2)	4.80(-3)	6.72(-2)	1.17(-2)	9.58(-2)	4.15(-2)	9.95(-2)	5.17(-2)	9.81(-2)	5.33(-2)
62	907.18	2.76(-2)	3.74(-3)	3.46(-2)	9.34(-3)	4.66(-2)	3.39(-2)	4.78(-2)	4.25(-2)	4.71(-2)	4.39(-2)
63	862.94	3.06(-2)	5.25(-3)	4.09(-2)	1.27(-2)	6.01(-2)	4.40(-2)	6.26(-2)	5.47(-2)	6.17(-2)	5.63(-2)

TABLE A10. (Continued)

Group	Eu	z=0		z=15.38		z=30.85		z=46.24		z=61.63	
		Fe	Na	Fe^+	Na	Fe^+	Na	Fe^+	Na	Fe^+	Na
64	820.85	1.79(-2)	2.81(-3)	2.35(-2)	6.51(-3)	3.31(-2)	2.16(-2)	3.41(-2)	2.66(-2)	3.35(-2)	2.73(-2)
65	780.82	1.15(-2)	2.99(-3)	1.54(-2)	7.13(-3)	2.20(-2)	2.45(-2)	2.27(-2)	3.04(-2)	2.24(-2)	3.13(-2)
66	742.74	3.07(-2)	2.38(-3)	4.02(-2)	4.95(-3)	5.59(-2)	1.45(-2)	5.73(-2)	1.74(-2)	5.63(-2)	1.78(-2)
67	706.51	3.60(-2)	2.94(-3)	4.75(-2)	5.88(-3)	6.66(-2)	1.62(-2)	6.84(-2)	1.93(-2)	6.73(-2)	1.96(-2)
68	672.06	3.46(-2)	5.81(-3)	4.55(-2)	1.19(-2)	6,38(-2)	3.31(-2)	6.57(-2)	3.92(-2)	6.47(-2)	3.97(-2)
69	639.28	3.21(-2)	7.67(-3)	4.25(-2)	1.60(-2)	5.98(-2)	4.45(-2)	6.16(-2)	5.25(-2)	6.07(-2)	5.31(-2)
70	608.10	5.14(-2)	8.06(-3)	6.73(-2)	1.63(-2)	9.15(-2)	4.29(-2)	9.33(-2)	4.99(-2)	9.17(-2)	5.03(-2)
71	578.44	3.60(-2)	1.03(-2)	4.70(-2)	2.25(-2)	6.33(-2)	6.55(-2)	6.45(-2)	7.76(-2)	6.34(-2)	7.84(-2)
72	550.23	3.90(-2)	1.87(-2)	5.25(-2)	4.67(-2)	7.57(-2)	1.61(-1)	7.84(-2)	1.98(-1)	7.73(-2)	2.02(-1)
73	523.40	3.12(-2)	3.70(-2)	4.50(-2)	1.22(-1)	7.83(-2)	5.88(-1)	8.57(-2)	7.75(-1)	8.56(-2)	8.15(-1)
74	497.87	6.17(-2)	5.44(-2)	7.94(-2)	1.44(-1)	9.72(-2)	5.34(-1)	9.56(-2)	6.62(-1)	9.34(-2)	6.78(-1)
75	450.49	2.36(-2)	2.93(-2)	2.83(-2)	7.14(-2)	2.75(-2)	2.32(-1)	2.53(-2)	2.80(-1)	2.46(-2)	2.84(-1)
76	407.62	1.35(-2)	8.87(-3)	1.55(-2)	1.95(-2)	1.32(-2)	5.56(-2)	1.16(-2)	6.53(-2)	1.12(-2)	6.58(-2)
77	387.74	3.25(-2)	1.89(-2)	3.62(-2)	4.00(-2)	3.01(-2)	1.08(-1)	2.67(-2)	1.26(-1)	2.64(-2)	1.26(-1)
78	368.83	6.03(-2)	5.98(-2)	6.70(-2)	1.32(-1)	5.50(-2)	3.81(-1)	4.90(-2)	4.49(-1)	4.87(-2)	4.52(-1)
79	333.73	9.25(-2)	7.66(-2)	9.92(-2)	1.53(-1)	7.35(-2)	3.83(-1)	6.41(-2)	4.41(-1)	6.50(-2)	4.42(-1)
80	301.97	1.15(-2)	4.28(-3)	1.23(-2)	7.94(-3)	1.12(-2)	1.88(-2)	1.10(-2)	2.18(-2)	1.12(-2)	2.20(-2)
81	298.50	3.96(-3)	3.60(-3)	4.44(-3)	7.55(-3)	4.60(-3)	2.09(-2)	4.68(-3)	2.47(-2)	4.78(-3)	2.50(-2)
82	297.20	9.35(-3)	3.61(-2)	1.43(-2)	1.55(-1)	3.65(-2)	9.71(-1)	4.73(-2)	1.36(0)	5.08(-2)	1.48(0)
83	294.52	1.24(-2)	3.48(-2)	1.36(-2)	9.30(-2)	1.10(-2)	3.49(-1)	1.05(-2)	4.36(-1)	1.10(-2)	4.47(-1)
84	287.25	1.74(-2)	3.88(-2)	1.75(-2)	8.89(-2)	9.52(-3)	2.64(-1)	7.64(-3)	3.13(-1)	8.23(-3)	3.15(-1)
85	273.24	3.31(-2)	4.64(-2)	3.10(-2)	9.34(-2)	1.42(-2)	2.23(-1)	1.19(-2)	2.52(-1)	1.40(-2)	2.50(-1)
86	247.24	1.42(-2)	1.39(-2)	1.28(-2)	2.52(-2)	5.38(-3)	5.15(-2)	4.46(-3)	5.65(-2)	5.34(-3)	5.60(-2)
87	235.18	1.56(-2)	2.18(-2)	1.43(-2)	4.25(-2)	5.39(-3)	9.78(-2)	3.13(-3)	1.10(-1)	3.25(-3)	1.09(-1)
88	223.71	1.58(-2)	1.49(-2)	1.39(-2)	2.73(-2)	6.23(-3)	5.77(-2)	6.59(-3)	6.41(-2)	8.63(-3)	6.39(-2)
89	212.80	8.26(-3)	1.15(-2)	7.29(-3)	2.15(-2)	2.77(-3)	4.60(-2)	1.91(-3)	5.09(-2)	2.14(-3)	5.05(-2)
90	202.42	6.35(-3)	2.69(-2)	5.85(-3)	5.55(-2)	2.43(-3)	1.37(-1)	1.64(-3)	1.56(-1)	1.75(-3)	1.55(-1)
91	192.55	1.07(-2)	3.55(-2)	9.73(-3)	7.29(-2)	5.50(-3)	1.82(-1)	6.41(-3)	2.07(-1)	8.14(-3)	2.06(-1)
92	183.16	1.79(-2)	3.89(-2)	1.57(-2)	7.69(-2)	6.81(-3)	1.82(-1)	6.66(-3)	2.06(-1)	8.51(-3)	2.05(-1)
93	174.22	1.02(-2)	3.55(-2)	8.98(-3)	7.12(-2)	5.92(-3)	1.72(-1)	9.60(-3)	1.95(-1)	1.36(-2)	1.94(-1)
94	165.73	6.60(-3)	3.30(-2)	5.75(-3)	6.66(-2)	3.52(-3)	1.60(-1)	4.68(-3)	1.80(-1)	6.11(-3)	1.79(-1)
95	157.64	7.17(-3)	3.06(-2)	6.15(-3)	6.18(-2)	2.86(-3)	1.47(-1)	2.87(-3)	1.65(-1)	3.51(-3)	1.63(-1)

TABLE A10. (Continued)

Group	Eu	z=0		z=15.38		z=30.85		z=46.24		z=61.63	
		Fe	Na	Fe^+	Na	Fe^+	Na	Fe^+	Na	Fe^+	Na
96	149.96	1.82(-3)	2.87(-2)	1.62(-3)	5.92(-2)	7.62(-4)	1.44(-1)	6.30(-4)	1.62(-1)	6.85(-4)	1.60(-1)
97	142.64	9.65(-3)	3.38(-2)	7.97(-3)	6.47(-2)	7.87(-3)	1.48(-1)	2.06(-2)	1.68(-1)	3.44(-2)	1.68(-1)
98	135.69	2.20(-2)	3.52(-2)	1.78(-2)	6.64(-2)	5.69(-3)	1.45(-1)	3.80(-3)	1.60(-1)	4.34(-3)	1.58(-1)
99	129.07	1.37(-2)	3.55(-2)	1.09(-2)	6.67(-2)	7.73(-3)	1.46(-1)	1.40(-2)	1.62(-1)	2.00(-2)	1.61(-1)
100	122.77	2.02(-2)	3.57(-2)	1.59(-2)	6.64(-2)	6.95(-3)	1.41(-1)	7.89(-3)	1.54(-1)	1.02(-2)	1.51(-1)
101	116.79	9.20(-3)	3.32(-2)	7.31(-3)	6.39(-2)	4.18(-3)	1.40(-1)	5.28(-3)	1.53(-1)	6.68(-3)	1.50(-1)
102	111.09	5.61(-3)	7.78(-2)	4.71(-3)	1.55(-1)	7.05(-3)	3.53(-1)	1.13(-2)	3.88(-1)	1.43(-2)	3.80(-1)
103	98.037	1.50(-2)	8.15(-2)	1.16(-2)	1.56(-1)	6.05(-3)	3.39(-1)	7.01(-3)	3.69(-1)	8.60(-3)	3.59(-1)
104	86.517	2.68(-3)	2.91(-2)	2.06(-3)	5.64(-2)	6.11(-4)	1.22(-1)	3.65(-4)	1.32(-1)	4.04(-4)	1.28(-1)
105	82.500	2.05(-2)	3.04(-2)	1.47(-2)	5.14(-2)	1.34(-2)	1.02(-1)	2.83(-2)	1.13(-1)	4.19(-2)	1.13(-1)
106	79.500	1.21(-2)	6.48(-2)	8.97(-3)	1.21(-1)	6.74(-3)	2.48(-1)	9.22(-3)	2.66(-1)	1.14(-2)	2.57(-1)
107	72.000	9.89(-3)	4.37(-2)	7.26(-3)	7.98(-2)	1.15(-2)	1.62(-1)	1.97(-2)	1.75(-1)	2.59(-2)	1.17(-1)
108	67.379	2.42(-2)	1.02(-1)	1.74(-2)	1.85(-1)	1.68(-2)	3.69(-1)	2.53(-2)	3.93(-1)	3.22(-2)	3.80(-1)
109	56.562	4.55(-3)	6.09(-3)	3.04(-3)	1.01(-2)	2.46(-3)	1.72(-2)	3.53(-3)	1.79(-2)	4.58(-3)	1.73(-2)
110	52.475	1.16(-2)	5.21(-2)	8.12(-3)	8.91(-2)	8.62(-3)	1.62(-1)	1.36(-2)	1.69(-1)	1.75(-2)	1.62(-1)
111	46.309	1.35(-2)	7.93(-2)	9.27(-3)	1.43(-1)	9.38(-3)	2.79(-1)	1.54(-2)	2.92(-1)	1.96(-2)	2.78(-1)
112	40.868	8.33(-3)	1.06(-1)	5.90(-3)	1.95(-1)	8.92(-3)	3.85(-1)	1.61(-2)	4.00(-1)	2.04(-2)	3.79(-1)
113	34.307	2.32(-3)	4.34(-2)	1.58(-3)	7.90(-2)	1.59(-3)	1.52(-1)	3.11(-3)	1.56(-1)	4.19(-3)	1.47(-1)
114	31.828	3.36(-4)	6.07(-2)	3.45(-4)	1.12(-1)	1.91(-3)	2.14(-1)	3.94(-3)	2.14(-1)	5.11(-3)	1.97(-1)
115	28.500	1.74(-4)	2.95(-2)	1.04(-4)	5.36(-2)	9.91(-5)	9.65(-2)	4.36(-4)	9.13(-2)	7.37(-4)	8.10(-2)
116	27.000	1.09(-3)	2.06(-2)	5.83(-4)	3.56(-2)	-1.87(-3)	6.06(-2)	-3.71(-3)	5.87(-2)	-4.53(-3)	5.46(-2)
117	26.058	7.15(-3)	3.39(-2)	5.10(-3)	5.34(-2)	3.71(-2)	9.69(-2)	1.02(-1)	1.15(-1)	1.59(-1)	1.24(-1)
118	24.788	2.13(-3)	1.71(-2)	1.22(-3)	2.67(-2)	8.95(-3)	5.83(-2)	5.37(-2)	8.65(-2)	1.24(-1)	1.06(-1)
119	24.176	1.19(-3)	1.60(-2)	6.44(-4)	2.62(-2)	7.82(-3)	6.13(-2)	4.82(-2)	8.56(-2)	1.10(-1)	9.62(-2)
120	23.579	4.67(-3)	4.52(-2)	2.94(-3)	7.74(-2)	3.85(-2)	1.81(-1)	1.53(-1)	2.10(-1)	2.84(-1)	1.94(-1)
121	21.875	4.72(-3)	6.99(-2)	4.09(-3)	1.24(-1)	8.15(-2)	2.55(-1)	2.35(-1)	2.20(-1)	3.53(-1)	1.50(-1)
122	19.305	1.11(-3)	1.27(-1)	5.75(-3)	2.28(-1)	1.63(-1)	3.59(-1)	3.20(-1)	1.94(-1)	3.68(-1)	8.29(-2)
123	15.034	3.01(-3)	1.12(-1)	8.54(-3)	1.90(-1)	1.37(-1)	1.89(-1)	1.88(-1)	4.97(-2)	1.79(-1)	9.71(-3)
124	11.709	4.91(-3)	8.94(-2)	8.83(-3)	1.45(-1)	7.31(-2)	9.86(-2)	7.49(-2)	1.32(-2)	6.70(-2)	1.21(-3)
125	9.1188	1.33(-3)	6.37(-2)	2.89(-3)	9.75(-2)	1.94(-2)	4.90(-2)	1.92(-2)	4.15(-3)	1.80(-2)	2.68(-4)

TABLE A10. (Continued)

Group	Eu	z=0		z=15.38		z=30.85		z=46.24		z=61.63	
		Fe	Na	Fe^{+}	Na	Fe^{+}	Na	Fe^{+}	Na	Fe^{+}	Na
126	7.1017	8.83(-4)	3.68(-2)	4.76(-3)	5.61(-2)	5.35(-2)	2.98(-2)	5.65(-2)	2.77(-3)	5.18(-2)	1.87(-4)
127	5.5308	8.19(-4)	1.39(-2)	4.58(-3)	2.18(-2)	7.02(-2)	1.41(-2)	7.52(-2)	1.49(-3)	6.70(-2)	9.71(-5)
128	4.3074	6.06(-4)	1.06(-3)	1.98(-3)	1.64(-3)	2.90(-2)	1.59(-3)	3.13(-2)	1.23(-4)	2.86(-2)	6.69(-6)
129	3.7074	6.42(-4)	-1.68(-3)	1.40(-3)	-2.31(-3)	2.27(-2)	-8.23(-4)	2.47(-2)	-9.76(-6)	2.25(-2)	1.41(-6)
130	3.3546	8.43(-4)	-2.27(-3)	1.14(-3)	-2.44(-3)	2.10(-2)	-1.46(-3)	2.31(-2)	-7.41(-5)	2.11(-2)	-1.71(-6)
131	3.0354	4.02(-4)	4.47(-3)	1.44(-3)	4.13(-3)	1.95(-2)	9.23(-4)	2.15(-2)	5.25(-6)	1.97(-2)	-8.06(-7)
132	2.7465	1.83(-4)	1.99(-3)	5.78(-4)	2.53(-3)	9.27(-3)	1.03(-3)	1.02(-2)	5.33(-5)	9.37(-3)	1.57(-6)
133	2.6126	1.39(-4)	9.98(-4)	5.22(-4)	1.22(-3)	8.94(-3)	7.12(-4)	9.81(-3)	4.62(-5)	9.03(-3)	1.56(-6)
134	2.4852	1.96(-4)	1.01(-3)	1.07(-3)	1.44(-3)	1.71(-2)	1.23(-3)	1.86(-2)	7.51(-5)	1.71(-2)	2.25(-6)
135	2.2487	4.50(-4)	1.98(-3)	1.36(-3)	3.23(-3)	1.64(-2)	1.62(-3)	1.75(-2)	8.26(-5)	1.61(-2)	2.20(-6)
136	2.0347	1.70(-3)	3.67(-2)	5.31(-3)	5.43(-2)	3.96(-2)	2.02(-2)	3.89(-2)	7.10(-4)	3.55(-2)	1.39(-5)
137	1.5846	3.22(-3)	1.06(-1)	8.09(-3)	1.58(-1)	3.90(-2)	5.44(-2)	3.45(-2)	1.58(-3)	3.13(-2)	2.38(-5)
138	1.2341	3.55(-3)	1.62(-1)	1.06(-2)	2.45(-1)	3.66(-2)	8.21(-2)	2.87(-2)	2.17(-3)	2.59(-2)	2.83(-5)
139	961.12 eV	2.81(-3)	2.02(-1)	1.61(-2)	3.11(-1)	4.43(-2)	1.03(-1)	2.88(-2)	2.60(-3)	2.54(-2)	3.11(-5)
140	748.52	2.65(-3)	2.20(-1)	2.11(-2)	3.35(-1)	4.71(-2)	1.06(-1)	2.65(-2)	2.42(-3)	2.31(-2)	2.56(-5)
141	582.95	2.26(-3)	2.28(-1)	2.70(-2)	3.42(-1)	5.10(-2)	1.02(-1)	2.48(-2)	2.14(-3)	2.14(-2)	2.02(-5)
142	454.00	4.96(-4)	2.32(-1)	3.39(-2)	3.41(-1)	5.61(-2)	9.62(-2)	2.39(-2)	1.84(-3)	2.04(-2)	1.56(-5)
143	353.58	5.23(-4)	2.36(-1)	4.28(-2)	3.37(-1)	6.17(-2)	8.90(-2)	2.29(-2)	1.56(-3)	1.94(-2)	1.18(-5)
144	275.36	1.13(-3)	2.38(-1)	5.34(-2)	3.28(-1)	6.81(-2)	8.11(-2)	2.22(-2)	1.29(-3)	1.85(-2)	8.81(-6)
145	214.45	9.91(-4)	2.37(-1)	6.55(-2)	3.16(-1)	7.52(-2)	7.24(-2)	2.17(-2)	1.04(-3)	1.79(-2)	6.42(-6)
146	167.02	8.07(-4)	2.37(-1)	7.94(-2)	3.03(-1)	8.28(-2)	6.40(-2)	2.12(-2)	8.33(-4)	1.72(-2)	4.59(-6)
147	130.07	6.39(-4)	2.35(-1)	9.46(-2)	2.87(-1)	9.00(-2)	5.54(-2)	2.00(-2)	6.47(-4)	1.59(-2)	3.18(-6)
148	101.30	4.93(-4)	2.31(-1)	1.11(-1)	2.69(-1)	9.64(-2)	4.70(-2)	1.83(-2)	4.89(-4)	1.42(-2)	2.13(-6)
149	78.893	3.72(-4)	2.30(-1)	1.31(-1)	2.49(-1)	1.05(-1)	3.91(-2)	1.87(-2)	3.59(-4)	1.45(-2)	1.38(-6)
150	61.442	2.74(-4)	2.27(-1)	1.50(-1)	2.28(-1)	1.11(-1)	3.18(-2)	1.85(-2)	2.56(-4)	1.42(-2)	8.63(-7)
151	47.851	1.97(-4)	2.23(-1)	1.69(-1)	2.06(-1)	1.17(-1)	2.53(-2)	1.78(-2)	1.77(-4)	1.35(-2)	5.19(-7)
152	37.267	1.34(-4)	2.12(-1)	1.82(-1)	1.79(-1)	1.17(-1)	1.91(-2)	1.67(-2)	1.15(-4)	1.25(-2)	2.91(-7)
153	29.203	9.67(-5)	2.16(-1)	2.09(-1)	1.66(-1)	1.26(-1)	1.53(-2)	1.63(-2)	7.91(-5)	1.20(-2)	1.73(-7)
154	22.603	6.16(-5)	2.07(-1)	2.20(-1)	1.39(-1)	1.24(-1)	1.08(-2)	1.55(-2)	4.68(-5)	1.13(-2)	8.66(-8)
155	17.603	3.91(-5)	2.00(-1)	2.32(-1)	1.18(-1)	1.24(-1)	7.64(-3)	1.46(-2)	2.76(-5)	1.05(-2)	4.32(-8)

TABLE A10. (Continued)

Group	Eu	z=0		z=15.38		z=30.85		z=46.24		z=61.63	
		Fe	Na	Fe†	Na	Fe†	Na	Fe†	Na	Fe†	Na
156	13.710	2.40(-5)	1.92(-1)	2.41(-1)	9.75(-2)	1.21(-1)	5.21(-3)	1.36(-2)	1.56(-5)	9.67(-3)	2.04(-8)
157	10.677	1.40(-5)	1.82(-1)	2.45(-1)	7.81(-2)	1.17(-1)	3.38(-3)	1.25(-2)	8.23(-6)	8.77(-3)	8.94(-9)
158	8.3153	7.83(-6)	1.72(-1)	2.44(-1)	6.13(-2)	1.11(-1)	2.11(-3)	1.14(-2)	4.14(-6)	7.87(-3)	3.70(-9)
159	6.4760	4.15(-6)	1.61(-1)	2.38(-1)	4.65(-2)	1.04(-1)	1.25(-3)	1.02(-2)	1.95(-6)	6.95(-3)	1.42(-9)
160	5.0435	2.09(-6)	1.50(-1)	2.27(-1)	3.40(-2)	9.51(-2)	6.97(-4)	9.04(-3)	8.53(-7)	6.05(-3)	5.00(-10)
161	3.9279	9.89(-7)	1.38(-1)	2.11(-1)	2.39(-2)	8.53(-2)	3.64(-4)	7.87(-3)	3.44(-7)	5.17(-3)	1.61(-10)
162	3.0590	4.42(-7)	1.28(-1)	1.94(-1)	1.62(-2)	7.60(-2)	1.79(-4)	6.80(-3)	1.29(-7)	4.39(-3)	4.74(-11)
163	2.3724	1.71(-7)	1.11(-1)	1.64(-1)	9.69(-3)	6.22(-2)	7.50(-5)	5.46(-3)	3.98(-8)	3.47(-3)	1.12(-11)
164	1.8554	6.46(-8)	9.90(-2)	1.40(-1)	5.74(-3)	5.20(-2)	3.08(-5)	4.47(-3)	1.21(-8)	2.79(-3)	2.65(-12)
165	1.4450	2.08(-8)	8.48(-2)	1.12(-1)	2.99(-3)	4.08(-2)	1.06(-5)	3.44(-3)	3.01(-9)	2.12(-3)	4.99(-13)
166	1.1254	5.72(-9)	6.96(-2)	8.37(-2)	1.36(-3)	3.00(-2)	3.10(-6)	2.51(-3)	6.18(-10)	1.52(-3)	7.62(-14)
167	0.87642	1.25(-9)	5.27(-2)	5.65(-2)	5.04(-4)	2.00(-2)	7.04(-7)	1.67(-3)	9.66(-11)	1.00(-3)	8.70(-15)
168	0.68256	2.03(-10)	3.57(-2)	3.29(-2)	1.39(-4)	1.16(-2)	1.13(-7)	9.67(-4)	1.04(-11)	5.78(-4)	6.73(-16)
169	0.53158	1.92(-11)	1.80(-2)	1.37(-2)	2.15(-5)	4.77(-3)	9.77(-9)	4.07(-4)	5.86(-13)	2.45(-4)	2.67(-17)
	0.41399										
Integral		1.7754	8.1857	6.1671	10.210	6.4445	13.282	5.5510	13.794	6.0583	13.748
Elastic		1.3165	7.7590	4.8433	9.934	4.8120	12.712	3.8895	13.023	4.3266	12.901
Inelastic		0.3988	0.0265	0.5487	0.093	1.1442	0.527	1.3826	0.751	1.4417	0.826

*Tabulated values are of the quantity: $-\frac{\Delta R}{R} / \frac{\Delta \Sigma_T}{\Sigma_T}$.

†Includes the iron in both the stainless and carbon steels. The two may be approximately separated by ascribing all the sensitivity above ∿ 500 keV to the stainless steel and below ∿ 500 keV to the carbon steel.

**Read as 3.80×10^{-5}, etc..

TABLE A11. Group Integrated Total Sensitivity Functions for the 4-in. Bonner Ball Behind 46.56 cm. SS + 459.83 cm. Na + z cm. CS*

	z=0		z=15.41		z=30.85		z=41.11		z=51.40		z=61.68	
Group	Fe	Na	Fe†	Na	Fe†	Na	Fe†	Na	Fe†	Na	Fe†	Na
1	6.61(-5)**	1.05(-5)	2.61(-4)	1.25(-4)	3.97(-3)	2.81(-3)	6.25(-3)	4.56(-3)	6.78(-3)	5.02(-3)	7.06(-3)	5.28(-3)
2	8.54(-5)	1.70(-5)	3.44(-4)	2.12(-4)	5.28(-3)	4.86(-3)	8.32(-3)	7.92(-3)	9.03(-3)	8.74(-3)	9.41(-3)	9.20(-3)
3	8.78(-5)	1.58(-5)	3.39(-4)	2.08(-4)	5.11(-3)	4.84(-3)	8.04(-3)	7.92(-3)	8.72(-3)	8.76(-3)	9.08(-3)	9.23(-3)
4	6.58(-5)	1.33(-5)	2.59(-4)	1.64(-4)	3.89(-3)	3.72(-3)	6.11(-3)	6.06(-3)	6.62(-3)	6.68(-3)	6.89(-3)	7.03(-3)
5	7.35(-5)	1.53(-5)	2.84(-4)	1.89(-4)	4.19(-3)	4.30(-3)	6.56(-3)	7.01(-3)	7.10(-3)	7.73(-3)	7.39(-3)	8.13(-3)
6	9.00(-5)	1.88(-5)	3.44(-4)	2.28(-4)	5.00(-3)	5.15(-3)	7.81(-3)	8.38(-3)	8.44(-3)	9.23(-3)	8.78(-3)	9.71(-3)
7	1.07(-4)	2.20(-5)	4.01(-4)	2.60(-4)	5.68(-3)	5.77(-3)	8.84(-3)	9.36(-3)	9.55(-3)	1.03(-2)	9.91(-3)	1.08(-2)
8	2.84(-4)	5.88(-5)	1.04(-3)	6.71(-4)	1.43(-2)	1.47(-2)	2.23(-2)	2.38(-2)	2.40(-2)	2.61(-2)	2.49(-2)	2.74(-2)
9	3.61(-4)	6.51(-5)	1.24(-3)	7.19(-4)	1.64(-2)	1.54(-2)	2.53(-2)	2.49(-2)	2.72(-2)	2.73(-2)	2.81(-2)	2.86(-2)
10	5.37(-4)	8.18(-5)	1.72(-3)	8.52(-4)	2.14(-2)	1.78(-2)	3.29(-2)	2.86(-2)	3.53(-2)	3.13(-2)	3.65(-2)	3.27(-2)
11	7.00(-4)	1.06(-4)	2.19(-3)	1.09(-3)	2.66(-2)	2.25(-2)	4.08(-2)	3.61(-2)	4.37(-2)	3.94(-2)	4.51(-2)	4.13(-2)
12	9.14(-4)	1.34(-4)	2.78(-3)	1.36(-3)	3.30(-2)	2.80(-2)	5.05(-2)	4.49(-2)	5.41(-2)	4.91(-2)	5.59(-2)	5.13(-2)
13	1.18(-3)	1.59(-4)	3.45(-3)	1.58(-3)	3.97(-2)	3.21(-2)	6.05(-2)	5.13(-2)	6.47(-2)	5.60(-2)	6.68(-2)	5.85(-2)
14	1.46(-3)	1.87(-4)	4.26(-3)	1.87(-3)	4.90(-2)	3.80(-2)	7.48(-2)	6.07(-2)	8.00(-2)	6.62(-2)	8.26(-2)	6.92(-2)
15	1.82(-3)	2.36(-4)	5.27(-3)	2.39(-3)	6.07(-2)	4.90(-2)	9.27(-2)	7.84(-2)	9.92(-2)	8.56(-2)	1.02(-1)	8.95(-2)
16	2.22(-3)	2.83(-4)	6.14(-3)	2.86(-3)	6.86(-2)	5.85(-2)	1.05(-1)	9.36(-2)	1.12(-1)	1.02(-1)	1.15(-1)	1.07(-1)
17	2.61(-3)	3.10(-4)	6.71(-3)	3.07(-3)	7.03(-2)	6.23(-2)	1.07(-1)	9.96(-2)	1.14(-1)	1.09(-1)	1.17(-1)	1.13(-1)
18	3.11(-3)	3.13(-4)	7.40(-3)	2.94(-3)	7.20(-2)	5.82(-2)	1.09(-1)	9.26(-2)	1.16(-1)	1.01(-1)	1.19(-1)	1.05(-1)
19	3.74(-3)	3.38(-4)	8.48(-3)	3.08(-3)	7.85(-2)	6.01(-2)	1.18(-1)	9.56(-2)	1.26(-1)	1.04(-1)	1.29(-1)	1.08(-1)
20	4.56(-3)	3.98(-4)	1.00(-2)	3.71(-3)	9.02(-2)	7.29(-2)	1.35(-1)	1.16(-1)	1.44(-1)	1.26(-1)	1.48(-1)	1.32(-1)
21	5.52(-3)	4.62(-4)	1.16(-2)	4.35(-3)	9.85(-2)	8.57(-2)	1.47(-1)	1.36(-1)	1.56(-1)	1.48(-1)	1.60(-1)	1.55(-1)
22	1.85(-3)	1.37(-4)	3.62(-3)	1.20(-3)	2.75(-2)	2.29(-2)	4.05(-2)	3.62(-2)	4.28(-2)	3.92(-2)	4.39(-2)	4.08(-2)
23	3.82(-3)	2.77(-4)	7.19(-3)	2.41(-3)	5.14(-2)	4.56(-2)	7.54(-2)	7.21(-2)	7.96(-2)	7.81(-2)	8.14(-2)	8.13(-2)
24	6.52(-3)	3.88(-4)	1.17(-2)	3.17(-3)	7.68(-2)	5.77(-2)	1.12(-1)	9.07(-2)	1.18(-1)	9.81(-2)	1.20(-1)	1.02(-1)
25	7.43(-3)	4.51(-4)	1.27(-2)	3.80(-3)	7.90(-2)	7.02(-2)	1.14(-1)	1.11(-1)	1.20(-1)	1.20(-1)	1.23(-1)	1.24(-1)
26	8.63(-3)	4.31(-4)	1.38(-2)	3.41(-3)	7.42(-2)	6.08(-2)	1.06(-1)	9.52(-2)	1.11(-1)	1.03(-1)	1.13(-1)	1.07(-1)
27	8.25(-3)	4.01(-4)	1.27(-2)	3.07(-3)	6.26(-2)	5.38(-2)	8.85(-2)	8.41(-2)	9.26(-2)	9.07(-2)	9.42(-2)	9.40(-2)
28	9.05(-3)	4.74(-4)	1.36(-2)	3.78(-3)	6.37(-2)	6.78(-2)	8.97(-2)	1.06(-1)	9.37(-2)	1.15(-1)	9.53(-2)	1.19(-1)
29	1.00(-2)	4.59(-4)	1.45(-2)	3.57(-3)	6.11(-2)	6.29(-2)	8.48(-2)	9.85(-2)	8.83(-2)	1.06(-1)	8.96(-2)	1.10(-1)
30	1.18(-2)	5.15(-4)	1.67(-2)	3.88(-3)	6.54(-2)	6.74(-2)	8.97(-2)	1.05(-1)	9.31(-2)	1.13(-1)	9.43(-2)	1.18(-1)

TABLE A11. (Continued)

Group	z=0		z=15.41		z=30.85		z=41.11		z=51.40		z=61.68	
	Fe	Na	Fe†	Na	Fe†	Na	Fe†	Na	Fe†	Na	Fe†	Na
31	2.18(-2)	9.43(-4)	3.03(-2)	6.48(-3)	1.09(-1)	1.07(-1)	1.47(-1)	1.65(-1)	1.52(-1)	1.78(-1)	1.53(-1)	1.84(-1)
32	2.62(-2)	9.40(-4)	3.51(-2)	6.03(-3)	1.12(-1)	9.47(-2)	1.48(-1)	1.46(-1)	1.52(-1)	1.56(-1)	1.53(-1)	1.61(-1)
33	2.75(-2)	1.21(-3)	3.86(-2)	7.33(-3)	1.33(-1)	1.10(-1)	1.76(-1)	1.69(-1)	1.81(-1)	1.81(-1)	1.82(-1)	1.86(-1)
34	1.48(-2)	7.66(-4)	2.11(-2)	4.80(-3)	7.50(-2)	7.34(-2)	9.98(-2)	1.13(-1)	1.02(-1)	1.20(-1)	1.03(-1)	1.24(-1)
35	1.58(-2)	1.48(-3)	2.31(-2)	1.10(-2)	8.80(-2)	1.86(-1)	1.18(-1)	2.88(-1)	1.21(-1)	3.10(-1)	1.22(-1)	3.20(-1)
36	1.79(-2)	1.07(-3)	2.46(-2)	6.33(-3)	6.71(-2)	9.15(-2)	8.40(-2)	1.39(-1)	8.46(-2)	1.48(-1)	8.42(-2)	1.52(-1)
37	1.86(-2)	1.07(-3)	2.52(-2)	5.72(-3)	6.23(-2)	7.67(-2)	7.61(-2)	1.16(-1)	7.63(-2)	1.23(-1)	7.57(-2)	1.26(-1)
38	2.02(-2)	1.44(-3)	2.73(-2)	7.56(-3)	6.35(-2)	9.91(-2)	7.65(-2)	1.49(-1)	7.64(-2)	1.57(-1)	7.57(-2)	1.61(-1)
39	1.95(-2)	1.07(-3)	2.44(-2)	5.22(-3)	4.20(-2)	6.46(-2)	4.71(-2)	9.65(-2)	4.66(-2)	1.02(-1)	4.60(-2)	1.04(-1)
40	1.29(-2)	6.02(-4)	1.62(-2)	2.73(-3)	2.69(-2)	3.19(-2)	2.98(-2)	4.74(-2)	2.94(-2)	4.99(-2)	2.90(-2)	5.10(-2)
41	4.54(-3)	2.24(-4)	5.92(-3)	9.75(-4)	1.11(-2)	1.09(-2)	1.27(-2)	1.62(-2)	1.26(-2)	1.70(-2)	1.24(-2)	1.73(-2)
42	5.27(-3)	2.99(-4)	7.05(-3)	1.23(-3)	1.42(-2)	1.31(-2)	1.65(-2)	1.92(-2)	1.63(-2)	2.01(-2)	1.61(-2)	2.04(-2)
43	7.47(-3)	4.96(-4)	9.35(-3)	2.15(-3)	1.57(-2)	2.39(-2)	1.74(-2)	3.53(-2)	1.72(-2)	3.71(-2)	1.70(-2)	3.78(-2)
44	1.74(-2)	1.05(-3)	2.21(-2)	4.18(-3)	3.83(-2)	4.30(-2)	4.28(-2)	6.29(-2)	4.22(-2)	6.59(-2)	4.16(-2)	6.70(-2)
45	2.32(-2)	1.34(-3)	2.86(-2)	5.26(-3)	4.61(-2)	5.30(-2)	5.07(-2)	7.73(-2)	4.99(-2)	8.09(-2)	4.92(-2)	8.22(-2)
46	1.94(-2)	1.18(-3)	2.33(-2)	4.65(-3)	3.62(-2)	4.72(-2)	3.95(-2)	6.89(-2)	3.89(-2)	7.21(-2)	3.84(-2)	7.34(-2)
47	2.03(-2)	1.78(-3)	2.55(-2)	7.18(-3)	4.61(-2)	7.40(-2)	5.23(-2)	1.08(-1)	5.17(-2)	1.13(-1)	5.10(-2)	1.15(-1)
48	2.25(-2)	4.45(-3)	3.09(-2)	2.06(-2)	7.22(-2)	2.40(-1)	8.64(-2)	3.55(-1)	8.61(-2)	3.73(-1)	8.53(-2)	3.80(-1)
49	1.89(-2)	2.53(-3)	2.46(-2)	8.81(-3)	4.08(-2)	7.77(-2)	4.41(-2)	1.12(-1)	4.31(-2)	1.16(-1)	4.23(-2)	1.18(-1)
50	1.80(-2)	3.50(-3)	2.41(-2)	1.23(-2)	4.13(-2)	1.08(-1)	4.48(-2)	1.55(-1)	4.38(-2)	1.61(-1)	4.30(-2)	1.63(-1)
51	1.47(-2)	2.61(-3)	1.93(-2)	8.79(-3)	3.04(-2)	7.41(-2)	3.21(-2)	1.06(-1)	3.13(-2)	1.10(-1)	3.07(-2)	1.11(-1)
52	1.25(-2)	4.59(-3)	1.71(-2)	1.80(-2)	2.91(-2)	1.75(-1)	3.15(-2)	2.54(-1)	3.07(-2)	2.65(-1)	3.02(-2)	2.69(-1)
53	1.43(-2)	4.00(-3)	1.79(-2)	1.46(-2)	2.26(-2)	1.33(-1)	2.21(-2)	1.91(-1)	2.14(-2)	1.98(-1)	2.10(-2)	2.01(-1)
54	2.71(-2)	4.73(-3)	3.35(-2)	1.44(-2)	3.81(-2)	1.06(-1)	3.56(-2)	1.49(-1)	3.42(-2)	1.54(-1)	3.34(-2)	1.56(-1)
55	1.93(-2)	3.59(-3)	2.30(-2)	1.00(-2)	2.32(-2)	6.72(-2)	2.07(-2)	9.38(-2)	1.99(-2)	9.68(-2)	1.94(-2)	9.76(-2)
56	1.79(-2)	3.34(-3)	2.12(-2)	9.00(-3)	2.07(-2)	5.72(-2)	1.82(-2)	7.94(-2)	1.74(-2)	8.18(-2)	1.70(-2)	8.25(-2)
57	4.15(-2)	5.88(-3)	5.03(-2)	1.31(-2)	4.99(-2)	5.97(-2)	4.37(-2)	7.96(-2)	4.18(-2)	8.13(-2)	4.09(-2)	8.16(-2)
58	3.88(-2)	5.84(-3)	4.62(-2)	1.26(-2)	4.37(-2)	5.34(-2)	3.77(-2)	7.02(-2)	3.61(-2)	7.16(-2)	3.53(-2)	7.17(-2)
59	6.99(-2)	1.06(-2)	8.21(-2)	2.18(-2)	7.49(-2)	8.37(-2)	6.36(-2)	1.08(-1)	6.08(-2)	1.10(-1)	5.95(-2)	1.10(-1)
60	2.75(-2)	5.43(-3)	3.21(-2)	1.15(-2)	2.86(-2)	4.59(-2)	2.40(-2)	5.97(-2)	2.30(-2)	6.07(-2)	2.25(-2)	6.07(-2)
61	6.47(-2)	9.16(-3)	7.54(-2)	1.65(-2)	6.64(-2)	4.60(-2)	5.56(-2)	5.64(-2)	5.33(-2)	5.69(-2)	5.23(-2)	5.67(-2)
62	3.36(-2)	7.25(-3)	3.85(-2)	1.33(-2)	3.28(-2)	3.86(-2)	2.72(-2)	4.77(-2)	2.60(-2)	4.81(-2)	2.55(-2)	4.81(-2)
63	3.91(-2)	9.98(-3)	4.64(-2)	1.77(-2)	4.14(-2)	4.68(-2)	3.46(-2)	5.68(-2)	3.31(-2)	5.72(-2)	3.25(-2)	5.70(-2)

TABLE A11. (Continued)

	z=0		z=15.41		z=30.85		z=41.11		z=51.40		z=61.68	
Group	Fe	Na	Fe^{+}	Na	Fe^{+}	Na	Fe^{+}	Na	Fe^{+}	Na	Fe^{+}	Na
64	2.27(-2)	5.20(-3)	2.66(-2)	9.03(-3)	2.30(-2)	2.35(-2)	1.90(-2)	2.85(-2)	1.81(-2)	2.88(-2)	1.78(-2)	2.87(-2)
65	1.49(-2)	5.64(-3)	1.76(-2)	1.00(-2)	1.54(-2)	2.75(-2)	1.28(-2)	3.38(-2)	1.22(-2)	3.41(-2)	1.20(-2)	3.41(-2)
66	3.87(-2)	4.10(-3)	4.51(-2)	6.63(-3)	3.87(-2)	1.47(-2)	3.19(-2)	1.74(-2)	3.05(-2)	1.75(-2)	2.99(-2)	1.74(-2)
67	4.56(-2)	4.94(-3)	5.34(-2)	7.73(-3)	4.61(-2)	1.54(-2)	3.82(-2)	1.77(-2)	3.65(-2)	1.78(-2)	3.58(-2)	1.77(-2)
68	4.39(-2)	9.99(-3)	5.14(-2)	1.57(-2)	4.46(-2)	2.94(-2)	3.72(-2)	3.30(-2)	3.59(-2)	3.28(-2)	3.54(-2)	3.27(-2)
69	4.10(-2)	1.34(-2)	4.83(-2)	2.10(-2)	4.18(-2)	3.79(-2)	3.49(-2)	4.18(-2)	3.37(-2)	4.15(-2)	3.33(-2)	4.12(-2)
70	6.47(-2)	1.38(-2)	7.52(-2)	2.12(-2)	6.36(-2)	3.51(-2)	5.23(-2)	3.77(-2)	5.02(-2)	3.73(-2)	4.94(-2)	3.70(-2)
71	4.55(-2)	1.85(-2)	5.28(-2)	2.99(-2)	4.45(-2)	5.50(-2)	3.67(-2)	6.05(-2)	3.53(-2)	5.99(-2)	3.48(-2)	5.93(-2)
72	5.06(-2)	3.65(-2)	6.02(-2)	6.43(-2)	5.37(-2)	1.41(-1)	4.53(-2)	1.60(-1)	4.35(-2)	1.58(-1)	4.28(-2)	1.56(-1)
73	4.41(-2)	8.52(-2)	5.60(-2)	1.89(-1)	6.21(-2)	7.16(-1)	5.75(-2)	9.00(-1)	5.55(-2)	8.99(-1)	5.44(-2)	8.89(-1)
74	8.02(-2)	1.10(-1)	9.20(-2)	2.02(-1)	7.12(-2)	4.76(-1)	5.62(-2)	5.46(-1)	5.44(-2)	5.38(-1)	5.40(-2)	5.30(-1)
75	2.95(-2)	5.68(-2)	3.20(-2)	9.76(-2)	2.25(-2)	2.00(-1)	1.74(-2)	2.24(-1)	1.70(-2)	2.21(-1)	1.71(-2)	2.19(-1)
76	1.64(-2)	1.62(-2)	1.72(-2)	2.60(-2)	1.12(-2)	4.74(-2)	8.37(-3)	5.21(-2)	8.12(-3)	5.15(-2)	8.08(-3)	5.10(-2)
77	3.77(-2)	3.36(-2)	3.88(-2)	5.25(-2)	2.51(-2)	8.70(-2)	1.94(-2)	9.27(-2)	1.95(-2)	9.13(-2)	1.99(-2)	9.03(-2)
78	7.00(-2)	1.09(-1)	7.17(-2)	1.75(-1)	4.53(-2)	3.00(-1)	3.46(-2)	3.19(-1)	3.51(-2)	3.13(-1)	3.63(-2)	3.08(-1)
79	1.05(-1)	1.31(-1)	1.04(-1)	1.98(-1)	6.45(-2)	3.13(-1)	5.01(-2)	3.31(-1)	5.18(-2)	3.25(-1)	5.43(-2)	3.22(-1)
80	1.23(-2)	6.93(-3)	1.24(-2)	1.02(-2)	1.17(-2)	1.88(-2)	1.16(-2)	2.14(-2)	1.18(-2)	2.13(-2)	1.20(-2)	2.12(-2)
81	4.44(-3)	6.33(-3)	4.66(-3)	1.01(-2)	4.85(-3)	2.06(-2)	4.98(-3)	2.36(-2)	5.05(-3)	2.35(-2)	5.10(-3)	2.33(-2)
82	1.39(-2)	9.86(-2)	2.02(-2)	3.21(-1)	5.85(-2)	2.73(0)	7.69(-2)	3.91(0)	7.98(-2)	4.05(0)	8.12(-2)	4.09(0)
83	1.47(-2)	7.12(-2)	1.48(-2)	1.34(-1)	8.27(-3)	3.65(-1)	6.47(-3)	4.36(-1)	7.16(-3)	4.32(-1)	7.84(-3)	4.27(-1)
84	1.95(-2)	7.28(-2)	1.82(-2)	1.20(-1)	7.85(-3)	2.26(-1)	5.10(-3)	2.48(-1)	5.93(-3)	2.44(-1)	6.75(-3)	2.40(-1)
85	3.38(-2)	8.01(-2)	2.98(-2)	1.21(-1)	1.30(-2)	1.68(-1)	1.05(-2)	1.69(-1)	1.30(-2)	1.65(-1)	1.52(-2)	1.63(-1)
86	1.40(-2)	2.25(-2)	1.20(-2)	3.16(-2)	5.30(-3)	4.00(-2)	4.50(-3)	3.94(-2)	5.52(-3)	3.86(-2)	6.39(-3)	3.81(-2)
87	1.58(-2)	3.71(-2)	1.37(-2)	5.47(-2)	4.90(-3)	7.94(-2)	2.31(-3)	8.17(-2)	2.53(-3)	8.01(-2)	2.84(-3)	7.90(-2)
88	1.51(-2)	2.42(-2)	1.27(-2)	3.45(-2)	6.48(-3)	4.85(-2)	7.27(-3)	5.01(-2)	9.49(-3)	4.94(-2)	1.13(-2)	4.90(-2)
89	7.60(-3)	1.90(-2)	6.35(-3)	2.73(-2)	2.68(-3)	3.85(-2)	1.96(-3)	3.94(-2)	2.25(-3)	3.87(-2)	2.53(-3)	3.81(-2)
90	6.36(-3)	4.76(-2)	5.56(-3)	7.27(-2)	2.32(-3)	1.11(-1)	1.47(-3)	1.14(-1)	1.61(-3)	1.11(-1)	1.78(-3)	1.09(-1)
91	1.12(-2)	6.24(-2)	9.66(-3)	9.52(-2)	6.09(-3)	1.45(-1)	7.32(-3)	1.50(-1)	9.13(-3)	1.46(-1)	1.06(-2)	1.44(-1)
92	1.74(-2)	6.67(-2)	1.46(-2)	9.93(-2)	6.93(-3)	1.45(-1)	6.88(-3)	1.48(-1)	8.77(-3)	1.45(-1)	1.03(-2)	1.43(-1)
93	1.01(-2)	6.16(-2)	8.42(-3)	9.24(-2)	6.73(-3)	1.37(-1)	1.09(-2)	1.42(-1)	1.48(-2)	1.39(-1)	1.80(-2)	1.37(-1)
94	6.40(-3)	5.75(-2)	5.32(-3)	8.66(-2)	4.04(-3)	1.28(-1)	5.55(-3)	1.31(-1)	6.95(-3)	1.28(-1)	8.04(-3)	1.25(-1)
95	6.72(-3)	5.35(-2)	5.53(-3)	8.05(-2)	3.16(-3)	1.18(-1)	3.38(-3)	1.20(-1)	4.01(-3)	1.16(-1)	4.53(-3)	1.14(-1)

TABLE A11. (Continued)

Group	z=0		z=15.41		z=30.85		z=41.11		z=51.40		z=61.68	
	Fe	Na	Fe†	Na	Fe†	Na	Fe†	Na	Fe†	Na	Fe†	Na
96	2.10(-3)	5.10(-2)	1.79(-3)	7.76(-2)	9.30(-4)	1.15(-1)	7.68(-4)	1.17(-1)	8.14(-4)	1.14(-1)	8.74(-4)	1.12(-1)
97	9.36(-3)	5.68(-2)	7.43(-3)	8.29(-2)	8.99(-3)	1.19(-1)	2.08(-2)	1.24(-1)	3.23(-2)	1.22(-1)	4.29(-2)	1.21(-1)
98	2.00(-2)	5.86(-2)	1.56(-2)	8.47(-2)	6.03(-3)	1.16(-1)	4.19(-3)	1.16(-1)	4.65(-3)	1.12(-1)	5.05(-3)	1.10(-1)
99	1.21(-2)	5.89(-2)	9.24(-3)	8.49(-2)	8.77(-3)	1.18(-1)	1.54(-2)	1.19(-1)	2.09(-2)	1.16(-1)	2.52(-2)	1.14(-1)
100	1.75(-2)	5.90(-2)	1.33(-2)	8.45(-2)	7.73(-3)	1.13(-1)	9.24(-3)	1.11(-1)	1.14(-2)	1.08(-1)	1.31(-2)	1.05(-1)
101	7.96(-3)	5.63(-2)	6.10(-3)	8.21(-2)	4.74(-3)	1.12(-1)	6.29(-3)	1.10(-1)	7.56(-3)	1.06(-1)	8.57(-3)	1.03(-1)
102	4.84(-3)	1.36(-1)	3.84(-3)	2.02(-1)	8.08(-3)	2.82(-1)	1.33(-2)	2.78(-1)	1.59(-2)	2.67(-1)	1.80(-2)	2.60(-1)
103	1.36(-2)	1.38(-1)	1.01(-2)	2.02(-1)	6.70(-3)	2.70(-1)	7.87(-3)	2.63(-1)	9.16(-3)	2.52(-1)	1.02(-2)	2.44(-1)
104	3.22(-3)	4.99(-2)	2.39(-3)	7.29(-2)	8.25(-4)	9.73(-2)	4.52(-4)	9.43(-2)	4.71(-4)	9.01(-2)	5.32(-4)	8.73(-2)
105	1.60(-2)	4.66(-2)	1.12(-2)	6.34(-2)	1.37(-2)	8.22(-2)	2.71(-2)	8.26(-2)	3.74(-2)	8.12(-2)	4.64(-2)	8.03(-2)
106	1.01(-2)	1.08(-1)	7.18(-3)	1.54(-1)	7.09(-3)	1.99(-1)	9.86(-3)	1.90(-1)	1.16(-2)	1.81(-1)	1.29(-2)	1.74(-1)
107	7.80(-3)	7.15(-2)	5.46(-3)	1.01(-1)	1.17(-2)	1.31(-1)	2.03(-2)	1.27(-1)	2.50(-2)	1.22(-1)	2.89(-2)	1.18(-1)
108	1.91(-2)	1.67(-1)	1.31(-2)	2.35(-1)	1.66(-2)	2.97(-1)	2.53(-2)	2.84(-1)	3.04(-2)	2.70(-1)	3.45(-2)	2.60(-1)
109	3.19(-3)	9.34(-3)	2.06(-3)	1.24(-2)	2.57(-3)	1.44(-2)	3.86(-3)	1.37(-2)	4.66(-3)	1.32(-2)	5.40(-3)	1.28(-2)
110	8.67(-3)	8.17(-2)	5.80(-3)	1.11(-1)	8.46(-3)	1.33(-1)	1.34(-2)	1.24(-1)	1.63(-2)	1.18(-1)	1.86(-2)	1.13(-1)
111	9.77(-3)	1.30(-1)	6.47(-3)	1.83(-1)	8.60(-3)	2.26(-1)	1.39(-2)	2.11(-1)	1.69(-2)	1.98(-1)	1.92(-2)	1.90(-1)
112	6.12(-3)	1.76(-1)	4.11(-3)	2.50(-1)	7.64(-3)	3.11(-1)	1.32(-2)	2.88(-1)	1.62(-2)	2.69(-1)	1.83(-2)	2.56(-1)
113	1.76(-3)	7.17(-2)	1.17(-3)	1.01(-1)	1.29(-3)	1.23(-1)	2.24(-3)	1.13(-1)	2.93(-3)	1.05(-1)	3.45(-3)	1.00(-1)
114	-3.48(-4)	1.02(-1)	-1.07(-4)	1.44(-1)	1.37(-3)	1.74(-1)	2.77(-3)	1.56(-1)	3.46(-3)	1.43(-1)	3.92(-3)	1.33(-1)
115	1.23(-3)	4.89(-2)	7.67(-4)	6.88(-2)	2.56(-4)	7.85(-2)	4.37(-4)	6.60(-2)	6.07(-4)	5.82(-2)	7.05(-4)	5.31(-2)
116	1.66(-3)	3.29(-2)	9.63(-4)	4.52(-2)	-1.35(-3)	4.79(-2)	-2.94(-3)	3.90(-2)	-3.48(-3)	3.51(-3)	-3.74(-3)	3.30(-2)
117	4.74(-3)	4.98(-2)	2.99(-3)	6.56(-2)	2.84(-2)	7.29(-2)	7.05(-2)	7.27(-2)	1.03(-1)	7.63(-2)	1.30(-1)	7.95(-2)
118	1.34(-3)	2.49(-2)	7.42(-4)	3.26(-2)	5.26(-3)	4.47(-2)	2.61(-2)	5.75(-2)	5.53(-2)	6.77(-2)	9.02(-2)	7.57(-2)
119	7.53(-4)	2.40(-2)	4.02(-4)	3.20(-2)	4.61(-3)	4.85(-2)	2.37(-2)	6.16(-2)	4.98(-2)	6.85(-2)	7.84(-2)	7.23(-2)
120	2.88(-3)	6.96(-2)	1.68(-3)	9.43(-2)	2.71(-2)	1.48(-1)	9.14(-2)	1.68(-1)	1.58(-1)	1.64(-1)	2.14(-1)	1.54(-1)
121	2.86(-3)	1.10(-1)	1.99(-3)	1.51(-1)	5.96(-2)	2.14(-1)	1.59(-1)	1.96(-1)	2.35(-1)	1.56(-1)	2.84(-1)	1.24(-1)
122	6.35(-4)	2.04(-1)	1.71(-3)	2.85(-1)	1.15(-1)	3.16(-1)	2.38(-1)	1.95(-1)	2.91(-1)	1.12(-1)	3.14(-1)	6.76(-2)
123	2.02(-3)	1.77(-1)	2.87(-3)	2.41(-1)	9.54(-2)	1.91(-1)	1.55(-1)	6.58(-2)	1.62(-1)	2.23(-2)	1.66(-1)	8.19(-3)
124	2.86(-3)	1.40(-1)	3.09(-3)	1.88(-1)	5.05(-2)	1.17(-1)	6.68(-2)	2.37(-2)	6.39(-2)	4.69(-3)	6.68(-2)	1.02(-3)
125	9.01(-4)	9.85(-2)	1.04(-3)	1.29(-1)	1.38(-2)	6.73(-2)	1.76(-2)	9.43(-3)	1.72(-2)	1.29(-3)	1.84(-2)	2.18(-4)

TABLE A11. (Continued)

Group	z=0		z=15.41		z=30.85		z=41.11		z=51.40		z=61.68	
	Fe	Na	Fe^{+}	Na	Fe^{+}	Na	Fe^{+}	Na	Fe^{+}	Na	Fe^{+}	Na
126	5.98(-4)	5.61(-2)	1.39(-3)	7.28(-2)	3.74(-2)	3.90(-2)	5.08(-2)	5.98(-3)	4.94(-2)	9.00(-4)	5.30(-2)	1.59(-4)
127	4.91(-4)	2.08(-2)	1.31(-3)	2.70(-2)	4.83(-2)	1.70(-2)	6.69(-2)	3.22(-3)	6.43(-2)	5.43(-4)	6.87(-2)	9.59(-5)
128	4.51(-4)	-7.73(-4)	5.61(-4)	1.40(-3)	2.02(-2)	4.48(-4)	2.81(-2)	2.21(-4)	2.74(-2)	4.00(-5)	2.99(-2)	6.71(-6)
129	3.81(-4)	-4.82(-3)	4.47(-4)	-6.21(-3)	1.58(-2)	-2.72(-3)	2.22(-2)	-2.53(-4)	2.16(-2)	-1.10(-5)	2.37(-2)	3.91(-7)
130	1.16(-4)	-6.23(-3)	7.33(-4)	-1.11(-2)	1.47(-2)	-5.21(-3)	2.07(-2)	-5.49(-4)	2.03(-2)	-4.34(-5)	2.23(-2)	-3.55(-6)
131	6.27(-4)	7.18(-3)	1.70(-4)	9.85(-3)	1.35(-2)	3.17(-3)	1.93(-2)	1.61(-4)	1.89(-2)	-5.00(-6)	2.09(-2)	-1.73(-6)
132	2.14(-4)	2.95(-3)	1.76(-4)	5.70(-3)	6.49(-3)	3.05(-3)	9.19(-3)	3.27(-4)	9.01(-3)	2.79(-5)	1.00(-2)	2.53(-6)
133	1.23(-4)	1.87(-3)	1.45(-4)	3.82(-3)	6.25(-3)	2.07(-3)	8.86(-3)	2.54(-4)	8.69(-3)	2.27(-5)	9.68(-3)	2.20(-6)
134	3.30(-5)	4.25(-3)	2.67(-4)	4.85(-3)	1.20(-2)	2.86(-3)	1.68(-2)	3.57(-4)	1.65(-2)	3.32(-5)	1.83(-2)	3.29(-6)
135	1.63(-4)	2.98(-3)	3.71(-4)	3.94(-3)	1.15(-2)	2.36(-3)	1.59(-2)	3.22(-4)	1.55(-2)	2.98(-5)	1.73(-2)	2.71(-6)
136	6.29(-4)	5.58(-2)	1.44(-3)	7.21(-2)	2.75(-2)	3.32(-2)	3.56(-2)	3.12(-3)	3.43(-2)	2.01(-4)	3.81(-2)	1.40(-5)
137	1.59(-3)	1.67(-1)	2.40(-3)	2.21(-1)	2.68(-2)	9.91(-2)	3.20(-2)	8.47(-3)	3.03(-2)	4.59(-4)	3.36(-2)	2.57(-5)
138	2.25(-3)	2.65(-1)	3.23(-3)	3.60(-1)	2.49(-2)	1.62(-1)	2.70(-2)	1.35(-2)	2.51(-2)	6.85(-4)	2.78(-2)	3.47(-5)
139	1.67(-3)	3.37(-1)	4.39(-3)	4.68(-1)	2.97(-2)	2.14(-1)	2.77(-2)	1.76(-2)	2.48(-2)	8.73(-4)	2.74(-2)	4.21(-5)
140	1.54(-3)	3.73(-1)	5.70(-3)	5.22(-1)	3.18(-2)	2.36(-1)	2.61(-2)	1.88(-2)	2.26(-2)	8.84(-4)	2.50(-2)	3.97(-5)
141	1.23(-3)	3.91(-1)	7.48(-3)	5.48(-1)	3.52(-2)	2.43(-1)	2.51(-2)	1.88(-2)	2.10(-2)	8.40(-4)	2.31(-2)	3.53(-5)
142	2.30(-4)	4.01(-1)	9.84(-3)	5.62(-1)	4.03(-2)	2.44(-1)	2.49(-2)	1.82(-2)	2.01(-2)	7.74(-4)	2.20(-2)	3.07(-5)
143	5.09(-4)	4.10(-1)	1.37(-2)	5.71(-1)	4.68(-2)	2.40(-1)	2.49(-2)	1.73(-2)	1.91(-2)	6.99(-4)	2.08(-2)	2.61(-5)
144	5.25(-4)	4.16(-1)	1.88(-2)	5.75(-1)	5.53(-2)	2.33(-1)	2.52(-2)	1.61(-2)	1.84(-2)	6.18(-4)	1.98(-2)	2.17(-5)
145	3.99(-4)	4.18(-1)	2.57(-2)	5.72(-1)	6.58(-2)	2.23(-1)	2.58(-2)	1.47(-2)	1.78(-2)	5.33(-4)	1.91(-2)	1.76(-5)
146	2.88(-4)	4.22(-1)	3.48(-2)	5.68(-1)	7.87(-2)	2.11(-1)	2.66(-2)	1.32(-2)	1.73(-2)	4.51(-4)	1.83(-2)	1.39(-5)
147	2.02(-4)	4.23(-1)	4.65(-2)	5.59(-1)	9.32(-2)	1.95(-1)	2.69(-2)	1.16(-2)	1.61(-2)	3.70(-4)	1.69(-2)	1.07(-5)
148	1.37(-4)	4.22(-1)	6.11(-2)	5.44(-1)	1.09(-1)	1.78(-1)	2.69(-2)	9.89(-3)	1.45(-2)	2.95(-4)	1.52(-2)	7.92(-6)
149	9.08(-5)	4.21(-1)	7.99(-2)	5.25(-1)	1.28(-1)	1.58(-1)	2.87(-2)	8.23(-3)	1.49(-2)	2.28(-4)	1.54(-2)	5.66(-6)
150	5.85(-5)	4.19(-1)	1.02(-1)	5.02(-1)	1.47(-1)	1.38(-1)	2.99(-2)	6.67(-3)	1.46(-2)	1.70(-4)	1.50(-2)	3.89(-6)
151	3.66(-5)	4.17(-1)	1.27(-1)	4.76(-1)	1.66(-1)	1.18(-1)	3.06(-2)	5.24(-3)	1.40(-2)	1.23(-4)	1.42(-2)	2.57(-6)
152	2.16(-5)	4.02(-1)	1.51(-1)	4.32(-1)	1.78(-1)	9.56(-2)	3.01(-2)	3.87(-3)	1.30(-2)	8.25(-5)	1.31(-2)	1.58(-6)
153	1.35(-5)	4.20(-1)	1.91(-1)	4.23(-1)	2.06(-1)	8.28(-2)	3.17(-2)	3.05(-3)	1.26(-2)	5.91(-5)	1.25(-2)	1.03(-6)
154	7.31(-6)	4.04(-1)	2.20(-1)	3.72(-1)	2.15(-1)	6.27(-2)	3.11(-2)	2.07(-3)	1.19(-2)	3.59(-5)	1.18(-2)	5.63(-7)
155	3.95(-6)	3.96(-1)	2.53(-1)	3.31(-1)	2.25(-1)	4.76(-2)	3.06(-2)	1.40(-3)	1.11(-2)	2.17(-5)	1.08(-2)	3.06(-7)

TABLE A11. (Continued)

Group	z=0		z=15.41		z=30.85		z=41.11		z=51.40		z=61.68	
	Fe	Na	Fe†	Na	Fe†	Na	Fe†	Na	Fe†	Na	Fe†	Na
156	2.05(-6)	3.87(-1)	2.86(-1)	2.88(-1)	2.32(-1)	3.48(-2)	2.98(-2)	9.08(-4)	1.03(-2)	1.25(-5)	9.90(-3)	1.57(-7)
157	1.00(-6)	3.72(-1)	3.14(-1)	2.42(-1)	2.35(-1)	2.41(-2)	2.86(-2)	5.52(-4)	9.39(-3)	6.69(-6)	8.92(-3)	7.44(-8)
158	4.64(-7)	3.57(-1)	3.38(-1)	2.00(-1)	2.32(-1)	1.61(-2)	2.72(-2)	3.19(-4)	8.48(-3)	3.39(-6)	7.95(-3)	3.32(-8)
159	2.03(-7)	3.39(-1)	3.54(-1)	1.59(-1)	2.26(-1)	1.01(-2)	2.55(-2)	1.73(-4)	7.56(-3)	1.59(-6)	6.97(-3)	1.37(-8)
160	8.41(-8)	3.20(-1)	3.61(-1)	1.22(-1)	2.14(-1)	6.02(-3)	2.36(-2)	8.76(-5)	6.63(-3)	6.93(-7)	6.02(-3)	5.18(-9)
161	3.24(-8)	2.99(-1)	3.57(-1)	8.97(-2)	1.98(-1)	3.34(-3)	2.14(-2)	4.09(-5)	5.72(-3)	2.76(-7)	5.11(-3)	1.78(-9)
162	1.17(-8)	2.81(-1)	3.49(-1)	6.38(-2)	1.82(-1)	1.75(-3)	1.93(-2)	1.79(-5)	4.91(-3)	1.02(-7)	4.30(-3)	5.64(-10)
163	3.60(-9)	2.46(-1)	3.10(-1)	4.00(-2)	1.53(-1)	7.75(-4)	1.61(-2)	6.44(-6)	3.91(-3)	3.05(-8)	3.36(-3)	1.42(-10)
164	1.09(-9)	2.24(-1)	2.79(-1)	2.48(-2)	1.32(-1)	3.37(-4)	1.37(-2)	2.29(-6)	3.18(-3)	9.04(-9)	2.68(-3)	3.57(-11)
165	2.74(-10)	1.94(-1)	2.34(-1)	1.35(-2)	1.06(-1)	1.23(-4)	1.09(-2)	6.69(-7)	2.44(-3)	2.17(-9)	2.01(-3)	7.15(-12)
166	5.77(-11)	1.61(-1)	1.82(-1)	6.43(-3)	7.98(-2)	3.78(-5)	8.16(-3)	1.62(-7)	1.77(-3)	4.24(-10)	1.43(-3)	1.16(-12)
167	9.40(-12)	1.24(-1)	1.28(-1)	2.50(-3)	5.45(-2)	9.06(-6)	5.54(-3)	3.00(-8)	1.17(-3)	6.27(-11)	9.28(-4)	1.39(-13)
168	1.12(-12)	8.55(-2)	7.66(-2)	7.16(-4)	3.20(-2)	1.53(-6)	3.24(-3)	3.86(-9)	6.78(-4)	6.33(-12)	5.29(-4)	1.14(-14)
169	7.54(-14)	4.45(-2)	3.25(-2)	1.16(-4)	1.34(-2)	1.39(-7)	1.36(-3)	2.60(-10)	2.86(-4)	3.31(-13)	2.20(-4)	4.74(-16)
Integral	2.0387	15.060	7.2981	17.115	8.5398	18.557	6.6626	18.439	6.7590	18.320	7.1357	18.255
Elastic	1.4822	14.408	5.6567	16.609	5.8896	16.358	3.7715	15.223	3.7989	14.898	4.1193	14.731
In-Elastic	0.5038	0.064	0.6829	0.202	1.9194	2.054	2.5117	3.089	2.5958	3.289	2.6289	3.386

*Tabulated values are of the quantity: $-\frac{\Delta R}{R} / \frac{\Delta \Sigma_T}{\Sigma_T}$.

†Includes the iron in both the stainless and carbon steels. The two may be approximately separated by ascribing all the sensitivity above ∿ 500 keV to the stainless steel and below ∿ 500 keV to the carbon steel.

**Read as 6.61×10^{-5}, etc..

TABLE A12. Group Integrated Total Sensitivity Functions for the 4-in. Bonner Ball Behind 30.90 cm. SS + 459.83 cm. Na + z cm. CS*

	z=0		z=15.41		z=30.85		z=41.11		z=61.68		z=90.06	
Group	Fe	Na	Fe†	Na	Fe†	Na	Fe†	Na	Fe†	Na	Fe†	Na
1	1.02(-4)**	4.62(-5)	4.86(-4)	4.56(-4)	3.53(-3)	4.33(-3)	4.38(-3)	5.53(-3)	4.85(-3)	6.31(-3)	5.20(-3)	6.90(-3)
2	1.31(-4)	7.17(-5)	6.32(-4)	7.41(-4)	4.61(-3)	7.19(-3)	5.73(-3)	9.23(-3)	6.36(-3)	1.06(-2)	6.82(-3)	1.16(-2)
3	1.39(-4)	7.34(-5)	6.64(-4)	7.92(-4)	4.83(-3)	7.82(-3)	6.00(-3)	1.01(-2)	6.66(-3)	1.16(-2)	7.14(-3)	1.27(-2)
4	1.01(-4)	5.60(-5)	4.71(-4)	5.72(-4)	3.37(-3)	5.52(-3)	4.17(-3)	7.08(-3)	4.61(-3)	8.11(-3)	4.93(-3)	8.88(-3)
5	1.12(-4)	6.33(-5)	5.14(-4)	6.48(-4)	3.62(-3)	6.25(-3)	4.48(-3)	8.02(-3)	4.95(-3)	9.17(-3)	5.29(-3)	1.00(-2)
6	1.36(-4)	7.65(-5)	6.13(-4)	7.69(-4)	4.25(-3)	7.36(-3)	5.25(-3)	9.42(-3)	5.78(-3)	1.08(-2)	6.16(-3)	1.18(-2)
7	1.60(-4)	8.83(-5)	7.02(-4)	8.61(-4)	4.76(-3)	8.12(-3)	5.85(-3)	1.04(-2)	6.42(-3)	1.18(-2)	6.82(-3)	1.29(-2)
8	4.22(-4)	2.31(-4)	1.79(-3)	2.18(-3)	1.18(-2)	2.02(-2)	1.45(-2)	2.58(-2)	1.59(-2)	2.92(-2)	1.68(-2)	3.18(-2)
9	5.52(-4)	2.74(-4)	2.23(-3)	2.49(-3)	1.42(-2)	2.26(-2)	1.73(-2)	2.87(-2)	1.88(-2)	3.24(-2)	1.99(-2)	3.51(-2)
10	8.32(-4)	3.66(-4)	3.18(-3)	3.13(-3)	1.94(-2)	2.76(-2)	2.35(-2)	3.49(-2)	2.55(-2)	3.92(-2)	2.68(-2)	4.23(-2)
11	1.10(-3)	4.81(-4)	4.11(-3)	4.07(-3)	2.47(-2)	3.57(-2)	2.99(-2)	4.49(-2)	3.23(-2)	5.04(-2)	3.39(-2)	5.43(-2)
12	1.45(-3)	6.22(-4)	5.31(-3)	5.20(-3)	3.15(-2)	4.54(-2)	3.80(-2)	5.71(-2)	4.09(-2)	6.40(-2)	4.30(-2)	6.89(-2)
13	1.86(-3)	7.57(-4)	6.65(-3)	6.18(-3)	3.85(-2)	5.32(-2)	4.64(-2)	6.68(-2)	4.99(-2)	7.46(-2)	5.23(-2)	8.03(-2)
14	2.38(-3)	9.27(-4)	8.53(-3)	7.58(-3)	4.99(-2)	6.52(-2)	6.01(-2)	8.18(-2)	6.47(-2)	9.14(-2)	6.78(-2)	9.83(-2)
15	3.03(-3)	1.20(-3)	1.10(-2)	9.96(-3)	6.45(-2)	8.63(-2)	7.78(-2)	1.08(-1)	8.38(-2)	1.21(-1)	8.79(-2)	1.31(-1)
16	3.68(-3)	1.47(-3)	1.30(-2)	1.22(-2)	7.53(-2)	1.06(-1)	9.07(-2)	1.33(-1)	9.77(-2)	1.48(-1)	1.02(-1)	1.60(-1)
17	4.30(-3)	1.68(-3)	1.44(-2)	1.36(-2)	8.07(-2)	1.17(-1)	9.69(-2)	1.46(-1)	1.04(-1)	1.64(-1)	1.09(-1)	1.76(-1)
18	5.03(-3)	1.78(-3)	1.59(-2)	1.36(-2)	8.56(-2)	1.14(-1)	1.02(-1)	1.42(-1)	1.09(-1)	1.58(-1)	1.14(-1)	1.69(-1)
19	6.04(-3)	2.00(-3)	1.85(-2)	1.49(-2)	9.73(-2)	1.22(-1)	1.16(-1)	1.52(-1)	1.24(-1)	1.69(-1)	1.29(-1)	1.81(-1)
20	7.43(-3)	2.46(-3)	2.27(-2)	1.87(-2)	1.18(-1)	1.55(-1)	1.41(-1)	1.93(-1)	1.50(-1)	2.14(-1)	1.56(-1)	2.29(-1)
21	9.06(-3)	2.99(-3)	2.69(-2)	2.29(-2)	1.37(-1)	1.90(-1)	1.62(-1)	2.36(-1)	1.72(-1)	2.62(-1)	1.79(-1)	2.81(-1)
22	2.96(-3)	8.95(-4)	8.13(-3)	6.37(-3)	3.83(-2)	5.08(-2)	4.50(-2)	6.30(-2)	4.74(-2)	6.94(-2)	4.88(-2)	7.38(-2)
23	6.03(-3)	1.84(-3)	1.60(-2)	1.30(-2)	7.32(-2)	1.03(-1)	8.58(-2)	1.28(-1)	9.01(-2)	1.41(-1)	9.27(-2)	1.50(-1)
24	1.01(-2)	2.66(-3)	2.54(-2)	1.76(-2)	1.11(-1)	1.34(-1)	1.29(-1)	1.65(-1)	1.35(-1)	1.80(-1)	1.38(-1)	1.91(-1)
25	1.15(-2)	3.22(-3)	2.83(-2)	2.19(-2)	1.21(-1)	1.69(-1)	1.41(-1)	2.09(-1)	1.48(-1)	2.29(-1)	1.52(-1)	2.42(-1)
26	1.29(-2)	3.20(-3)	2.94(-2)	2.03(-2)	1.16(-1)	1.51(-1)	1.34(-1)	1.85(-1)	1.39(-1)	2.01(-1)	1.42(-1)	2.12(-1)
27	1.20(-2)	3.00(-3)	2.63(-2)	1.84(-2)	9.85(-2)	1.34(-1)	1.13(-1)	1.64(-1)	1.17(-1)	1.78(-1)	1.19(-1)	1.88(-1)
28	1.31(-2)	3.63(-3)	2.83(-2)	2.32(-2)	1.05(-1)	1.73(-1)	1.20(-1)	2.12(-1)	1.24(-1)	2.31(-1)	1.26(-1)	2.44(-1)
29	1.42(-2)	3.61(-3)	2.91(-2)	2.24(-2)	1.01(-1)	1.63(-1)	1.15(-1)	2.00(-1)	1.18(-1)	2.17(-1)	1.20(-1)	2.29(-1)
30	1.64(-2)	4.10(-3)	3.22(-2)	2.46(-2)	1.05(-1)	1.77(-1)	1.19(-1)	2.16(-1)	1.21(-1)	2.34(-1)	1.23(-1)	2.46(-1)

TABLE A12. (Continued)

Group	z=0		z=15.41		z=30.85		z=41.11		z=61.68		z=90.06	
	Fe	Na	Fe^{+}	Na	Fe^{+}	Na	Fe^{+}	Na	Fe^{+}	Na	Fe^{+}	Na
31	2.92(-2)	7.24(-3)	5.42(-2)	3.98(-2)	1.61(-1)	2.71(-1)	1.79(-1)	3.29(-1)	1.82(-1)	3.54(-1)	1.82(-1)	3.71(-1)
32	3.38(-2)	7.21(-3)	5.94(-2)	3.70(-2)	1.61(-1)	2.40(-1)	1.77(-1)	2.89(-1)	1.77(-1)	3.09(-1)	1.77(-1)	3.22(-1)
33	3.63(-2)	8.70(-3)	6.54(-2)	4.28(-2)	1.75(-1)	2.69(-1)	1.91(-1)	3.22(-1)	1.91(-1)	3.42(-1)	1.89(-1)	3.55(-1)
34	2.01(-2)	5.42(-3)	3.69(-2)	2.76(-2)	1.01(-1)	1.77(-1)	1.10(-1)	2.12(-1)	1.10(-1)	2.26(-1)	1.09(-1)	2.34(-1)
35	2.29(-2)	1.02(-2)	4.44(-2)	6.23(-2)	1.29(-1)	4.43(-1)	1.42(-1)	5.39(-1)	1.42(-1)	5.81(-1)	1.41(-1)	6.09(-1)
36	2.45(-2)	7.38(-3)	4.04(-2)	3.55(-2)	8.20(-2)	2.16(-1)	8.52(-2)	2.57(-1)	8.21(-2)	2.71(-1)	7.95(-2)	2.80(-1)
37	2.48(-2)	7.17(-3)	3.94(-2)	3.16(-2)	7.14(-2)	1.78(-1)	7.28(-2)	2.10(-1)	6.95(-2)	2.20(-1)	6.68(-2)	2.26(-1)
38	2.65(-2)	9.36(-3)	4.14(-2)	4.07(-2)	7.12(-2)	2.26(-1)	7.19(-2)	2.65(-1)	6.82(-2)	2.78(-1)	6.55(-2)	2.84(-1)
39	2.29(-2)	6.98(-3)	3.19(-2)	2.81(-2)	4.26(-2)	1.47(-1)	4.12(-2)	1.72(-1)	3.86(-2)	1.79(-1)	3.67(-2)	1.83(-1)
40	1.42(-2)	3.88(-3)	1.96(-2)	1.46(-2)	2.45(-2)	7.24(-2)	2.35(-2)	8.41(-2)	2.19(-2)	8.72(-2)	2.08(-2)	8.88(-2)
41	5.09(-3)	1.40(-3)	7.30(-3)	5.10(-3)	9.78(-3)	2.45(-2)	9.44(-3)	2.83(-2)	8.82(-3)	2.93(-2)	8.37(-3)	2.98(-2)
42	5.91(-3)	1.76(-3)	8.63(-3)	6.14(-3)	1.19(-2)	2.84(-2)	1.16(-2)	3.26(-2)	1.08(-2)	3.36(-2)	1.03(-2)	3.41(-2)
43	8.10(-3)	2.96(-3)	1.11(-2)	1.09(-2)	1.36(-2)	5.24(-2)	1.29(-2)	6.06(-2)	1.21(-2)	6.26(-2)	1.15(-2)	6.36(-2)
44	1.88(-2)	5.98(-3)	2.58(-2)	2.04(-2)	3.12(-2)	9.22(-2)	2.96(-2)	1.06(-1)	2.75(-2)	1.09(-1)	2.61(-2)	1.10(-1)
45	2.54(-2)	7.62(-3)	3.36(-2)	2.55(-2)	3.81(-2)	1.13(-1)	3.58(-2)	1.29(-1)	3.33(-2)	1.33(-1)	3.15(-2)	1.34(-1)
46	2.18(-2)	6.75(-3)	2.81(-2)	2.27(-2)	3.10(-2)	1.01(-1)	2.90(-2)	1.16(-1)	2.70(-2)	1.19(-1)	2.55(-2)	1.20(-1)
47	2.40(-2)	9.98(-3)	3.25(-2)	3.44(-2)	3.98(-2)	1.56(-1)	3.79(-2)	1.79(-1)	3.53(-2)	1.84(-1)	3.36(-2)	1.87(-1)
48	2.86(-2)	2.29(-2)	4.27(-2)	9.11(-2)	6.43(-2)	4.69(-1)	6.35(-2)	5.46(-1)	6.01(-2)	5.66(-1)	5.77(-2)	5.77(-1)
49	2.16(-2)	1.23(-2)	2.84(-2)	3.77(-2)	2.81(-2)	1.53(-1)	2.54(-2)	1.74(-1)	2.33(-2)	1.77(-1)	2.21(-2)	1.79(-1)
50	2.10(-2)	1.62(-2)	2.84(-2)	5.05(-2)	2.89(-2)	2.06(-1)	2.62(-2)	2.34(-1)	2.41(-2)	2.39(-1)	2.29(-2)	2.41(-1)
51	1.75(-2)	1.21(-2)	2.31(-2)	3.62(-2)	2.16(-2)	1.43(-1)	1.92(-2)	1.61(-1)	1.75(-2)	1.64(-1)	1.66(-2)	1.65(-1)
52	1.62(-2)	2.12(-2)	2.24(-2)	7.32(-2)	2.31(-2)	3.27(-1)	2.10(-2)	3.75(-1)	1.94(-2)	3.84(-1)	1.86(-2)	3.88(-1)
53	1.60(-2)	1.85(-2)	1.99(-2)	5.96(-2)	1.50(-2)	2.51(-1)	1.27(-2)	2.85(-1)	1.17(-2)	2.91(-1)	1.13(-2)	2.92(-1)
54	2.64(-2)	1.95(-2)	3.11(-2)	5.37(-2)	1.95(-2)	1.94(-1)	1.56(-2)	2.18(-1)	1.44(-2)	2.21(-1)	1.40(-2)	2.21(-1)
55	1.83(-2)	1.47(-2)	2.06(-2)	3.73(-2)	1.11(-2)	1.25(-1)	8.63(-3)	1.39(-1)	8.10(-3)	1.40(-1)	8.01(-3)	1.40(-1)
56	1.68(-2)	1.34(-2)	1.85(-2)	3.30(-2)	9.48(-3)	1.06(-1)	7.14(-3)	1.18(-1)	6.63(-3)	1.19(-1)	6.49(-3)	1.19(-1)
57	3.31(-2)	1.84(-2)	3.67(-2)	3.85(-2)	1.82(-2)	1.01(-1)	1.36(-2)	1.10(-1)	1.27(-2)	1.10(-1)	1.26(-2)	1.09(-1)
58	3.00(-2)	1.72(-2)	3.24(-2)	3.51(-2)	1.53(-2)	8.78(-2)	1.14(-2)	9.49(-2)	1.07(-2)	9.47(-2)	1.05(-2)	9.40(-2)
59	5.09(-2)	2.90(-2)	5.34(-2)	5.68(-2)	2.39(-2)	1.34(-1)	1.73(-2)	1.44(-1)	1.62(-2)	1.43(-1)	1.60(-2)	1.42(-1)
60	1.88(-2)	1.47(-2)	1.95(-2)	2.98(-2)	8.56(-3)	7.25(-2)	6.21(-3)	7.81(-2)	5.86(-3)	7.78(-2)	5.83(-3)	7.73(-2)
61	3.63(-2)	1.96(-2)	3.68(-2)	3.36(-2)	1.55(-2)	6.42(-2)	1.14(-2)	6.76(-2)	1.15(-2)	6.73(-2)	1.20(-2)	6.70(-2)
62	1.91(-2)	1.58(-2)	1.90(-2)	2.77(-2)	7.89(-2)	5.49(-2)	5.77(-3)	5.80(-2)	5.67(-3)	5.79(-2)	5.90(-3)	5.79(-2)
63	1.85(-2)	2.02(-2)	1.91(-2)	3.41(-2)	8.32(-3)	6.26(-2)	6.23(-3)	6.58(-2)	6.46(-3)	6.58(-2)	7.09(-3)	6.59(-2)
64	1.04(-2)	1.09(-2)	1.07(-2)	1.79(-2)	4.41(-3)	3.26(-2)	3.15(-3)	3.43(-2)	3.09(-3)	3.43(-2)	3.24(-3)	3.43(-2)
65	6.63(-3)	1.20(-2)	6.92(-3)	2.04(-2)	2.99(-3)	3.89(-2)	2.19(-3)	4.12(-2)	2.20(-3)	4.12(-2)	2.36(-3)	4.12(-2)

TABLE A12. (Continued)

	z=0		z=15.41		z=30.85		z=41.11		z=61.68		z=90.06	
Group	Fe	Na	Fe^{+}	Na	Fe^{+}	Na	Fe^{+}	Na	Fe^{+}	Na	Fe^{+}	Na
66	1.55(-2)	8.28(-3)	1.58(-2)	1.24(-2)	6.46(-3)	1.95(-2)	4.59(-3)	2.01(-2)	4.55(-3)	2.01(-2)	4.82(-3)	2.00(-2)
67	1.78(-2)	9.24(-3)	1.84(-2)	1.33(-2)	7.68(-3)	1.89(-2)	5.59(-3)	1.93(-2)	5.73(-3)	1.93(-2)	6.25(-3)	1.93(-2)
68	1.84(-2)	1.65(-2)	1.89(-2)	2.39(-2)	8.18(-3)	3.27(-2)	6.60(-3)	3.31(-2)	8.08(-3)	3.30(-2)	1.02(-2)	3.31(-2)
69	1.17(-2)	2.03(-2)	1.78(-2)	2.95(-2)	7.75(-3)	3.93(-2)	6.32(-3)	3.97(-2)	7.92(-3)	3.95(-2)	1.01(-2)	3.96(-2)
70	2.51(-2)	1.90(-2)	2.59(-2)	2.69(-2)	1.07(-2)	3.39(-2)	8.10(-3)	3.38(-2)	8.87(-3)	3.36(-2)	1.02(-2)	3.36(-2)
71	2.01(-2)	2.58(-2)	2.08(-2)	3.89(-2)	9.03(-3)	5.42(-2)	7.10(-3)	5.46(-2)	7.95(-3)	5.38(-2)	9.20(-3)	5.33(-2)
72	2.48(-2)	5.06(-2)	2.65(-2)	8.34(-2)	1.23(-2)	1.31(-1)	9.46(-3)	1.32(-1)	9.84(-3)	1.29(-1)	1.08(-2)	1.27(-1)
73	2.49(-2)	1.20(-1)	2.87(-2)	2.46(-1)	1.67(-2)	5.53(-1)	1.38(-2)	5.81(-1)	1.39(-2)	5.66(-1)	1.47(-2)	5.54(-1)
74	3.88(-2)	1.49(-1)	4.00(-2)	2.54(-1)	1.73(-2)	4.19(-1)	1.42(-2)	4.25(-1)	1.66(-2)	4.14(-1)	2.00(-2)	4.05(-1)
75	1.34(-2)	7.80(-2)	1.31(-2)	1.26(-1)	5.71(-3)	1.94(-1)	5.03(-3)	1.96(-1)	6.20(-3)	1.92(-1)	7.59(-3)	1.88(-1)
76	6.56(-3)	2.22(-2)	6.18(-3)	3.36(-2)	2.10(-3)	4.76(-2)	1.49(-3)	4.79(-2)	1.64(-3)	4.69(-2)	1.88(-3)	4.60(-2)
77	1.49(-2)	4.28(-2)	1.36(-2)	6.29(-2)	6.14(-3)	8.27(-2)	6.68(-3)	8.26(-2)	1.02(-2)	8.09(-2)	1.42(-2)	7.98(-2)
78	2.74(-2)	1.31(-1)	2.48(-2)	1.99(-1)	1.14(-2)	2.68(-1)	1.32(-2)	2.66(-1)	2.19(-2)	2.60(-1)	3.18(-2)	2.56(-1)
79	3.50(-2)	1.39(-1)	3.06(-2)	1.99(-1)	1.33(-2)	2.48(-1)	1.74(-2)	2.45(-1)	3.50(-2)	2.39(-1)	5.70(-2)	2.35(-1)
80	4.43(-3)	7.12(-3)	4.06(-3)	9.94(-3)	2.33(-3)	1.31(-2)	2.53(-3)	1.32(-2)	3.78(-3)	1.29(-2)	5.29(-3)	1.26(-2)
81	1.77(-3)	6.56(-3)	1.67(-3)	9.87(-3)	1.07(-3)	1.42(-2)	1.14(-3)	1.42(-2)	1.55(-3)	1.38(-2)	2.03(-3)	1.34(-2)
82	6.61(-3)	1.01(-1)	8.59(-3)	2.97(-1)	1.44(-2)	1.18(0)	1.68(-2)	1.33(0)	1.93(-2)	1.33(0)	2.17(-2)	1.32(0)
83	6.40(-3)	7.71(-2)	5.79(-3)	1.36(-1)	4.12(-3)	2.38(-1)	5.09(-3)	2.42(-1)	7.14(-3)	2.32(-1)	9.17(-3)	2.23(-1)
84	8.03(-3)	8.06(-2)	6.74(-3)	1.26(-1)	4.68(-3)	1.77(-1)	6.40(-3)	1.76(-1)	9.99(-3)	1.69(-1)	1.37(-2)	1.62(-1)
85	1.30(-2)	8.79(-2)	1.02(-2)	1.26(-1)	8.27(-3)	1.52(-1)	1.27(-2)	1.49(-1)	2.14(-2)	1.44(-1)	3.04(-2)	1.40(-1)
86	5.41(-3)	2.41(-2)	4.13(-3)	3.23(-2)	3.48(-3)	3.63(-2)	5.29(-3)	3.54(-2)	8.71(-3)	3.42(-2)	1.23(-2)	3.32(-2)
87	6.48(-3)	3.95(-2)	4.97(-3)	5.58(-2)	2.27(-3)	6.75(-2)	2.64(-3)	6.60(-2)	3.83(-3)	6.32(-2)	5.09(-3)	6.08(-2)
88	5.81(-3)	2.52(-2)	4.37(-3)	3.45(-2)	5.08(-3)	4.11(-2)	8.70(-3)	4.05(-2)	1.55(-2)	3.93(-2)	2.26(-2)	3.83(-2)
89	3.14(-3)	2.02(-2)	2.40(-3)	2.78(-2)	1.97(-3)	3.27(-2)	2.60(-3)	3.18(-2)	3.69(-3)	3.03(-2)	4.81(-3)	2.91(-2)
90	2.68(-3)	5.12(-2)	2.14(-3)	7.48(-2)	1.63(-3)	9.24(-2)	2.02(-3)	8.96(-2)	2.65(-3)	8.47(-2)	3.26(-3)	8.04(-2)
91	4.50(-3)	6.62(-2)	3.58(-3)	9.64(-2)	5.57(-3)	1.20(-1)	8.73(-3)	1.16(-1)	1.38(-2)	1.11(-1)	1.90(-2)	1.06(-1)
92	7.03(-3)	6.88(-2)	5.29(-3)	9.81(-2)	5.20(-3)	1.19(-1)	8.27(-3)	1.16(-1)	1.39(-2)	1.11(-1)	1.98(-2)	1.06(-1)
93	4.12(-3)	6.38(-2)	3.16(-3)	9.18(-2)	7.30(-3)	1.13(-1)	1.34(-2)	1.11(-1)	2.44(-2)	1.06(-1)	3.62(-2)	1.02(-1)
94	2.71(-3)	5.99(-2)	2.13(-3)	8.64(-2)	4.62(-3)	1.05(-1)	7.26(-3)	1.02(-1)	1.11(-2)	9.65(-2)	1.52(-2)	9.17(-2)
95	2.81(-3)	5.59(-2)	2.17(-3)	8.05(-2)	3.30(-3)	9.69(-2)	4.67(-3)	9.34(-2)	6.48(-3)	8.77(-2)	8.29(-3)	8.28(-2)

TABLE A12. (Continued)

Group	z=0		z=15.41		z=30.85		z=41.11		z=61.68		z=90.06	
	Fe	Na	Fe^{+}	Na	Fe^{+}	Na	Fe^{+}	Na	Fe^{+}	Na	Fe^{+}	Na
96	7.87(-4)	5.39(-2)	6.21(-4)	7.85(-2)	5.22(-4)	9.51(-2)	5.51(-4)	9.15(-2)	5.86(-4)	8.57(-2)	6.81(-4)	8.07(-2)
97	3.60(-3)	5.83(-2)	2.59(-3)	8.16(-2)	1.12(-2)	9.98(-2)	2.62(-2)	9.91(-2)	6.05(-2)	9.69(-2)	1.04(-1)	9.47(-2)
98	8.01(-3)	5.91(-2)	5.55(-3)	8.23(-2)	3.94(-3)	9.48(-2)	4.99(-3)	9.03(-2)	6.60(-3)	8.39(-2)	8.01(-3)	7.82(-2)
99	4.71(-3)	5.88(-2)	3.34(-3)	8.20(-2)	1.03(-2)	9.73(-2)	1.86(-2)	9.41(-2)	3.26(-2)	8.88(-2)	4.76(-2)	8.39(-2)
100	6.74(-3)	5.83(-2)	4.70(-3)	8.09(-2)	7.43(-3)	9.16(-2)	1.10(-2)	8.67(-2)	1.63(-2)	8.00(-2)	2.17(-2)	7.41(-2)
101	3.34(-3)	5.65(-2)	2.45(-3)	7.96(-2)	5.41(-3)	9.05(-2)	7.74(-3)	8.52(-2)	1.07(-2)	7.82(-2)	1.37(-2)	7.19(-2)
102	1.97(-3)	1.38(-1)	1.95(-3)	1.98(-1)	1.15(-2)	2.27(-1)	1.65(-2)	2.13(-1)	2.23(-2)	1.94(-1)	2.78(-2)	1.78(-1)
103	5.54(-3)	1.39(-1)	4.01(-3)	1.95(-1)	7.91(-3)	2.16(-1)	1.06(-2)	2.01(-1)	1.36(-2)	1.82(-1)	1.60(-2)	1.65(-1)
104	1.07(-3)	5.04(-2)	6.65(-4)	7.09(-2)	-3.99(-4)	7.83(-2)	-7.09(-4)	7.27(-2)	-9.01(-4)	6.55(-2)	-9.19(-4)	5.95(-2)
105	5.43(-3)	4.40(-2)	3.54(-3)	5.87(-2)	1.66(-2)	6.72(-2)	3.12(-2)	6.55(-2)	5.69(-2)	6.28(-2)	8.66(-2)	5.99(-2)
106	3.99(-3)	1.06(-1)	2.92(-3)	1.47(-1)	8.44(-3)	1.58(-1)	1.14(-2)	1.45(-1)	1.47(-2)	1.29(-1)	1.75(-2)	1.16(-1)
107	3.03(-3)	6.99(-2)	2.38(-3)	9.61(-2)	1.51(-2)	1.05(-1)	2.26(-2)	9.84(-2)	3.27(-2)	8.93(-2)	4.31(-2)	8.09(-2)
108	7.62(-3)	1.62(-1)	5.59(-3)	2.22(-1)	2.08(-2)	2.37(-1)	2.91(-2)	2.18(-1)	3.91(-2)	1.94(-1)	4.81(-2)	1.74(-1)
109	1.28(-3)	9.10(-3)	9.02(-4)	1.18(-2)	3.05(-3)	1.20(-2)	4.18(-3)	1.12(-2)	5.72(-3)	1.01(-2)	7.39(-3)	9.07(-3)
110	3.51(-3)	7.91(-2)	2.69(-3)	1.05(-1)	1.13(-2)	1.07(-1)	1.60(-2)	9.78(-2)	2.14(-2)	8.61(-2)	2.60(-2)	7.63(-2)
111	3.92(-3)	1.26(-1)	2.92(-3)	1.72(-1)	1.22(-2)	1.78(-1)	1.77(-2)	1.61(-1)	2.33(-2)	1.40(-1)	2.73(-2)	1.23(-1)
112	2.52(-3)	1.70(-1)	2.14(-3)	2.35(-1)	1.30(-2)	2.43(-1)	1.93(-2)	2.18(-1)	2.49(-2)	1.87(-1)	2.80(-2)	1.63(-1)
113	7.67(-4)	6.96(-2)	6.20(-4)	9.52(-2)	4.11(-3)	9.76(-2)	6.14(-3)	8.70(-2)	7.82(-3)	7.39(-2)	8.59(-3)	6.38(-2)
114	1.13(-4)	9.92(-2)	3.65(-4)	1.36(-1)	8.99(-3)	1.37(-1)	1.41(-2)	1.19(-1)	1.77(-2)	9.75(-2)	1.89(-2)	8.15(-2)
115	8.17(-5)	4.77(-2)	5.31(-5)	6.50(-2)	-2.45(-3)	6.11(-2)	-2.96(-3)	5.05(-2)	-1.48(-3)	3.87(-2)	-3.95(-5)	3.06(-2)
116	3.26(-4)	3.18(-2)	-3.19(-4)	4.23(-2)	-1.11(-2)	3.68(-2)	-1.66(-2)	3.04(-2)	-2.06(-2)	2.53(-2)	-2.19(-2)	2.25(-2)
117	1.56(-3)	4.67(-2)	1.53(-3)	6.00(-2)	3.06(-2)	5.76(-2)	6.43(-2)	5.81(-2)	1.33(-1)	6.34(-2)	2.07(-1)	6.54(-2)
118	4.56(-4)	2.31(-2)	1.61(-4)	2.97(-2)	6.15(-3)	3.76(-2)	2.87(-2)	4.67(-2)	1.17(-1)	6.17(-2)	2.86(-1)	7.40(-2)
119	2.69(-4)	2.24(-2)	5.11(-5)	2.95(-2)	5.50(-3)	4.14(-2)	2.52(-2)	4.91(-2)	9.95(-2)	5.61(-2)	2.32(-1)	5.70(-2)
120	1.07(-3)	6.53(-2)	7.82(-4)	8.81(-2)	3.38(-2)	1.26(-1)	9.07(-2)	1.31(-1)	2.34(-1)	1.10(-1)	4.14(-1)	7.82(-2)
121	1.09(-3)	1.04(-1)	1.86(-3)	1.42(-1)	7.41(-2)	1.79(-1)	1.51(-1)	1.50(-1)	2.70(-1)	8.09(-2)	3.75(-1)	3.24(-2)
122	2.43(-4)	1.94(-1)	4.29(-3)	2.67(-1)	1.38(-1)	2.41(-1)	2.16(-1)	1.42(-1)	2.62(-1)	3.99(-2)	3.03(-1)	7.04(-3)
123	7.44(-4)	1.67(-1)	5.70(-3)	2.23(-1)	1.12(-1)	1.29(-1)	1.38(-1)	4.51(-2)	1.29(-1)	4.47(-3)	1.50(-1)	1.64(-4)
124	1.13(-3)	1.33(-1)	5.47(-3)	1.73(-1)	5.96(-2)	6.98(-2)	6.00(-2)	1.49(-2)	5.04(-2)	5.34(-4)	6.27(-2)	3.03(-6)
125	3.19(-4)	9.34(-2)	1.95(-3)	1.18(-1)	1.69(-2)	3.61(-2)	1.65(-2)	5.35(-3)	1.46(-2)	1.14(-4)	1.79(-2)	3.64(-7)

TABLE A12. (Continued)

	z=0		z=15.41		z=30.85		z=41.11		z=61.68		z=90.06	
Group	Fe	Na	Fe^+	Na	Fe^+	Na	Fe^+	Na	Fe^+	Na	Fe^+	Na
126	1.84(-4)	5.33(-2)	2.78(-3)	6.68(-2)	4.18(-2)	2.19(-2)	4.52(-2)	3.58(-3)	4.04(-2)	8.39(-5)	5.08(-2)	2.76(-7)
127	1.69(-4)	1.98(-2)	2.72(-3)	2.51(-2)	5.38(-2)	1.04(-2)	5.88(-2)	2.00(-3)	5.07(-2)	4.73(-5)	6.44(-2)	1.34(-7)
128	1.30(-4)	-2.26(-4)	1.09(-3)	1.25(-3)	2.25(-2)	9.27(-4)	2.50(-2)	1.62(-4)	2.22(-2)	3.27(-6)	2.86(-2)	5.33(-9)
129	1.23(-4)	-4.44(-3)	7.03(-4)	-3.54(-3)	1.75(-2)	-8,32(-4)	1.96(-2)	-5.88(-5)	1.73(-2)	5.98(-7)	2.26(-2)	1.71(-9)
130	8.51(-5)	-6.80(-3)	7.18(-4)	-5.32(-3)	1.63(-2)	-1.44(-3)	1.84(-2)	-1.62(-4)	1.63(-2)	-1.12(-6)	2.14(-2)	-5.51(-11)
131	2.77(-4)	6.23(-3)	5.71(-4)	3.79(-3)	1.52(-2)	4.52(-4)	1.71(-2)	-7.23(-6)	1.53(-2)	-8.83(-7)	2.01(-2)	-6.42(-10)
132	9.15(-5)	2.86(-3)	3.27(-4)	3.54(-3)	7.29(-3)	8.92(-4)	8.18(-3)	1.05(-4)	7.30(-3)	8.89(-7)	9.64(-3)	4.29(-10)
133	3.91(-5)	1.93(-3)	3.18(-4)	2.88(-3)	7.05(-3)	7.16(-4)	7.89(-3)	8.80(-5)	7.05(-3)	8.54(-7)	9.32(-3)	4.60(-10)
134	3.08(-5)	3.81(-3)	7.10(-4)	3.94(-3)	1.35(-2)	1.23(-3)	1.50(-2)	1.52(-4)	1.34(-2)	1.28(-6)	1.77(-2)	7.46(-10)
135	9.13(-5)	2.74(-3)	9.05(-4)	3.67(-3)	1.31(-2)	1.26(-3)	1.42(-2)	1.54(-4)	1.26(-2)	1.11(-6)	1.67(-2)	4.79(-10)
136	3.26(-4)	5.27(-2)	3.51(-3)	6.55(-2)	3.15(-2)	1.61(-2)	3.19(-2)	1.41(-3)	2.79(-2)	6.08(-6)	3.67(-2)	1.87(-9)
137	6.90(-4)	1.57(-1)	4.94(-3)	1.98(-1)	3.05(-2)	4.48(-2)	2.87(-2)	3.39(-3)	2.48(-2)	9.57(-6)	3.25(-2)	1.63(-9)
138	8.25(-4)	2.48(-1)	6.38(-3)	3.18(-1)	2.80(-2)	7.07(-2)	2.42(-2)	5.04(-3)	2.07(-2)	1.14(-5)	2.69(-2)	1.31(-9)
139	6.33(-4)	3.15(-1)	9.48(-3)	4.12(-1)	3.21(-2)	9.16(-2)	2.45(-2)	6.38(-3)	2.01(-2)	1.30(-5)	2.66(-2)	1.19(-9)
140	5.84(-4)	3.47(-1)	1.20(-2)	4.56(-1)	3.29(-2)	9.85(-2)	2.28(-2)	6.53(-3)	1.85(-2)	1.13(-5)	2.43(-2)	7.76(-10)
141	4.75(-4)	3.64(-1)	1.53(-2)	4.76(-1)	3.45(-2)	9.96(-2)	2.16(-2)	6.31(-3)	1.71(-2)	9.53(-6)	2.25(-2)	5.11(-10)
142	9.83(-5)	3.73(-1)	1.95(-2)	4.86(-1)	3.72(-2)	9.83(-2)	2.11(-2)	5.95(-3)	1.64(-2)	7.89(-6)	2.14(-2)	3.41(-10)
143	1.39(-4)	3.81(-1)	2.50(-2)	4.91(-1)	4.05(-2)	9.53(-2)	2.06(-2)	5.51(-3)	1.57(-2)	6.44(-6)	2.03(-2)	2.27(-10)
144	1.88(-4)	3.86(-1)	3.21(-2)	4.92(-1)	4.46(-2)	9.12(-2)	2.03(-2)	5.02(-3)	1.50(-2)	5.17(-6)	1.94(-2)	1.50(-10)
145	1.46(-4)	3.88(-1)	4.10(-2)	4.87(-1)	4.95(-2)	8.57(-2)	2.02(-2)	4.48(-3)	1.45(-2)	4.06(-6)	1.86(-2)	9.74(-11)
146	1.06(-4)	3.91(-1)	5.23(-2)	4.81(-1)	5.53(-2)	7.99(-2)	2.02(-2)	3.94(-3)	1.41(-2)	3.13(-6)	1.79(-2)	6.20(-11)
147	7.49(-5)	3.91(-1)	6.58(-2)	4.70(-1)	6.12(-2)	7.30(-2)	1.95(-2)	3.39(-3)	1.30(-2)	2.34(-6)	1.65(-2)	3.81(-11)
148	5.11(-5)	3.90(-1)	8.19(-2)	4.55(-1)	6.71(-2)	6.55(-2)	1.85(-2)	2.84(-3)	1.15(-2)	1.69(-6)	1.48(-2)	2.24(-11)
149	3.39(-5)	3.89(-1)	1.02(-1)	4.36(-1)	7.51(-2)	5.76(-2)	1.92(-2)	2.32(-3)	1.18(-2)	1.18(-6)	1.50(-2)	1.27(-11)
150	2.18(-5)	3.87(-1)	1.24(-1)	4.14(-1)	8.25(-2)	4.96(-2)	1.94(-2)	1.85(-3)	1.16(-2)	7.94(-7)	1.46(-2)	6.84(-12)
151	1.36(-5)	3.85(-1)	1.49(-1)	3.89(-1)	8.91(-2)	4.18(-2)	1.92(-2)	1.43(-3)	1.11(-2)	5.14(-7)	1.39(-2)	3.52(-12)
152	8.02(-6)	3.71(-1)	1.70(-1)	3.51(-1)	9.22(-2)	3.34(-2)	1.83(-2)	1.04(-3)	1.03(-2)	3.10(-7)	1.28(-2)	1.66(-12)
153	4.99(-6)	3.86(-1)	2.08(-1)	3.40(-1)	1.03(-1)	2.85(-2)	1.85(-2)	8.07(-4)	9.81(-3)	1.99(-7)	1.22(-2)	8.42(-13)
154	2.69(-6)	3.71(-1)	2.33(-1)	2.97(-1)	1.04(-1)	2.13(-2)	1.78(-2)	5.40(-4)	9.35(-3)	1.07(-7)	1.14(-2)	3.42(-13)
155	1.45(-6)	3.63(-1)	2.60(-1)	2.62(-1)	1.06(-1)	1.60(-2)	1.71(-2)	3.61(-4)	8.69(-3)	5.71(-8)	1.06(-2)	1.39(-13)
156	7.46(-7)	3.54(-1)	2.85(-1)	2.26(-1)	1.07(-1)	1.15(-2)	1.62(-2)	2.30(-4)	8.00(-3)	2.88(-8)	9.62(-3)	5.28(-14)

TABLE A12. (Continued)

Group	z=0		z=15.41		z=30.85		z=41.11		z=61.68		z=90.06	
	Fe	Na	Fe†	Na	Fe†	Na	Fe†	Na	Fe†	Na	Fe†	Na
157	3.63(-7)	3.40(-1)	3.05(-1)	1.89(-1)	1.06(-1)	7.90(-3)	1.53(-2)	1.38(-4)	7.27(-3)	1.35(-8)	8.67(-3)	1.83(-14)
158	1.67(-7)	3.26(-1)	3.20(-1)	1.54(-1)	1.03(-1)	5.21(-3)	1.42(-2)	7.90(-5)	6.53(-3)	5.95(-9)	7.71(-3)	5.92(-15)
159	7.28(-8)	3.08(-1)	3.28(-1)	1.22(-1)	9.81(-2)	3.24(-3)	1.30(-2)	4.23(-5)	5.78(-3)	2.42(-9)	6.76(-3)	1.74(-15)
160	2.99(-8)	2.90(-1)	3.28(-1)	9.27(-2)	9.19(-2)	1.91(-3)	1.18(-2)	2.12(-5)	5.04(-3)	9.06(-10)	5.83(-3)	4.63(-16)
161	1.14(-8)	2.71(-1)	3.19(-1)	6.76(-2)	8.40(-2)	1.05(-3)	1.05(-2)	9.79(-6)	4.32(-3)	3.08(-10)	4.93(-3)	1.10(-16)
162	4.09(-9)	2.54(-1)	3.06(-1)	4.77(-2)	7.64(-2)	5.44(-4)	9.24(-3)	4.23(-6)	3.67(-3)	9.63(-11)	4.14(-3)	2.37(-17)
163	1.24(-9)	2.22(-1)	2.68(-1)	2.96(-2)	6.36(-2)	2.39(-4)	7.55(-3)	1.51(-6)	2.90(-3)	2.40(-11)	3.23(-3)	3.86(-18)
164	3.71(-10)	2.01(-1)	2.37(-1)	1.82(-2)	5.42(-2)	1.03(-4)	6.30(-3)	5.32(-7)	2.34(-3)	5.99(-12)	2.57(-3)	6.55(-19)
165	9.22(-11)	1.73(-1)	1.96(-1)	9.87(-3)	4.32(-2)	3.72(-5)	4.94(-3)	1.54(-7)	1.78(-3)	1.19(-12)	1.92(-3)	8.40(-20)
166	1.91(-11)	1.43(-1)	1.51(-1)	4.64(-3)	3.23(-2)	1.13(-5)	3.65(-3)	3.69(-8)	1.29(-3)	1.90(-13)	1.36(-3)	8.49(-21)
167	3.06(-12)	1.09(-1)	1.05(-1)	1.78(-3)	2.19(-2)	2.69(-6)	2.45(-3)	6.78(-9)	8.49(-4)	2.27(-14)	8.82(-4)	6.24(-22)
168	3.57(-13)	7.44(-2)	6.25(-2)	5.08(-4)	1.28(-2)	4.51(-7)	1.43(-3)	8.63(-10)	4.94(-4)	1.83(-15)	5.02(-4)	3.02(-23)
169	2.36(-14)	3.79(-2)	2.64(-2)	8.16(-5)	5.35(-3)	4.05(-8)	5.98(-4)	5.78(-11)	2.12(-4)	7.59(-17)	2.09(-4)	7.30(-25)
Integral	1.38299	14.682	6.7379	16.599	6.4152	17.404	5.6275	17.282	6.2405	17.181	7.4290	17.120
Elastic	0.83093	13.900	4.9815	15.522	3.7907	12.931	2.9189	11.973	3.4511	11.508	4.5429	11.205
In-Elastic	0.52021	0.226	0.8597	0.803	2.1472	4.320	2.3834	5.151	2.4417	5.499	2.4757	5.728

*Tabulated values are of the quantity: $-\frac{\Delta R}{R} / \frac{\Delta \Sigma_T}{\Sigma_T}$.

†Includes the iron in both the stainless and carbon steels. The two may be approximately separated by ascribing all the sensitivity above ∿ 500 keV to the stainless steel and below ∿ 500 keV to the carbon steel.

**Read as 1.02×10^{-4}, etc..

ORNL-5259
(ENDF-258)
Distribution Category UC-79d

INTERNAL DISTRIBUTION

1- 3. L. S. Abbott
4. D. E. Bartine
5. R. L. Childs
6. C. E. Clifford
7. F. L. Culler
8. G. F. Flanagan
9. H. Goldstein (Consultant)
10. W. O. Harms
11. K. M. Henry
12. R. F. Hibbs
13. L. B. Holland
14. J. L. Hull
15. J. Lewin
16-20. R. E. Maerker
21-22. F. C. Maienschein
23. J. J. Manning
24. J. N. Money
25. F. J. Muckenthaler
26. F. R. Mynatt
27. R. W. Peelle
28. H. Postma
29. C. O. Slater
30. P. N. Stevens
31. M. L. Tobias
32. D. B. Trauger
33. C. R. Weisbin
34. A. Zucker
35. P. Greebler (Consultant)
36. W. W. Havens, Jr. (Consultant)
37. A. F. Henry (Consultant)
38. R. E. Uhrig (Consultant)
39-40. Central Research Library
41. ORNL Y-12 Technical Library
Document Reference Section
42-43. Laboratory Records
44. Laboratory Records ORNL RC
45. ORNL Patent Office
46. RSIC

EXTERNAL DISTRIBUTION

47- 48. USERDA Division of Reactor Development and Demonstration, Washington, D. C. 20545: Director

49. USERDA Oak Ridge Operations, Research and Technical Support Division, P. O. Box E, Oak Ridge, TN 37830: Director

50. USERDA Oak Ridge Operations, Reactor Division, P. O. Box E, Oak Ridge, TN 37830: Director

51-296. For distribution as shown in TID-4500 Distribution Category UC-79d - LMFBR Physics

297-358. Evaluated Neutron Data File Distribution

UNITED STATES DEPARTMENT OF ENERGY
P.O. BOX 62
OAK RIDGE, TENNESSEE 37830

OFFICIAL BUSINESS
PENALTY FOR PRIVATE USE, $300

POSTAGE AND FEES PAID
UNITED STATES
DEPARTMENT OF ENERGY

Brookhaven National Laboratory ENDF
ATTN: Dr. Charles L. Dunford
National Nuclear Data Center
Building 197
Upton, NY 11973

PRINTED MATTER – BOOKS